IN-05

p. 250

NASA Contractor Report 177585

Technology Needs for High-Speed Rotorcraft (I)

J. B. Wilkerson, J. J. Schneider, and K. M. Bartie

CONTRACT NAS2-13041
May 1991

National Aeronautics and
Space Administration

NASA Contractor Report 177585

Technology Needs for High-Speed Rotorcraft (I)

J. B. Wilkerson, J. J. Schneider, and K. M. Bartie

Boeing Helicopters
P.O. Box 16858
Philadelphia, PA 19142

Prepared for
Ames Research Center
CONTRACT NAS2-13041
May 1991

National Aeronautics and
Space Administration

Ames Research Center
Moffett Field, California 94035-1000

TABLE OF CONTENTS

TABLE OF CONTENTS - Continued

PAGE

PREFACE

This report was prepared for the National Aeronautics and Space Admnistration, NASA, Ames Research Center, Moffett Field, CA., in fulfillment of NASA Contract NAS2-13041.

The study was performed for NASA Ames Research Center by Boeing Helicopters during the period June 1989 through November 1990. Mr. Peter Talbot and Mr. Marty Maisel of NASA Ames Research Center were the technical monitors.

The Boeing Helicopters Program Manager was Mr. J. B. Wilkerson and the Configuration Manager was Mr. J. J. Schneider. Volume I of this report was prepared by Mr. J. Schneider and Mr. J. Wilkerson. Volume II was prepared by Mr. J. Wilkerson. Mr. K. Bartie prepared all the graphics, assisted in final report preparaton, and did the final report layup. Ms. M. McGuire typed the report. In addition, the following Boeing Helicopters engineering and management personnel made significant contributions to this study effort in either configuration analysis or in preparing the enabling technology plans:

Acoustics:	H. Sternfeld P. Ziegenbein
Aerodynamics:	L. Dadone J. Liu D. Paisley
Cost Analysis:	B. Celani Z. Jasnoff M. Smith
Dynamics:	R. Gabel P. Lang F. Tarzanin B. Vlaminck
Flight Controls:	F. Dones
Handling Qualities:	R. Lacy
Structures and Materials:	G. Rossi
Propulsion:	R. Semple D. Woodley
Weights:	S. Dyess J. Wisniewski

J B Wilkerson

Joseph B. Wilkerson

SUMMARY

The objective of this study was to identify high-speed rotorcraft concepts and the corresponding technology needed to greatly extend the cruise capabilities of rotorcraft beyond current capabilities, up to 450 knots, while retaining the helicopter attributes of low downwash velocities and temperatures: the so-called "soft footprint" characteristic.

Task I conducted a broad survey which identified 20 candidate rotorcraft concepts with high-speed potential. These concepts were qualitatively evaluated and graded against 17 key discriminators. The five concepts with the most potential were:

1. Conventional tiltrotor (a baseline rotorcraft)
2. Forward-swept-wing/canard tiltrotor with advanced- geometry rotor
3. Forward-swept-wing/canard tiltrotor with variable diameter rotor
4. Forward-swept-wing/canard folding tiltrotor with convertible engine
5. Two-prop tiltwing.

These five rotorcraft concepts were designed and sized to the NASA-defined military transport mission (6,000-lb payload, 450-knot cruise speed, and 350-nmi radius). Wing loading and disc loading tradeoffs were analyzed to arrive at the optimum combination for each concept, that which minimized vehicle gross weight. These five optimum vehicle designs were quantitatively compared against 11 key criteria; gross weight, speed potential, hover efficiency and downwash, conversion maneuverability, cruise range factor, aeroelastic considerations, R&M, survivability, LCC and applicability to other missions. The two highest ranking concepts were selected for further study in Task II: the canard tiltrotor and the folding tiltrotor. The selective process is schematically shown in Figure 1.

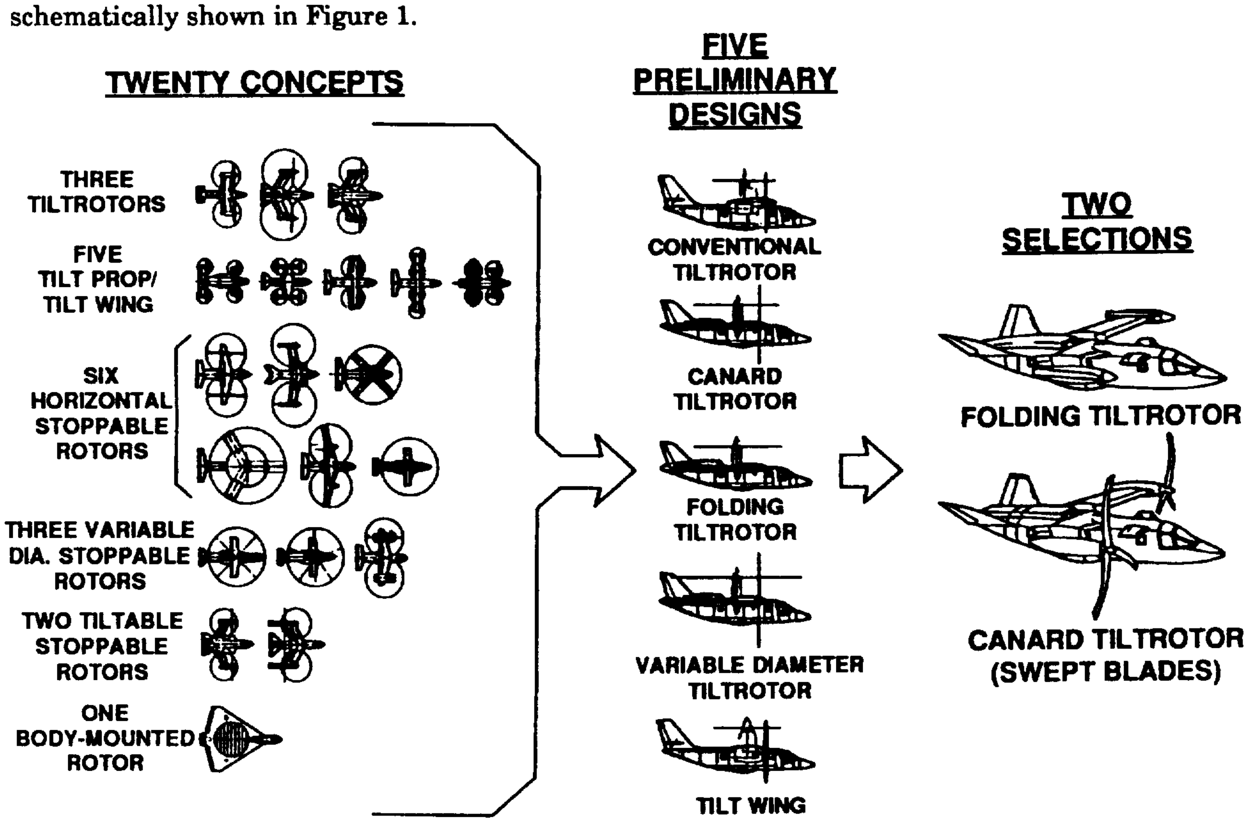

Figure 1. Candidate High-Speed Rotorcraft Selection

The folding tiltrotor had the highest speed potential, best specific range at 450-knots, and the best survivability characteristics, giving it greater design flexibility and a higher potential military worth than the other configurations. It was applied to the NASA military transport mission. The canard tiltrotor with an advanced-geometry rotor design had the lowest gross weight and lowest estimated cost to build, which made it ideally suited to the highly cost-competitive market of civil airline operations. It was applied to the NASA 30-passenger civil mission.

Task II refined the two selected concepts for their respective missions. Technologies were examined in more detail, component weights were reestimated, and the vehicles were resized to satisfy mission requirements and design criteria appropriate to the mission. With 1990 technology, the high-speed civil tiltrotor was resized to a 38,380 lb gross weight aircraft capable of carrying 30 passengers over a 600-nautical -mile (nmi) range at an altitude of 25,000 ft and cruise speed of 450 knots TAS. It can hover out of ground effect (OGE) with one engine inoperative. The military folding tiltrotor sized out to a 51,406 lb gross weight rotorcraft- capable of carrying 6,000 lb of cargo or troops round trip over a 350 nmi radius with a 15 minute hover and a 30 minute loiter at the destination. Artist's renderings of the military folding tiltrotor and high-speed civil tiltrotor are shown in Figures 2 and 3, respectively.

Many performance characteristics were generated, such as prop-rotor performance maps, airframe drag polars, climb rates, conversion corridors, flight envelopes, and STOL performance. STO performance for the high-speed civil tiltrotor, for example, showed a 30% increase in useful load capability for only a 220-ft ground roll (550-ft clearway). This corresponds to almost a 50% increase in payload, assuming no structural changes were necessitated.

Sensitivity studies indicated vehicle gross weight and installed power to be quite sensitive to mission parameters. A 50-knot increase in design speed, for instance, resulted in about a 15% increase in gross weight for the folding tiltrotor with its convertible engine, and a similar percentage increase in installed power. But a 50-knot increase for the tiltrotor resulted in a 45% increase in gross weight, driven by over twice as much installed power required with its speed-sensitive prop-rotor propulsion. Advanced-technology factors were also evaluated. A 2-square-foot decrease in flat-plate area gave about an 8% decrease in gross weight and about 18% lower power installed. Year 2000 engine technology, estimated from the IHPTET Phase II objectives, gave a 10% reduction in gross weight. The combined year 2000 engine technology and drag reduction for the military folding tiltrotor yielded a 16% reduction in gross weight. An advanced-geometry prop-rotor for the civil tiltrotor yielded a 7.5% reduction in gross weight and a 17% reduction in installed power. The combined year 2000 engine technology, drag reduction, and advanced-geometry prop-rotor on the high-speed civil tiltrotor gave an 18% overall decrease in gross weight and 32% decrease in installed power.

Task III developed an enabling technology plan. Design issues and technologies critical for concept maturity were defined for each concept. The objective was to establish the fundamental understanding and technical maturity necessary for a low-risk, full-scale development program by 1997. As an example, a critical design issue for the civil tiltrotor is development of an advanced-geometry prop-rotor for the gross weight and power benefits stated above. Another critical design issue is development of an automated, reversible, stop/fold procedure for the folding tiltrotor. Development of such an automated control system process requires a valid data base and a thorough understanding of blade loads for the current prop-rotor blade and hub design. These are examples of multidisciplinary technology issues requiring a concurrent engineering design approach. The overall enabling technology plan consists of several individual technology plans, each addressing a separate critical design issue. These plans address required improvements in technical analyses and development of data bases to support high performance

Figure 2. Artist's Rendering of Military Folding Tiltrotor

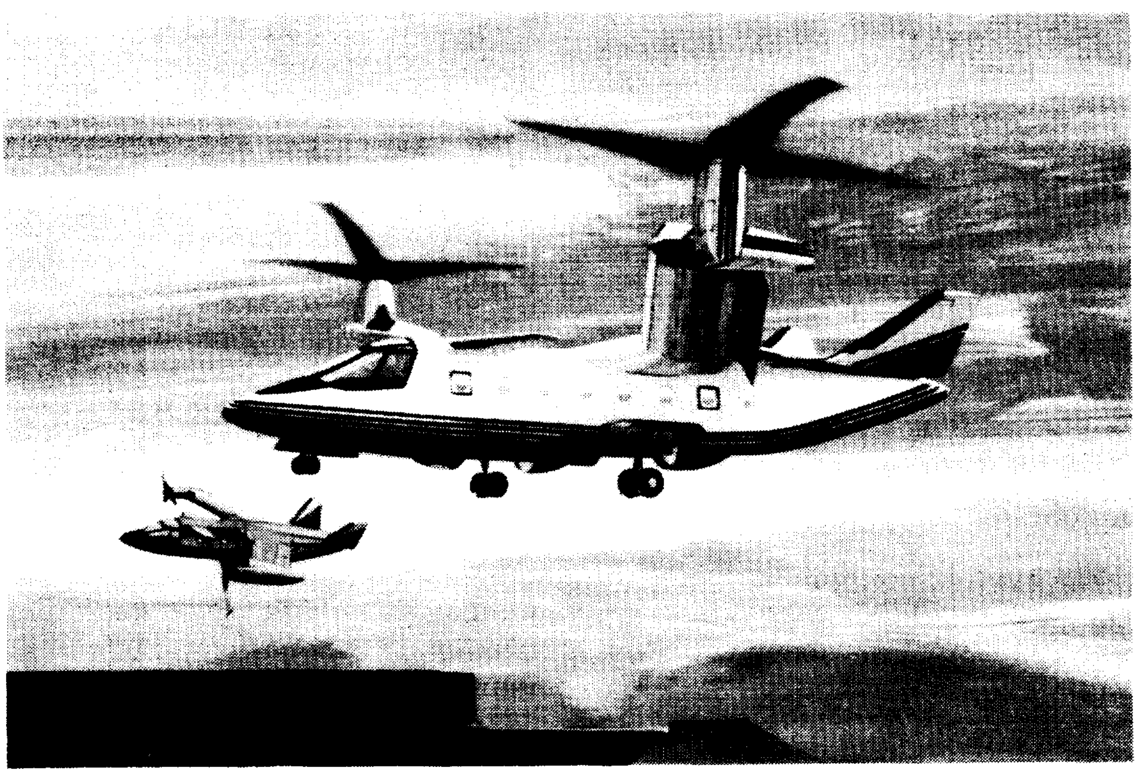

Figure 3. Artist's Rendering of High-Speed Civil Tiltrotor

integrated designs. Tables 1 and 2 identify the critical design issues for the military folding tiltrotor and for the high-speed civil tiltrotor, respectively. The tables provide a summary of the rationale for the enabling technology plan, showing the 1990 baseline performance, the advanced-technology goals, and the benefit or requirement for reaching these goals. The figure numbers are a reference to the technology plan presented in Section 3 of this report.

The military folding tiltrotor and high-speed civil tiltrotor had several design issues in common by virtue of their similarity. The common design issues were (1) aeroelastic/structural design of the forward-swept wing to avoid whirl flutter instability on the high-speed tiltrotor and static divergence on the folding tiltrotor, (2) aerodynamic design of the wing, canard, and tail to maximize cruise L/D and to provide suitable static margin and control authority over the speed range in airplane mode, (3) minimize the structural weight fraction by concurrent engineering solutions (e.g., the wing structural design and manufacturing methods), and (4) simulation of flight control laws to verify control sensitivity and load-limiting features for helicopter mode, through transition, and up to 540 knots in the airplane mode.

Table 1. Summary of Enabling Technologies for Military Folding Tiltrotor

CRITICAL DESIGN ISSUE	BASELINE 1990 PERFORMANCE	YEAR 2000 GOAL	BENEFIT OR REQUIREMENT	TECHNOLOGY PLAN (REF.)
FOLDING HUB DESIGN	• Limited 1969-72 wind tunnel database	• Analytical loads estimation • Hub concept/detailed design • Automated/reversible fold procedure	• Required for development • Operational effectiveness	Figure 92, 93
WING STATIC DIVERGENCE AND FLUTTER	• No database or analysis for forward swept wing with tip pod • Stiffness approach	• Design, test and verify structurally efficient forward swept wing • Active flutter suppression	• Required to satisfy static divergence and weight objectives	Figure 94
WING-CANARD AERODYNAMICS	• L/D = 10.4	• L/D = 11.5 • Minimum trim drag • Minimum interference drag • Minimum tip pod drag	• - 7% gross weight and - 16% shp	Figure 82
ACOUSTICS-EXTERNAL	• High hover sideline noise	• Improved sideline noise	• Detection requirements	Figure 88
HANDLING QUALITIES	• Non-optimum canard	• Optimized size and location	• Min. size, min. trim drag	Figure 95
FLIGHT CONTROLS	• Manual nacelle conversion	• Auto-nacelle conversion • Automated fold system • Aeroservoelastic compensation	• Operational effectiveness	Figure 95
STRUCTURES AND MATERIALS	• Graphite skin and stringer construction	• 15% lighter body • 14% lighter wing • 22% lighter engine • 8% lighter flight controls	• - 16% gross weight and - 13.5% shp	Figure 84
CONVERTIBLE ENGINE DEVELOPMENT	• IHPTET Phase I • VIGV/VEGV have high blade stresses, noise, and residual thrust in the turboshaft mode	• IHPTET Phase II (- 5% sfc) • Full-scale development and test stand verification	• - 10% gross weight and - 9.1% shp	Figure 91
COMBINED POTENTIAL IMPACT OF ADVANCED TECHNOLOGIES:			- 25% GW, - 27% INSTALLED THRUST AND - 30% RECURRING COST	

Table 2. Summary of Enabling Technologies for High-Speed Civil Tiltrotor

CRITICAL DESIGN ISSUE	BASELINE 1990 PERFORMANCE	YEAR 2000 GOAL	BENEFIT OR REQUIREMENT	TECHNOLOGY PLAN (REF.)
ROTOR CRUISE PROPULSIVE EFFICIENCY	• Unswept blade • t/c = 18% - 9% • $\eta = 0.71$	• Swept blade • t/c = 8% • $\eta = 0.79$	• - 7.3% gross weight and - 16.5% shp	Figure 85
WHIRL FLUTTER ANALYSIS AND PREVENTION	• Uncoupled torsion • Spanwise fibers • Stiffness approach	• Fully coupled • Tailored mode shapes • Active flutter suppression	• Required to makeup 80 KEAS shortfall	Figure 86, 87
WING-CANARD AERODYNAMICS	• L/D = 9.2	• L/D = 10.8 • Minimum trim drag • Minimum interference drag	• - 8.2% gross weight and - 18.7% shp	Figure 82
VIBRATION CONTROL	• Vibration suppressors • Post design tuning	• Low vibration rotor • Airframe structure optimization	• 0.05g vibration levels in cruise, cabin and cockpit	Figure 89
ACOUSTICS-EXTERNAL	• High hover sideline noise • Meets ICAO standard	• Improved sideline noise • Exceed min. requirement	• Satisfaction of local community ordinances	Figure 88
ACOUSTICS-INTERNAL	• Meets 85 dBA with conventional treatment	• Meet 78 dBA with active noise suppression	• Passenger comfort and acceptance	Figure 88
HANDLING QUALITIES	• Non-optimum canard	• Optimized size and location	• Min. size, min. trim drag	Figure 90
FLIGHT CONTROLS	• Manual nacelle conversion	• Auto-nacelle conversion • Aeroservoelastic compensation	• Reduced pilot workload	Figure 90
STRUCTURES AND MATERIALS	• Graphite skin and stringer construction	• 15% lighter body • 14% lighter wing • 22% lighter engine • 8% lighter flight controls	• - 16% gross weight and - 13.5% shp	Figure 84
TURBOSHAFT ENGINES	• IHPTET Phase I	• IHPTET Phase II (- 12.5% sfc)	• - 10% gross weight and - 9.1% shp	
COMBINED POTENTIAL IMPACT OF ADVANCED TECHNOLOGIES:			- 25% GW, - 35% SHP AND - 30% RECURRING COST	

LIST OF FIGURES

PAGE

LIST OF FIGURES - Continued

PAGE

LIST OF FIGURES - Continued

LIST OF TABLES

INTRODUCTION

A number of attractive high performance rotorcraft concepts were conceived over the past 40 years of VTOL research: Development of many of these concepts had to be deferred until enabling technologies could provide lighter structures, significant improvements in propulsion system weight or fuel fraction, and solutions for previously limiting loads and aeroelastic characteristics. Technological advances such as turboshaft engines, bearingless rotor hubs, and a multitude of vibration suppressors and absorbers have been the keys in bringing rotorcraft to higher levels of efficiency, reduced maintenance, and more acceptable comfort levels for passengers and crew. Still, rotary-wing aircraft are generally noted by the public as being rather small, noisy, marginally safe aircraft best suited for very limited uses such as emergency medical transportation, police work, border patrols, or executive/business applications which require the helicopter's main attribute of vertical takeoff and landing. Certainly, the helicopter has never had a public image of being a large, safe, quiet, comfortable, highly reliable machine suitable for significant civil transportation over substantial distances; not like a fixed-wing aircraft.

Opportunities for helicopter-like vertical flight and fixed-wing-like cruise began to arise in the 1950s with NASA and DOD funding of many types of advanced VTOL aircraft. Many of these aircraft were funded through the development and flight testing of concept demonstrators, with varying degrees of success. These include nonrotary-wing vehicles such as the Hawker-Siddeley P1127 direct-lift jet, the Ryan X-13 jet-powered tailsitter, the AvroCar VZ-9 body-mounted rotor, the Ryan XV-5A fan-in-wing, and the North American XFV-12A augmentor-wing. Many rotary-wing aircraft were also built and flight-tested: among them, the Bell XV-3 and XV-15 tiltrotors, the LTV XC-142 tiltwing, the Curtiss-Wright X-19 tiltprop, and the Bell X-22 tiltduct. Section 1 of this report provides a survey and discussion of rotorcraft concepts which are of relatively low disc loading and are capable of high cruise speeds. But in the last 20 years only one hovercraft has successfully transitioned to full-scale production: the AV-8A/B Harrier direct-lift jet (not rotary-wing); and only one other has been under serious development for military airlift: the MV-22 Osprey tiltrotor. Doubtless to say, neither of these aircraft would have arrived at its current level of capability without numerous technical developments and several flight research aircraft contributing to their heritage and maturity.

It is wise, if not necessary, to occasionally reevaluate old and new concepts in light of the currently available technology. This serves to redefine concept feasibility, especially against new requirements. Such was the case with this study.

The study objectives were to identify those rotorcraft concepts with the best potential for achieving a 450-knot cruise speed while retaining the helicopter attributes of efficient hover, good low-speed handling, and relatively low downwash velocities and temperatures: the so-called "soft footprint" characteristics. The choice of rotorcraft concept is inexorably tied to the concepts' fundamental strengths and weaknesses. Section 1 of this report describes 20 different candidate high-speed rotorcraft. The two most attractive concepts were chosen and then designed to NASA-defined missions requiring 450-knot cruise speeds. The two selected candidates were a high-speed tiltrotor applied to a civil mission and a folding tiltrotor applied to a military transport mission. Both choices reflected the best combination of speed capability, cruise efficiency, and relative life-cycle cost. They represent the potential for another quantum jump in capability: from the 300-knot speed of the V-22 to a 450-knot cruise speed.

Changing technology and future technology advances have an obvious impact on vehicle size and performance. It is therefore desirable to make a projection of this impact when evaluating and comparing the different rotorcraft concepts. Two technology levels were considered; baseline designs used 1990 technology levels and projections were made to year 2000 technology levels.

Vehicle sensitivity to selected year 2000 technologies was then evaluated to determine the relative impact on concept attributes such as size, weight, installed power, and cost. Section 2 describes the attributes of the baseline 1990 vehicles and their sensitivity to the projected year 2000 technology. In order to keep Volume I of this report to a readable size, many of the technical details generated for these vehicles were put in Appendices A and B, Volume II of this report.

Critical technologies were identified as a product of the design and sensitivity activities. Critical technologies were defined as those requiring further development to achieve the prerequisite low risk level needed before entering preliminary design. Finally, a set of development plans was prepared showing a path to achieving technology maturity in preparation for low-risk, full-scale development. The identification of critical technologies and the development plans are described in Section 3, Enabling Technology Plans.

SECTION 1. INITIAL CANDIDATE CONCEPTS

Task I of the study was to survey current and previous rotorcraft concepts to identify those with a high-speed potential. Twenty candidate concepts were identified and then narrowed down to 5 concepts. These 5 were further defined, sized to the NASA mission, compared to one another, and then given relative rankings. The two most attractive concepts were recommended for continuation into Task II.

A three-view sketch of each configuration was prepared. In some cases, further exploratory design layout was done in order to size important elements such as transmission retracting methods, rotor blade retraction reels, rotor blade/disc interfaces, rotor blade stowage volume, swept wing/rotor tilt axis/CG interfaces, sweep effects on tiltwing, and rotor blade telescoping concepts. Drive system schematics were prepared for all configurations defining gearboxes, shafting, clutches, gear sets, rotor brakes, and engines.

Candidate High-Speed Rotorcraft Concepts

During the past 50 years of rotorcraft development, many concepts have been suggested for their potential high-speed capability. While most of these were never developed, some concepts were carried through wind tunnel programs and a few were either developed in test-bed demonstration programs or progressed as far as operational test aircraft.

Boeing Helicopters participated in many of these studies and developments and previous records were researched in order to define the candidate concepts. In addition, a brainstorming session was undertaken to explore any new ideas for conceptual high-speed rotorcraft. Figure 4 summarizes these candidate high-speed rotorcraft concepts. Fourteen basic approaches were defined, resulting in a total of more then 20 configurations (varying numbers of rotors, wings, etc) that were evaluated. Four missions (two civil and two military) were defined by NASA as shown in Table 3. For the initial evaluation, Boeing selected the military transport mission because of its similarity to the V-22 Osprey requirements.

Sizing and Constraints

Initial trend studies established a first-cut gross weight of about 50,000 pounds for the 6,000-pound-payload military transport mission. The V-22 carries 24 troops (5,760 lb) in a 6-ft x 6-ft x 21-ft cabin at approximately 275 knots. Gross weight for this mission is about 40,000 pounds. Of course, the V-22 is only a conceptual baseline since the aerodynamics and propulsion must be significantly improved in order to meet the 450-knot speed requirement. However, the V-22 provides a reasonable basis for comparison and for realism in weight and performance analysis.

Downwash (disc loading) constraints were implied by the RFP. Working from those desires, the downwash criteria of Table 4 were established from many helicopter and VTOL tests; references 1 through 3 provide significant information in this area. Although there are many criteria of

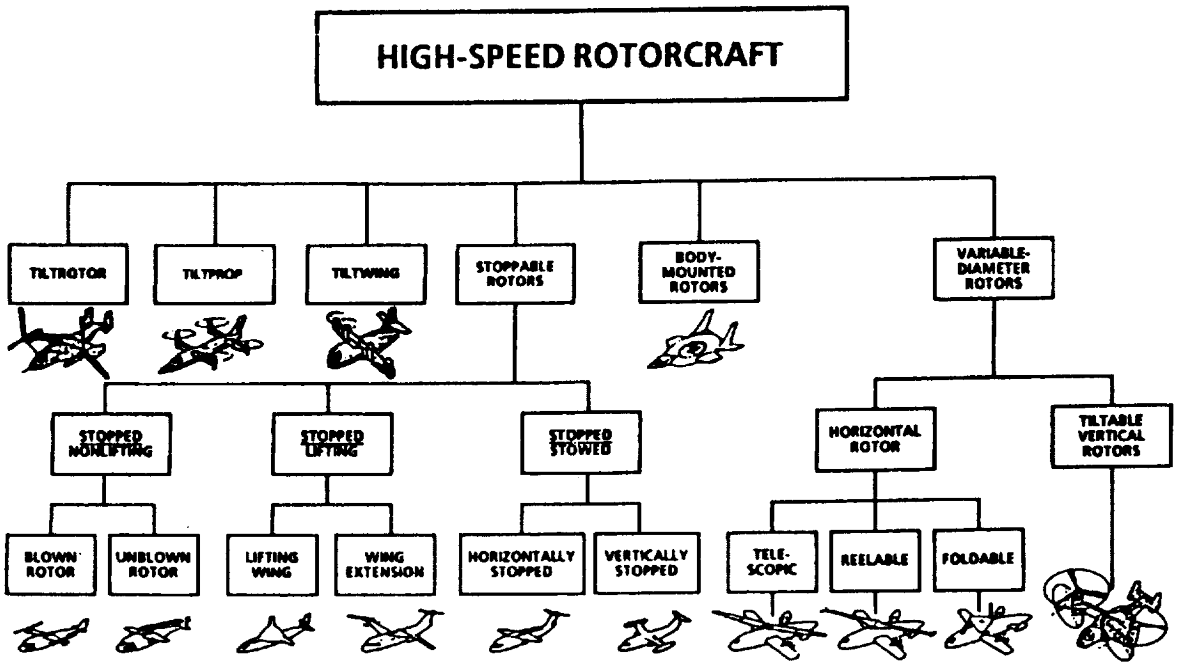

Figure 4. Candidate High-Speed Rotorcraft Concepts

Table 3. Mission Definitions

MISSION	MILITARY TRANSPORT	MILITARY ATTACK	CIVIL TRANSPORT	CIVIL COMMUTER
BASIC LAYOUT	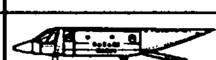		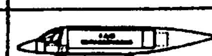	
MISSION DEFINITION	• ISA + 15°C • VTO and convert/climb • Dash 350 nmi at 450 knots • Hover OGE 15 minutes • Loiter 30 minutes • Cruise back • 10% fuel reserves	• 4,000 ft, 95°F • VTO and convert • Cruise 150 nmi • Dash 50 nmi at 400 knots • NOE maneuver — 15 minutes at hover OGE and 15 minutes at 40 knots • 5 minutes attack at IRP • Cruise back • 10% fuel reserves	• ISA + 15°C • VTO and convert/climb • Cruise 600 nmi at 450 knots • 10% fuel reserves	• ISA + 15°C • VTO and convert/climb • Cruise 600 nmi at 450 knots • 10% fuel reserves
DEFINED WEIGHTS	Payload 6,000 lb Fixed equipment 3,000 lb Mission equipment 2,900 lb Crew 470 lb	Payload 3,000 lb Fixed equipment 2,000 lb Mission equipment 2,900 lb Crew 470 lb	Payload 6,000 lb (30 passengers) Fixed equipment 4,000 lb Avionics 800 lb Operational items and crew 625 lb	Payload 3,000 lb (15 passengers) Fixed equipment 2,900 lb Avionics 600 lb Operational items and crew 435 lb

Table 4. Downwash Criteria

CONCERN	CRITERIA
1. Overturning personnel	Disc loading / diameter limits
2. Walking without assistance	Max 40 psf disc loading
3. Overturning:	
Tents	Max 35-40 psf disc loading
Empty 55 gal. drums	Separation distance
4. Debris / stone transport	Cleanliness / altitude separation
5. Dust / water vapor clouds	Sufficient altitude
6. Eye tissue damage	Max 35-40 psf
7. Rotor-engine re-ingestion	Configuration dependent
8. Tree thrashing	Sufficient altitude
9. Noise	Moderate tip speeds Moderate disc loading Configuration clearances
10. Temperature	Low disc loading IR suppressors

interest for a definitive aircraft development and further definition may be needed, only the first two constraints are illustrated in Figure 5. The limiting personnel overturning moment constraints from the Wernicke paper[1] for a single- and twin-rotor aircraft are shown along with various rotorcraft and V/STOL test points.

For those multirotor concepts whose outwash layer is very thin (close to the ground) but very fast, a constraint is required that will allow close-in walking around a hovering aircraft. Operational testing[2] of the XC-142 assault transport defined the difficulty of approaching the aircraft at 40-psf disc loading. Other tests (CL-84 and Vanguard 2D) were judged as very close to the limit for walking in thin, fast outwash. Therefore, Table 4 limits constrained the rotor sizing for all concepts, eliminating any consideration of high-disc loading-concepts such as tilt-duct, fan-in-wing, ejector, or jet-lifters in this study.

Since disc loading and diameter define gross weight, the 50,000-lb gross weight trends for 1-, 2-, and 4-rotor concepts can be superimposed on the constraints of Figure 5 as seen in Figure 6. Therefore, the minimum diameter for all single-rotor concepts is 70 ft (except for the body-mounted rotor concept), the minimum for the four-rotor concepts is 20 ft, whereas the twin-rotor diameters were optimized for each concept at no less than 28 ft.

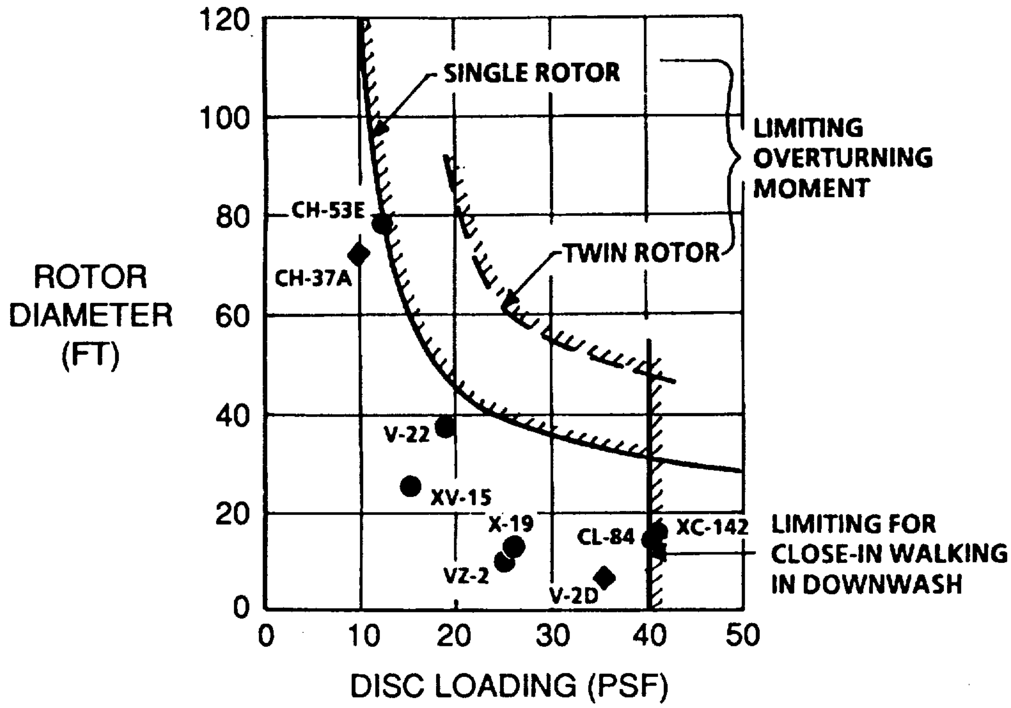

Figure 5. Downwash Limitations

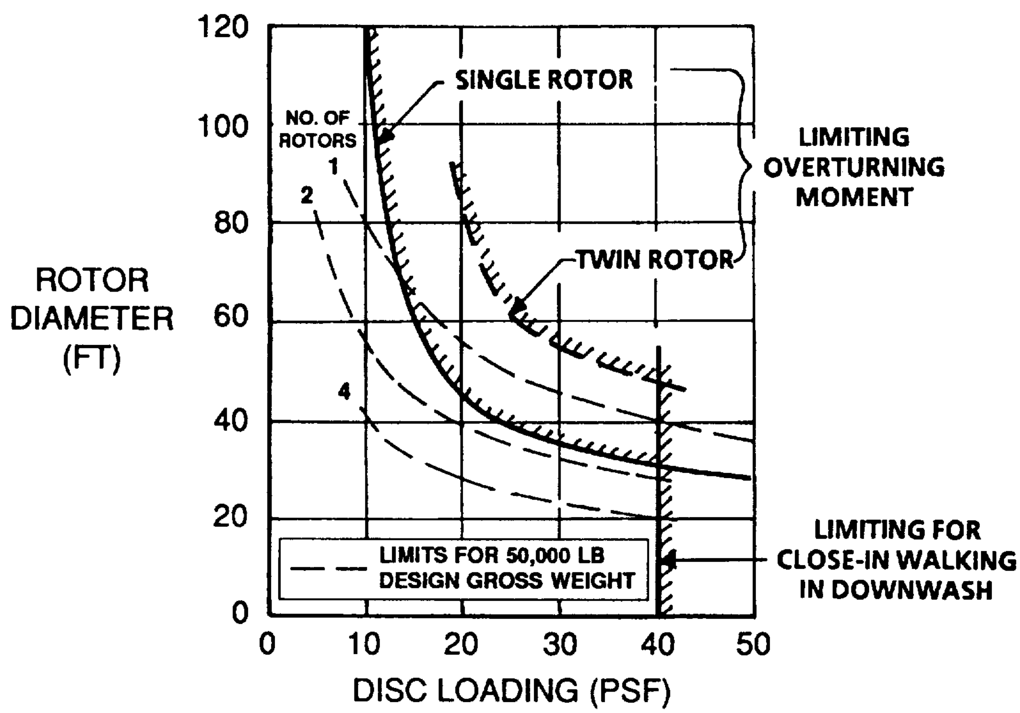

Figure 6. Sizing Constraints

Concept Definition

In the following, the candidate conceptual configurations are defined in sufficient detail for an evaluation leading to the selection of five concepts having the highest potential for a 450+ knot V/STOL rotorcraft. The format for each concept consists of background, configuration description, configuration issues (technology barriers), and mission suitability.

Tiltrotor

The tiltrotor concept (Figure 7) has a long history of development starting with the early inventors[4]. In the late 30's and early 40's, the Baynes Heliplane and the Focke-Achgelis FA-269 tiltrotor concepts saw some design development. However, no aircraft were developed. Then, in the late 1940's, Dr. LePage suggested the tiltrotor transport shown here (Figure 8). One of his former employees, along with Mario Guerierri, began the development of the Transcendental Model 1g. Robert Lichten left Transcendental to lead the tiltrotor XV-3 development for Bell Helicopter. Following successful demonstrations of the XV-3 in the early 60's, and further technology studies and wind tunnel testing, the development of the XV-15 was undertaken by the Bell/Army/NASA team in 1973[5]. The outstanding success of this program fostered the current development of the vertical-lift V-22 Osprey tiltrotor for the U.S. Marine Corps.

FOCKE-ACHGELIS FA-269
PUSHER TILT-ROTOR

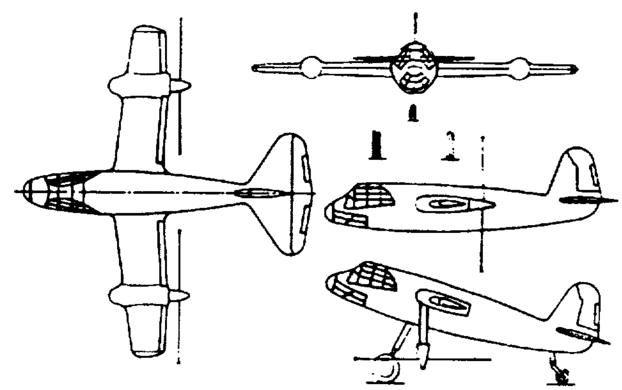

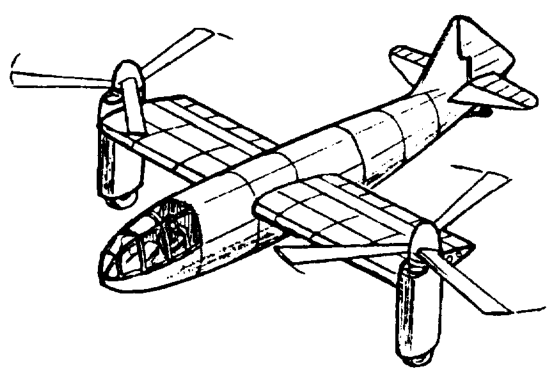

1937 BAYNES HELIPLANE TILT-ROTOR

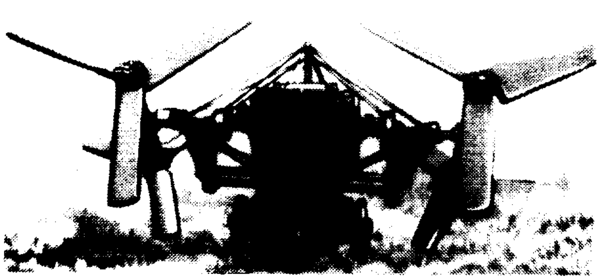

LEINWEBER-CURTISS

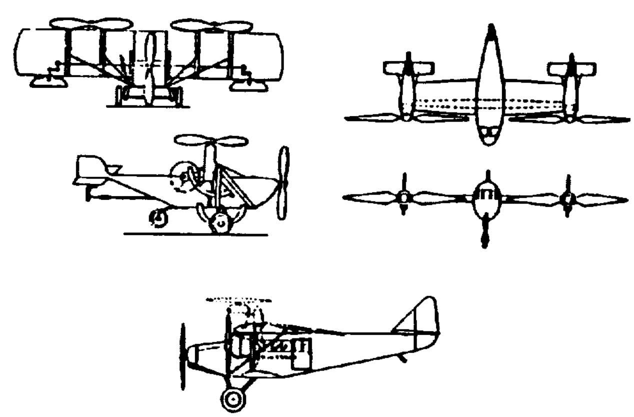

U.S. PATENT DRAWINGS

Figure 7. Tiltrotor Background - Early Years

LePAGE's TILTROTOR

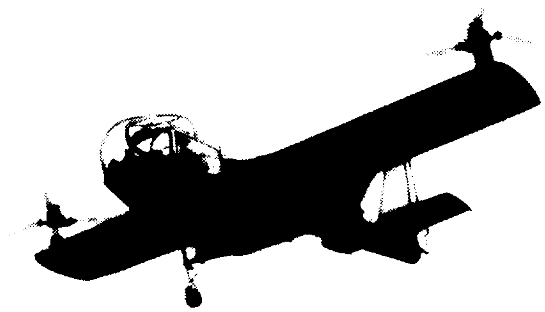

TRANSCENDENTAL MODEL 1-G

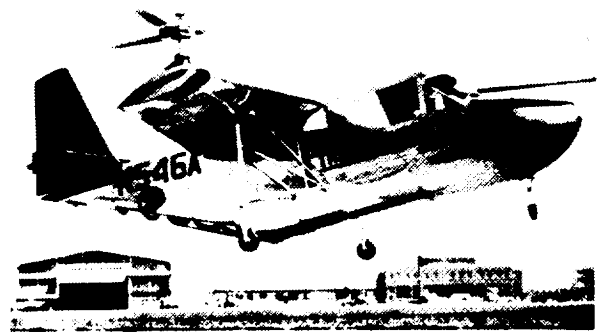

TRANSCENDENTAL MODEL 2

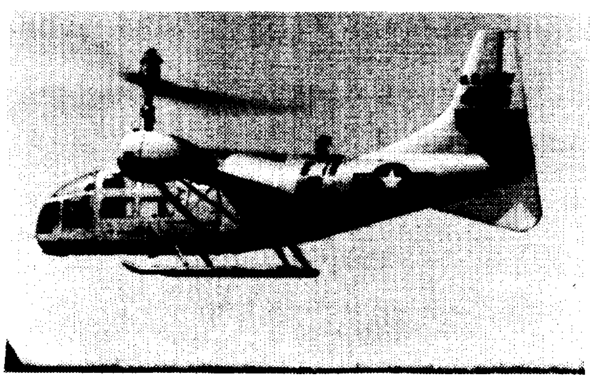

BELL XV-3

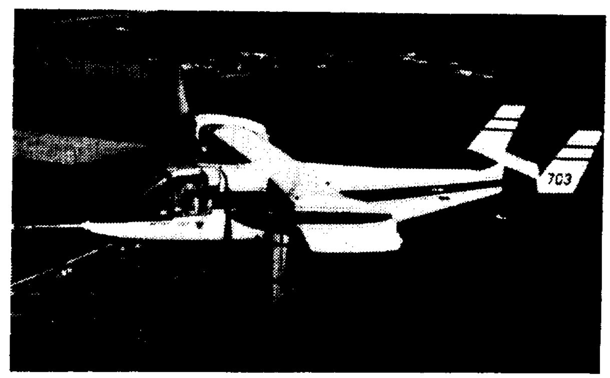

BELL XV-15

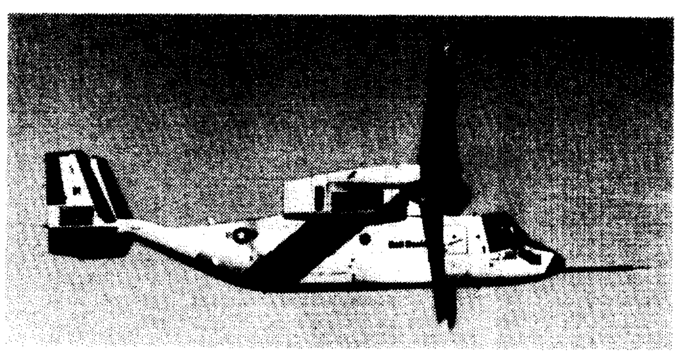

BELL BOEING V-22

Figure 8. Tiltrotor Background - Past 45 Years

The conventional tiltrotor military transport shown in Figure 9 is very similar to the V-22 except for speed-enhancing improvements. Since the power for high speed is about twice the hover requirement, optimum disc loading generally increases. Rotor diameter is 38 ft for a disc loading of 22 psf; the wing loading is 100 psf. The large fuel sponsons of the V-22 were removed, leaving small fairings for the landing gear. Improvements in the aerodynamics of the nose and afterbody were assumed. Fuel was located in the subfloor and wing torque box. Major configuration issues of the conventional tiltrotor are:

- Wing thickness effects
- Drive system design torque
- Rotor and wing aeroelastics
- Speed limited to Mach 0.7

Since the wing of a tiltrotor aircraft needs a relatively large thickness in order to alleviate aeroelastic problems at high speed, the wing must be optimized by trades between wing loading, thickness ratio, sweep, structural tailoring (weight), and low-drag airfoil sections. As speed increases, helical tip Mach number limitations result in a need to slow the rotor rpm. This trend, combined with the power increases (for speed), result in an exponential increase in drive system design torque (and weight).

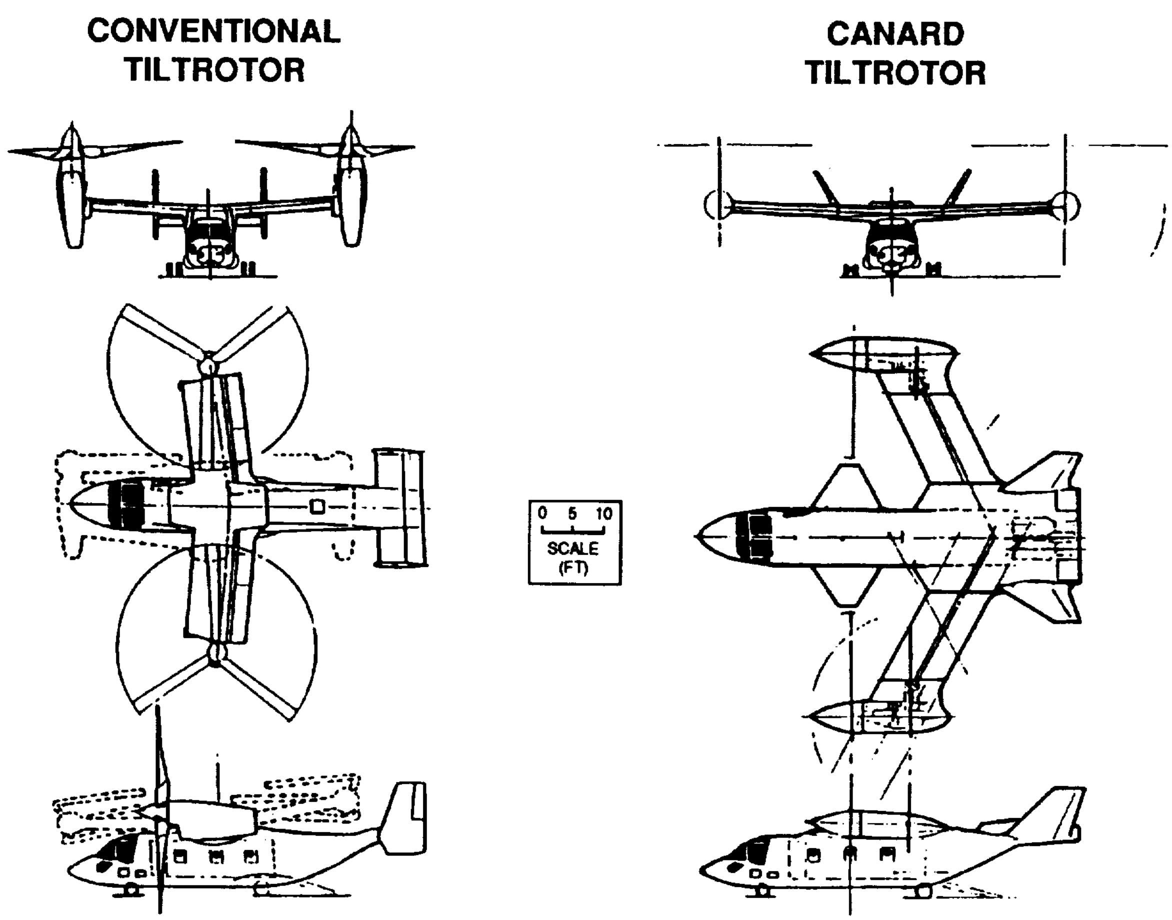

Figure 9. Tiltrotor Candidate Configurations

The cited issues, including the margins required for prop-rotor whirl-flutter modes, tend to limit the speed capability of the conventional tiltrotor defined here to approximately Mach 0.7. Major configuration changes can delay this speed limit - and they are incorporated in the so-called canard tiltrotor (Figure 9).

The canard tiltrotor results from the desire for forward wing sweep angles of substantially more than 10°. For small sweep angles, the conversion axis/drive shaft interface can be easily handled, but at high sweep angles the conversion axis is outside the planform of the wing structure. Therefore, some form of canard configuration is required to move the equivalent MAC forward such that the conversion axis/driveshaft can be accommodated within the wing planform[6]. There can be many canard variants, long-coupled and short-coupled, etc.

Due to the adverse drive system torque (and weight) trends, an advanced rotor is desirable for the higher speed canard tiltrotor. The swept rotor can allow higher speeds at essentially constant rpm and meet the helical tip mach number limits. Alternatively, the variable-diameter rotor could also allow constant rpm for the same helical tip mach number. First evaluations would indicate that the swept rotor is the better selection because of the safety and complexity issues of the variable-diameter rotor. More detailed design studies of both are required to determine the performance and weight tradeoffs.

The canard tiltrotor shown in Figure 9 has 33-ft. diameter advanced rotors with a 29-psf disc loading. The short-coupled canard configuration results in a higher wing aspect ratio and a lower wing loading (87 psf). In order to reduce the peak cross-sectional area distribution, the engines are integrated into the afterbody. Configuration issues are:

- Swept-forward wing/canard
- Swept rotor blades
- Rotor and wing aeroelastics
- Speed limited to ~ Mach 0.8

Although there are many canard arrangements possible, studies and testing are required to optimize the layout, performance, and weights. The optimum-swept blades and rotor/wing aeroelastics must be determined for the potentially higher speed capability of the canard tiltrotor. The tiltrotor concept has been the subject of many application studies and (within its speed capabilities) can be effective in many military and civil missions. Some recent applications range from small ground attack aircraft to advanced escorts and to civil canard feeder-liners, as well as medium to large civil tiltrotor concepts.

Tiltprop

The tiltprop concept (Figure 10) has several developments in its background[7]. After World War II, Prof. Heinrich Focke initiated a four-propeller configuration under contract to a Brazilian company. Although never flown during the early 50's, a ground test rig was built and tested and the flight test vehicle was nearly completed. During the late 50's, Curtiss-Wright, under Henry Borst's direction, built and successfully demonstrated the two-prop X-100 utilizing the lift force from the inclined propellers for transition: the so-called radial lift force capability. This was followed during the 60's by one of the winners in the Tri-Service Transport competition, the Curtiss-Wright X-19 four-propeller/tandem-wing tiltprop[8]. Unfortunately, a fatigue-caused gearcase failure destroyed the aircraft and cut short the test program.

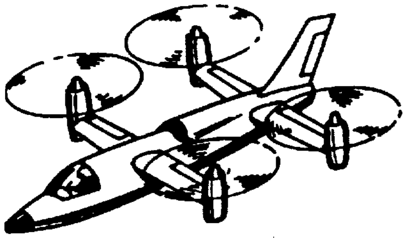

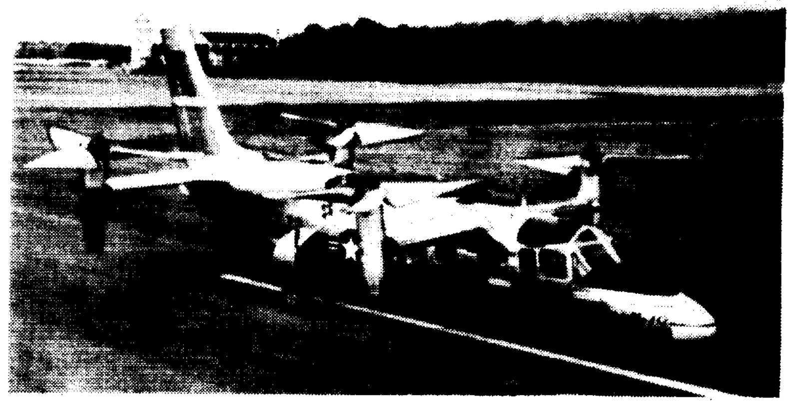

CURTISS-WRIGHT X-19

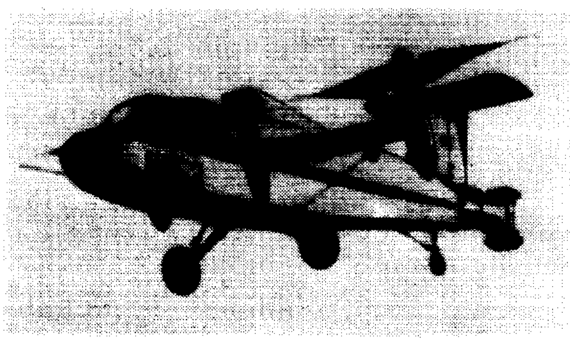

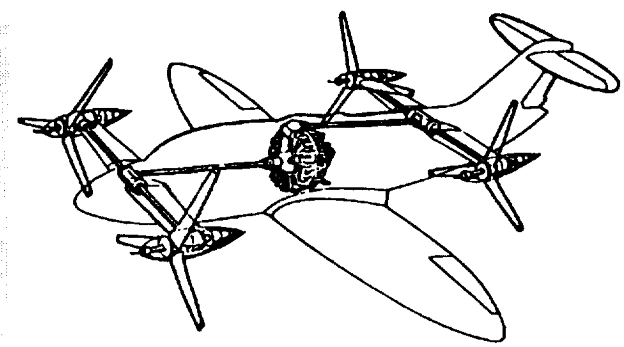

CURTISS-WRIGHT X-100 PROF. FOCKE's BRAZILIAN VTOL PROJECT

Figure 10. Tiltprop Background

The tandem-wing tiltprop configuration defined in Figure 11 has four 20-ft-diameter propellers with a 40-psf disc loading. Tandem wings based on X-19 scaling are shown with a wing loading of 110 psf. Primary configuration issues of this arrangement are:

- Drive system complexity
- Transition corridor
- Prop-prop interference
- Shipboard folding complexity
- Rotor and wing aeroelastics
- Speed limited to ~ Mach 0.7

The single-wing/four-propeller variant (Figure 11) was also considered. Disc-loading and wing-loading characteristics are the same as before. Configuration issues are:

- Drive system complexity
- Prop-prop interference
- Rotor and wing aeroelastics
- Aft propeller safety in hover
- Swept-wing lift balance
- Speed limited to ~ Mach 0.8

Most issues are self-evident except for the lift balance. If a large amount of leading-edge sweep is desired for high speed, the concept layout is very difficult in matching the hover lift center to the CG/MAC required for cruise. Use of the tapered planform shown allows the lift center (for two equal-diameter propellers) to be near the quarter-chord MAC. However, highly swept wings tend to require a large tail due to the aft CG/lift center location.

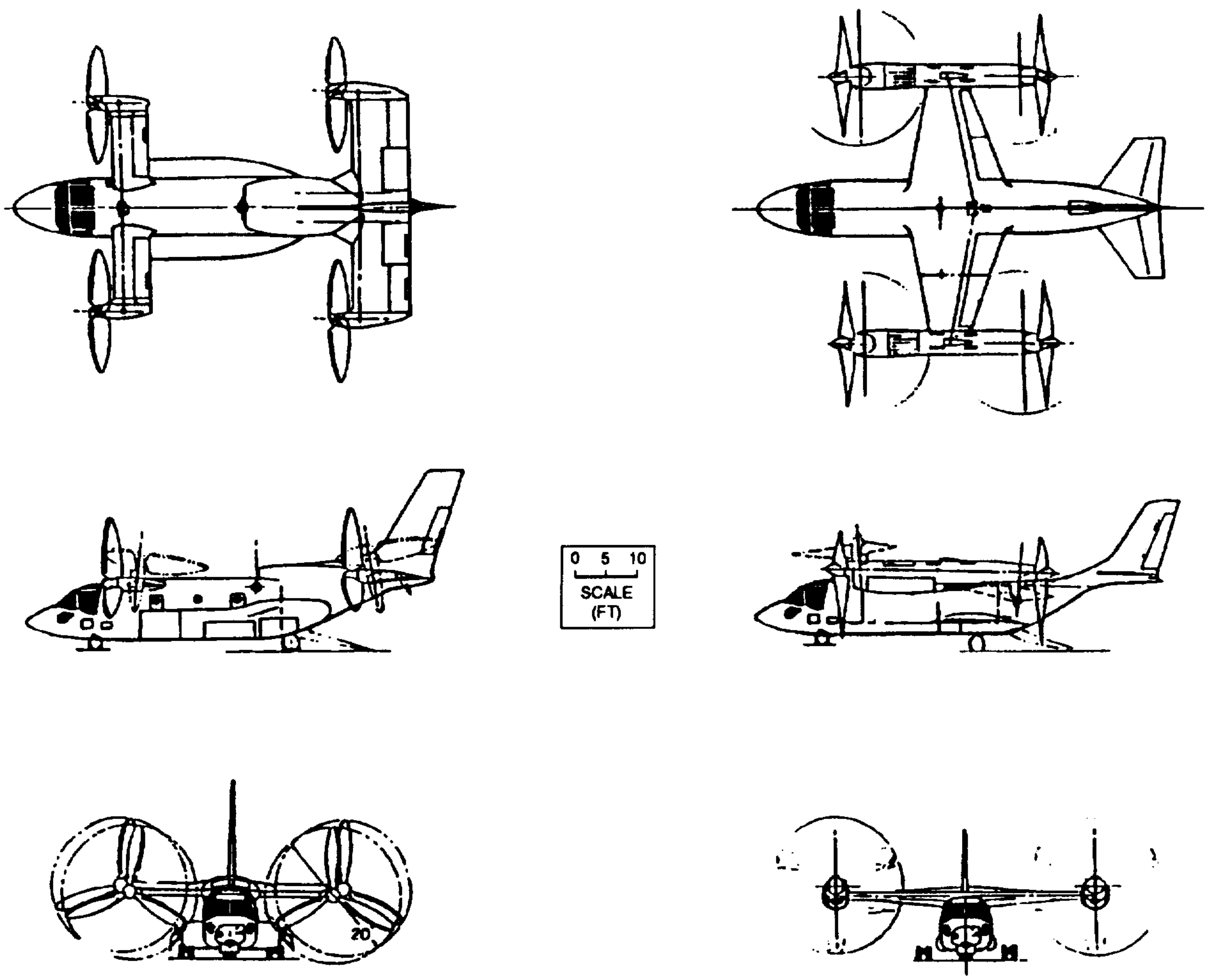

Figure 11. Tiltprop Candidate Configurations

Tiltwing

The tiltwing concept (Figure 12) has four significant test bed/demonstrator aircraft programs in its background[7]. In addition, there were considerable wind tunnel investigations by DOD, NASA, and industry for programs such as the Light Intratheater Transport (LIT), Advanced Aerial Fire Support System (AAFSS), etc.

The Boeing VZ-2A tiltwing test bed[9], along with extensive NASA wind tunnel testing, proved the tiltwing principles and led to the Tri-Service Transport Program development of the XC-142A[10]. In the meantime, USAF-sponsored development of the X-18A was proceeding[11]. However, the X-18 had been designed around the earlier Pogo engines (XT-40) and their coaxial propellers. Reliability problems of the propulsion system resulted in cancellation of the program prior to full conversion.

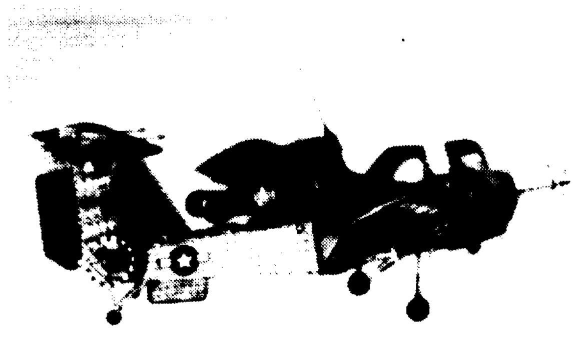

BOEING VERTOL VZ-2

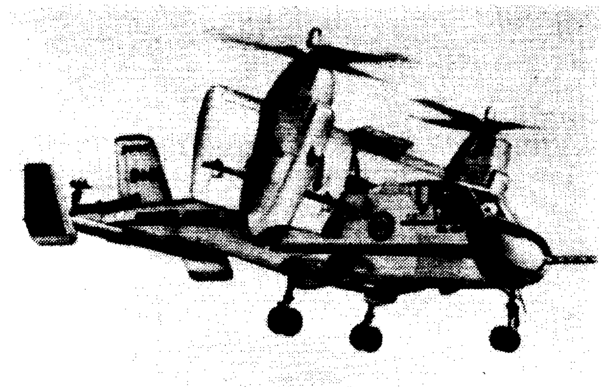

CANADAIR CL-84

HILLER X-18

LTV-HILLER-RYAN XC-142A

Figure 12. Tiltwing Background

Five XC-142A operational test aircraft were completed and 420 hours of testing were accomplished in this tri-service program. The program was completed in 1967. While there were deficiencies in the aircraft, tiltwing demonstration was successfully accomplished.

Canadair began development of the CL-84 in the late 50's[12]. Four aircraft were built and successful technology and operational demonstrations were completed by 1974. A total of 476 hours were flown on these aircraft.

Three variants of the tiltwing concept were evaluated in Task 1. The two-propeller tiltwing of Figure 13 has 28-ft-diameter propellers of 40-psf disc loading; wing loading is 72 psf. Configuration issues of the two-propeller tiltwing are:

- Chord/diameter effects
- Wing sweep impractical
- Rotor and wing aeroelastics
- Hingeless prop-rotor cyclic control
- 360° vision in hover (wing up)
- Recirculation in short landings
- Speed limited to ~ Mach 0.7

One of the elemental problems of the tiltwing is the necessity to keep the wing/flap system fully immersed in the propeller slipstream during the approach/descent mode. This leads to geometry considerations such as chord-to-diameter ratio, disc area-to-wing area ratio, propeller plane

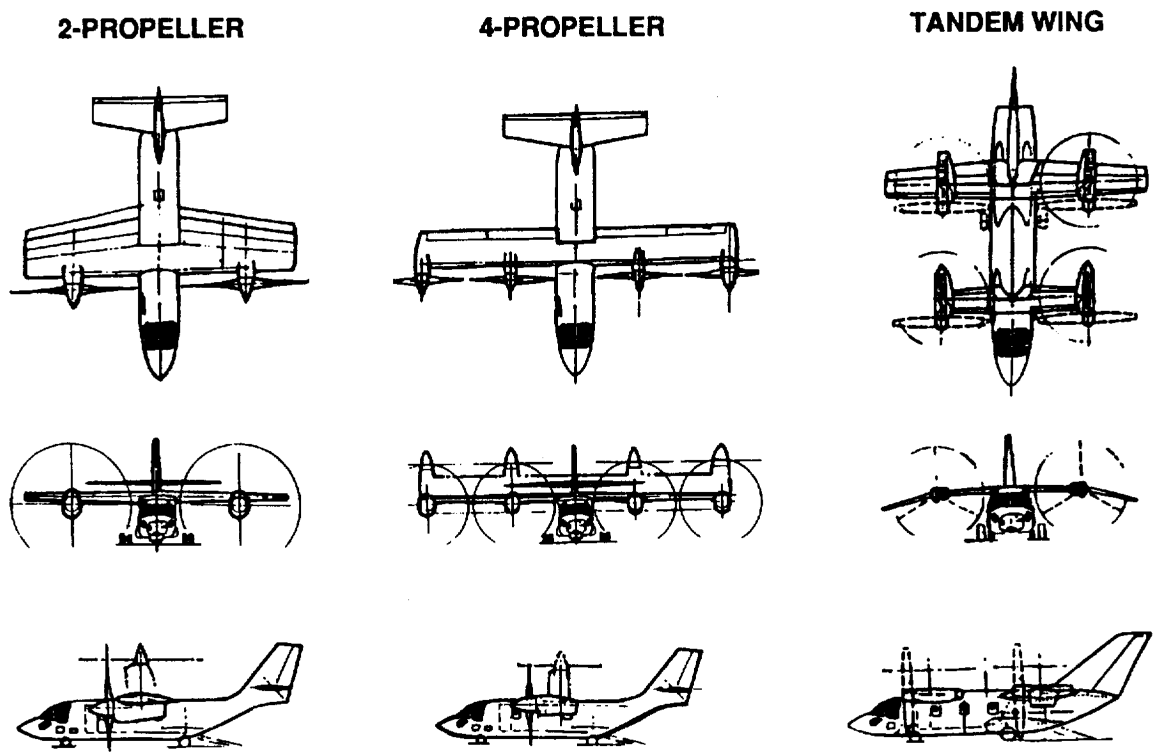

Figure 13. Tiltwing Candidate Configurations

position forward of the leading edge, propeller centerline location below the wing plane, etc. The relationship of chord/diameter ratio and wing loading shows that a maximum wing loading of about 80 psf is probably within the tiltwing state of the art. Actually, maximum wing loading will vary with disc loading as well as C/D ratio and may need to be as low as 60 psf for a 40-psf disc loading. This low wing loading has a major impact on wing weight and drag for a high-speed tiltwing, as will be seen later in the parametric studies.

Since we are considering a minimum high speed of 450 knots, wing sweep also becomes of interest for a tiltwing concept. While a small angle (forward or aft) may be possible within the propeller positioning constraints, large sweep angles appear to be completely unacceptable both from the slipstream immersion geometry requirements as well as ground and overall height limitations. Figure 14 (while rather negative sketches) serves to illustrate the problem for a military transport. Aeroelastic issues for all prop/rotor-wing concepts are self-evident. The hingeless propeller cyclic pitch control (in lieu of a prop/fan at the tail) was never fully demonstrated. In an attack variant, where allaround vision is extremely important, the wing position in hover severely limits its capability. Another problem revealed by the XC-142A tests was the rollup of the ground vortex in a short landing when the speed decreased below about 30 knots, resulting in directional instabilities.

Figure 13 also illustrates the four-propeller/single-wing variant (which is very similar to the XC-142A). Propeller diameter is 20 ft with a disc loading of 40 psf and a wing loading of 76 psf.

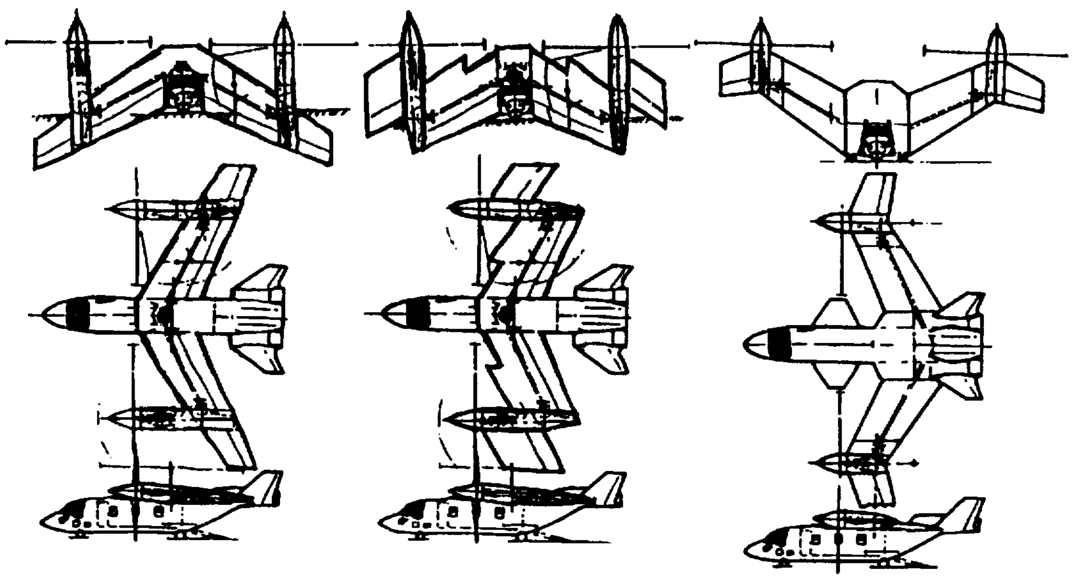

Figure 14. Tiltwing Alternatives

Configuration issues are generally the same as previously shown for the two-propeller variant:

- Drive system complexity
- Rotor and wing aeroelastics
- Shipboard folding complexity
- Wing sweep impractical
- 360° vision in hover
- Recirculation in short landings
- Speed limited to ~ Mach 0.7

Figure 13 illustrates the four-propeller/tandem-wing arrangement with 20-ft-diameter propellers and a 40-psf disc loading. The wing loading shown is 89 psf and is based on work of the German VFW company in the late 60's[13]. Configuration issues of this concept are also generally the same as for the other tiltwing concepts:

- Drive system complexity
- Rotor and wing aeroelastics
- Shipboard folding complexity
- Prop-prop interference
- 360° vision in hover
- Recirculation in short landings
- Speed limited to ~ Mach 0.7

While there have been many application studies for slower speed tiltwings, high-speed (> 450 knots) variants do not appear to offer any advantages for the reasons discussed here.

Non-Lifting Stoppable Rotors

Although ideas for these concepts date back more than 40 years, more definitive efforts began in the mid-60's with blown and unblown rotors - all aimed at simply stopping the rotors (with some minimum folding) and flying with exposed rotor blades in the cruise mode (Figure 15).

Dr. Ian Cheeseman's efforts to develop the "Stopped Pipe-Rotor" were based on blowing air out along spanwise slots in a circular "pipe" blade section. When stopped (with air off) it appeared as a low-drag, simple concept[14]. Hawker-Siddeley followed these ground tests with studies of elliptical sections with more complex folding arrangements. Lockheed initiated stopped-rotor tests of an XH-51 rigid rotor in the mid-60's based on conceptual studies of many arrangements (some included folding and trailing exposed blades)[15]. In Germany, VFW studied stopping a Flettner rotating-cylinder-blade concept (Magnus effect).

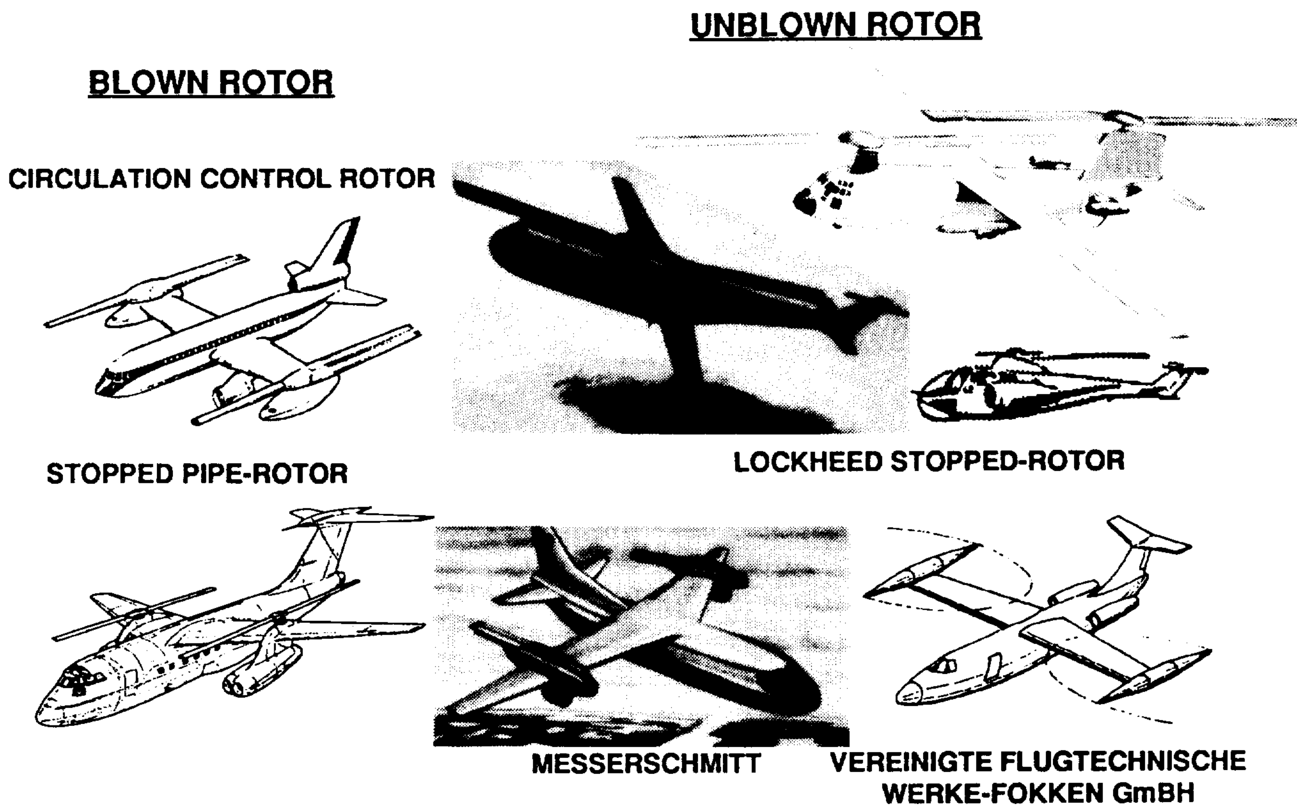

Figure 15. Stopped / Non-Lifting Rotor Background

While these efforts all came to naught, two concepts were envisioned for evaluation in this category. The blown-rotor variant shown in Figure 16 has 49-ft elliptical-section rotors with a 13-psf disc loading. Wing loading is an independent variable and assumed to be 90 psf. Configuration issues of this configuration are:

- Conversion dynamics/time
- Conversion period maneuverability
- Drive/blowing complexity
- Shipboard folding
- High blowing power
- Exposed-blade dynamics
- Poor high-speed area distribution
- Drag limits high speed

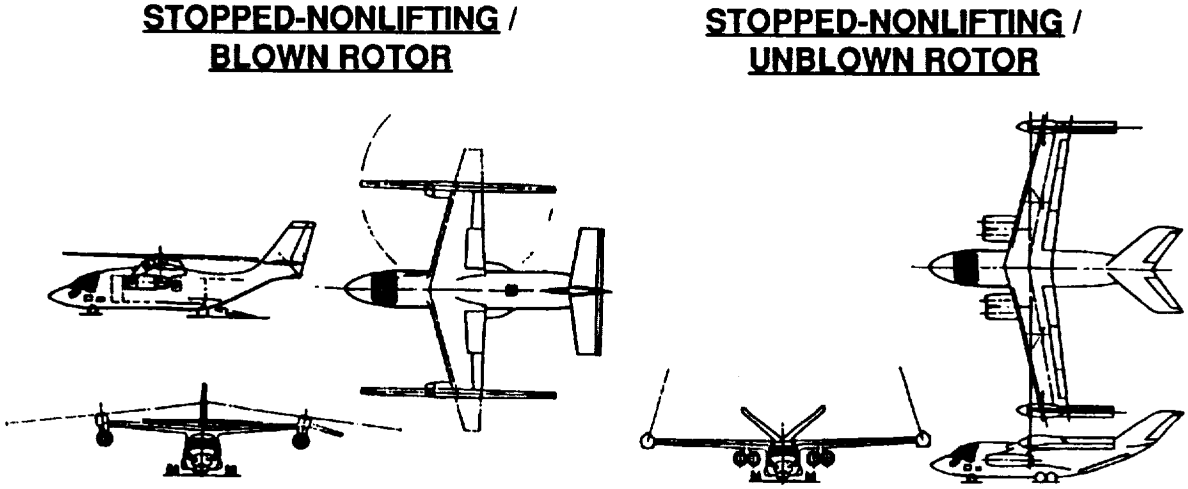

Figure 16. Blown / Unblown-Rotor Candidate Configurations

The unblown-rotor concept (Figure 16) selected is one being studied by the USAF. The rotor is flown as a helicopter, stopped during conversion in a horizontal plane, then tilted forward and down as the blades are folded aft into a trailed position. Rotor diameter is 45-ft for a 16-psf disc loading. Wing area was unnecessarily excessive and is shown as 73 psf. Configuration issues are:

- Conversion dynamics/time
- Conversion period maneuverability
- Exposed-blade dynamics
- Poor high-speed area distribution
- Drag limits high speed

Lifting Stoppable Rotors

Probably the earliest example of these concepts is that of Gerrard Herrick (Figure 17) whose "biplane" aircraft took off and flew as an airplane, but had the capability to unlock the top "wing" and autorotate to a landing. The Herrick HV-2A was demonstrated in the late 30's in northeast Philadelphia[4]. This was followed by disc-wing approaches with retracting blades by Gray Goose Airways and Piasecki Helicopter around 1950.

Hughes Helicopters began disc-wing studies[16] in the 1960's and Lockheed began various wing/ rotor variants in the late 60's, leading to the X-wing program of the 80's[17]. Many variations are possible and have been proposed by Kaman, Ryan, etc.

Wing extension concepts were patented by A. Kisovec[18], followed by variations by Bell and Lockheed. Kisovec's concept featured a single counterbalanced blade on each wing that stopped in a position creating outer panels for a very high-aspect-ratio wing. Others had 2- and 3-bladed rotor approaches to improve the dynamic problems of the single-blade rotor.

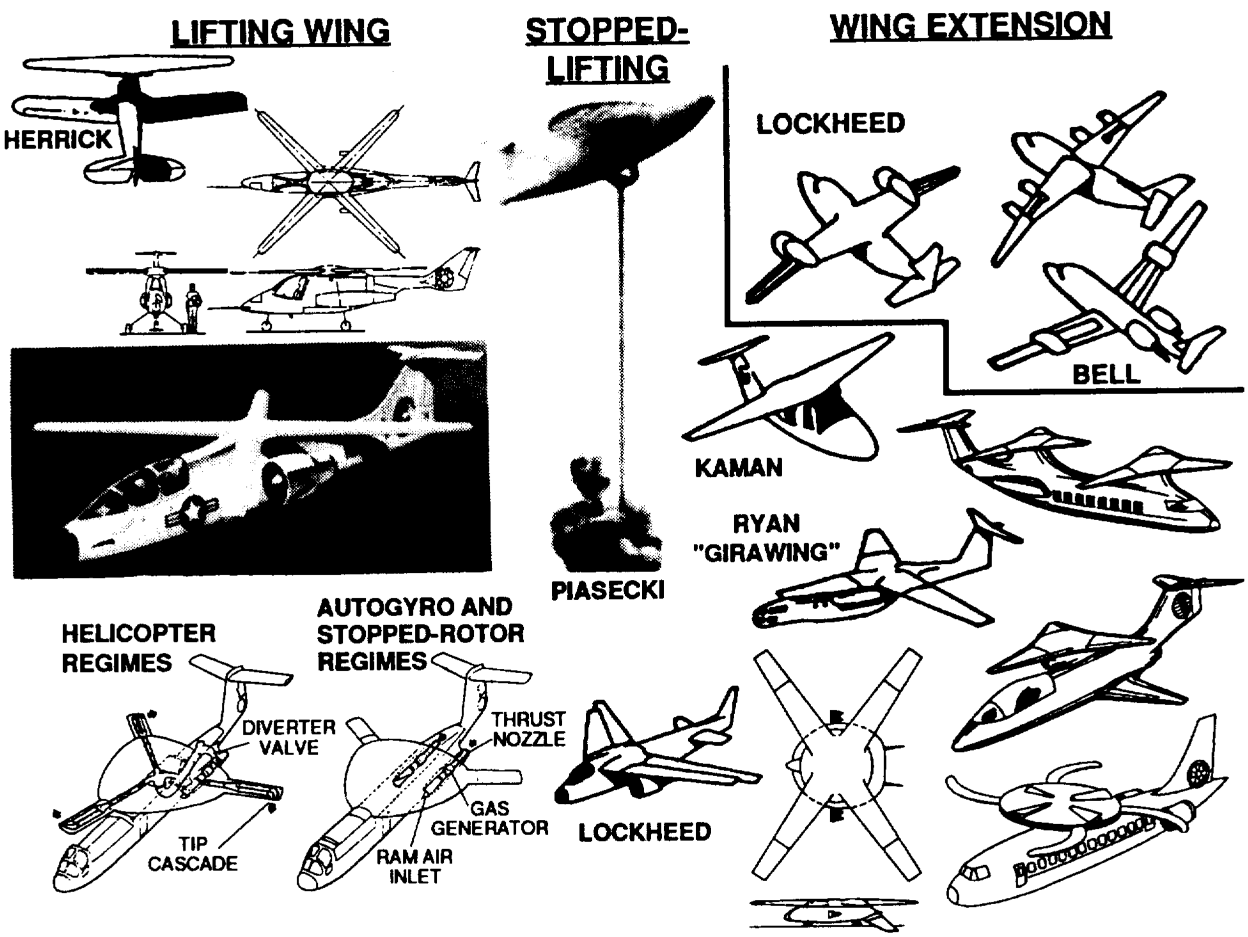

Figure 17. Stopped / Lifting-Rotor Background

The disc-wing concept shown in Figure 18 is sized on the basis of an annular disc loading in order to meet the downwash criteria. This results in a 90-ft-diameter rotor and an 11-psf disc loading. Based on a 55% disc/rotor diameter ratio, the cruise wing loading is 21 psf and is most detrimental to the efficiency of this concept. The excessive wing area results in a low high-speed cruise L/D. Other major configuration issues are:

- Poor hover figure of merit
- Conversion attitude
- Poor cruise L/D
- Upward pilot vision/ejection
- Out of proportion/ship compatibility
- Poor blade/disc interface
- Airplane mode lateral control
- Drag limits high speed
- Conversion dynamics/time
- Conversion roll control
- Conversion period maneuverability

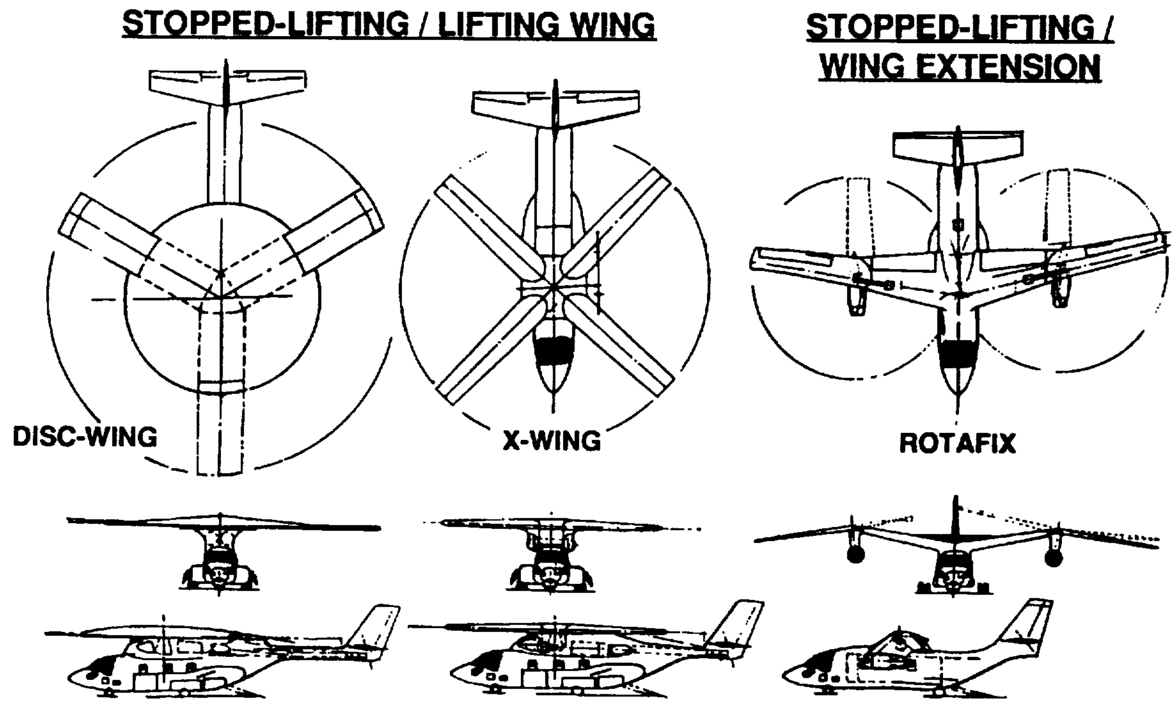

Figure 18. Stopped / Lifting-Wing Candidate Configurations

Conversion attitude variations of this concept are an issue. Although the angles might be held to less than typical jet transport rotation angles, this is poor in comparison to the constant fuselage attitude capability of the tiltrotor concepts.

The X-wing concept shown in Figure 18 has a 70-ft-diameter rotor with 13-psf disc loading. Although early X-wing studies were based on rotor solidities of 0.13, later calculations and wind tunnel data indicated that a solidity of about 0.26 was required in order to convert. Therefore, wing loading for this concept is 56 psf and, aside from the excessive rotor weight, results in a low high-speed cruise L/D (see Figure A-10). Configuration issues of this concept are:

- Conversion dynamics/time
- Conversion effects on solidity
- Conversion period maneuverability
- Complex HHC/blowing system
- Low L/D - low wing loading
- Large pitching moment
- Drag limits high speed

The wing extension stoppable rotor concept seen in Figure 18 (commonly called Rotafix) has a rotor diameter of 49 ft with a 13-psf disc loading.

Although the stopped single-blade "outer panel" increases the wing aspect ratio to 12, the excessive wing area results in a 60-psf wing loading and a poor L/D in high-speed cruise. At lower speeds (around 150 knots), the Rotafix does have a very high L/D. Configuration issues are:

- Conversion dynamics/time
- Conversion period maneuverability
- Poor figure of merit
- Poor L/D (good at 150 knots)
- Complex shipboard folding
- Out of proportion
- Drag limits high speed

Stowed Stoppable Rotors

Perhaps the first technical development of this concept was as one of the three concepts ordered by the USAF in the 1950 convertiplane competition. The XV-2 (Sikorsky S-57) shown in Figure 19 was a single-counterbalanced-blade arrangement where the rotor was stopped and retracted into the fuselage cavity. Although considerable wind tunnel testing was accomplished, the concept was not selected for prototyping (as were the XV-1 and XV-3)[19]. Later, two-blade arrangements were also studied and model-tested. Then in the mid-60's, a Lockheed concept was studied in the Army's Composite Aircraft Program[20].

The horizontally stopped stowed rotor shown in Figure 20 has a 70-ft-diameter rotor with 13-psf disc loading. Since the wing sizing can be independent of the rotor, a wing loading of 107 psf was

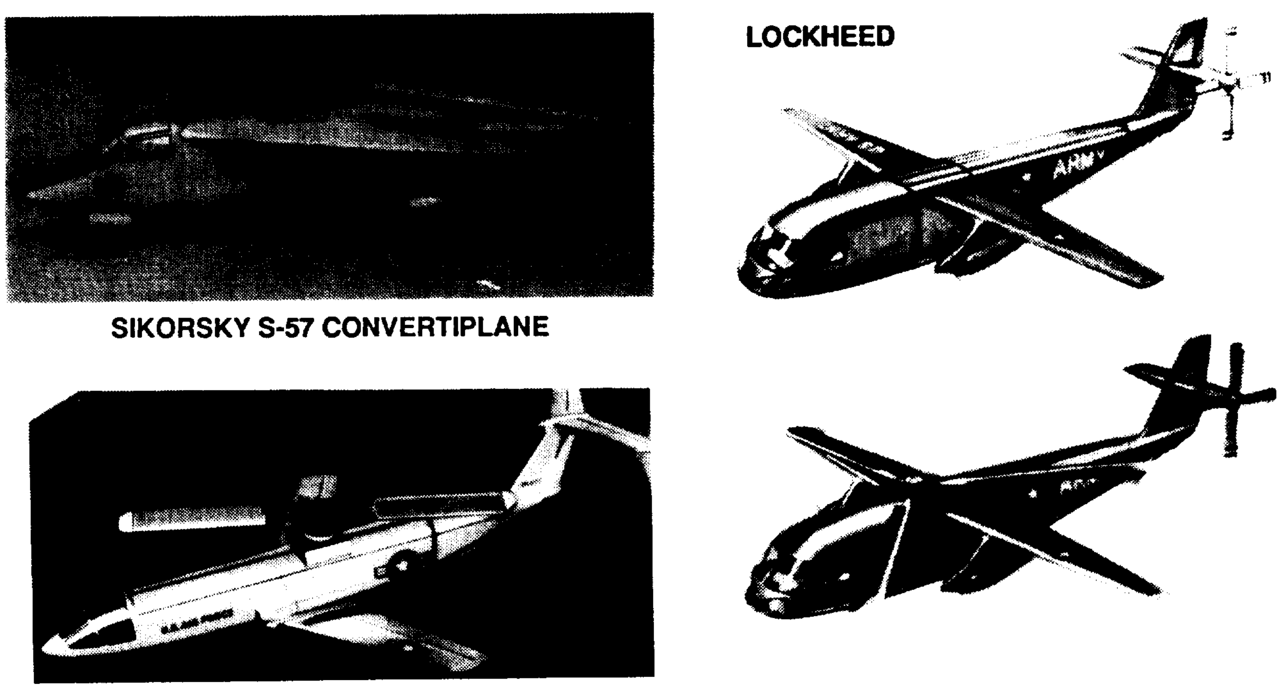

Figure 19. Stopped / Stowed-Rotor Background - Horizontally Stopped

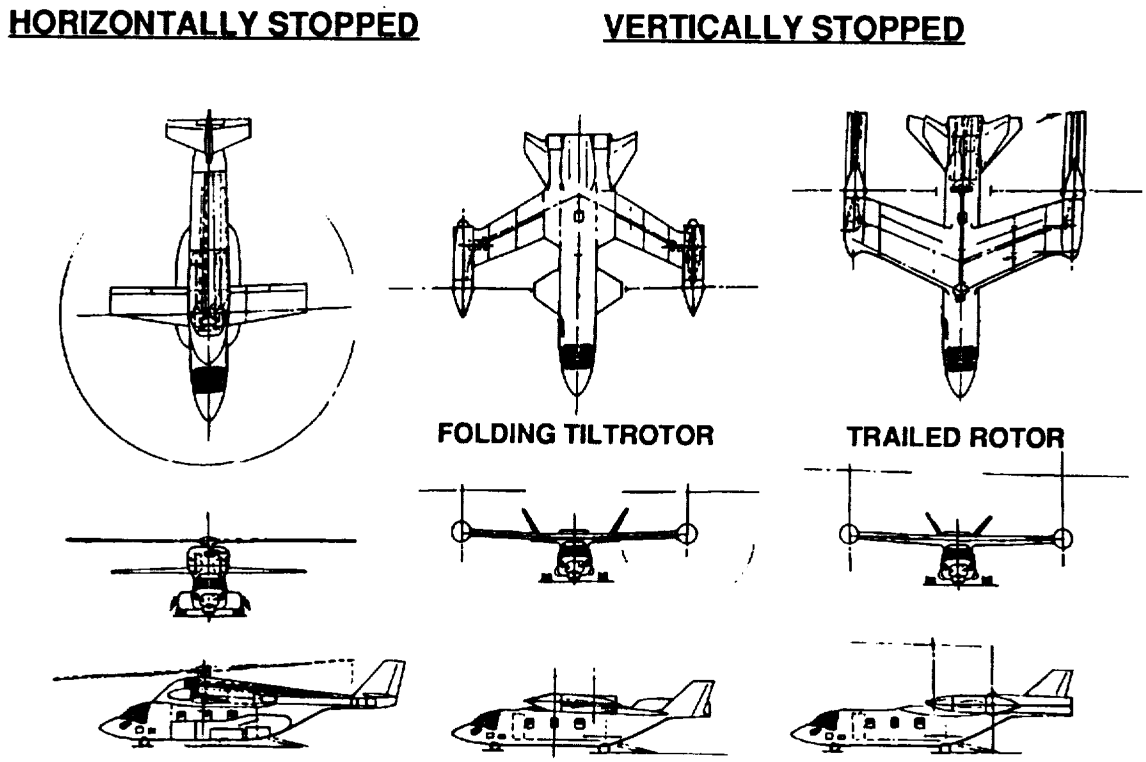

Figure 20. Stopped / Stowed-Rotor Candidate Configurations

shown. The rotor and transmission are mounted on a four-bar linkage for retraction into the fuselage. Configuration issues of this concept are:

- Conversion dynamics/time
- Conversion period maneuverability
- Complex drive retraction
- High-torque clutching
- Highly loaded rotor covers/doors

The vertically stopped stowed rotor concepts are shown in Figure 21. In 1964 both Bell Helicopter and Boeing Helicopters initiated design and wind tunnel studies on the vertically stopped/stowed concepts - Boeing with the folding tiltrotor[21] and Bell with the trailed rotor[22]. After early studies, it became obvious that the trailed-rotor concept did not possess the characteristics desired for a high-speed variant of the tiltrotor. The trailed rotor could not utilize the tilting rotor for good takeoff acceleration and STOL capability nor could it operate in the efficient prop-rotor loiter mode. In those low-speed regimes, it either operated as a helicopter (with about 15° forward tilt capability) or as a compound helicopter using very inefficient jet-thrusting means. Therefore, both Bell and Boeing (and later Sikorsky) continued to explore and further develop folding tiltrotor configurations, leading up to the 1970's series of U.S. Air Force and NASA studies and wind tunnel full-scale rotor and model tests[23,24,25].

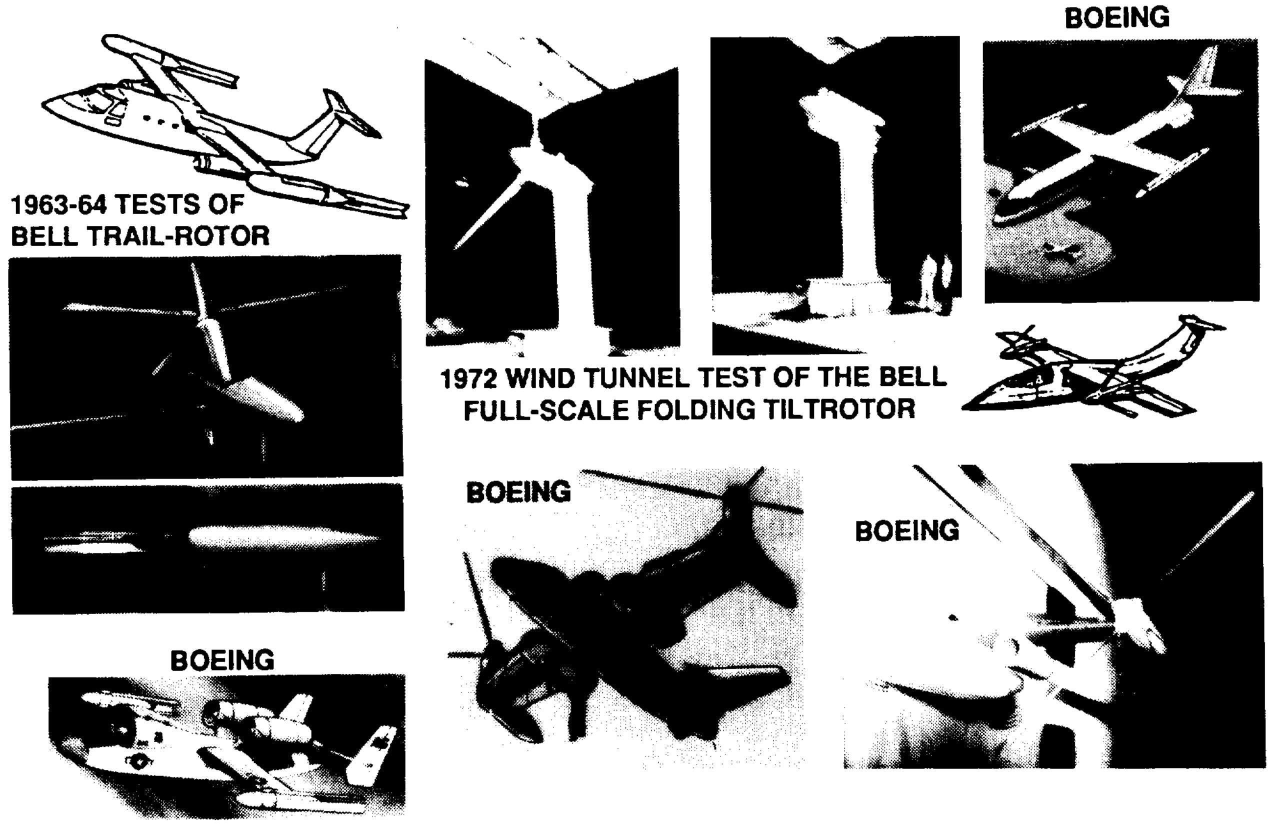

Figure 21. Stopped / Stowed-Rotor Background - Vertically Stopped

The folding tiltrotor is essentially a tiltrotor during hovering and low speed flight. The rotors are used in the upright position for hovering and for vertical takeoff and landing. For transition to forward flight, the rotors are tilted through 90 degrees. When full wing lift is achieved, the forward thrust is transferred to the cruise fans and the rotors are feathered and stopped; the blades are then folded along the wingtip nacelles. The conversion corridor speed is of the order of 120 to 180 knots.

During the 1970's studies and evaluations for the U.S. Air Force, NASA and industry concluded that the folding tiltrotor concept is most attractive because it has the least risk associated with the conversion sequence (stopping and folding the rotors). Since the rotors are stopped and folded in a relatively constant aerodynamic environment, as opposed to the constantly changing one faced by horizontal stopping rotors, it faces fewer aerodynamic and dynamic design problems. The folding tiltrotor offers the greatest operational flexibility. It has good vertical takeoff capability and it can tilt its rotors for acceleration, good STOL, and climb-out capability. In addition, by using its rotors as propellers, it has the potential of operating efficiently in three distinct flight regimes.

Following the Air Force and NASA wind tunnel testing in the early seventies, conclusions were that the folding tiltrotor concept showed much promise with no fundamental problems encountered! The program was, however, delayed until after the basic tiltrotor (XV-15) had been demonstrated. In the interim, some studies of the X-Wing stopped rotor concept held out a high potential, if its problems could be overcome. So far, that concept has not been proven and (probably) has been discarded.

Figure 20 also illustrates one approach to a high-speed folding tiltrotor with a short-coupled canard arrangement. The rotor diameter is 33 ft with a 29-psf disc loading. Wing loading is 89 psf. Configuration issues are:

- Swept-forward wing/canard
- Wing aeroelastics
- Speed limited to ~ Mach 1.5 (for attack variants)

Reference 6 discusses the tests performed under USAF and NASA contracts. The results of all this effort showed that there are no significant technical obstacles to the development of a folding-tiltrotor aircraft beyond those normally encountered in any new aircraft development.

Over the years, mission applications have been explored starting with the 1965 NASA Shorthaul Transport studies, the USAF Advanced Rescue and Assault Transport Missions, etc. Recent design studies have explored STOVL configurations.

The trailed-rotor variant of the vertically stopped stowed rotor is also illustrated in Figure 20. Rotor diameter is 38 ft for a disc loading of 22 psf. Although drawn for a 25° aft-swept wing, the concept is probably only acceptable for small sweep angles due to the relationship of the tilt axis (at the CG) and the proper location on the MAC. If placed where stability requires, a very long overhang results as shown with severe weight, balance, and operational problems. Other configuration issues are:

- Aft-swept wing aeroelastics
- Exposed-blade dynamics
- Tilt axis/CG/MAC/overhang
- Wing wake effects on folding
- Autogyro mode
- Inefficient loiter mode
- Conversion time
- Poor STO capability
- Sweep/drag limit high speed

Variable-Diameter Rotors

Figure 22 illustrates some of the background for the three major variants of the Variable-diameter-rotor concept. In the mid-40's, Vittorio Isacco built a 10-to-1 diameter-ratio telescoping rotor. [26] Apparently it was ground-tested but never flown. This was followed in the early 50's by the Piasecki Helicopter/Vertol Aircraft telescoping rotors.[27] Although a rotor was built for testing, none was accomplished. Later, Sikorsky conducted wind tunnel testing of its TRAC telescoping rotor. In the 1950's, Hiller built a full-scale wind tunnel model of the foldable concept shown; again, never tested. In the reelable rotor, many variations are possible. The Barish/Vidya/Martin concepts of Figure 22 were seriously investigated in the late 50's. The Martin Company built a test rotor[28], as did Kellett Aircraft[29], and a fabric rotor was tested on a home-made helicopter by Edward Glatfelter.

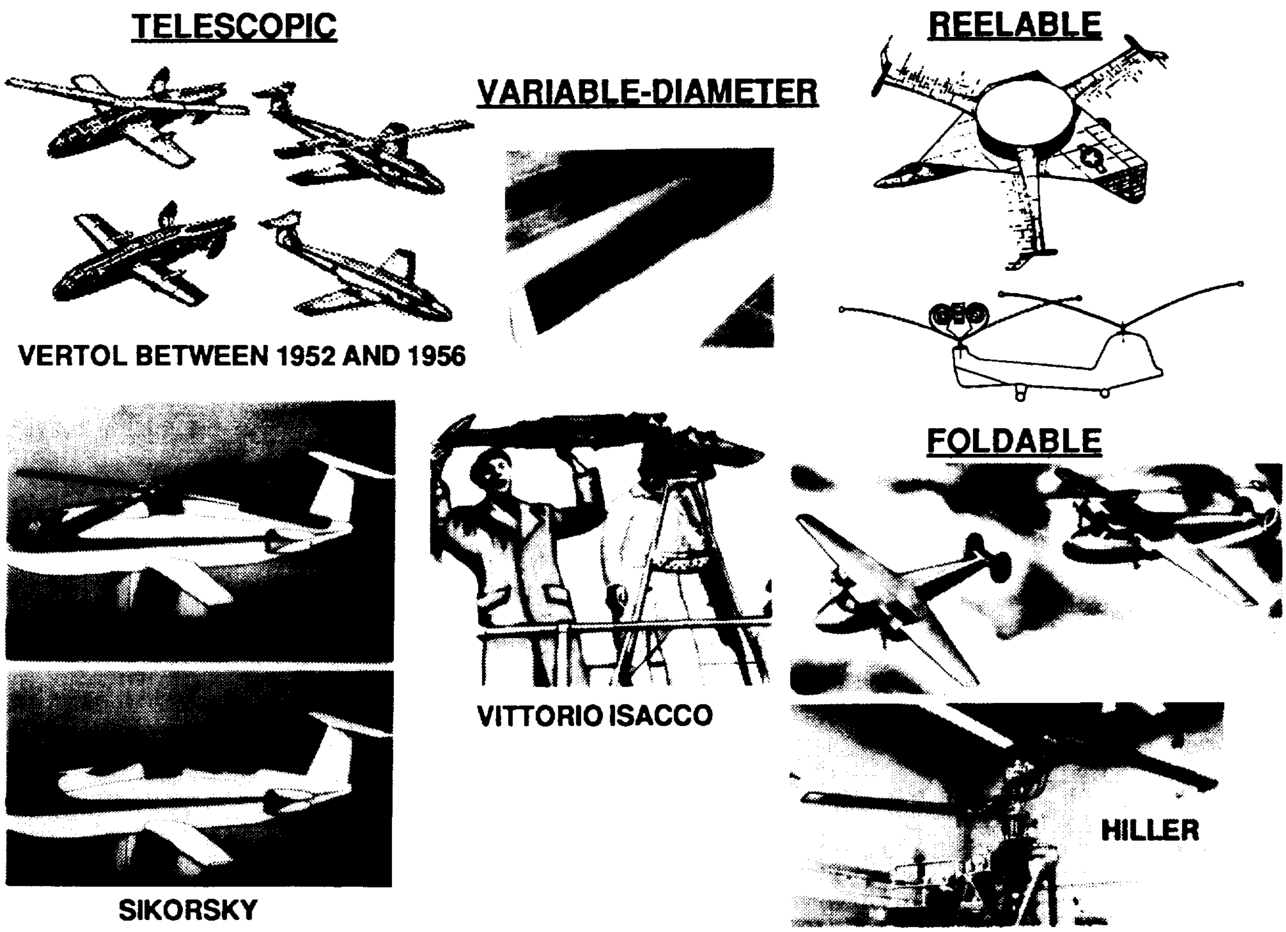

Figure 22. Variable-Diameter Background - Horizontal Rotors

The telescoping-rotor variant (Figure 23) has a 70-ft-diameter rotor with 13-psf disc loading telescoping to 60% diameter for stopping and stowing. Although the reduction in diameter eases the stowing volume required, the fuselage (as shown) has an excessive cabin length (10 ft). Wing loading can be optimized to suit conversion/cruise requirements and is shown as 107 psf. Configuration issues are:

- Conversion dynamics/time
- Conversion period maneuverability
- Complex telescoping/folding
- High-torque clutching
- Highly loaded rotor covers/doors
- Out-of-proportion/excessive fuselage
- Drag limits high speed

The reelable rotor variant (Figure 23) is similar in layout with a 70-ft-diameter rotor at 13-psf disc loading. In order to accommodate the five reels for blade retraction, a large-diameter "tub" is buried in the rotor hub fairing (and spins with the rotor). Several blade concepts (deflatable, coiled sheet, segmented) were analyzed for the tub and disc sizing shown. Configuration issues are:

- Conversion dynamics/time
- Conversion period maneuverability
- Complex reel drive system
- Rotor figure of merit/lift capability
- Blade design/materials/etc.
- Drag limits high speed

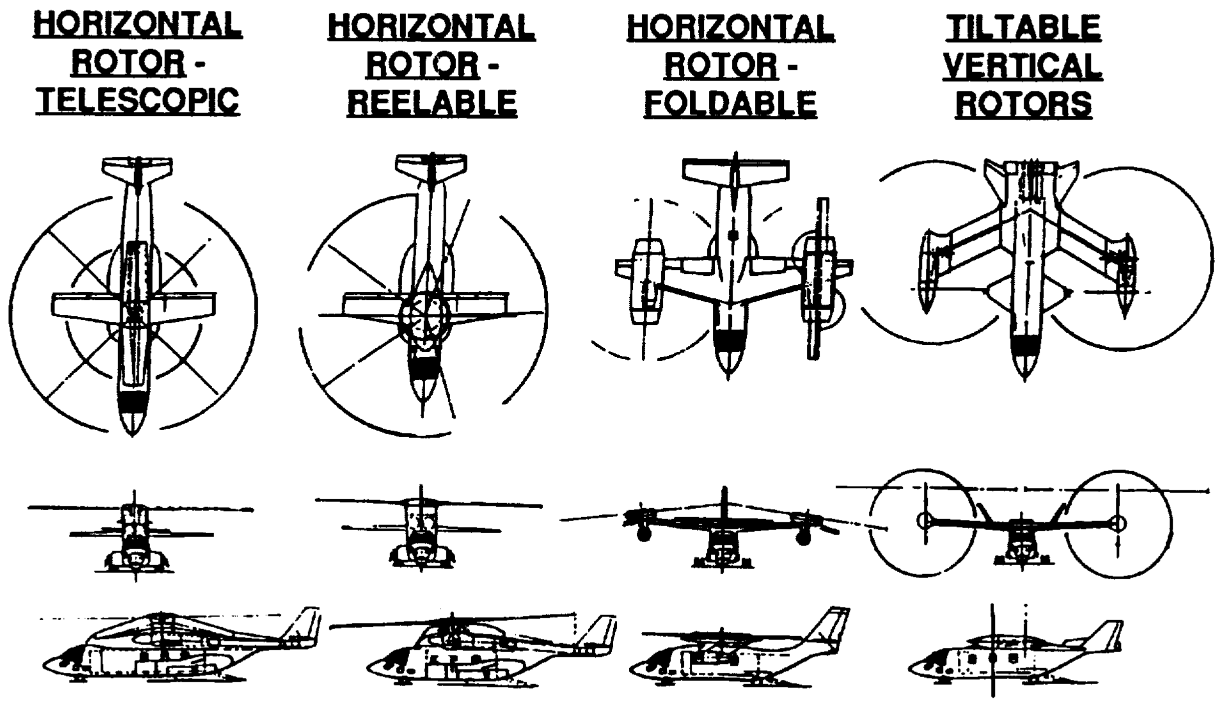

Figure 23. Variable-Diameter Rotor Concepts

The foldable-rotor variant (Figure 23) has 49-ft-diameter rotors with 13-psf disc loading. Blade folding hinges are at about 33% span (similar to the Hiller 1950's concept) and the blades fold to lie parallel to each other. Large segmented doors roll up to cover the folded blades and hub, providing a relatively low-drag package. Configuration issues are:

- Conversion dynamics/time
- Conversion period maneuverability
- Hig- torque clutching
- Highly loaded rotor covers/doors
- High download
- Sweep/drag limits high speed

Variable-Diameter Tiltable Rotors

In the 1960's, Bell and Boeing considered the variable-diameter tiltrotor as appropriate for a high-speed tiltrotor to alleviate the severe penalty of rotor tip speed reduction.[30] Bell brought Arthur Young back to active status and a test rotor was developed and demonstrated in ground tests (Figure 24).[31,32] Later, Sikorsky envisioned a tiltrotor variant of their telescoping rotor (TRAC) concept for compound helicopters.[33]

Figure 23 illustrates a variable-diameter (telescoping) rotor applied to the canard tiltrotor discussed earlier. Although listed and evaluated separately in this overview, the variable-diameter rotor itself is considered to be another option for the advanced rotor system of a very high-speed

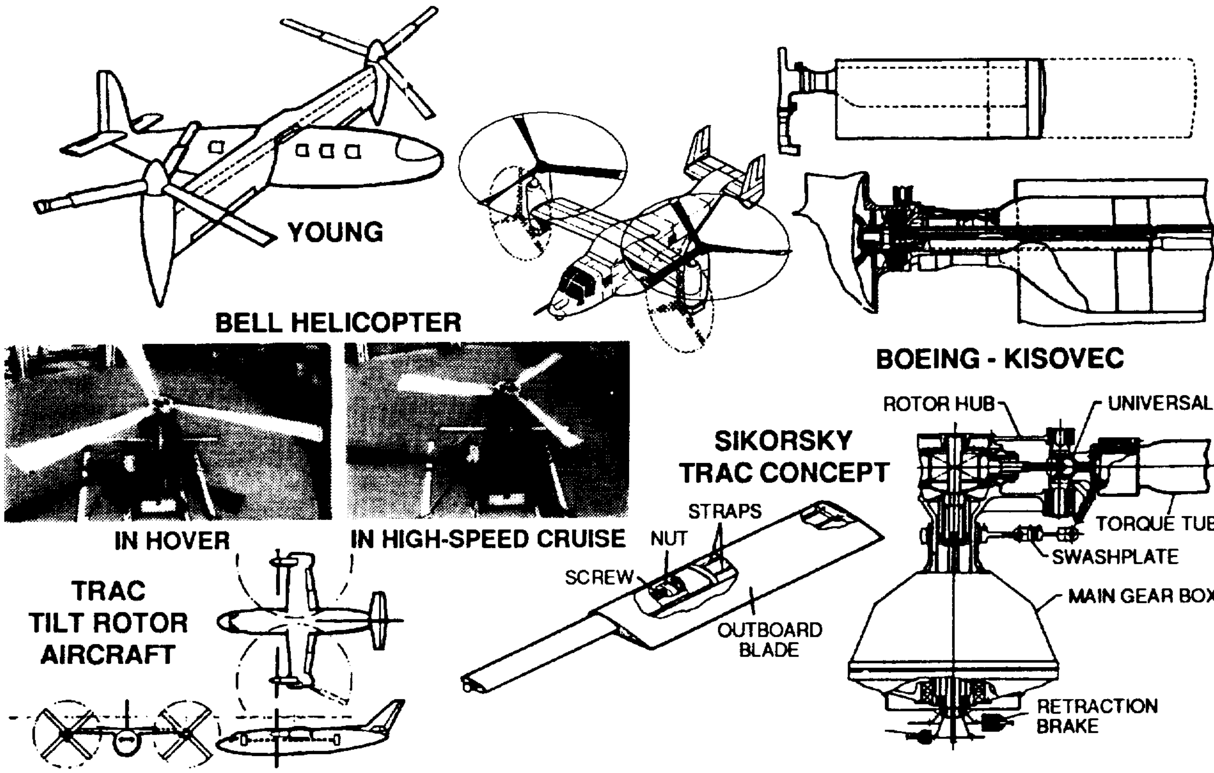

Figure 24. Variable-Diameter Background - Tiltable Vertical Rotors

tiltrotor. The aircraft shown has the full 40% diameter reduction, from a 55-ft-diameter in hover to 33 ft in cruise. Hover disc loading was 11 psf and a wing loading of 87 psf is shown. Configuration issues are:

- Swept-forward wing/canard
- Rotor and wing aeroelastics
- Complex blade retraction/drive
- Shipboard folding complexity
- Speed limited to ~ Mach 0.8

Body-Mounted Rotors

Body-mounted rotors have had an attraction for many inventors over the years, starting possibly with the "Flying Saucer" stories of the early 50's leading to Avro Aircraft's version for the USAF,[34] which then led to the "ground-effect" Avrocar saucer for the U.S. Army.[35] Other entrepreneurs such as Rotavion, Sadleir, and Moller have proposed single and multiple variants as seen in Figure 25.[36,37]

A single-rotor example was selected for evaluation as shown in Figure 26. A 42-ft-diameter rotor is buried in the delta wing. Actually, it is a ducted rotor/fan, thereby meeting the downwash constraints. Probably the most detrimental characteristic of these concepts is the excessive wing area. The aircraft depicted has a 3200-sq-ft wing area in cruise flight. Although drawn for the

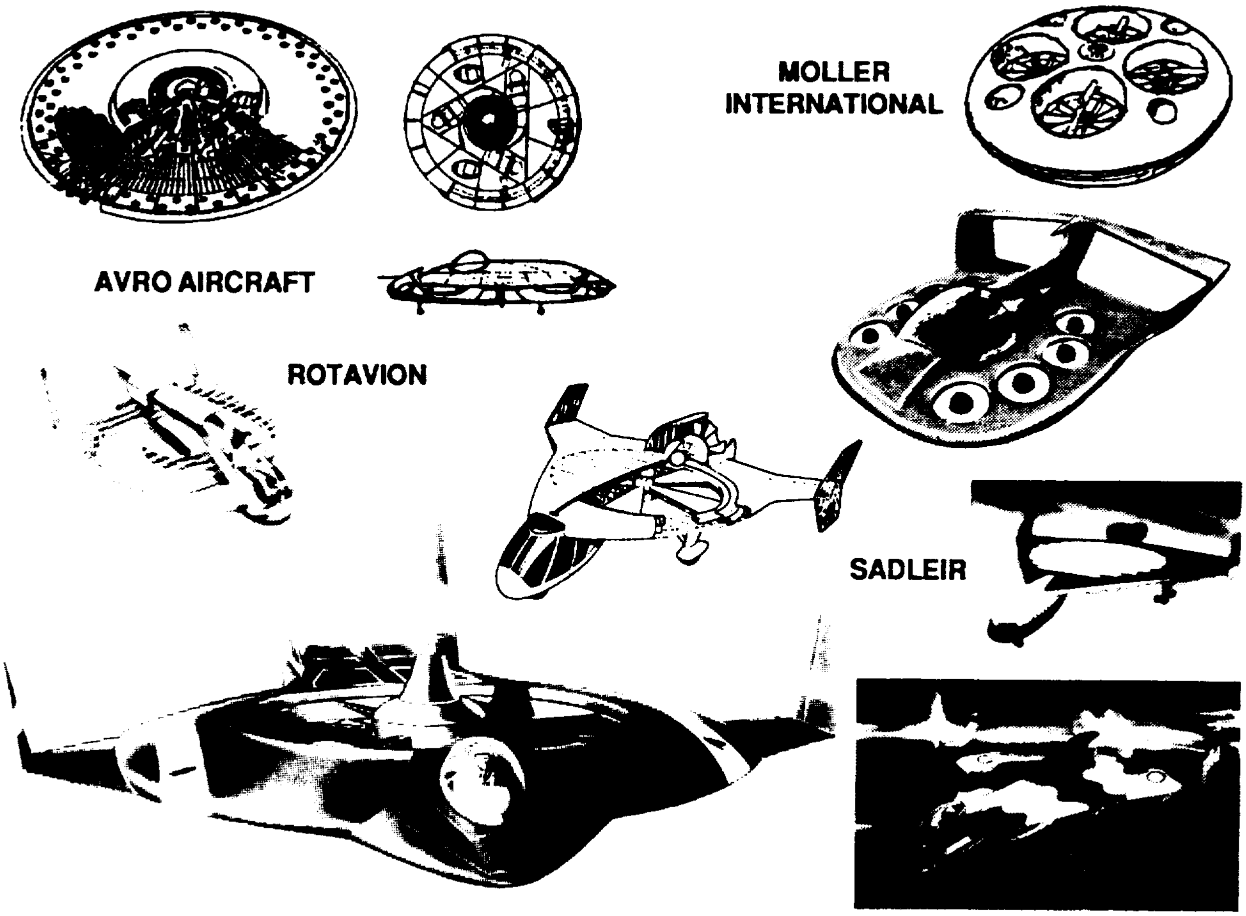

Figure 25. Body-Mounted Rotor Background

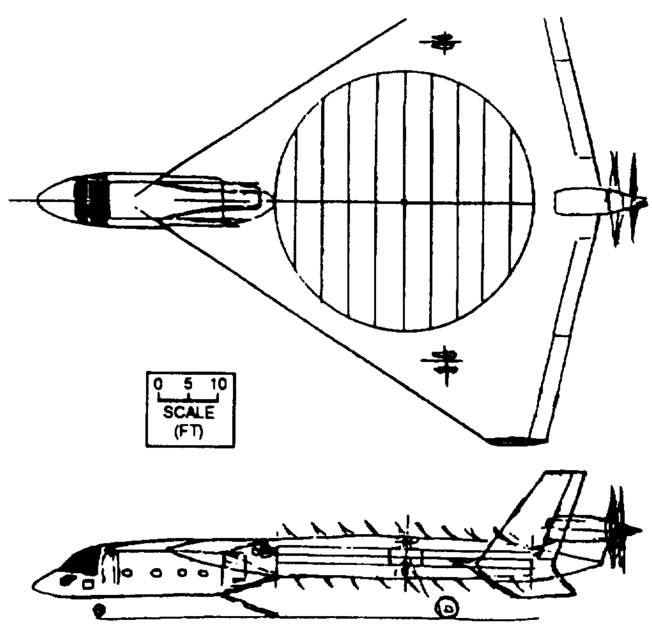

Figure 26. Body-Mounted Rotor Candidate Configuration

hypothetical 50,000-lb design point, the large areas of the wing, upper closures, and bottom vane/ closures would seriously escalate the empty weight. Configuration issues are:

- Grossly out of proportion
- Low L/D
- Extremely low wing loading
- Balance
- Shipboard compatibility
- Drag limits high speed

Candidate High-Speed Rotorcraft Selection

Figure 27 summarizes the 20 concepts identified,evaluated, and down-selected to five preliminary designs and leading to the selection of two concepts for the Task II assessment.

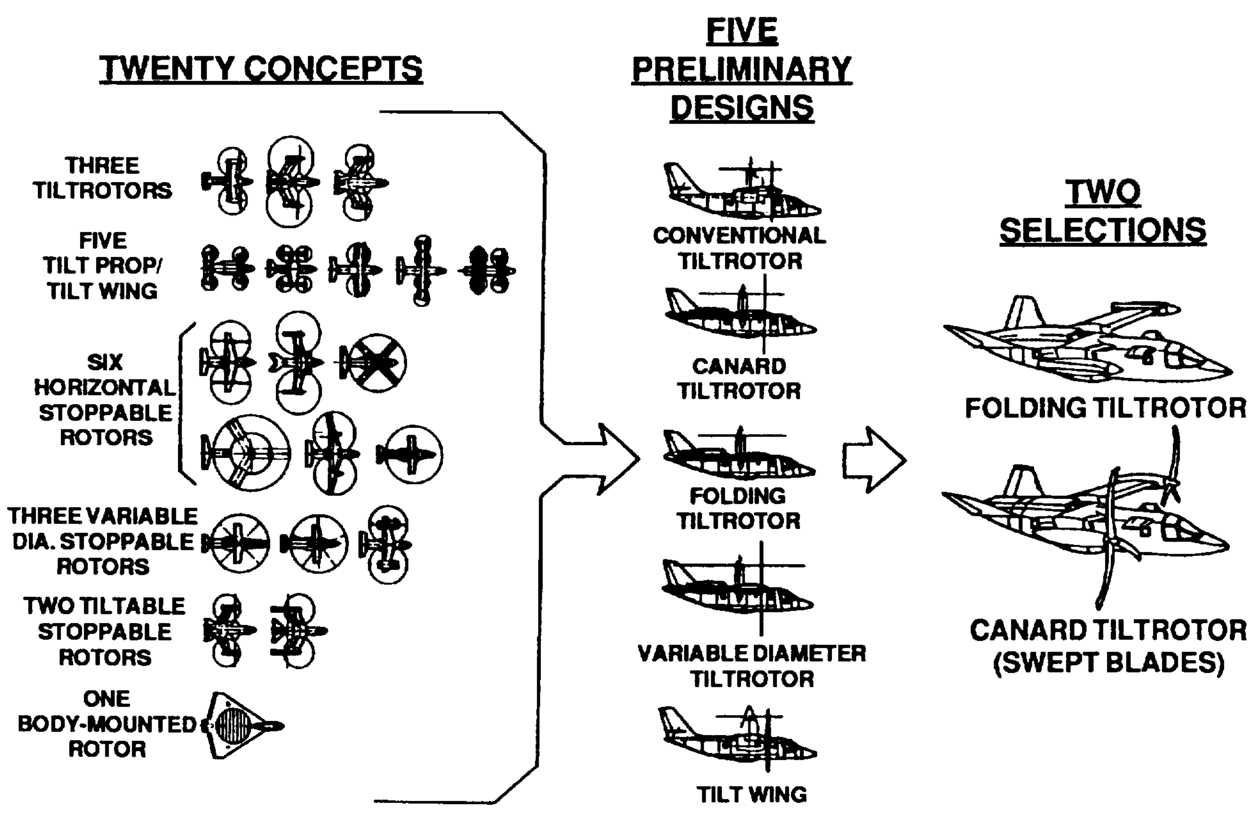

Figure 27. Candidate High-Speed Rotorcraft Selection

Downselect to Five Candidates

Measures of effectiveness (MoE) and measures of performance (MoP) were developed and are reported in Appendix A, Table A-3. A list of key discriminators was developed mostly from the MoE's and MoP's to address the important features and differences between the concepts. Key discriminators, their definition, and their importance are as follows:

Empty Weight-to-Gross Weight Ratio

Aircraft payload fractions depend directly on a concept's EW/GW ratio. Generally speaking, larger ratios imply more components such as extra wings or rotors or engines; or some components may be heavier than normal, reflecting higher drive system ratings, higher wing stiffness requirements, or a more complex control system. Higher EW/GW ratios leave a lower percentage of the GW for useful load (payload + fuel) and usually reflect a less efficient rotorcraft. Thus, lower EW/GW ratios are desirable.

Hover Disc Loading

Disc loading has a prime influence on both downwash velocity and hover fuel flow. Low downwash was a stated objective of this study and is considered here through the disc-loading term.

Hover Maneuverability

Some rotorcraft concepts have less hover maneuverability than others. Low-disc-loading rotors with full cyclic control are the best. High-disc-loading concepts with a relatively high inertia about either control axis may tend to be sluggish in their hover maneuverability.

Conversion Time

The time to convert is a measure of how long the vehicle is in the process of changing over to a cruise mode. (It does not include time involved in normal transition from hover to helicopter-type forward flight.) This is a reflection of how many different things have to occur in the conversion process. In some concepts this is a drawn-out process, during which the vehicle and crew are more vulnerable and less able to carry out other mission duties. Conversion should be a smooth, continuous process, and reversible from any point. Thus, conversion time can be very important to survivability.

Conversion Maneuverability

Many of the high-speed rotorcraft concepts are operating near operational boundaries during conversion. Indeed, many must have rotors and/or wing designs compromised to satisfy the conversion lift and trim requirements. Thus maneuverability is often minimal here and so it is of prime importance, whether in a military attack role or for evasive maneuvering in a transport role.

Conversion Fold / Stow Penalty

All the high-speed rotorcraft concepts go through some mechanical change between hover mode and cruise mode, generally either tilting, stopping, folding, or some combination . The mechanical complexity and volumetric requirements for this process are considered together here as an indicator of the conversion penalty.

Cruise Speed Potential

The study objective and mission profiles specify a 450-knot speed requirement. Some of the concepts considered can barely meet this, while others may have higher speed potential. This discriminator allows recognition of that potential.

Cruise Flat-Plate Area

Cruise power required at 450 knots is primarily determined by flat-plate area and compressibility drag. A high flat-plate area results in high cruise drag and high installed-power requirements, leading to larger, heavier airframes. This discriminator allows elimination of concepts which inherently result in high flat-plate areas. This may be driven by an oversized wing or wing-rotor blade combination, or an abnormally large fuselage to house folded/stowed rotor blades, or rotor blades and shafts left exposed in the airstream during cruise flight.

Cruise Wing Loading

Does the concept allow the wing to be sized for the cruise mode or must it be significantly compromised to satisfy another flight regime (usually conversion)?

Cruise Lift / Drag Ratio

The concept's cruise L/D depends on many geometric factors such as flat-plate area, interference effects, compressibility, and cruise altitude. Its importance lies in its heavy contribution to the cruise fuel requirement and range factor and hence the impact on overall vehicle gross weight.

Propulsion Limits

Several discriminators are listed here which are based on past experience with configurations which required more than two rotors, more than two engines, or more than two types of engine (both a turboshaft and a turbofan). These have proven to be heavier and more complex arrangements for rotorcraft (requiring more interconnect shafting) and are avoided in this study by use of this discriminator .

Propulsion Efficiency

Prop-rotor cruise efficiency drops significantly past the 400- to 450-knot speed range. However, convertible engines and single-rotation propellers retain high efficiency to much higher speeds. While this discriminator did not eliminate any concept, its use does allow the higher efficiency systems to be pointed out.

Concept Layout / Appearance

This discriminator considers items such as rational proportions of wing area, tail areas and disc area and whether the concept lends itself to folding for shipboard compatibility and for air transportability .

Aeroelastic Limits and Vibrations

Some rotorcraft concepts are known to have speed-limiting aeroelastic boundaries. Other concepts have substantial vibration problems during the slowing and stopping process of the conversion mode. This discriminator allows for qualitative grading of the severity of this class of problem. Low scores generally indicate that the problem has proven to be extremely difficult to treat, or that it is a significant problem but very little is known about it.

Complexity

The drive system and number of gearboxes required were used as one guide to the concept complexity. Other factors considered were the relative difficulty of the slowing-stopping-folding schemes, extra sets of louvers or doors to cover stopped rotors, and perceived extra functions required of the flight control system for the hover-conversion-forward flight modes.

Table 5 summarizes the evaluation of the 20 candidate rotorcraft concepts using those key discriminators. The purpose of the chart is to establish a pass/fail grade through which to eliminate the least desirable concepts and to select the most desirable concepts. Five concepts received passing grades. These were selected for further study:

(1) A tiltrotor of conventional layout (similar to a V-22)

(2) A canard tiltrotor with forward-swept wing and advanced rotor geometry

(3) A canard tiltrotor with forward-swept wing and variable-diameter rotor

(4) A folding tiltrotor with forward-swept wing and canard

(5) A tiltwing with 2 prop-rotors

Table 5. Comparative Evaluation of 20 Candidate Rotorcraft Concepts

KEY DISCRIMINATORS	TILTROTOR		TILTWING			TILTPROP		STOPPED ROTORS					STOPPED AND STOWED ROTORS			VARIABLE DIAMETER CONCEPTS				BODY MOUNTED ROTORS
								NON-LIFTING		LIFTING			HORIZ. STOPPED	AXIALLY STOPPED (TILTROTORS)		HORIZONTALLY STOPPED			AXIAL	
	CONV.	CANARD	1 WING 2 PROP	1 WING 4 PROP	2 WING 4 PROP	PUSHER TRACTOR	TANDEM 4 PROP	BLOWN	UN-BLOWN	DISC WING	X-WING	ROTA-FIX	SINGLE ROTOR	FTR CANARD	TRAIL ROTOR	TELE-SCOPING	REEL-ABLE	FOLD-ABLE	TILT-ROTOR	
EMPTY WEIGHT / GROSS WEIGHT	☆	☆								D	F									D
HOVER: DISC LOADING, MANEUVERABILITY	☆	☆			☆	☆	☆	☆	☆ ☆		D	D	☆ ☆ ☆	☆	☆	☆ ☆ ☆	☆ ☆ ☆	☆ ☆ ☆	☆ ☆ ☆	D
CONVERSION: <30 SECOND EXPOSURE, MANEUVERABILITY, FOLD/STOW PENALTY	☆ ☆ ☆	☆ ☆ ☆	☆ ☆	☆ ☆	☆	☆ D D	☆ D	F F	F F	D F	F F	F F	D F D	☆ ☆ ☆	D D	F F D	F D	F F D		
CRUISE: SPEED POTENTIAL, FE, WING LOADING, L/D	☆ ☆	☆	☆	D ☆	D ☆	D D	D D	D ☆	☆ D D	☆ F F D	☆ D D	D D D	☆		D D				☆	F F F D
PROPULSION: 2 ROTOR LIMIT, 2 ENGINE LIMIT, SINGLE ENGINE TYPE, EFFICIENCY				F	F	F	F	☆	☆	☆	☆	☆	☆	☆	☆	☆	☆	☆		☆
LAYOUT/APPEARANCE: PRACTICAL AND SENSIBLE	☆	☆	☆			D	D		F			D		☆		D	F	D		D
AEROELASTIC LIMITS/VIBRATION			☆					D		D	D	F	D				D			
COMPLEXITY	☆	☆	☆	D	D	F	F	D	D		F	D	F			F	F	F		
SELECTION	✓	✓	✓											✓					✓	

☆ - EXCELLENT CHARACTERISTICS D - POOR CHARACTERISTICS F - UNACCEPTABLE CHARACTERISTICS

Design Requirements

Mission Profiles

The NASA-defined military transport mission (6,000-lb payload) was chosen as the basis for evaluating the five selected high-speed rotorcraft. Each concept was sized for this mission profile, described in Table 3, with a 450 knot cruise speed. The weight of airframe equipment, mission equipment, armor, mission kit, and crew was specified to be 6,370 lb in the NASA military transport. The NASA-defined 30-passenger civil mission (6,000-lb payload) was subsequently chosen for one of the two final rotorcraft concepts. This mission profile is also described in Table 3. The weight of fixed equipment, avionics, and fixed useful load was specified to be 5,425 lb for the NASA 30-passenger civil mission. The civil mission has a shorter range and a lighter equipment package than the military transport, leading one to expect a lighter and somewhat smaller aircraft to perform the civil mission.

Military Transport Rotorcraft

All five rotorcraft selected were designed to structural design criteria appropriate to the military transport mission. The structural design gross weight (SDGW) was defined as the primary mission gross weight (PMGW) less 40% of the mission fuel. The airplane-mode limit load factor (LLF) was adopted from the V-22 specification to be 4.0 g's at the SDGW. The rotorcraft were designed to a 2.0-g VTO jump takeoff which sizes the wingroot strength for tiltrotor concepts. The helo-mode airframe LLF criteria were taken from ADS-29 for a class IV transport. A low-speed maneuver requirement of 1.7 g's at 60 knots airspeed was also imposed. This required higher tiltrotor solidity at higher wing loadings. These are summarized below:

Airplane LLF:	**4.0 g's at SDGW**
Jump takeoff LLF:	**2.0 g's**
Helo-mode LLF:	**3.0 g's/-0.5 g's**
Low-speed maneuver:	**1.7 g's at 60 knots**
Hover yaw acceleration:	**20 deg/sec^2**

These are rational choices for the military transport mission.

Civil Passenger Rotorcraft

Future, civil high-speed rotorcraft will probably be certified under the FAA's new Draft Interim Airworthiness Criteria for Powered-Lift Transport Category Aircraft. For this study the following criteria were used:

Airplane LLF:	**2.6 g's/-1.0 g's at DGW**
Jump takeoff LLF:	**2.0 g's**
Hover yaw acceleration:	**15 deg/sec^2**
Low-speed maneuver:	**45 deg bank turn**

Mission Analysis

A number of military transport missions were examined to determine the relative need for high speed and good VTO capability. Of those examined the most frequent missions were priority resupply of components, special operations forces (SOF) in wartime, medevac, and combat search and rescue (CSAR). Considering frequency to be an indication of relative need and military mission importance, these four missions were focused on.

VTO Requirement - The SOF, medevac, and CSAR missions all require midpoint hover capability to perform their missions without the advantage of any prepared landing site or field. The priority resupply mission must deliver its cargo as near as possible to the user. In many cases the nearest runway may be destroyed or damaged beyond use, making VTO capability very important to a timely delivery.

Speed Requirement - The SOF missions must employ nighttime operations wherever possible to reduce detection, thereby enhancing mission success. A nighttime SOF operation over a 1200-nmi radius requires cruise speeds of about 350 knots, allowing 1 hour at the mission destination. Medevac statistics show that the trauma mortality rate can be reduced up to 20% if 1 hour of elapsed time can be saved in getting wounded to a rear area hospital. CSAR statistics indicate that the capture rate of downed aircrew can be reduced by 36% if the land rescue time can be cut to 10 minutes. The priority resupply mission is to deliver critical depot components in a timely manner to win the battle. All of these transport category missions can use the advantage of speed to directly and quantitatively improve their mission performance.

Figure 28 shows a scattergram of several mission payload and radius requirements. The NASA defined military missions of 6000-lb and 3000-lb payload are also spotted on the figure. The dashed payload-radius line passing through the NASA mission requirement is currently only an approximation of the long-range potential of a high-speed rotorcraft. It does, however, indicate that a vehicle designed to the NASA 6000-lb military transport mission could also handle most of the other mission requirements reviewed by Boeing.

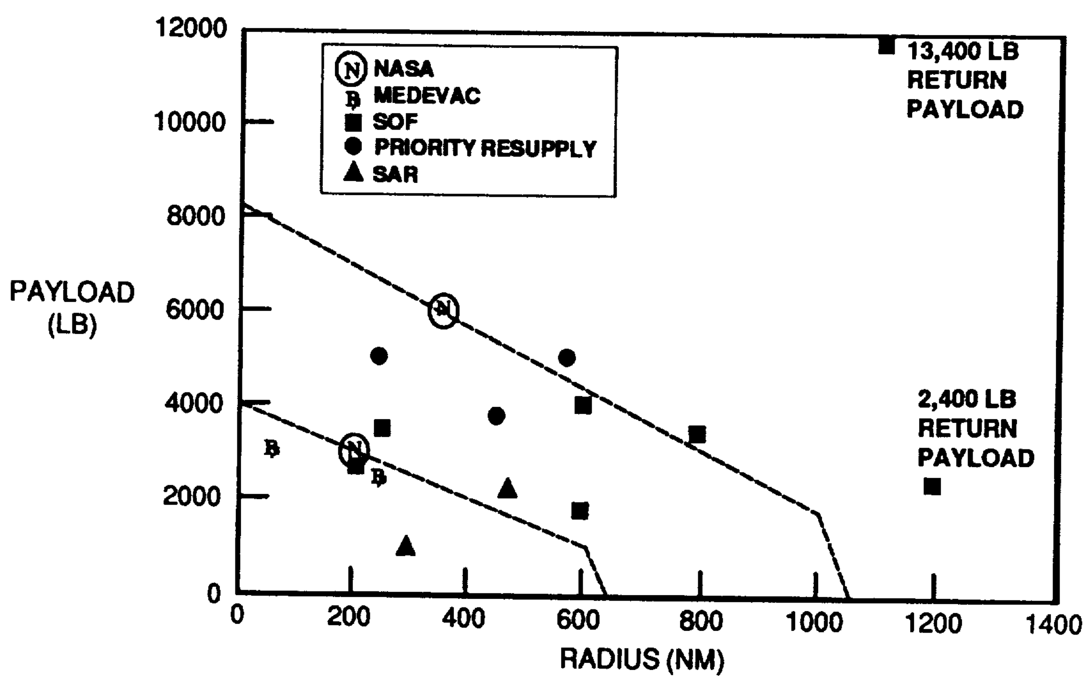

Figure 28. Composite Payload-Radius Curve for Transport Missions

Technology Definition

Two levels of technology were addressed during the study; a 1990 technology and a year 2000 technology. Figure 29 gives a graphical explanation of these technology levels. It shows the relationship between the airframe development cycle and the engine development cycle. Engine demonstration go-ahead must occur about 2 years prior to the beginning of the airframe preliminary design phase. Also, the engine preliminary preflight rating test (PPFRT) should coincide with the airframe first flight. Finally, the engine maturity phase ends with the airframe first delivery. These are fundamental milestones in any development cycle, although the actual times vary according to a wide range of factors (technical difficulties, funding limitations, changing operational concepts, and political events, to mention a few).

The definition of 1990 technology, for this study, is that 1990 technology is the available technology (reasonably mature and low-risk) which the airframer is willing to incorporate in a preliminary design beginning in 1990. Likewise, year 2000 technology is the available technology which the airframer is willing to incorporate in a preliminary design beginning in the year 2000. With this interpretation, 1990 technology has an IOC date of about 2001, and year 2000 technology has an IOC date of about 2011.

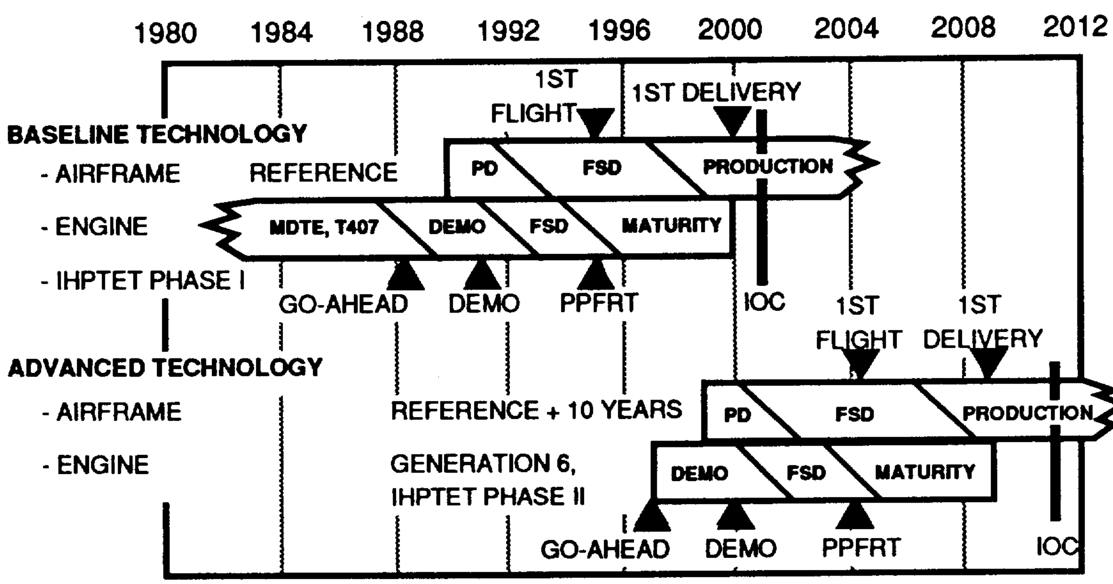

Figure 29. Airframe and Propulsion Technology Development Cycles

Weights

A review of past performance on the all-composite Bell-Boeing V-22 Osprey and the Boeing Model 360 all-composite tandem helicopter gave a good indication of progress in the area of weights for both primary structure and for rotor blades and hubs. Boeing involvement in other programs such as ADOCS, IHPTET, and ART (Advanced Rotorcraft Transmissions) gave the weight group specific knowledge and a substantial data base for estimation of future weight savings.

There are specific concept-related weight penalties to consider. Component weights for the five rotorcraft concepts were estimated by the weight trend equations in VASCOMP II, a V/STOL aircraft sizing and performance computer program[6]. Technology factors were applied to the component weights to adjust for 1990 and year 2000 capabilities, see Table A-4 in Appendix A. Further discussion of weights is provided in Appendix A, Technology Assessment - Weights. Wing weights for all of the tiltrotor concepts were generated from a Boeing Helicopters-developed tiltrotor wing weight trend. This methodology accounts for both the wing strength and stiffness requirements. Strength requirements are dictated by the wing bending moments imposed by the VTO jump takeoff, in both vertical bending and wing torsion. The wing box spar stiffness requirement is dictated by the aeroelastic stability boundary.

The rotor group also required specific weight penalties associated with the rotor concept geometry and complexity.

Aerodynamics

The aerodynamic analysis required for the five concepts can be summarized in the categories of airframe aerodynamics and performance and rotor aerodynamics and performance.

The primary airframe aerodynamic characteristics as they relate to aircraft sizing are parasite drag, drag due to lift, and compressibility drag. The basic parasite drags of the concepts differ primarily because of the different wing and nacelle size and their layouts. The basic fuselage geometry is unaltered among the various designs, apart from the engine mounting, for purposes of this comparison.

Resultant equivalent parasite areas (f_e) for the five concepts are shown in Figure 30. Drag improvements relative to the V-22 come from a smoother afterbody fairing, elimination of sponsons, smaller nacelles (for body-mounted engine configurations), and reductions in protuberances which are required for a 450-knot design.

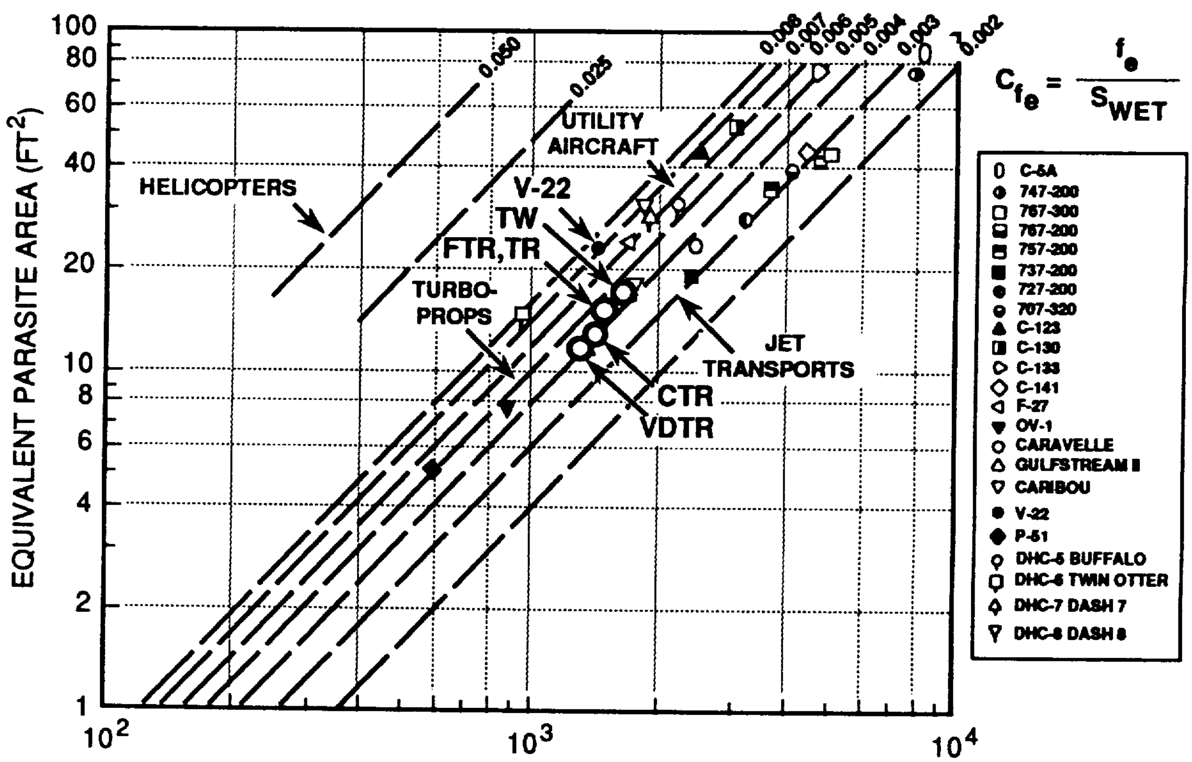

Figure 30. Aerodynamic Cleanliness Comparison

About a 10% reduction in skin friction drag comes with the higher cruise Reynolds number. A comparison to other types of aircraft shows the estimated f_e values to fall slightly below those for turboprops, but not as good as large, civil transports.

Compressibility drag is a very important driver in determining wing section geometry, particularly thickness/chord ratio. The challenge is to choose a high value of t/c for structural reasons while keeping close to the boundary for drag divergence at the design Mach number. The test and theory data for wing drag divergence shows a gain of 0.06 Mach in drag divergence by changing from the V-22 wing airfoil to a 20% thick Boeing TR38 advanced airfoil. A further 0.05 Mach can be gained by reducing the thickness to 15%. A review of the speed and altitude requirements for the vehicles indicated a need for airfoils in the 18% to 14% t/c range to avoid severe compressibility effects. The compressible drag increment was derived from the TR38 2-D characteristics and then corrected to 3-D. Figure 31 shows the resulting drag rise curves.

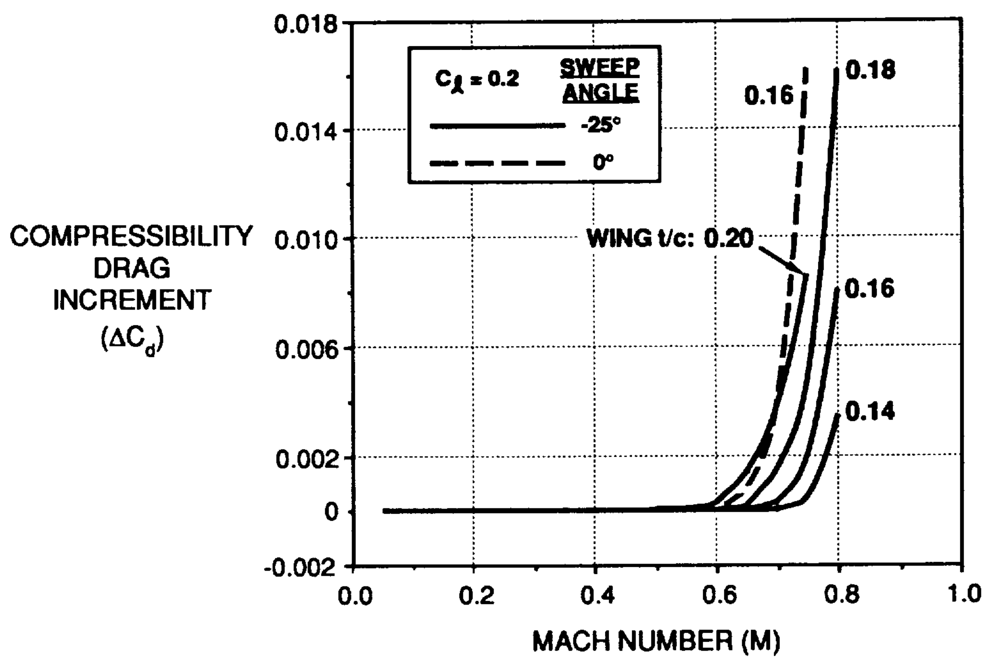

Figure 31. Compressibility Drag Increments

Each vehicle concept had a different rotor design. The rotor blade twist was determined by the cruise condition. This resulted in an almost linear twist of close to 35°, which performs adequately in hover. The aircraft propulsion systems are all sized for cruise, resulting in their being considerably oversized for hover. This renders hover performance of little consequence, except for verifying its adequacy. Should OEI performance become an issue, however, hover would be of prime importance.

Propulsion

Turboshaft engines were used with all of the concepts except the folding tiltrotor, which required a convertible engine. Engine lapse rate and sfc characteristics with speed, altitude, and part power were based on a growth version of the GE38 core engine. The absolute weight and fuel flow values were adjusted to IHPTET Phase I for the baseline 1990 technology and to IHPTET Phase II for the year 2000 technology.

Figure 32 shows a historical trend of turboshaft engine SFC and weight trends. Obviously, the 1990 and year 2000 technology SFC values represent a substantial improvement from the trend line. The weight objectives, however, are more in line with the historical trends.

The convertible engine characteristics were based on a variable-inlet guidevane/variable-exit guide vane configuration with a high bypass ratio of 6.0 and a 1.75 overall pressure ratio. A thrust-to-horsepower ratio of 1.47 was used for the 1990 technology convertible. SFC values were adjusted to reflect the IHPTET goals as explained previously. Further discussion of convertible engine characteristics is included in Appendix A, Technology Assessment - Propulsion and in Appendix B, Military Folding Tiltrotor Propulsion System.

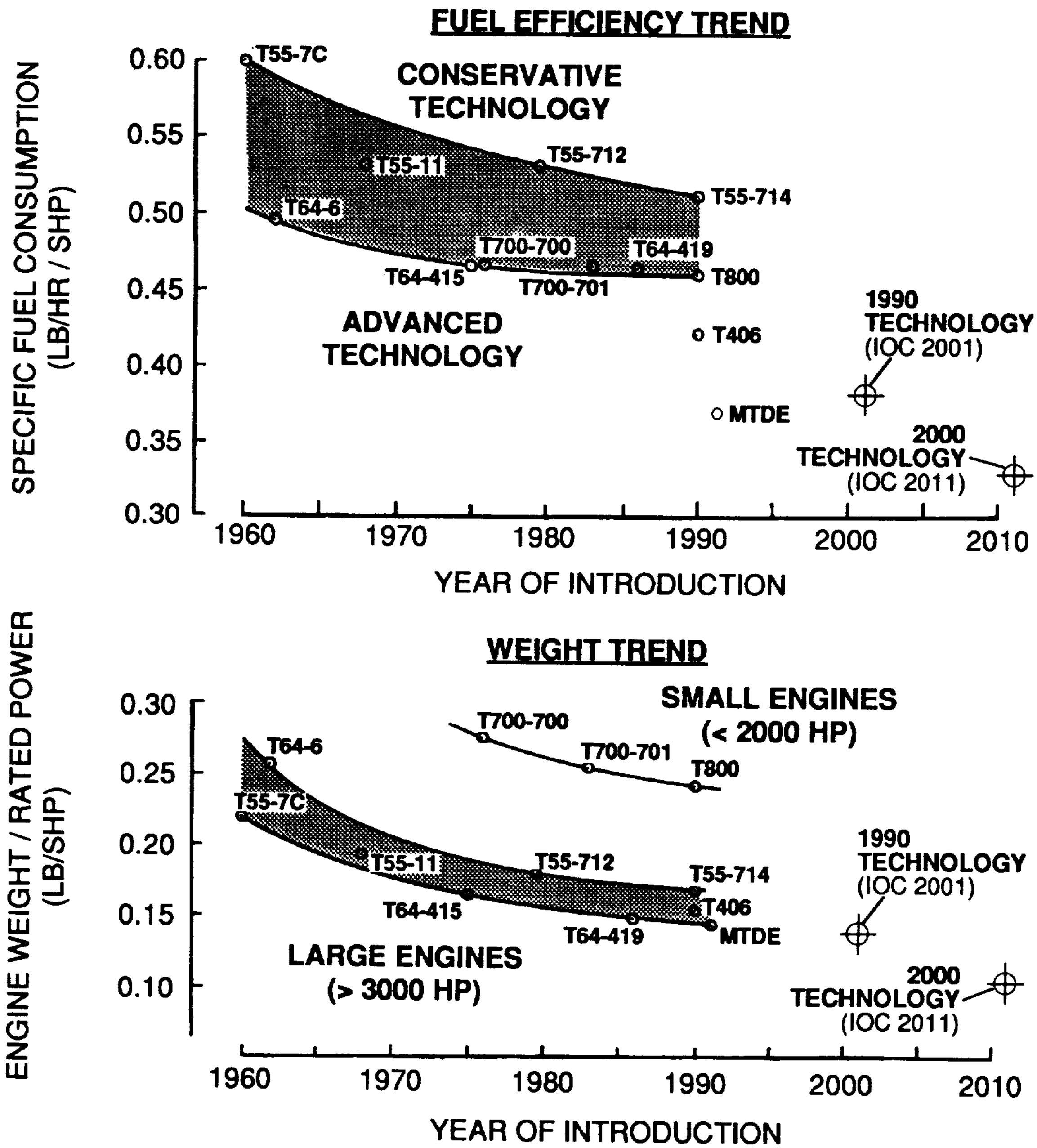

Figure 32. Turboshaft Engine Fuel Efficiency and Weight Trends

Task I Concept Tradeoffs

The concepts were designed to achieve a 450-knot true airspeed at the altitude which gave the lightest gross-weight solution. This required some iteration during the study, since the correct combination of t/c and wing loading at which to run the altitude variations is not initially known.

Still, the prop-rotor-driven (turboshaft engine) concepts tended to optimize at about 15,000 ft cruise altitude and the folding tiltrotor (convertible engine) concept optimized at about 25,000 ft cruise altitude. Allowing the design altitude to be different affects both the equivalent airspeed and the Mach number. A 450-KTAS design speed at sea level corresponds to about 540-KEAS dive speed, but at 25,000 feet is only 350-KEAS dive speed. The higher altitude thus gives a structural/weight benefit via the lower EAS dive speed, as well as a substantial L/D improvement. The disadvantage of higher cruise altitudes is that Mach number creeps up. This impacts both the vehicle compressibility drag and the propeller efficiency (higher helical tip Mach numbers). A further adverse effect of higher cruise altitude is the growth in installed engine SHP required to compensate for the reduced SHP available at altitude.

Concept Description and Sizing

Three-view drawings of the five high-speed rotorcraft concepts are shown in Figure 33. A detailed description of each will not be provided here. Suffice it to point out that the straight wings of the conventional tiltrotor and the tiltwing make it difficult for these two to achieve 450 KTAS (M = 0.72). The forward-swept-wing configurations are much better suited for high subsonic speeds. The three forward-swept-wing concepts also have body-mounted engines, thus reducing the wingtip nacelle size and reducing flat-plate area.

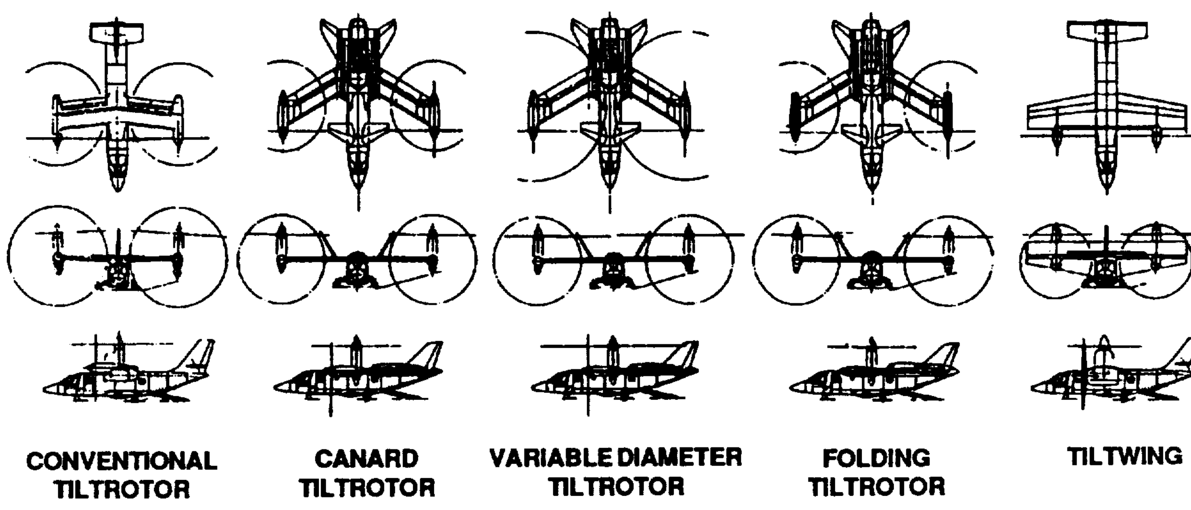

Figure 33. Three-View Drawings of 5 High-Speed Rotorcraft

Conventional Tiltrotor: The conventional tiltrotor (TR) operates very similarly to the V-22 transport. Rotor analysis tradeoffs showed a 575-fps tip speed gave about the best cruise propulsive efficiency, corresponding to 0.87 helical tip Mach number at the 450-KTAS cruise condition. This requires a substantial rpm reduction from hover, which penalizes the drive system weight by requiring higher torque ratings. A rotor propulsive efficiency of 0.67 was achieved at the 450-knot cruise condition. The optimum cruise altitude was about 15,000 ft and the optimum wing thickness ratio was 0.14.

Parametric tradeoffs of wing loading and disc loading for the TR are shown in Figure 34. The choice of disc loading W/A was limited to a maximum of 25 psf in keeping with the study objective of low downwash. This limit was well within the disk loading constraints shown in Figure 6, but was chosen in Task I based on past experience. This selection was later supported by the more detailed downwash evaluation conducted in Task II, which showed these disk loadings to create a thinner jet outwash than the CH-53E but of higher velocity; see Appendix B, Downwash Charactericstics. Note that GW is not sensitive to W/A for the TR. At this W/A the minimum-gross-weight point occurred at a wing-loading W/S of 140 psf. However, wing loadings were limited to a maximum value of 120 psf based on conversion corridor and stall considerations. The selected point for the TR is W/A=25 psf and W/S=120 psf, giving a 56,072-lb GW.

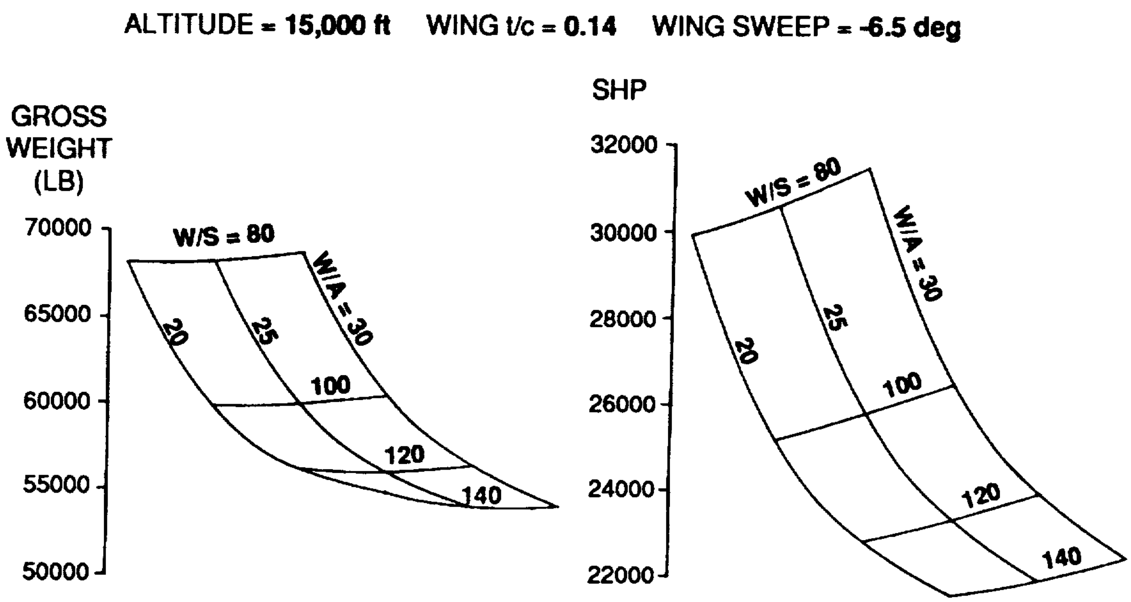

Figure 34. Conventional Tiltrotor Parametric Tradeoffs

Canard Tiltrotor: The canard tiltrotor (CTR) has a forward-swept wing and advanced-geometry rotors incorporating swept blades. The forward-swept wing is employed to achieve higher drag-divergence Mach numbers. A 0.16 wing thickness ratio gave the least-gross-weight solution for CTR. One penalty of the canard configuration is that the rotors must be outside of the canard tips, resulting in a higher wing aspect ratio. This rotor-canard arrangement is considered necessary to avoid rotor-canard vortex interaction (unless wind tunnel tests can verify that rotor tip vortices on canards or canard-induced velocities on rotors are inconsequential). The rotor and wing must be designed for 620 KTAS stability boundaries (450 KTAS * 1.2 * 1.15), including the whirl-flutter boundary. The difficulty in achieving this stability boundary is compounded by the increased aspect ratio and by the wing's forward-sweep geometry.

Rotor tip speeds in cruise can be higher for the advanced-geometry rotor. Estimates of cruise propulsive efficiency for this rotor geometry exceeded 0.8 for the 450-KTAS cruise condition. The optimum cruise altitude was about 15,000 ft.

Parametric tradeoffs of wing loading and disc loading for the CTR are shown in Figure 35. Here the wing weight penalty for higher aspect ratio shows up by increasing GW at the higher W/S values (lower chord, higher aspect ratio). A 25-psf W/A value was taken as the upper limit, giving a minimum GW of 46,480 lb at W/S=100 psf and W/A=25 psf.

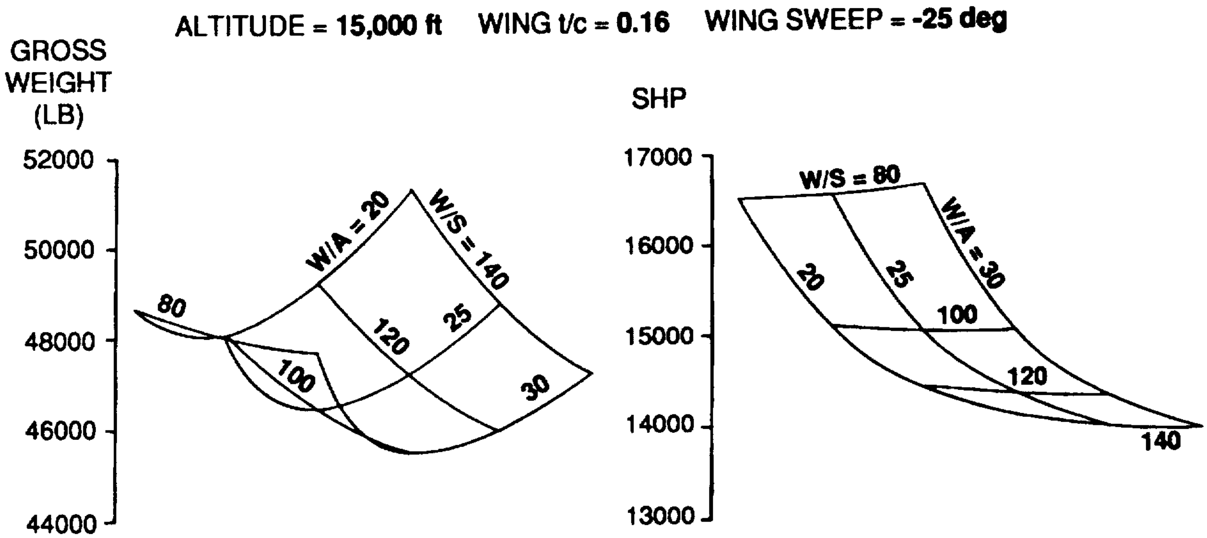

Figure 35. Canard Tiltrotor Parametric Tradeoffs

Variable-Diameter Tiltrotor: The variable-diameter tiltrotor (VDTR) has the same forward-swept wing and canard configuration as the CTR. The difference is that the variable-diameter rotor allows the rotor tips to be closer together in the hover mode, as indicated in the 3-view drawing of Figure 33. Rotor diameter is reduced during conversion to the airplane mode until the point where the blade tips will clear the canard tips. This layout results in a lower wing aspect ratio, which is better from weight considerations. But it has the penalty of a heavier and more complex rotor hub and blade design to accommodate the variable diameter. As on the CTR, this concept has a wing t/c of 0.16 and optimum cruise altitude of about 15,000 ft.

The parametric tradeoffs of W/A and W/S are shown in Figure 36. Higher disc loadings generally gave lighter GW, especially at the higher W/S values. However, staying with the 25-psf upper limit for W/A gave an optimum GW of 46,455 lb at W/S=120 psf and W/A=25 psf.

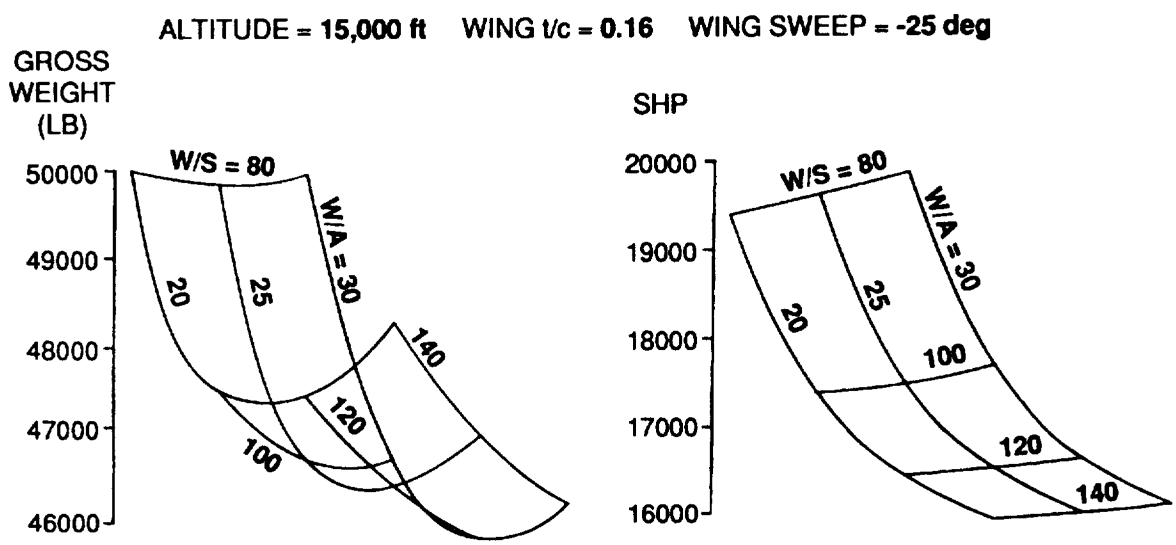

Figure 36. Variable Diameter Tiltrotor Parametric Tradeoffs

Folding Tiltrotor: The folding tiltrotor (FTR) has the same forward-swept wing and canard configuration as the two previous concepts. Body-mounted convertible engines provide propulsive thrust in cruise and shaft power for the two rotors in hover and during conversion to the airplane mode. This concept does not need to meet a high whirl-mode-stability boundary, since the rotor blades would be folded at about 200 KTAS. Leaving a 50-knot operational margin would give only a 250-KTAS flight envelope in the prop-rotor mode. This corresponds to a 345-KTAS whirl-mode-stability boundary requirement (13% less than V-22 requirement at sea level). Thus a wing weight savings may be expected here.

The FTR rotor can be optimized for hover and low-speed flight since it is not used above 200 KTAS. Also, rotor tip speed can always operate at the optimum hover value, even during conversion to the airplane mode. (A 790-fps hover tip speed gives a helical tip Mach number of 0.8 at 250 KTAS.) The high tip speed reduces the required rotor solidity and the constant rpm simplifies the drive system design. Also, the drive system need only be sized for hover and low-speed flight up to 200-250 KTAS in the prop-rotor mode, yielding a much lighter drive system than the other concepts. The weight advantage is partially offset by the added weight of a convertible engine with its extra fan and VIGV components. The FTR optimized at a cruise altitude of 25,000 ft and a 0.15 wing t/c.

Parametric tradeoffs of W/S and W/A are shown in Figure 37. The optimum configuration was chosen at W/S = 90 psf and W/A = 25 psf, giving a 53,600-lb GW. At the optimum W/S of 90 psf the 25-psf disc loading was also at a relative minimum point.

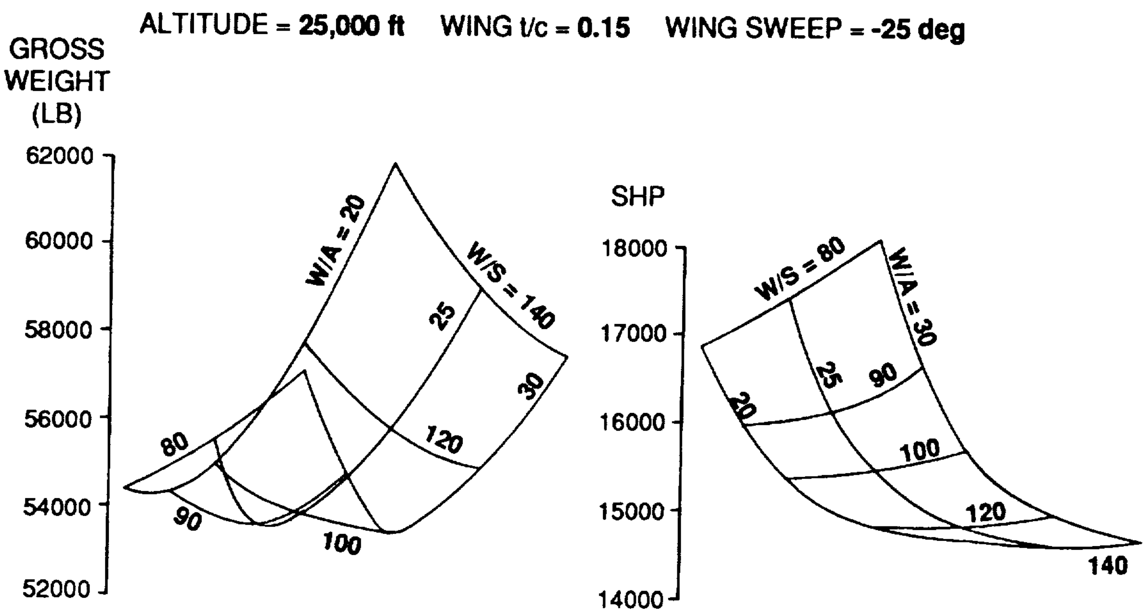

Figure 37. Folding Tiltrotor Parametric Tradeoffs

Tiltwing: The tiltwing (TW) concept is embodied as a single, unswept wing with two props. The straight wing was used to provide a wing-to-rotor proximity which is necessary for good conversion and low-speed control. Since the tiltwing wing is always aligned with the propwash, it has the distinct advantage of a low download in the hover mode. Pitch control in hover and low-speed flight would be provided by either monocyclic rotor control or by a free-floating wing with geared flap control system as described by Churchill in U.S. patent 3,029,043. Tail rotors have been avoided due to complexity and the problems they would present in high-speed flight.

The tiltwing has lower wing root bending moments in the jump takeoff maneuver than a tiltrotor. This lower wing root bending moment is carried in the stronger wing chord direction during jump takeoff since the wing is tilted with the rotors. These two factors make TW wing structural design easier than tiltrotor wing design. Also,the smaller rotor diameter and shorter distance from wing root to rotor centerline make it easier to meet whirl-flutter requirements. Thus, wing thickness ratio can be relatively low without a high wing weight penalty.

The large midwing engine nacelle increases drag. It gives twice the wing-nacelle interference drag as the tip-mounted tiltrotor nacelles; it does not give the beneficial effects of tip nacelle end-plating; and the nacelle wetted area must be larger to house the engines. All three factors drive down the vehicle L/D. As will be shown, the optimum TW is constrained to lower wing loadings than the tiltrotor concepts. This increased wing area means higher flat-plate area which further reduces L/D values for the concept. As with the other propeller-driven concepts, the TW optimized at a cruise altitude of about 15,000 ft.

Parametric tradeoffs of W/S and W/A on TW gross weight are shown in Figure 38. Higher wing loadings give lower gross weights, at least up through the 140-psf W/S considered here. This trend is different from the canard tiltrotors primarily because of the different wing weight requirements. A prime consideration in tiltwing design is the chord-to-diameter ratio, c/D.

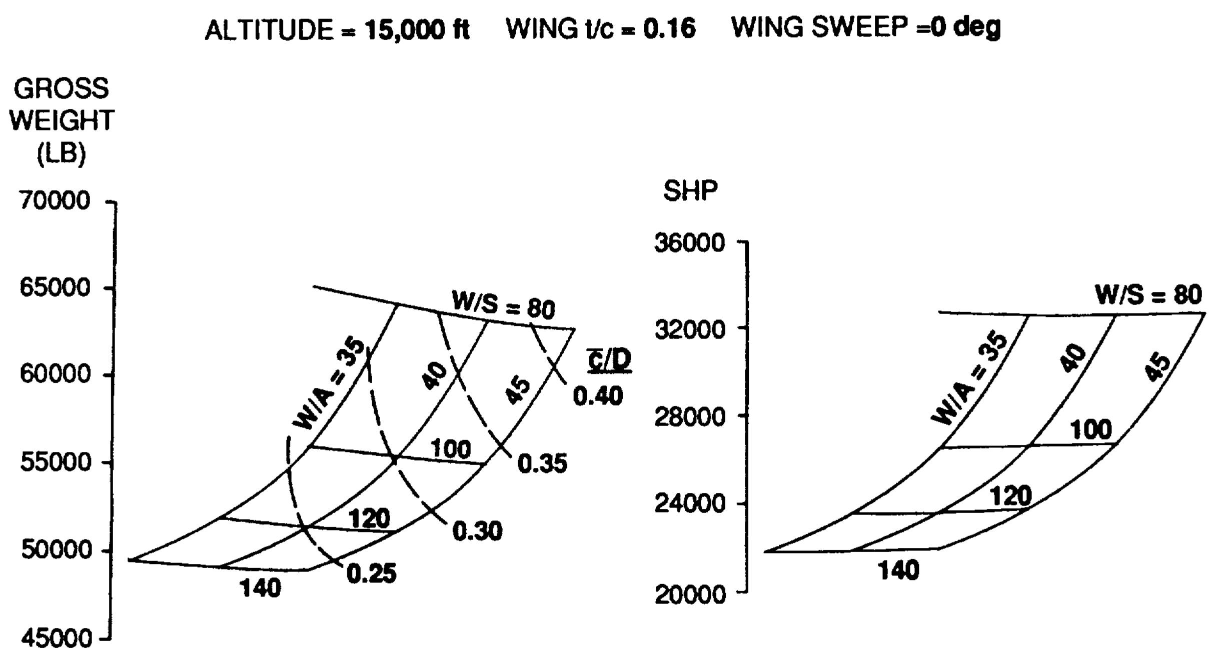

Figure 38. Tiltwing Parametric Tradeoffs

Bounds of this parameter are shown in Figure 39. Data from wind tunnel programs, such as LIT, indicate that the lower bound for the c/D should be about 0.43. This stems from control considerations and the wing stall phenomenon while in a partial-power, low-speed-descent mode. Imposing this c/D restriction on the GW trends of Figure 38 forces a choice at the corner: W/S = 80 psf and W/A = 45 psf, giving a 59,340-lb gross weight.

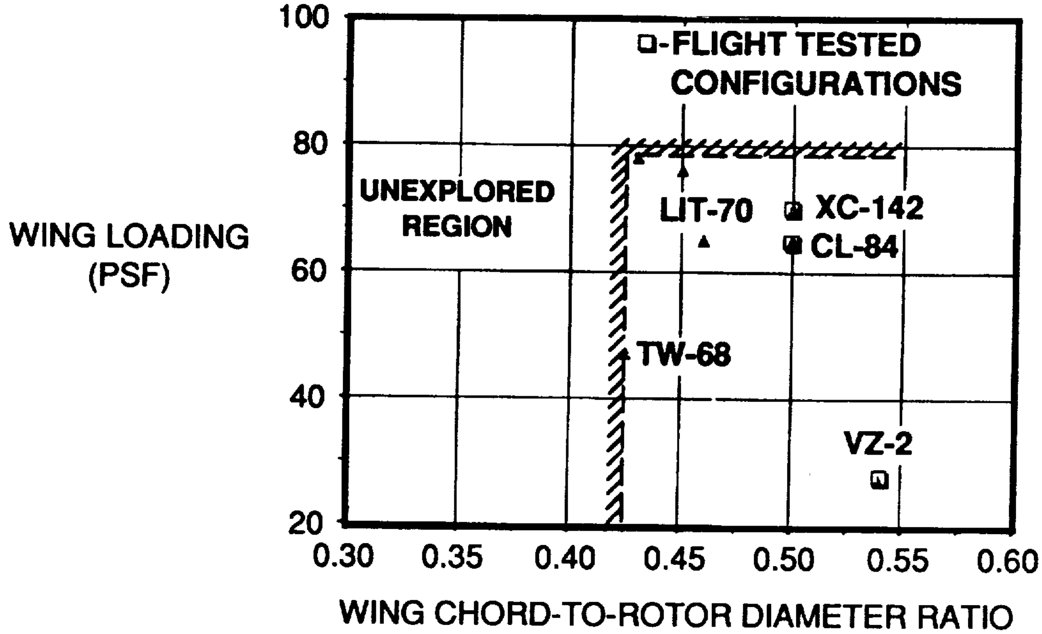

Figure 39. Tiltwing Design Constraint

Concept Comparison

The conventional tiltrotor and tiltwing have the highest gross weight and also the highest installed-power requirements. Both concepts suffer from a straight wing with no relief for compressibility drag and from the added flat-plate area of the larger nacelles which house the engines. They also show the lowest specific range and range factor values.

Clearly, the canard tiltrotor (CTR) and variable-diameter tiltrotor (VDTR) have the lowest gross weight (and horsepower required). The folding tiltrotor (FTR) has a higher gross weight than those two, but less gross weight than the conventional tiltrotor or the tiltwing. Its 25,000-ft design cruise altitude gives it substantially better values of specific range and range factor at the 450-knot required cruise speed. Also, the FTR has much greater speed potential than any of the propeller-driven concepts. Thus, from a weight and performance point of view the CTR, VDTR, and FTR are attractive candidates for Task II.

How well do these five high-speed rotorcraft compare with hover-designed helicopters and cruise-designed fixed-wing aircraft? Figure 40 shows this comparison to both helicopters and fixed-wing aircraft in terms of hover factor and range factor. The five high-speed rotorcraft concepts have about 80% of the helicopter's hover factor, defined as GW divided by fuel flow with units of hours. They also are competitive with the fixed-wings' in terms of range factor, defined as nm/lb fuel times GW with the units of nm. Actually achieving these predicted performance levels in a prototype vehicle would be a major accomplishment, requiring considerable R&D to realize the weights, performance, and propulsion goals which are reflected herein. But the potential is there and is within reach.

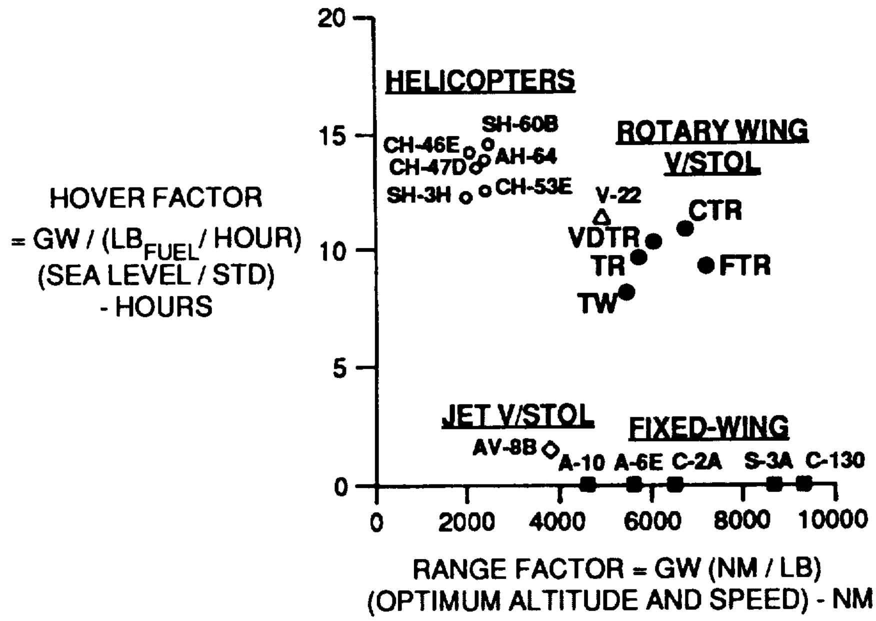

Figure 40. Minimizing the V/STOL Compromise

Sensitivity Study

Each of the five concepts was evaluated for its sensitivity to a combination of three technology factors: flat-plate area, prop-rotor cruise efficiency, and year 2000 engine technology. While this list of tech improvements is not comprehensive, it served as a gage of what may be expected. The tiltwing and conventional tiltrotor concept baselines were the heaviest, required the most installed power, and had the worst specific range and the highest fuel fraction. It should not be surprising that these two concepts benefited the most from the year 2000 engine technology. The CTR and VDTR were the lightest and had good SFCs, so they benefited the least.

The vehicles' sensitivity to design speed was also examined. The baseline 1990 cases were resized for a range of design speeds from 350 KTAS to 500 KTAS. The resulting trends in GW are shown in Figure 41. Starting at the 350-knot design speed, the FTR is obviously the heaviest solution. The prop-rotor driven concepts with turboshaft engines give the lightest GW vehicle up to about a 470-knot design airspeed. The TW and TR have unswept wings and simply did not converge beyond 450 knots. This is not to say that a carefully optimized design in either of these configurations could not be designed beyond 450 knots. But it does say that those two concepts are rapidly approaching their practical limits. The CTR and VDTR are lighter in weight up to about 465 knots, but they did not converge beyond 475 knots. Prop-rotor cruise efficiency drops off very rapidly at higher airspeed, suggesting that 475 knots is the upper limit for prop-rotor-driven concepts. Finall, the FTR shows its speed advantage with lighter gross weights beyond 465-knot design speeds. No convergence problems were encountered for the FTR baseline configuration up to 500 knots and no concept-related limitations exist which would keep the FTR from being designed for much higher dash speeds.

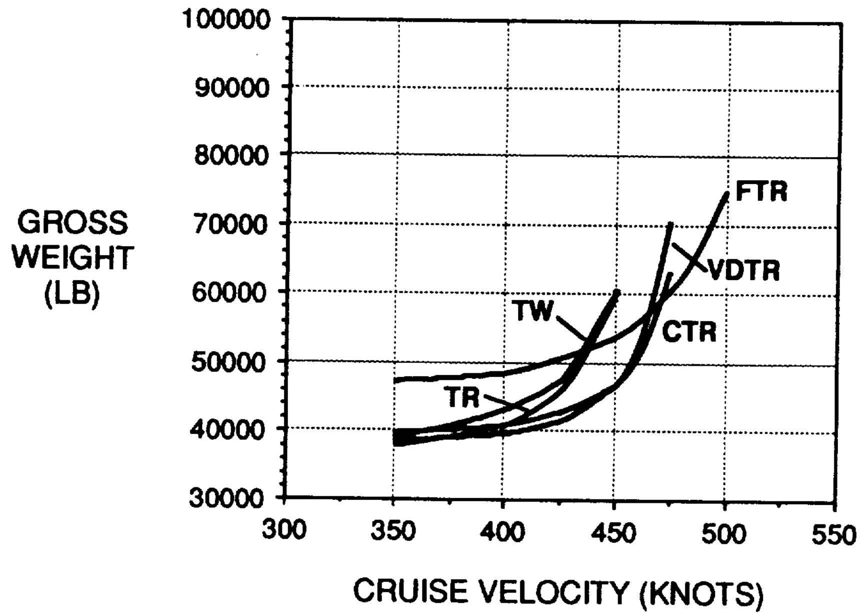

Figure 41. Gross Weight Sensitivity to Design Airspeed

Relative Cost

Life-cycle cost (LCC) estimates were made for each of the five concepts in order to obtain comparative cost data. A parametric approach was chosen for the initial estimate. In preliminary design, the available data is for relatively top-level parameters; mission gross weight, fuel system capacity, wing area, fuel consumption, and fuselage volume are typical products. A description of LCC can be found in Appendix A, Task I Cost Comparisons.

Over 100 discrete parameters were evaluated for each of the concepts and used in the LCC estimate. The technical and performance data which served as the foundation of the estimates were derived from the baseline 1990 optimum configurations. These baseline configurations had been selected on the basis of gross weight, not cost. However, the correlation between weight and cost has been demonstrated to be very high and therefore qualifies weight as a legitimate discriminator for conceptual design.

The results of the LCC analysis were normalized to the conventional tiltrotor design. The aircraft with the highest gross weight, e.g., tiltwing, resulted in the highest LCC. Similarly, those with the lowest gross weight, e.g., CTR and VDTR, projected the lowest LCC.

Down-Select to 2 Concepts

A summary of the five concepts' minimum gross weight, geometry, and cruise performance is shown in Table 6. The conventional tiltrotor and tiltwing have the highest gross weight and also the highest installed-power requirements. Both concepts suffer from a straight wing with no relief for compressibility drag and from the added flat-plate area of the larger nacelles which house the engines. They also show the lowest specific range and range factor values.

The canard tiltrotor and variable-diameter tiltrotor were the lightest, being about the same weight. Their specific range was about 50% better than the other two prop-driven candidates.

Table 6. Summary of Rotorcraft Geometry and Performance

	TILTROTOR	CANARD TILTROTOR	VARIABLE DIAMETER TILTROTOR	FOLDING TILTROTOR	TILT WING
GROSS WEIGHT	56,072	46,481	46,455	53,600	59,340
WING LOADING	120	100	120	90	80
ASPECT RATIO	4.6	6.9	6.0	5.9	5.3
WING t/c	0.14	0.16	0.16	0.15	0.15
WING SWEEP	-6°	-25°	-25°	-25°	0°
DISK LOADING SOLIDITY	25 0.141	25 0.137	25 0.140	25 0.118	45 0.254
SHAFT HP	23,360	15,024	16,536	16,123	29,586
DESIGN ALTITUDE	15,000 FT	15,000 FT	15,000 FT	25,000 FT	15,000 FT
SPECIFIC RANGE (NM/LB):					
AT 450 KNOTS	0.057	0.091	0.080	0.113	0.056
AT $V_{.99BR}$	0.103	0.149	0.132	0.133	0.093
RANGE FACTOR (NM):					
AT 450 KNOTS	3190	4247	3734	6078	3322
AT $V_{.99BR}$	5792	6935	6136	7130	5518

The folding tiltrotor had the next highest gross weight and a further 25% improvement in specific range at 450 knots (owing largely to better L/D at its 25,000-ft cruise altitude).

Final concept ranking was conducted against 11 key criteria to decide upon 2 concepts. A comparison to Table A-3 in Appendix A shows that most of these key criteria were taken directly from the measures of effectiveness and performance. For instance, cruise range in Table 7 is equivalent to range factor in Table A-3. Aeroelasticity however is less obvious, as it reflects vibration and ride quality from Table A-3 as well as a subjective assessment of difficulty in establishing a stable, flutter-free platform for each concept. Each criterion was given a potential number of points related to Boeing's judgement of its importance in this study. The best concept was given the maximum points for a given criterion and the other concepts received points in proportion to their ability relative to the best. The key criteria included speed potential, hover downwash, gross weight, maneuverability, aeroelasticity, R&M, survivability, and life-cycle cost. They are shown in Table 7 along with the assigned criteria weights. This multidisciplinary approach gave a broad, quantitative evaluation including a parametric estimate of life-cycle cost for each concept.

Quantitative ratings shown in Table 7 were scored according to the assessments made of each concept's capability relative to the others. The gross weight rating for example has a criteria weight of 100, which is then the best score going to lightest weight concept. Other concepts received ratings proportional to their gross weight. The tilt wing rating is simply:

= (Criteria Weight) x Least Gross Weight / Tilt Wing GW

= 100 x 46,455 / 59,340

= 78

Supporting data for ratings in the other criteria can be found elsewhere in this section of the report, or in Appendix A.

The folding tiltrotor received the highest score and the tiltwing received the lowest. Percentage rankings are shown at the bottom of Table 7. From this ranking the folding tiltrotor was selected for application to the military transport mission. The folding tiltrotor speed potential and survivability characteristics give it the greatest design flexibility and a high potential military worth. Its convertible engine allows the vehicle an expanded flight envelope, 25,000 to 30,000-ft altitude. The higher operational altitude also gives the folding tiltrotor a substantially better specific range at the 450-knot cruise speed.

The canard tiltrotor was selected as the second configuration and was applied to the NASA 30-passenger civil mission which was developed in Task II.

Table 7. Concept Evaluation Chart

KEY CRITERIA	CRITERIA WEIGHTS	TILTROTOR	CANARD TILTROTOR	VARIABLE DIAMETER TILTROTOR	FOLDING TILTROTOR	TILT WING
SPEED POTENTIAL	150	50	100	100	150	50
HOVER EFFICIENCY	50	50	50	50	50	40
HOVER DOWNWASH	50	50	50	50	50	20
GROSS WEIGHT	100	83	100	100	87	78
CONVERSION MANEUVERABILITY	50	50	50	50	50	30
CRUISE RANGE FACTOR, 450 KNOTS	50	30	39	35	50	25
OTHER MISSION APPLICABILITY	50	50	50	50	50	40
AEROELASTICITY	50	40	30	35	48	50
R&M	50	50	43	40	39	49
SURVIVABILITY	50	49	43	41	50	49
LIFE CYCLE COST	50	45	50	50	43	39
TOTAL SCORE	700	547	605	601	667	470
RANKING		82%	90%	90%	100%	70%

The payload-to-gross weight ratio of the two high-speed rotorcraft is shown in Figure 42. Clearly, the family of high-speed canard tiltrotors performs very well for design speeds up to about 0.7 Mach number. The exact PL/GW value is, however, very sensitive to prop-rotor cruise efficiency, wing weight fractions, and L/D values. It is also clear that the folding tiltrotor concept has a distinct advantage when design speeds are above about 0.7 Mach number. In fact, folding tiltrotor is the only low-disc-loading rotorcraft concept out of the group which has a realistic, near-term potential for supersonic flight in attack missions.

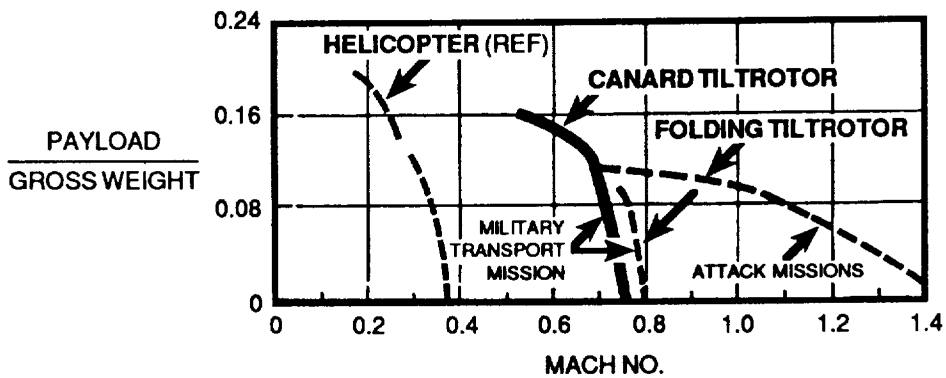

Figure 42. Rotorcraft Payload / Gross Weight vs. Mach No. Comparison

SECTION 2 - TECHNOLOGY EVALUATION

The two chosen concepts are further evaluated in this section to a conceptual level adequate for performance evaluation and for estimating concept sensitivities to advanced technologies. Technologies were examined and in several cases adjusted from those used in Section 1. The rotorcraft were then resized to their respective missions.

The high-speed tiltrotor concept was applied to the NASA civil mission and the folding tiltrotor concept was applied to the NASA military transport mission. A description of these two missions was given in Table 3 and their respective design criteria were discussed in Section 1. Figure 43 is a composite graph showing the maneuver criteria used to design the rotorcraft, having been superimposed on a graph of helicopter-mode and airplane-mode design load factors versus airspeed. The low-speed-maneuver criteria can determine the rotor solidity, which can have a significant influence on rotor weight. So rotor solidity was chosen on the basis of a hover C_T/σ of 0.15 or to satisfy the low speed maneuver criteria, whichever was greater. Airplane-mode maneuver criteria were checked after initial aircraft sizing and found to be satisfactory. Finally, minor adjustments were made to the canard and tail surfaces as needed to satisfy static stability requirements.

Several technology areas were examined in more detail. Estimates of aerodynamic drag were built up from component wetted areas and Reynolds numbers appropriate to the component. Wetted areas were also more accurate; nacelle sizes were scaled to proper engine dimensions, for instance. Induced drag and compressibility drag were estimated using a more accurate computer analysis which accounted for all three lifting surfaces. Another area of change was in component weights. Civil weight trend lines were established for the civil tiltrotor, being different from the military weight trends used to size the concepts in Section 1.

Supplemental data for Task II may be found in Appendix B.

Concept Definitions

High-Speed Civil Tiltrotor

Design layouts for the civil tiltrotor were derived from Task I. A new fuselage was designed to accommodate 30 passengers in a four-abreast, pressurized cabin of nearly circular cross section. Baggage area is provided on the passenger level at the rearmost cabin within the pressure bulkhead. A separate, outside access door is provided for the baggage compartment. A lavatory, galley, and flight attendant seat are also provided. The basic airframe design retained the forward-swept wing and canard arrangement, but increased the wing sweep up to 30 degrees to eliminate compressibility drag in cruise. Engines are placed at the wingtip for maximum separation from the cabin (noise and safety considerations) and to minimize cross-shaft loading. Since there is no infrared (IR) suppressor, the engine exhaust is on the order of 1,100°F during vertical takeoff. The engines are nontilting to avoid hot exhaust impingement on the tarmac or on service vehicles and personnel.

The canard was placed at the same longitudinal location as the rotor tip path plane in the airplane mode. The benefit of this configuration is a very comfortable 5-foot separation between the

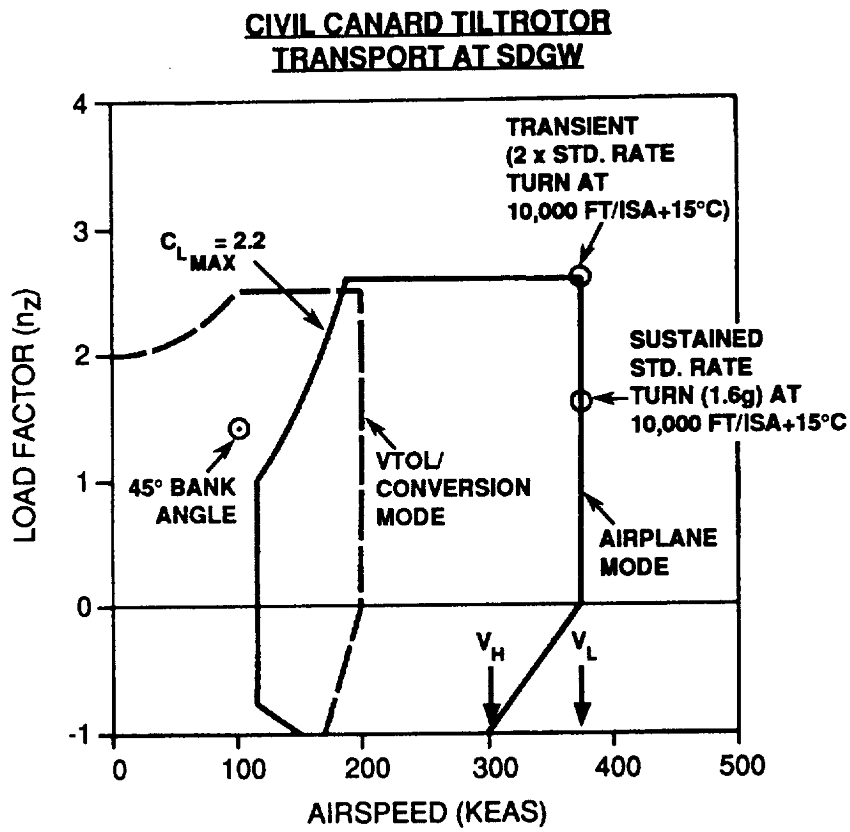

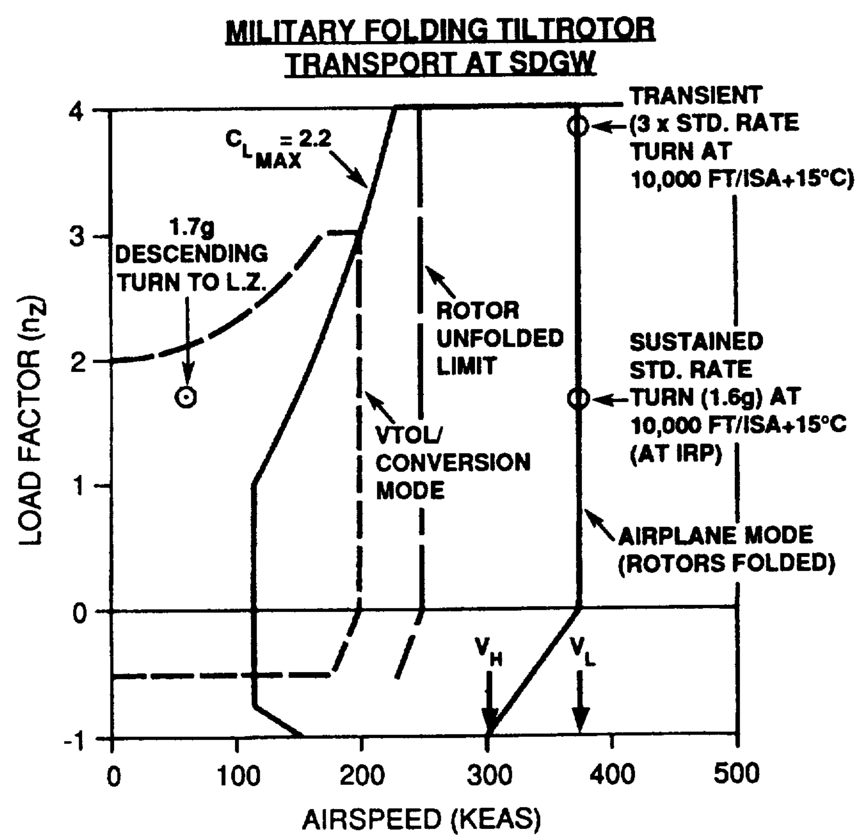

Figure 43. Design Criteria

body and the rotor tips, which significantly improves low-frequency noise in the passenger compartment from rotor tip passage. However, it forces a higher wingspan to position the rotor hubs out to that spacing. The resulting wing aspect ratio of 6.07 is well within reason and yields better aerodynamic cruise efficiency than would a shorter wingspan with a lower aspect ratio. The disadvantage is a penalty in wing weight due to the increased wingspan and higher aspect ratio than would be required for closer body-prop spacings. The wing weight penalty is partially offset by reduced acoustic treatment weight by virtue of the better spacing.

Performance characteristics from Section 1 for the canard tiltrotor were limited by prop-rotor performance at altitude. The optimum altitude of about 15,000 feet was a direct result of increasing Mach numbers at higher altitudes, reducing rotor cruise propulsion efficiency. Operation at higher altitudes was achieved in this part of the study by specifically designing the rotor for operation at 25,000 feet, thereby allowing the civil high-speed tiltrotor to take advantage of the improved airframe L/D available at that altitude. Rotor tip speeds were 750-fps in hover and 600-fps in cruise mode. Considerable effort was devoted to this rotor definition and is discussed later in more detail.

Sizing runs were conducted to determine the best combination of cruise altitude and wing thickness ratio, as was done for the military folding tiltrotor. Lower wing thickness ratios improved compressibility drag but gave higher wing weights, especially for the high-speed tiltrotor which must satisfy whirl-flutter divergence at its cruise speed. Results showed that a 25,000-foot cruise altitude with a 16% wing thickness was a good combination. Tradeoffs were then made on wing loading and disc loading on vehicle gross weight, shown in the carpet plot of Figure 44. A 25-psf disc loading was chosen for the civil high-speed tiltrotor in keeping with the original objective of low downwash velocities. Disk loadings above 25-psf were found to reduce the gross weight by only a few hundred pounds. Furthermore, maximum velocity in the ground wall jet for a 25-psf disk loading at a 25-ft wheel height hover condition was estimated to be nearly 80-knots at one rotor diameter from the rotor centerline. This analysis, shown in Appendix B, was reason enough to limit the disk loading to 25-psf for this commercial application. Also, a point of diminishing returns had been reached; going to a 30-psf disc loading would have given only a 500-lb gross

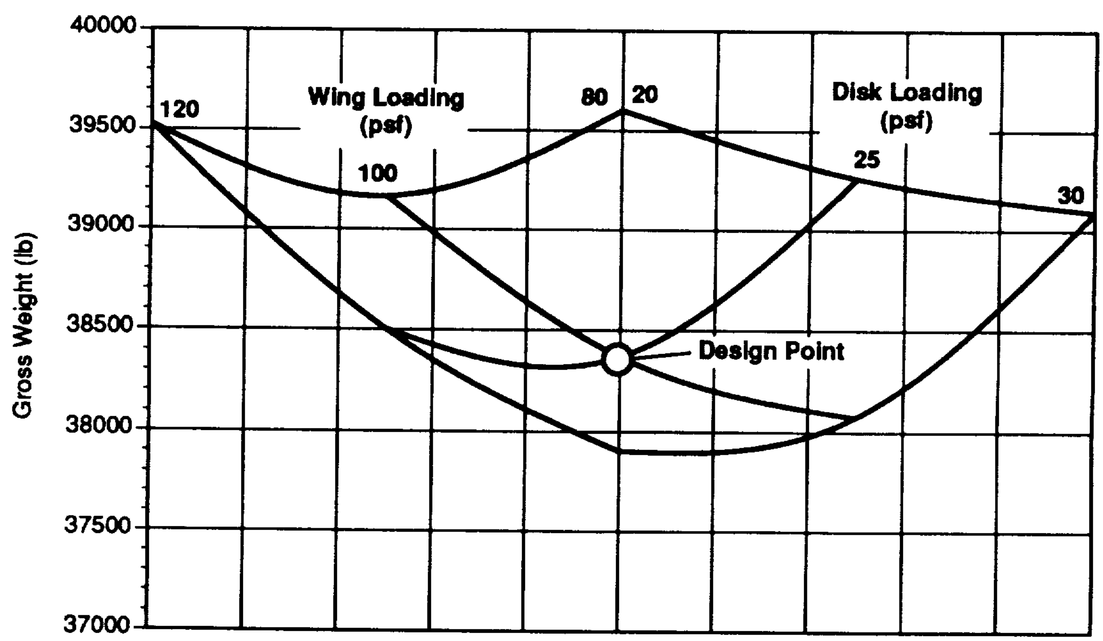

Figure 44. Civil Tiltrotor Wing Loading and Disk Loading Trade-Off

weight reduction. A 100-psf wing loading was selected for the minimum gross weight at the 25-psf disc loading. A 3-view drawing of this configuration is shown in Figure 45 and the interior arrangement is shown in Figure 46. A summary of geometric features, installed power, and transmission ratings is given in Table 8. Wetted areas and frontal areas are given in Appendix B, Table B-4.

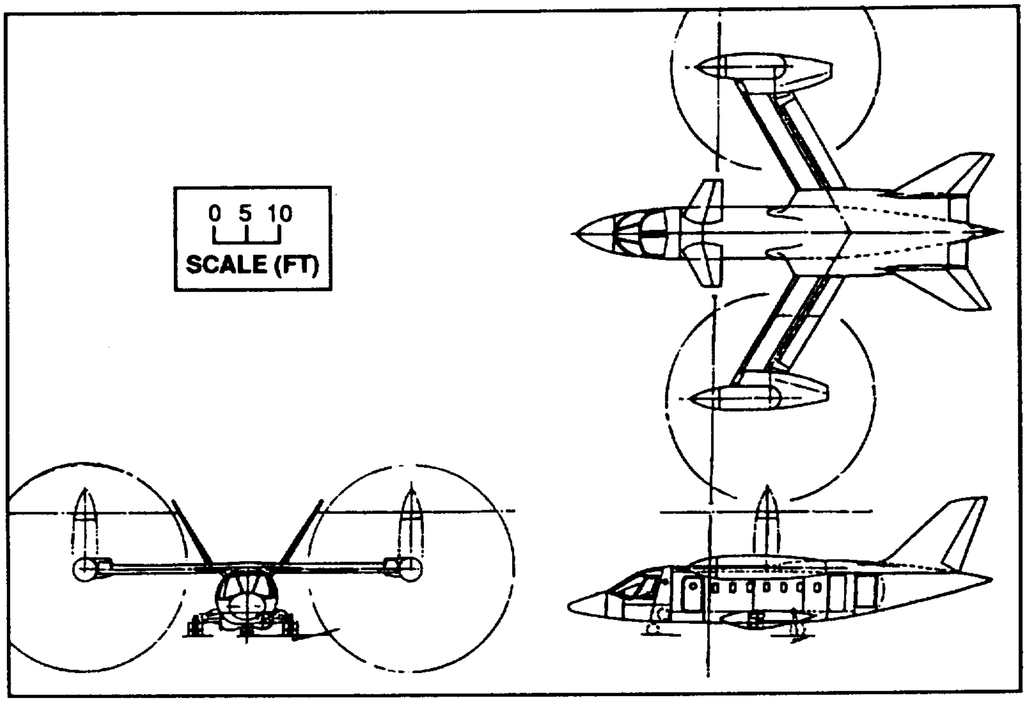

Figure 45. Civil Tiltrotor Three-View Drawing

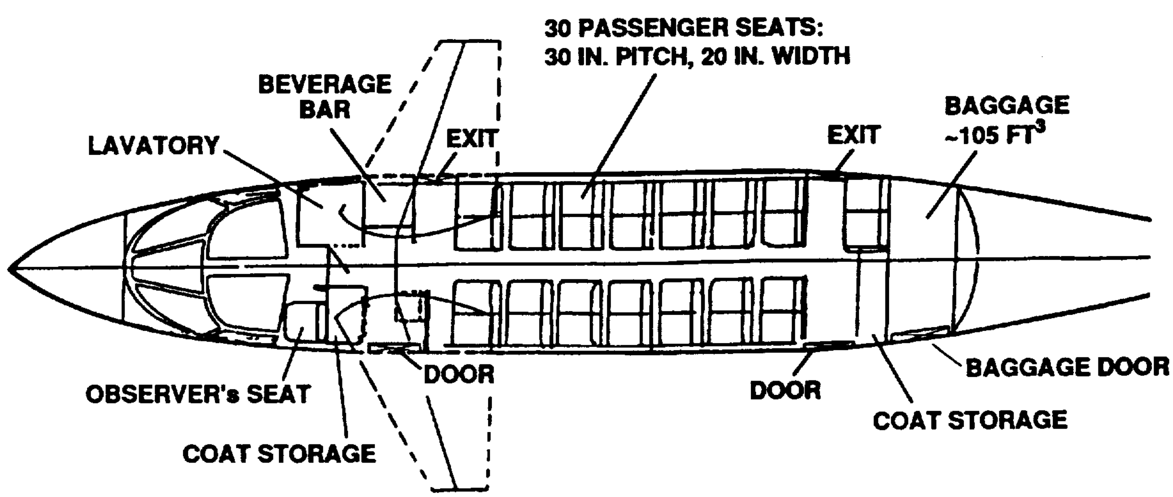

Figure 46. Civil Tiltrotor Interior Arrangement

Table 8. High-Speed Civil Tiltrotor Design Details

Gross Weight: **38,380 lb. (1.0)**	Empty Weight: **26,414 lb. (0.69)**	Fuel: **5226 lb. (0.14)**

Wing Loading:	**100 psf**	Rotor Geometry:	**Advanced Tapered Tip**
Wing Span:	**48.3 ft.**	Disk Loading:	**25 psf**
Wing Area:	**384 sq. ft.**	Rotor Diameter:	**31.3 ft.**
Mean Aero. Chord:	**8.0 ft.**	No. of Rotors:	**2**
Aspect Ratio:	**6.07**	Solidity:	**0.167** (Geometric)
Sweep at c/4:	**-30 deg.**	No. of Blades:	**4**
Taper Ratio:	**1.0**	Blade t/c:	**0.08**
Thickness Ratio:	**0.16**	Twist:	**-37 deg.**
		Tip Speed:	**750 fps** (Hover) / **600 fps** (Cruise)

	CANARD	V-TAIL		
Area (Theoretical):	**84.0 sq. ft.**	**165 sq. ft.** (total)	Power Plant Type:	**Turboshaft Engine**
Span:	**16.0 ft.**	**10.1 ft.**	Installed Power, Static, SLS:	**17357 shp**
Aspect Ratio:	**3.05**	**1.25**		
Sweep at c/4:	**24 deg.**	**40 deg.**	XMSN Rating	
Taper Ratio:	**0.40**	**0.6**	- Hover:	**10669 rhp at 457 rpm**
Thickness Ratio:	**0.12**	**0.09**		
Moment Arm:*	**11.2 ft.**	**27.2 ft.**	- Cruise:	**8535 rhp at 366 rpm**
Tail Volume Coeff.:	**0.306**	**0.24**		

*** From aft CG limit**

Another feature of the high-speed civil tiltrotor is the ability to hover out of ground effect (HOGE) with one engine inoperative (OEI). This was a civil design criterion from the start. As with the folding tiltrotor, installed power was determined by the cruise condition, 450-knots TAS at 25,000 ft. The installed horsepower (5-minute civil takeoff rating) for the civil high-speed tiltrotor was 210% of that required for 1g HOGE at sea level, ISA+15°C. This excess power then allows full hover capability for OEI conditions, with a small 5% power margin for maneuvers. Hover OEI under more demanding ambient conditions, hotter or higher, would still require use of an emergency engine rating. Note that higher disc loading designs would not have this benefit. Transmission size was based on power and torque required in cruise. The cruise torque was about 27% higher than hover torque required, due mostly to the reduced cruise rpm.

Military Folding Tiltrotor

The final version of the military folding tiltrotor looks very similar to that in Section 1. Changes include moving the high-bypass convertible engines from an over-the-wing location to a body-side-mounted location, aft of the main wing. The body-mounted engines allow continued flight in turbofan mode in the event of a single engine failure. A T-tail empennage was used in favor of the prior V-tail arrangement. The folding tiltrotor sized out slightly lighter than before due to small improvements in the engine characteristics and more forward sweep on the wing, 30 degrees instead of 25 degrees, which eliminated any compressibility drag penalty.

Preliminary sizing runs were conducted to determine the best combination of cruise altitude and wing thickness ratio. The results depend to some extent on engine characteristics, too, since higher design altitudes demand a larger installed engine to compensate for the engine lapse rate in thrust available. Lower wing thickness ratios improve on compressibility drag but yield higher wing weights, especially on tiltrotors. Results showed that a 25,000-foot cruise altitude with a 15% wing thickness was a good combination. Tradeoffs were then made on wing loading and disc loading on vehicle gross weight. The carpet plot shown in Figure 47 shows the optimum to occur at a 25-psf disc loading and a 90-psf wing loading. A 3-view drawing of this configuration is shown in Figure 48. A summary of geometric features, installed power, and transmission ratings is given in Table 9. Wetted areas and frontal areas are given in Appendix B, Table B-4.

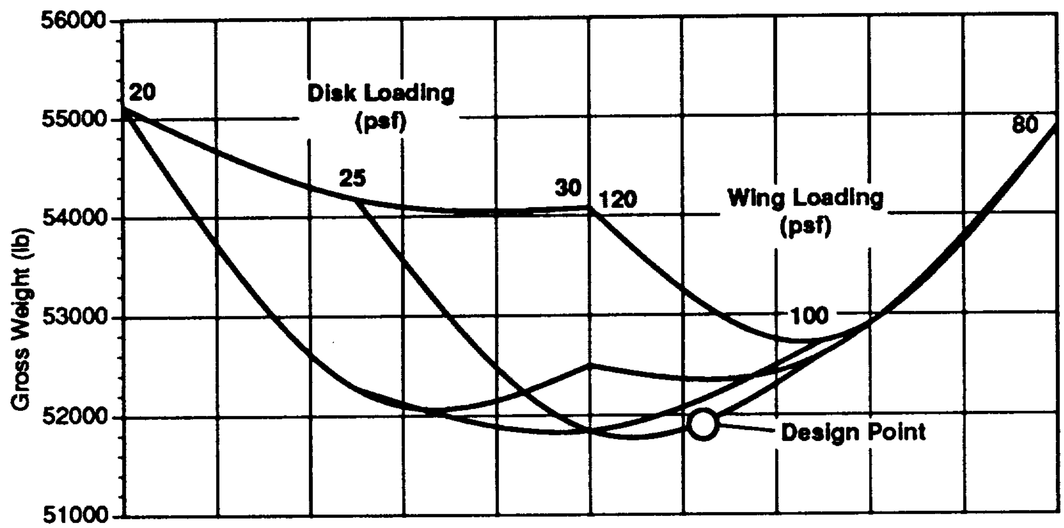

Figure 47. Military Folding Tiltrotor Wing Loading and Disk Loading Trade-Off

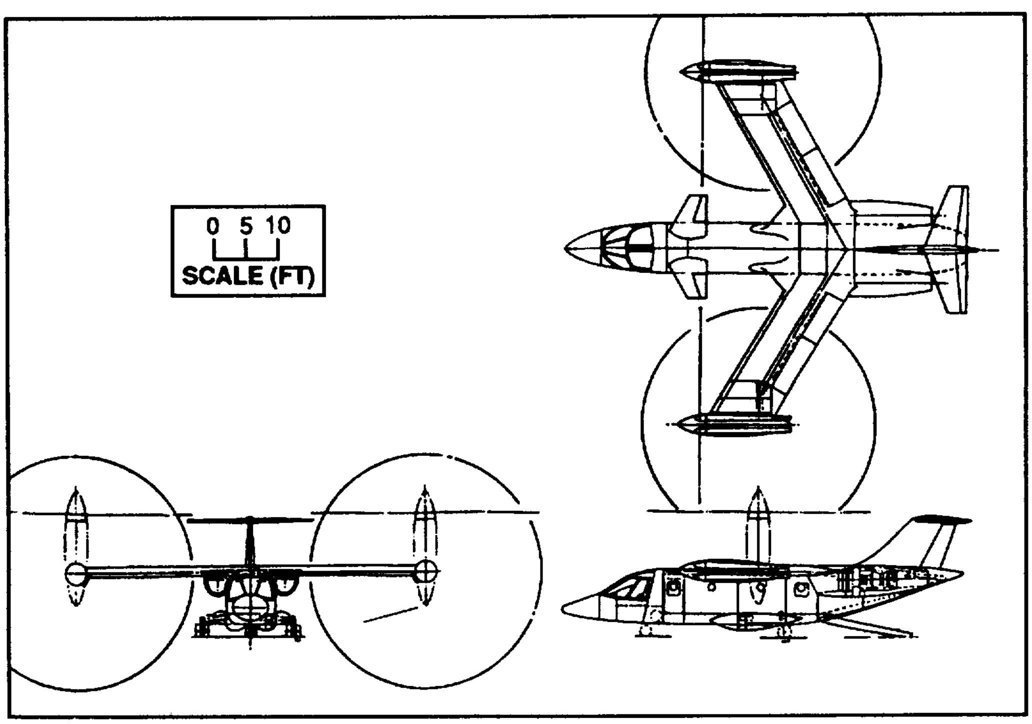

Figure 48. Military Folding Tiltrotor Three-View Drawing

Table 9. Military Folding Tiltrotor Design Details

Gross Weight: 51,406 lb. (1.0)	Empty Weight: 33,877 lb. (0.66)	Fuel: 10,945 lb. (0.213)

Wing Loading:	90 psf	Rotor Geometry:	V-22 Style (Tapered)
Wing Span:	55.2 ft.	Disk Loading:	25 psf
Wing Area:	571 sq. ft.	Rotor Diameter:	36.2 ft.
Mean Aero. Chord:	10.4 ft.	No. of Rotors:	2
Aspect Ratio:	5.33	Solidity:	0.122 (Geometric)
Sweep at c/4:	-30 deg.	No. of Blades:	4
Taper Ratio:	1.0	Blade t/c:	0.18 - 0.09
Thickness Ratio:	0.15	Twist:	-20 deg. linear
		Tip Speed:	750 fps

	CANARD	HORIZ. TAIL	VERT. TAIL
Area (Theoretical):	80 sq. ft.	125 sq. ft.	120 sq. ft.
Span:	15.0 ft.	21.7 ft.	12.2 ft.
Aspect Ratio:	3.2	4.1	1.24
Sweep at c/4:	24 deg.	16 deg.	40 deg.
Taper Ratio:	0.40	0.46	0.60
Thickness Ratio:	0.12	0.12	0.12
Moment Arm: *	15.0 ft.	25.8 ft.	19.3 ft.
Tail Volume Coeff.:	0.20	0.54	0.073

Power Plant Type:	Convertible with VIGV/VEGV
Installed Power, Static, SLS:	15,570 shp
Equivalent Static Thrust, SLS:	22,888 lb.
XMSN Rating, Hover and Cruise:	10,390 rhp at 395 rpm

* From aft CG limit

The folding tiltrotor's rotor design must operate well in the hover mode, in transition, and in turboprop cruise flight up to about 250 knots. Thus, the rotor design can be similar to that of the V-22 rotor, that is, a gimbaled rotor system with airfoil thickness ratios in the range of 18% inboard to 9% outboard. However, a 450-knot design speed in the turbofan mode does not give a power match between hover and cruise flight. Ample hover power is available, alleviating the need to optimize the rotor for hover performance. The twist distribution was chosen as a compromise between hover performance and blade contour compatibility with the nacelle in its folded mode and will be described later.

The installed power was determined by the cruise condition, 450-knots TAS at 25,000 ft. Maximum installed horsepower was about 50% greater than that required for 1g hover out of ground effect (HOGE), giving ample margin for high-hot hover and higher gross weights for VTO operations. Transmission size was based on the HOGE condition.

Rotor rpm was constant for all helicopter and turboprop airplane operations for the folding tiltrotor. A constant 750-fps tip speed gives a 0.77 helical tip Mach number at the 250-knot maximum speed in the turboprop airplane mode, which is well within the rotor airfoils' capabilities. This somewhat simplifies structural dynamics problems. It eliminated design problems associated with avoiding frequency coalescence for two different operating rpms.

High-Speed Civil Tiltrotor

Rotor Performance

The primary design objective for 450-knot prop-rotor design must be to provide good cruise propulsive efficiency and acceptable hover performance. A second design objective is that the rotor system be reasonably light and operationally simple.

There are several conflicting design considerations for a high-speed prop-rotor. The prop-rotor blades must operate in a high Mach number environment at 450-knots and 25,000-ft altitude. The inboard airfoil experiences about Mach 0.75 and the blade tip experiences nearly Mach 1 (theoretically). Rotational tip speed must be reduced in cruise to ease this Mach problem, and blade sweep must be considered as an available means of reducing the effective chordwise Mach numbers experienced near the blade tip. So cruise conditions demand thin blade airfoils in order to achieve high drag-divergence Mach numbers. But thin airfoils have lower values of maximum lift coefficient $C_{l_{max}}$. Reduced $C_{l_{max}}$ in turn reduces the rotor's maximum thrust coefficient/solidity ratio. The net effect is to require higher rotor solidity to satisfy hover. The rotor solidity was sized for a hover $C_T/\sigma = 0.128$ at SL ISA+15°C for a 750-fps tip speed. The low speed maneuver capability exceeded the 45° banked turn requirement; see Appedix B, Figure B-34. Higher solidity results in higher levels of parasite power in cruise, slightly reducing cruise performance. Obviously there is an important tradeoff between airfoil thickness ratio and blade sweep angle as they influence both hover and cruise performance.

Figure 49 illustrates a preliminary high-speed prop-rotor blade. The planform has a 3:1 taper between 0.75R and the tip. Tip sweep starts at 0.60R and the 8% thick VR-15 airfoil is employed outboard of 0.60R. The combination of sweep, twist, and airfoils was selected to meet the 450-knot cruise requirement with a tip speed of 600-fps. Figure 50 shows a comparison of cruise performance for two advanced rotor blade designs. Both use tip taper, optimum twist for 450-knot cruise and thin outboard airfoils. The difference in propulsive efficiency between the two designs is due to blade sweep, as depicted in Figure 49. The unswept blade provides a cruise propulsive efficiency of about 0.71; the swept-blade design could achieve a cruise propulsive efficiency of nearly 0.80. This 13% increase in cruise efficiency would save about 11% on fuel. The net impact of swept-blade performance would be to reduce total rotorcraft DGW by 7 percent.

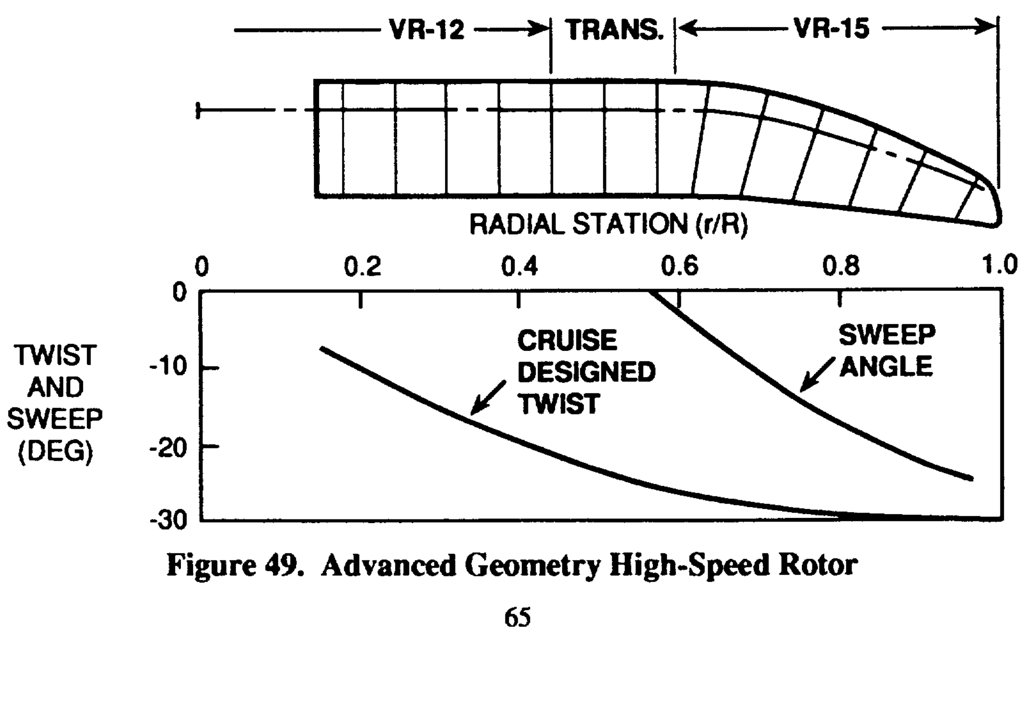

Figure 49. Advanced Geometry High-Speed Rotor

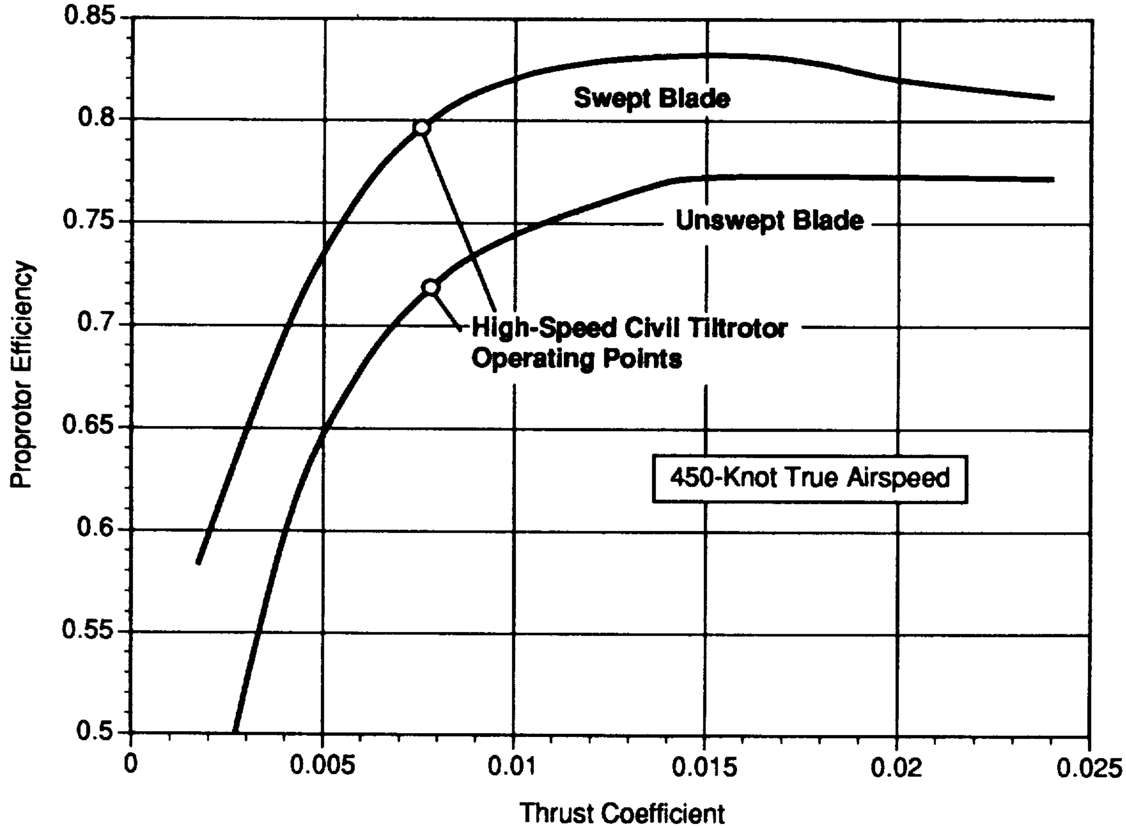

Figure 50. Effect of Blade Sweep on Prop-Rotor Cruise Efficiency

This aerodynamic rotor design is based purely on performance goals. Its advanced contours suggest considerable design and development work to ensure that blade loads, dynamic coupling, and stress are thoroughly evaluated before any commitment could be made to the design. Thus, this swept design is considered to be more like a 1995 technology rather than a state-of-the-art 1990 technology.

Hover performance for the advanced-geometry rotor is shown in Figure 51. Maximum hover figure of merit is quite good, exceeding 0.80, but efficiency falls off rapidly at higher values of C_T/σ owing to the reduced $C_{l_{max}}$ of the thin airfoils. It should be noted that only in the past 5 years has rotor data become available for the relatively high disc loadings and high twists of tiltrotors such as the V-22 design. The data has shown that the hover figure of merit versus C_T/σ curve is much flatter than earlier predictions, retaining high figures of merit out to higher C_T/σ values. This suggests airfoil stall boundaries are not reached until higher C_T/σ values. One explanation of this discrepancy is that inboard inflow angles are lower than predicted, thus delaying the airfoils' stall conditions until higher C_T/σ . Regardless of the cause, it must be acknowledged that rotor thrust capability is generally beyond the predicted stall boundary, making current estimates conservative.

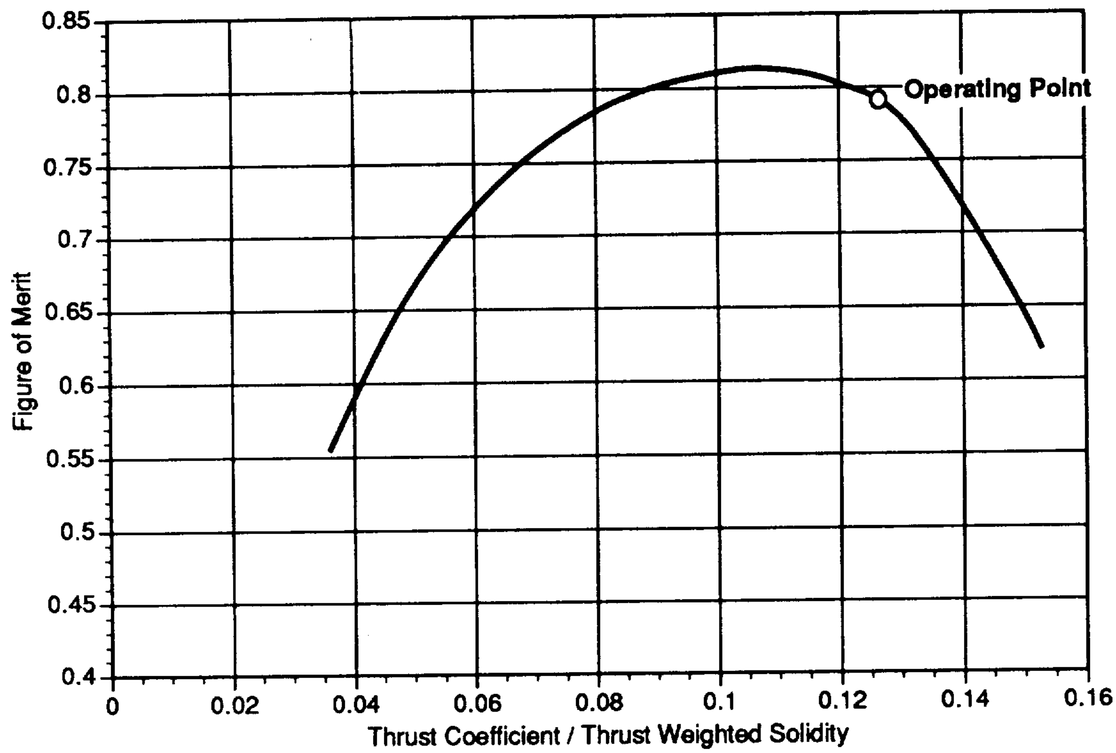

Figure 51. Civil Tiltrotor Hover Figure of Merit

Vehicle Performance

The high-speed civil tiltrotor was designed to the 600-nmi civil mission in the 30-passenger size using 1990 technology. This resulted in a 38,380-lb rotorcraft with a wing loading of 100-psf and a disc loading of 25-psf, shown in Figure 45. Two turboshaft engines of 8,700 shp each provide sufficient power to cruise at 450 knots, 25,000 ft, and to hover with one engine inoperative.

The high-speed civil tiltrotor flight envelope is shown in Figure 52. It would allow operation at altitudes up to about 32,000 feet, but at cruise speeds less than the 450-knot design speed. Operation at higher altitudes and somewhat lower speeds would provide substantial savings in fuel costs for a given range or could be taken as an increase in aircraft range. Maximum cruise speed capability for altitudes below about 24,000 feet is limited by the transmission torque limit, sized to the 450-knot design speed at 25,000 feet altitude. Maximum speed at higher altitudes and ceiling altitudes is determined by available power.

Lower airspeeds in the conversion envelope are limited by power available and by blade loads, depending on the nacelle angle. The conversion corridor limits, shown in Figure 53, indicate the nacelle angle required for force and moment trim of the rotorcraft versus airspeed for several fuselage pitch attitudes. The conversion corridor has assumed an autoschedule for flap settings; 40 degrees for nacelle angles greater than 60 degrees, 20 degrees for nacelle angles less than 60 but greater than 0 degrees, and 0 flap setting for 0 nacelle angle. The upper boundary is limited by transmission limits and the lower boundary is restricted by practical limits on the fuselage attitude reflecting the wing stall angle limit (about +20 degrees). The curve shows that full conversion to the airplane mode could be achieved with 1g flight, no flap deflection, at about 160 knots for a +10-degree attitude. Lower airspeeds could be trimmed in level flight using the flaps but would be subject to transmission torque limits.

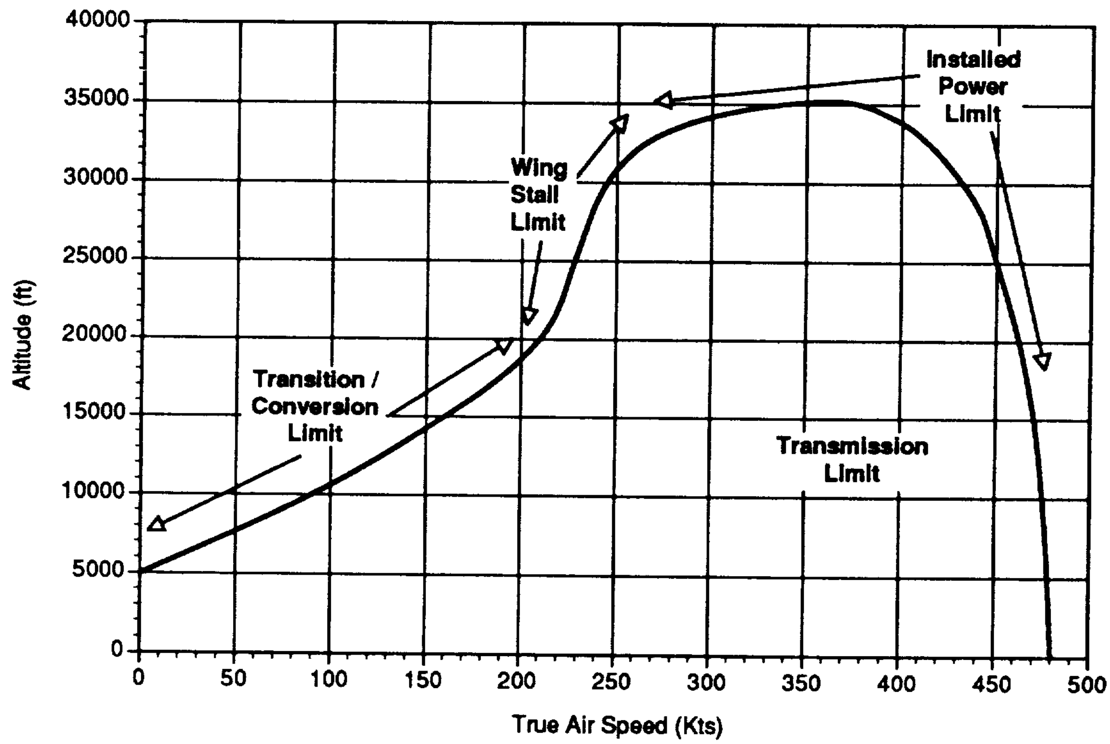

Figure 52. Civil Tiltrotor Flight Envelope

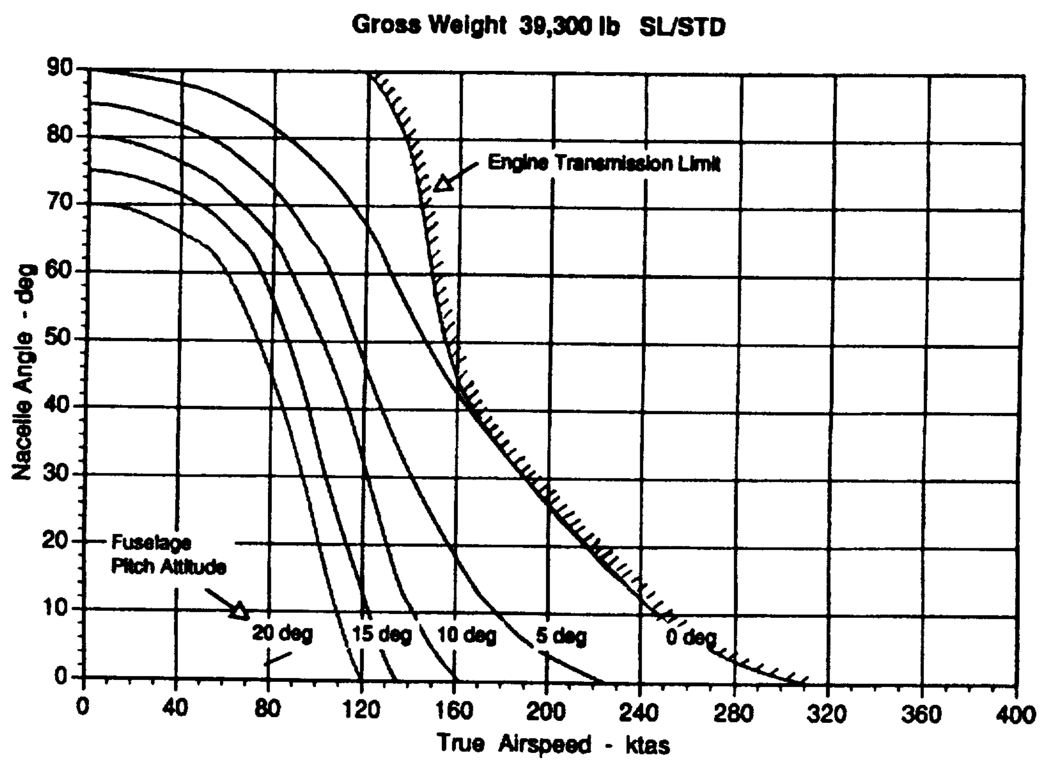

Figure 53. Level Flight Conversion Corridor for Civil Tiltrotor

Drag polars for the high-speed civil tiltrotor are shown in Figure 54 for several Mach numbers. The flat-plate area corresponds to a mean skin friction coefficient of 0.0043, which is not as good as jet transports (Figure 30). The wing sweep-and-thickness ratio combination push the occurrence of compressibility drag out beyond the 0.725 cruise Mach number, eliminating compressibility drag. The resulting lift-to-drag ratio (L/D) curves are shown in Figure 55 for SLS conditions. Maximum L/D is about 12, but L/D at the 450-knot cruise condition is down to 9.16 (ISA+15°C) because of choosing the 100-psf optimum wing loading; see Figure 44. As with the folding tiltrotor, cruise L/D is substantially improved at higher altitudes for the 450-knot design airspeed.

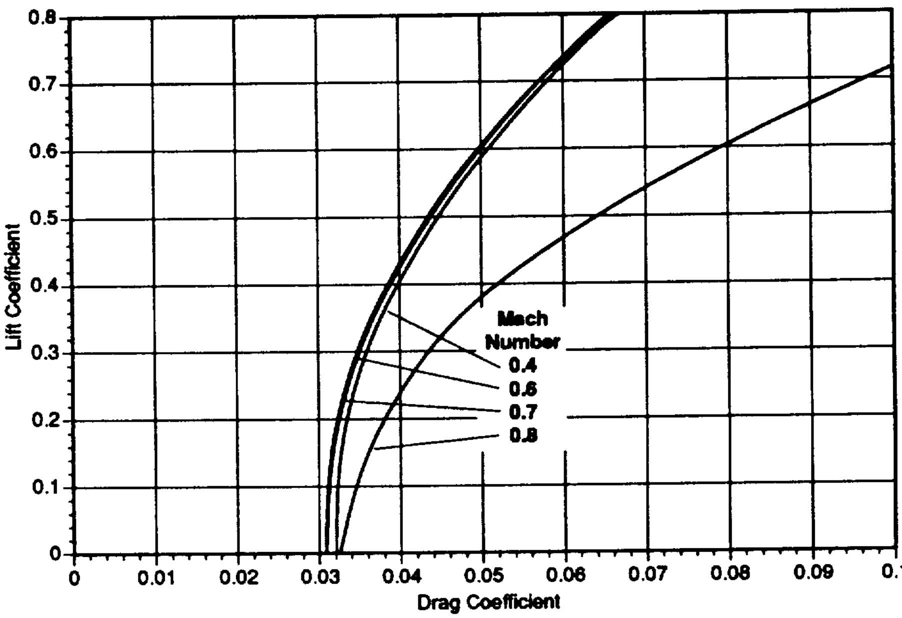

Figure 54. Civil Tiltrotor Drag Polar

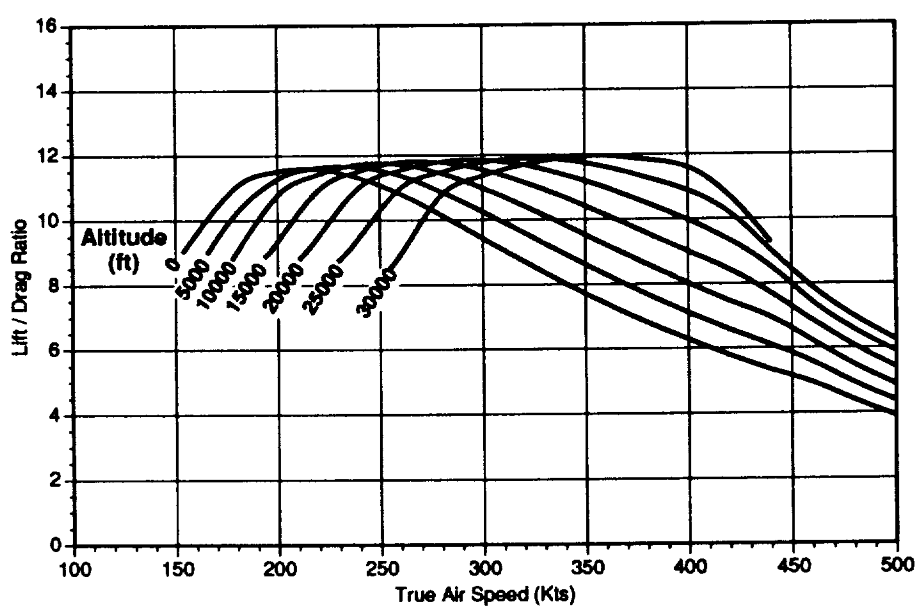

Figure 55. Civil Tiltrotor Lift / Drag Ratio (Standard Day)

The specific range curves in Figure 56 show the advantage of operating at higher altitudes. They also show a considerable fuel savings for rotorcraft operation at the long-range speed (99% best-range speed) rather than the specified 450 knots true airspeed. This suggests an operational tradeoff between direct fuel costs (favoring the lower speed) and other maintenance costs which are more directly related to flight hours (favoring the 450-knot speed). Such an evaluation is an important factor in building commercially competitive aircraft but was beyond the scope of this study.

Many more details on the high-speed civil tiltrotor's performance and other characteristics have been generated; these can be found in Appendix B.

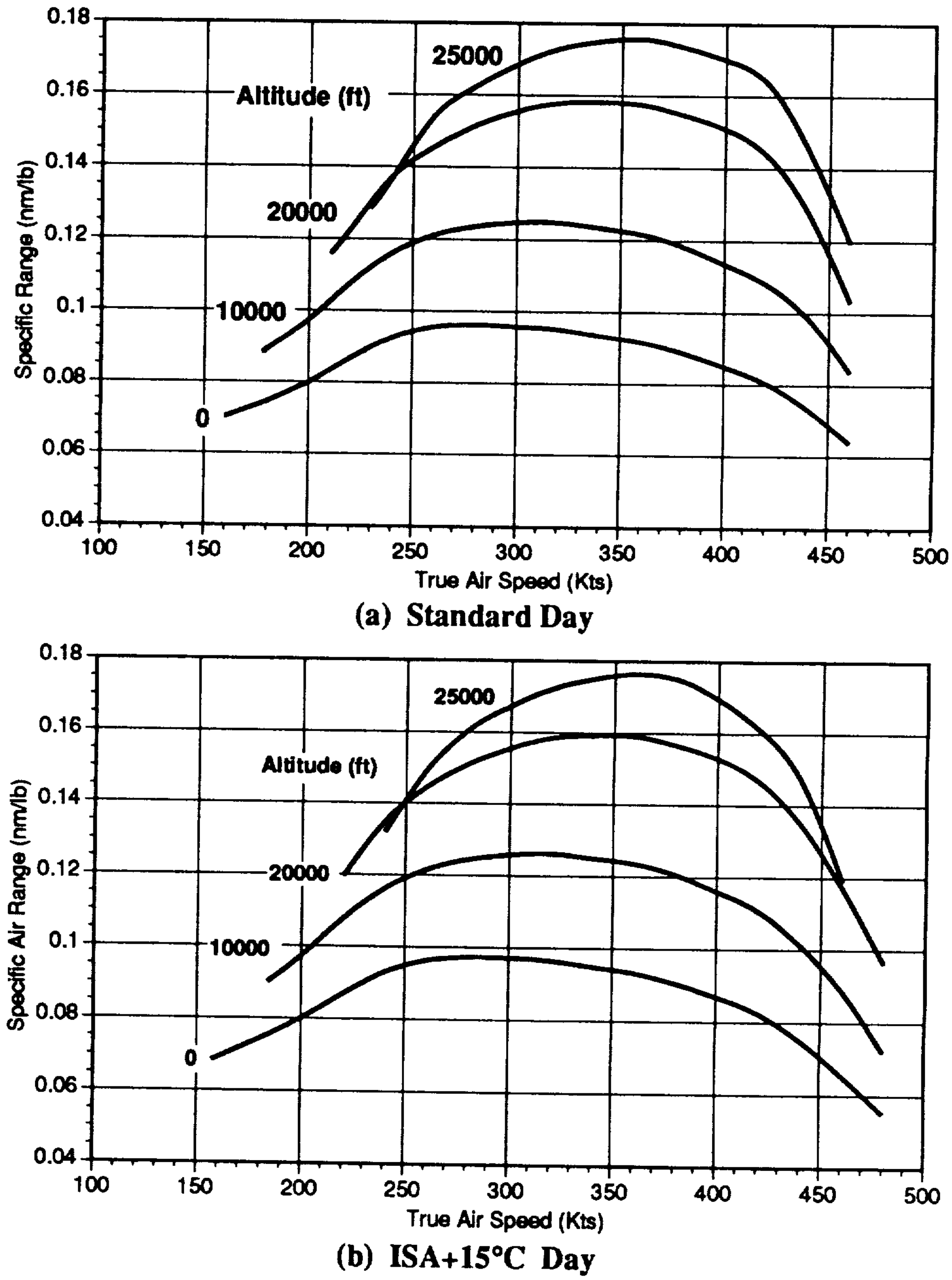

Figure 56. Civil Tiltrotor Specific Range

Acoustics

Special attention was given to the civil tiltrotor's acoustic characteristics in recognition of the external-noise importance to community acceptance and of the internal-noise importance to passenger comfort and acceptance. An overview of these results is included here. A more detailed discussion and graphs of the acoustic noise spectrum are provided in Appendix B.

ICAO Departure, Flyover, and Approach Noise Levels - Currently, neither the FAA nor ICAO (International Civil Aviation Organization) has developed certification levels or procedures for tiltrotor aircraft; therefore the procedures for helicopter certification given in Reference 39 have been applied. The tiltrotor has many varied options for approach, flyover, and departure methods which could be used to reduce or redistribute the resultant noise. For the purpose of this report the helicopter certification procedures have been followed. The resultant predictions show that the levels required for ICAO certification can be met by the tiltrotor, though consideration to engine noise and blade-vortex interaction noise is required. These results are summarized in Table 10.

Table 10. Summary of Predicted Civil Tiltrotor Perceived Noise Levels

(ICAO PROCEDURES)

CONDITION	ESTIMATED NOISE (EPNdB)	ICAO STANDARD (EPNdB)
Departure (80 knots, 60° nacelle, 2800 fpm R/C)	101.0	102.5
Flyover (180 knots, A/P mode, 500 ft altitude)	91.0	101.5
Approach (80 knots, 6° glide slope, 60° nacelle)		
With BVI	105.3	103.5
Without BVI	103.7	

NOTE: Normal engine installation

The predicted departure effective perceived noise level (EPNL) for the high-speed civil tiltrotor with a normal engine installation is 101, which is below the ICAO standard level of 102.5. The ICAO procedure specifies that the best rate of climb speed, Vy, is used, which was determined to be 80-knots for the civil tiltrotor with a nacelle tilt of 60 degrees and a rate of climb of 2,800 feet per minute. Rotor-loading noise predominated, with the engine noise contributing only a small amount.

The predicted flyover EPNL for the high-speed civil tiltrotor with a normal engine installation is 91 EPNL, which is considerably below the ICAO standard of 101.5. The airplane mode was used in calculating the flyover noise at a flight speed of 180-knots. The lightly loaded rotors are very quiet in the airplane mode. The flyover noise is therefore dominated by the engine noise, which could be acoustically optimized either in design and/or with acoustic treatments. Predicted EPNL levels for the centerline and sideline microphones are summarized in Table 10.

The predicted approach noise level for the high-speed civil tiltrotor with a normal engine installation and assuming no blade-vortex interaction (BVI) noise is 103.7, which nominally meets the ICAO standard level of 103.5. Rotor-loading noise was found to dominate the approach EPNL, but engine noise and blade-vortex interaction noise components were also found to be significant contributors. Possible noise abatement approach procedures (i.e. flight profiles) could also reduce and/or redistribute the resulting noise footprint.

The hover sideline sound spectrum was predicted at a 500-foot sideline position for the high-speed civil tiltrotor hovering at a 100-foot altitude. Engine noise, rotor-loading noise, rotor broadband noise, and blade-vortex interaction noise all contributed to the total noise levels. The resulting dBA and dBC levels are given below, along with the resultant levels for several acoustic optimizations.

	DISK LOADING (PSF)	WITH ROTOR BVI	dBA	dBC
Normal Installed Engine	25	Yes	90.5	95.3
Acoustically Optimized Engine	25	Yes	88.1	93.9
Acoustically Optimized Engine	25	No	87.6	93.0
Acoustically Optimized Engine	20	No	85.5	90.8
Acoustically Optimized Engine	19	No	85.1	90.3

The engine compressor noise could be reduced by increasing the inlet guide vane-to-fan spacing, or inlet duct acoustic treatment could be considered. Further reductions in the sound pressure levels could be obtained by reducing the blade-vortex or blade-wake interaction noise. Additional reductions are achievable by reducing the disc loading. A 20-psf disc loading, versus the 25-psf design, would give an aggregate reduction of 5 dBA and correspond to a 3.7-ft increase in rotor diameter. Increases to the rotor diameter would also require an increase in wingspan.

Military Folding Tiltrotor

Rotor Performance

The rotor system for the military folding tiltrotor must be designed for reasonable hover efficiency and for contour compatibility with the nacelle when in the folded mode. The prop-rotor airplane mode was not a critical factor for the folding tiltrotor since loiter time in the military mission was performed in the folded, turbofan mode. The rotor is not used in high-speed flight, so the design is not restricted by the need to operate in a high-Mach-number environment. Thus, it can use relatively thick blade airfoils like those on the V-22 rotor, which have high values of maximum lift coefficient ($C_{l_{max}}$). High $C_{l_{max}}$ allows the rotor to be designed with a lower solidity ratio, saving rotor and hub weight. Rotor solidity is sized for a hover $C_T/\sigma = 0.146$ at SL ISA+15°C for a 750-fps tip speed. This also just meets the 1.7g low speed maneuver requirement at the selected wing loading of 90-psf; see Appendix B, Figure B-54.

The turbofan cruise at 450-knots determined installed power, providing more than ample power for hover and thereby alleviating the need to optimize rotor geometry for hover performance. So takeoff and the 15-minute midpoint hover became the most important rotorborne flight modes. Several blade twist distributions were examined to quantify its influence on hover figure of merit and cruise propulsive efficiency. The best cruise twist would be over 50 degrees of nonlinear twist, whereas the best hover twist would be 25 to 30 degrees, depending on the operating thrust coefficient, see Figure 57. Samples of folded blade arrangements for three- and four-bladed rotors

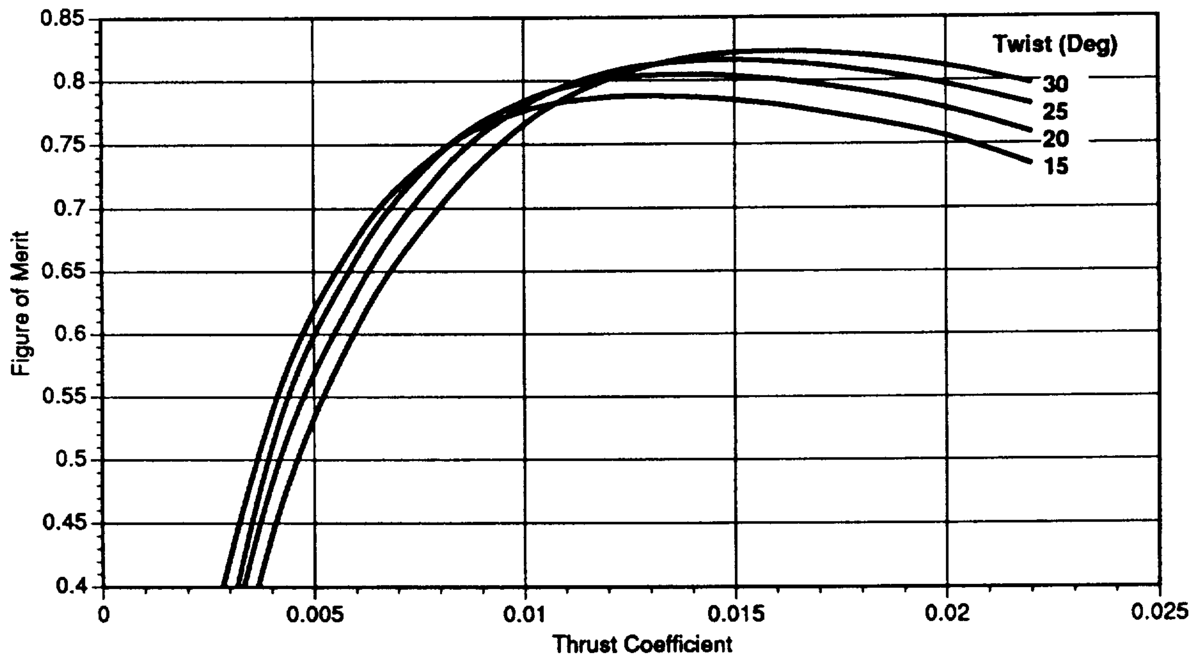

Figure 57. Effect of Linear Twist on Military Folding Tiltrotor Hover Figure of Merit

are shown in Figure 58. Folding schemes for high-solidity rotors and for rotors with more than four blades would probably require an increase in tip pod diameter. First-order estimates of the folded blade-nacelle compatibility issue were made by constructing three-dimensional CATIA drawings for a four-bladed rotor and nacelle. A blade with 20 degrees of linear twist is shown in Figure 59 laid flatwise into a nacelle cutout. This was found to be marginally acceptable, with the blade inboard trailing edge digging rather substantially into the nacelle contours. If the inboard trailing edge were moved up to better conform to the nacelle, then the tip trailing edge would be sticking out into the airstream. This diagram shows the spatial problem. It does not provide a solution, but it does point to the need for definitive work in this area to achieve aerodynamically clean contours and perhaps low signature contours. A compromised linear blade twist of 20 degrees was chosen from this very cursory examination, yielding a very acceptable hover figure of merit of about 0.77 at design gross weight.

The prop-rotor cruise efficiency for the chosen twist and solidity is shown in Figure 60 as a function of thrust coefficient, C_T. The operating C_T is spotted on the curve for three airspeeds.

LUBRICATED BEARINGS

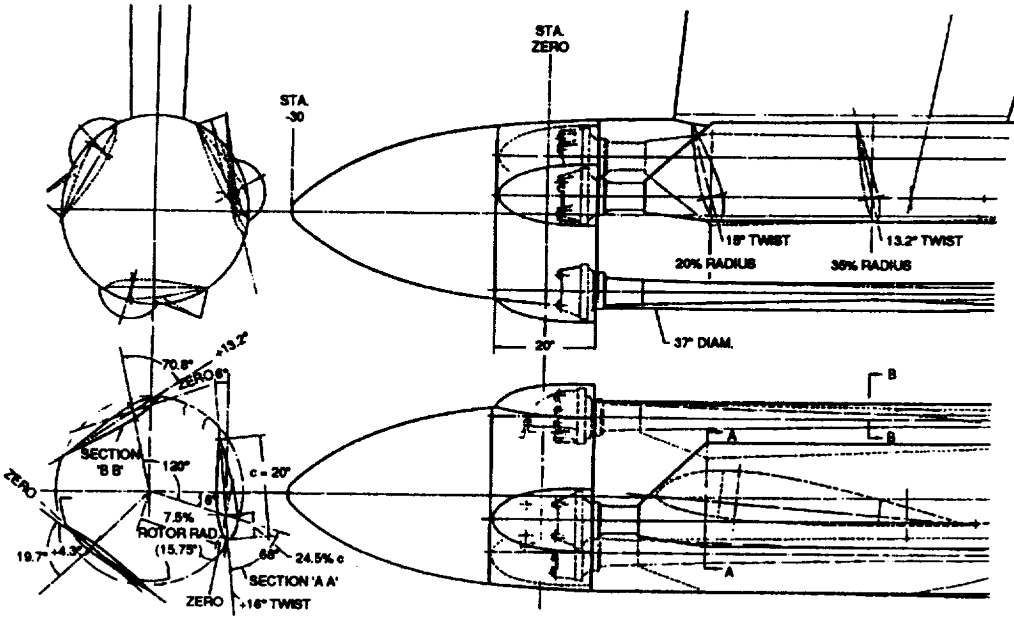

(a) 3-Bladed

FOUR-BLADE GIMBALLED STIFF-IN-PLANE FLEX-BEAM/ELASTOMERIC

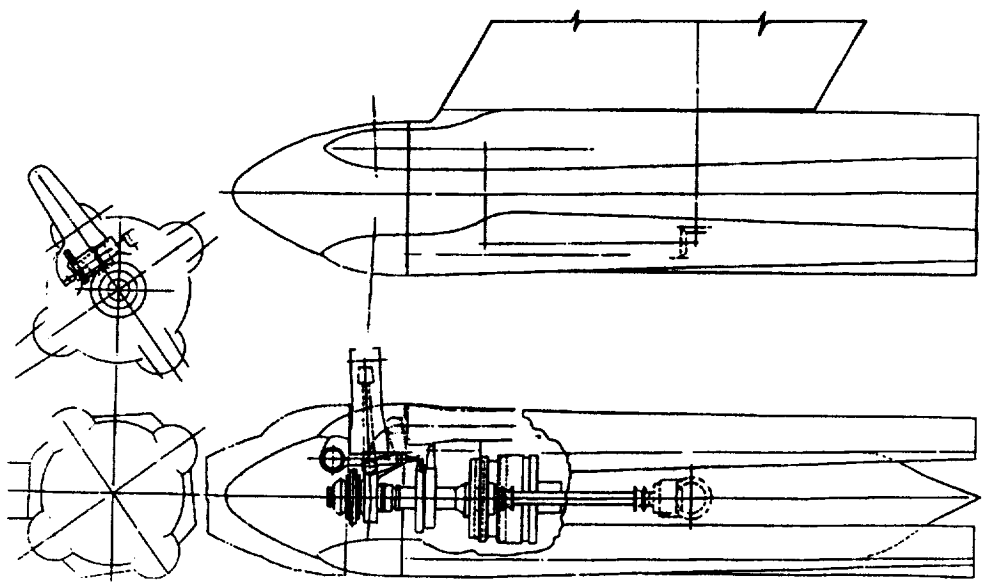

(b) 4-Bladed

Figure 58. Folded Rotor Schematic Diagrams

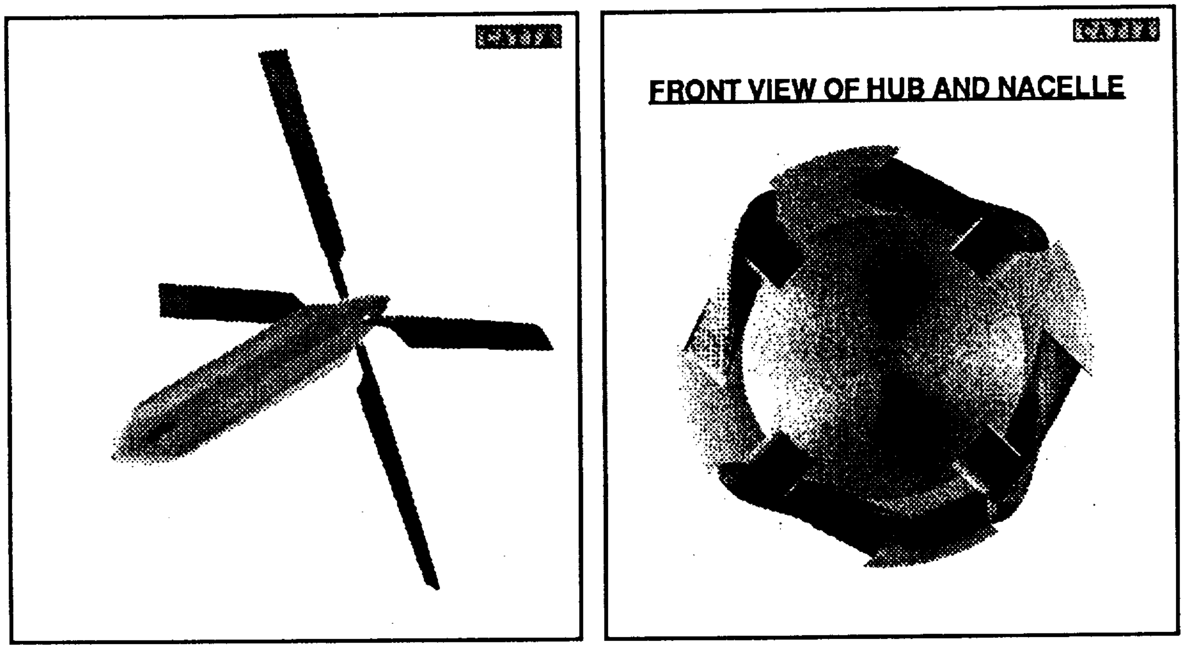

Figure 59. 3-D CATIA Models for Military Folding Tiltrotor

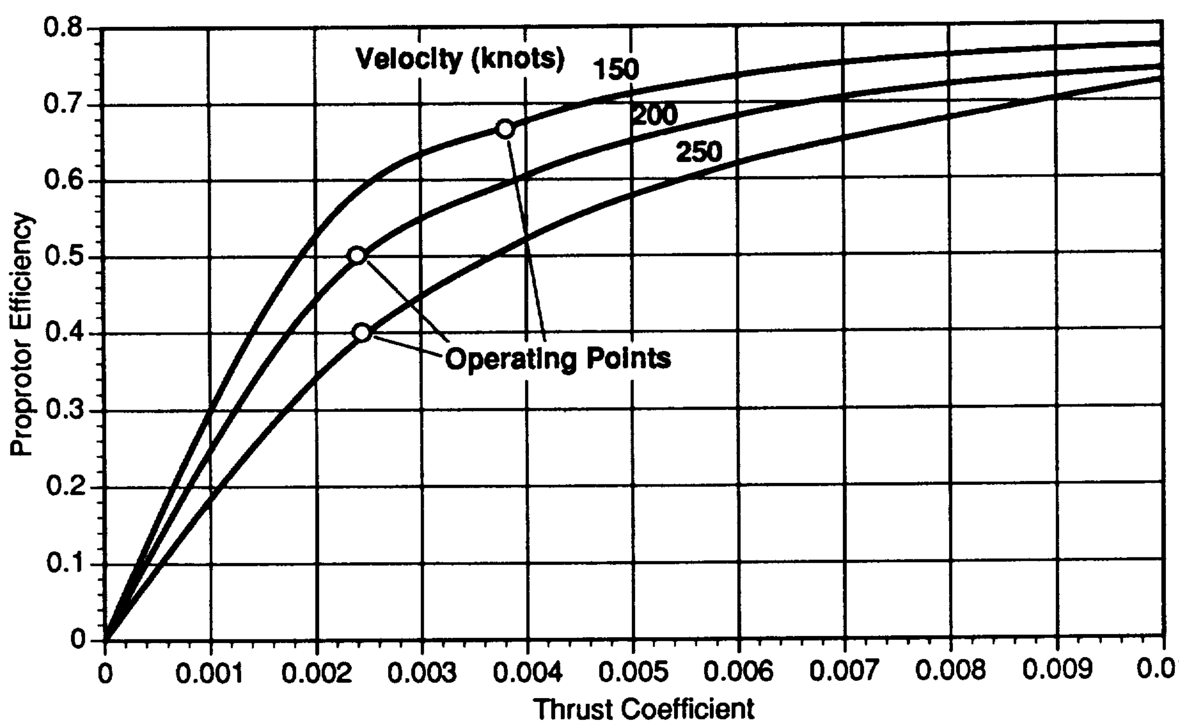

Figure 60. Military Folding Tiltrotor Prop-Rotor Cruise Propulsive Efficiency

Vehicle Performance

Overall vehicle performance was generated for the folding-tiltrotor geometry described in Table 9. All cruise performance was generated for the turbofan mode of operation. The flight envelope is shown in Figure 61. In the airplane mode with blades folded the flight envelope is limited in the same way as a conventional turbojet fixed-wing airplane.

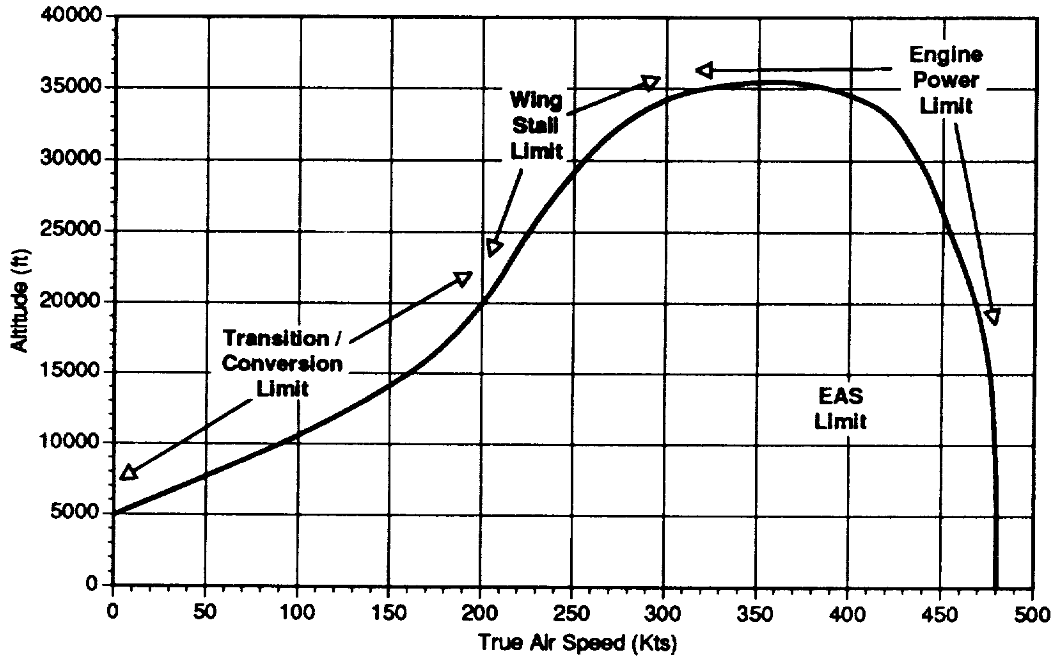

Figure 61. Military Folding Tiltrotor Flight Envelope for Standard Day

The folding tiltrotor's maneuver capability in the helicopter mode and turboprop mode would likely be similar to that of the V-22, but would of course be designed to the required capability. Sustained maneuver capability during transition to the turbofan mode is not expected to be affected by the rotor stop and fold process. However, an automated and fully reversible stop and fold process is considered to be necessary for any production folding tiltrotor, and the development of this process would naturally consider such effects as hub loads and blade loads. Further discussion of the automated process can be found in Section 3 Enabling Technology Plan and some additional discussion of the stop and fold maneuverability is given in Appendix B. Finally, maneuver capability in the turbofan mode is completely free of prop-rotor boundaries such as hub loads or whirl-flutter instability.

Lower airspeeds in the conversion envelope are limited by power available and by blade loads, depending on the nacelle angle. The conversion corridor limits shown in Figure 62 indicate the nacelle angle required for force and moment trim of the rotorcraft versus airspeed for several fuselage pitch attitudes. The conversion corridor has assumed an autoschedule for flap settings: 40 degrees for nacelle angles greater than 60 degrees, 20 degrees for nacelle angles less than 60 but greater than 0 degrees, and 0 flap setting for 0 nacelle angle. The upper boundary is limited by transmission limits and the lower boundary is restricted by practical limits on the fuselage attitude reflecting the wing stall angle limit (about +20 degrees). The curve shows that full conversion to the airplane mode could be achieved with 1g flight, no flap deflection, at about 160 knots for a +10-degree attitude. Lower airspeeds could be trimmed in level flight using the flaps but would be subject to transmission torque limits.

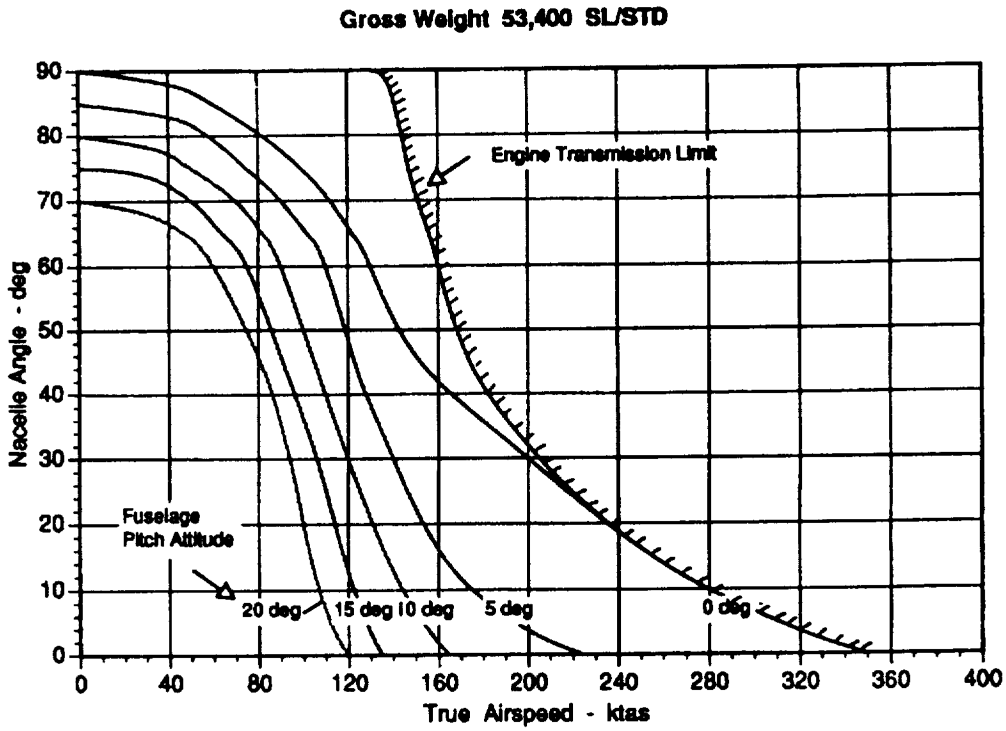

Figure 62. Level Flight Conversion Corridor for Military Folding Tiltrotor

The folding tiltrotor drag polar is shown in Figure 63 for several Mach numbers. The flat-plate area corresponds to a mean skin friction coefficient of 0.0044, being only slightly better than that of most turboprops but not as good as jet transports (Figure 30). The wing sweep-and-thickness ratio combination push the occurrence of compressibility drag out beyond the 0.725 cruise Mach

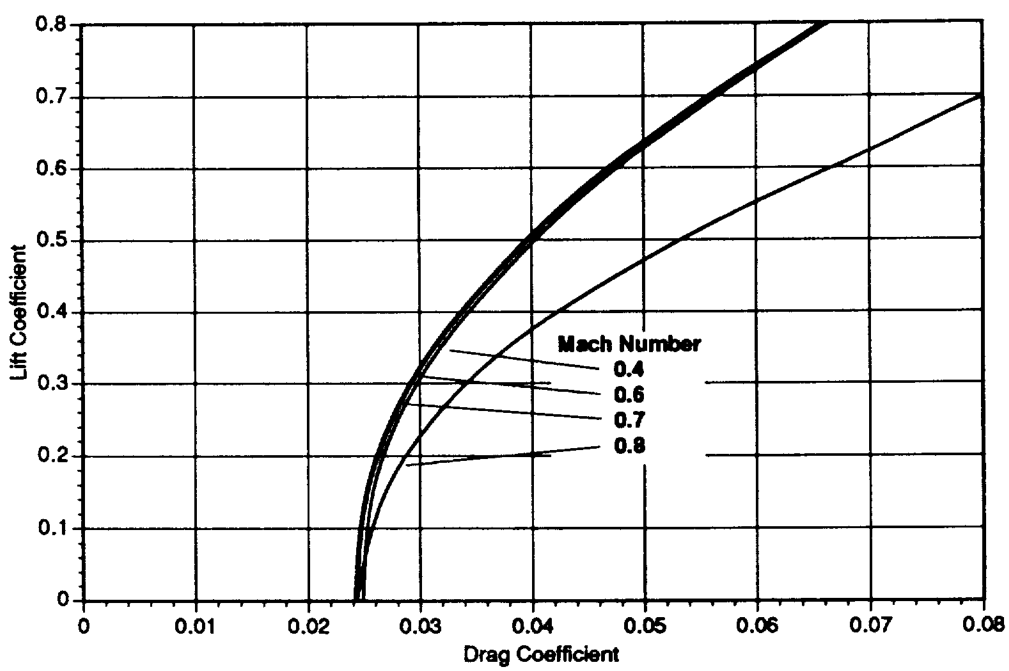

Figure 63. Military Folding Tiltrotor Drag Polar

number, eliminating compressibility drag. The resulting lift-to-drag ratio (L/D) curves are shown in Figure 64 at SLS conditions. The maximum L/D hardly changes with altitude, but clearly airframe L/D at a fixed 450-knot airspeed is significantly improved by cruising at higher altitudes. Reduced density requires a higher lift coefficient at higher altitudes, resulting in operation closer to the C_l for maximum L/D.

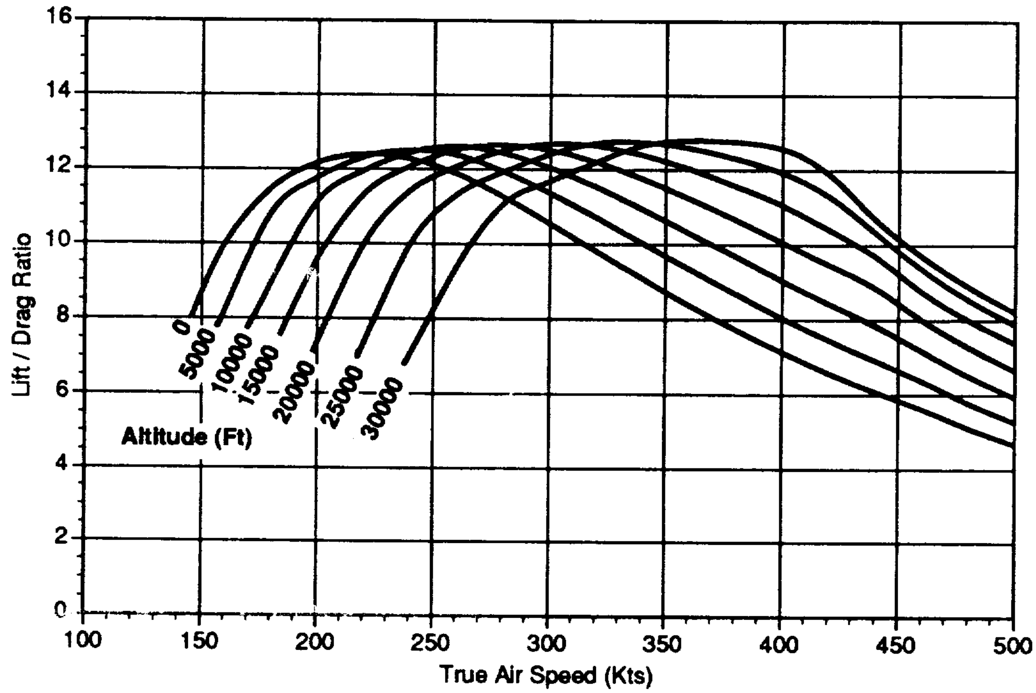

Figure 64. Military Folding Tiltrotor Lift / Drag Ratio (Standard Day)

Specific range is defined as speed divided by fuel flow to give nautical miles per pound of fuel. But fuel flow depends on many parameters such as airframe drag (L/D), altitude, ambient temperature, and the basic engine characteristics. For a given airframe, altitude and temperature (the L/D shown in Figure 64, at a 25,000-ft cruise altitude) the specific range then depends on engine performance. The data of Figure 65 show that peak specific range capability increases at higher altitudes even though maximum L/D hardly changes with altitude. This characteristic is an indication of the engine's basic performance improvement with altitude.

Many more details on the military folding-tiltrotor's performance and other characteristics have been generated and can be found in Appendix B.

Acoustics

External noise for the military folding tiltrotor may be a detection issue in the helicopter mode and turboprop airplane mode. Estimates were made for the 500-foot sideline noise for a folding tiltrotor hovering at a 100-foot wheel height.

Hover sideline sound spectra were predicted at a 500-foot sideline for the folding tiltrotor hovering at a 100-foot altitude. The resultant A-weighted and C-weighted levels with various combina-

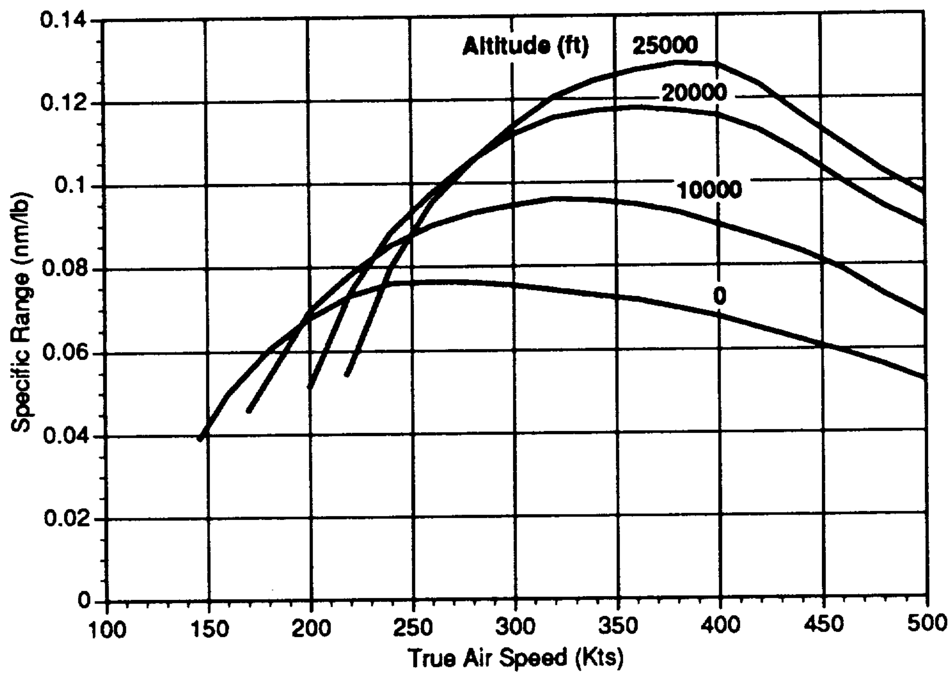

(a) Standard Day

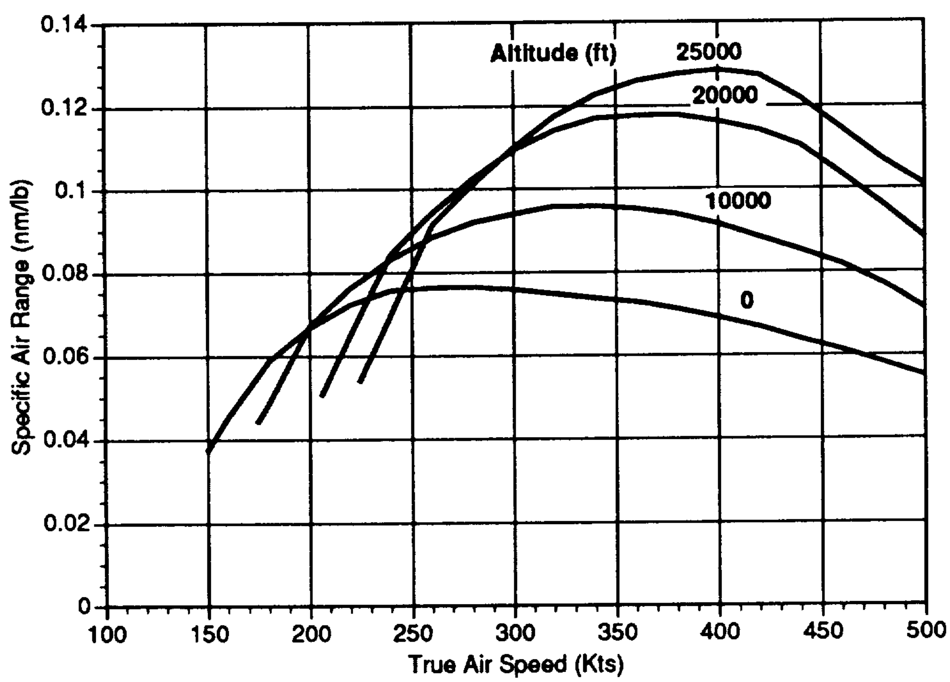

(b) ISA+15°C Day

Figure 65. Military Folding Tiltrotor Specific Range

tions of acoustical improvements are summarized in Table 11. Assuming a normal engine installation enclosed in an untreated nacelle, the engine combustor noise dominated. The treated engine corresponds to a modest 3-dB engine noise reduction by nacelle treatment. These calculations assumed rectangular-planform blades. If tapered blades were used the rotor noise would be reduced by approximately 2-dB. The resultant predicted A-weighted level with a normal engine installation was 96.7, and noise-reducing treatment to the nacelles would result in 94.7-dBA. Nacelle treatment to reduce combustor noise, allows the engine compressor noise to become the dominant contributor. The convertible engine has a VIGV/blade/VEGV spacing as low as 0.5 chords, whereas the data, which the prediction procedure of Reference 40 was based on, have 2.0 chords minimum spacing. A correction value of 8-dB was added to the predicted compressor noise levels to account for this. If the design of the engine was optimized for noise (increased VIGV/blade/VEGV spacings) the compressor noise could be reduced by 8-dB. The reduction of compressor noise, the reduction of the radiated combustor noise, and the tapered rotor blades resulted in predicted levels of 92.5-dBA and 98.2-dBC. Relative to the baseline design, this gives a reduction of approximately 5-dBA. Further reduction is achievable by reducing the disc loading from 25-psf to approximately 20-psf.

Table 11. Summary of Predicted Folding Tiltrotor Sideline Noise

	ROTOR NOISE ONLY	NORMAL ENGINE		TREATED ENGINE		ACOUSTICALLY OPTIMIZED ENGINE	
		ENGINE ONLY	ENGINE + ROTOR	ENGINE ONLY	ENGINE + ROTOR	ENGINE ONLY	ENGINE + ROTOR
Rectangular Blades							
dBA	92.8	95.4	97.3	92.4	95.6	87.5	93.9
dBC	99.3	97.4	101.5	94.4	100.5	90.4	99.8
Tapered Blades (from 75% outboard)							
dBA	90.9	95.4	96.7	92.4	94.7	87.5	92.5
dBC	97.4	97.4	100.4	94.4	99.2	90.4	98.2

Vehicle Sensitivity

Both the high-speed civil tiltrotor and the military folding tiltrotor were examined to quantify their sensitivity to changes in the mission design parameters and to changes in the technology. The following sections describe these sensitivities.

Design Parameter Sensitivity

Perturbations to the mission design parameters were made and the vehicle was resized to reflect the modified value. The following perturbations were made: (1) a 100% increase in hover time, (2) a 20% change in cruise L/D, and (3) changing the design cruise speed from 450-knots to 350-knots and to 500-knots.

A 100% change in hover time made very little difference to the civil tiltrotor, changing the total from 2 minutes to 4 minutes, a delta of only 2 minutes. However, a 100% change in hover time for the military folding tiltrotor affected not only the 1-minute takeoff and landing mission legs, but also the 15-minute midpoint HOGE requirement. This changed the folding tiltrotor hover time from 17 minutes to 34 minutes, a delta of 17 minutes of HOGE time. The resulting impacts on gross weight, empty weight, and installed shaft horsepower are shown in Figure 66. Perhaps a better comparison is the percentage of gross weight change per minute of additional HOGE. This yields a 0.4% growth in gross weight per minute of additional hover for the civil tiltrotor and 0.57% growth in gross weight per minute of additional hover for the military folding tiltrotor. Since the rotors have the same disc loading and nearly the same hover figure of merit, the different sensitivity must be a reflection of overall vehicle size and mission.

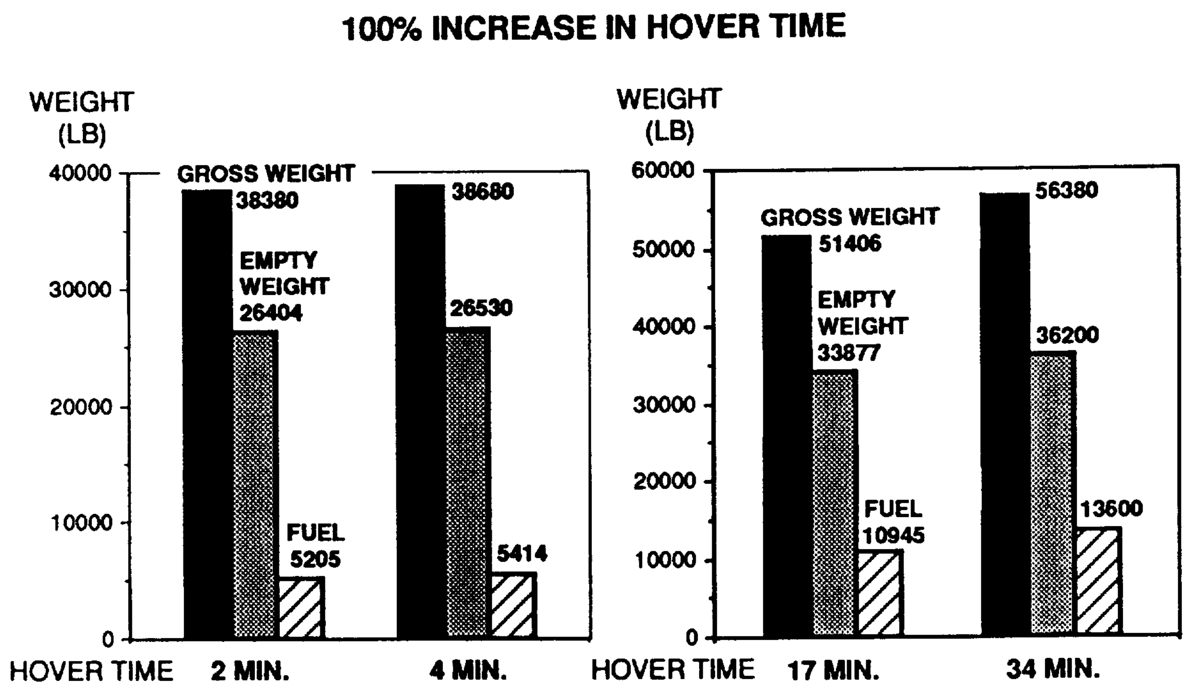

(a) High-Speed Civil Tiltrotor (b) Military Folding Tiltrotor

Figure 66. Sensitivity to Mission Hover Time

The cruise L/D was indirectly changed by modifying the flat-plate area in VASCOMP. This approach gave approximately 20% perturbations in the cruise L/D. Figure 67 shows the impact of this L/D change to the gross weight and power required for both concepts.

Concept sensitivity to design speed varied considerably between the prop-driven high-speed tiltrotor and the turbofan-driven folding tiltrotor. These differences are a consequence of concept attributes rather than mission application. Figure 68 shows the absolute growth of rotorcraft gross weight (pounds) and of installed shaft horsepower or thrust (shp or lb-t) for both the high-speed civil tiltrotor and the folding tiltrotor. The rotorcraft were resized for a lower design speed of 350-knots and a higher design speed of 500-knots to generate the curves. But the basic design choices of wing t/c and wing sweep angle and the prop-rotor design were unchanged from that based on a 450-knot speed. Thus, the rotorcraft push into drag divergence for the 500-knot design

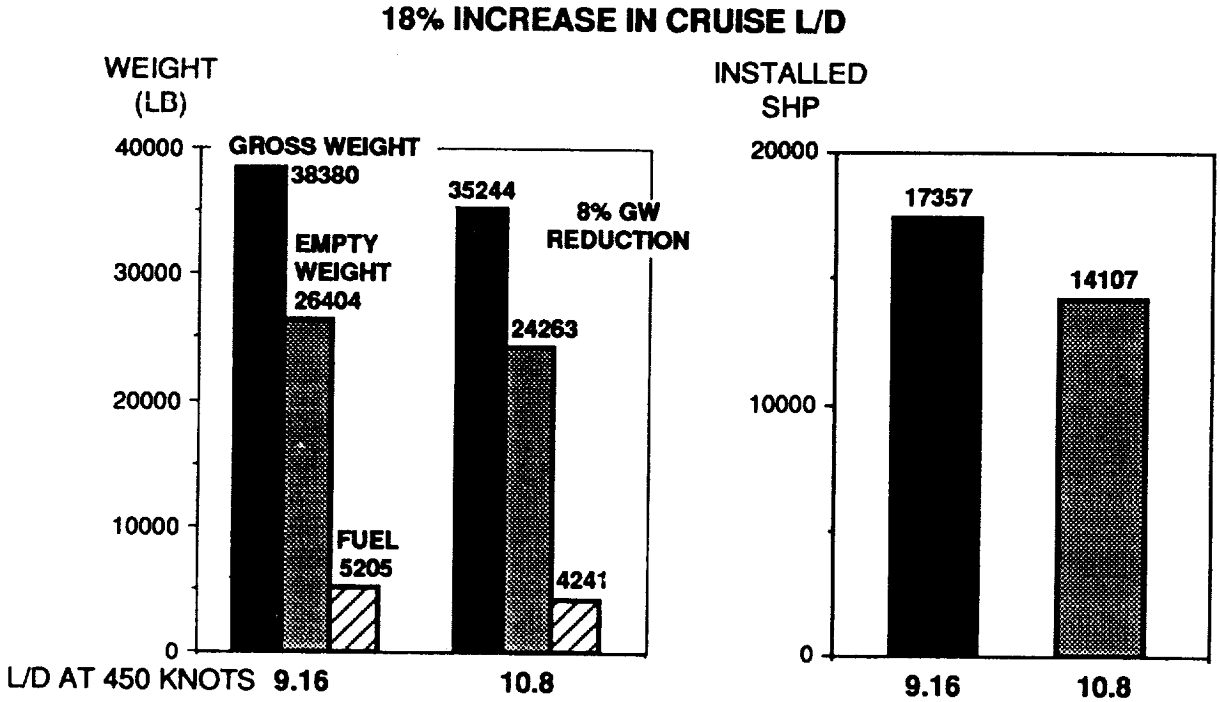

(a) High-Speed Civil Tiltrotor

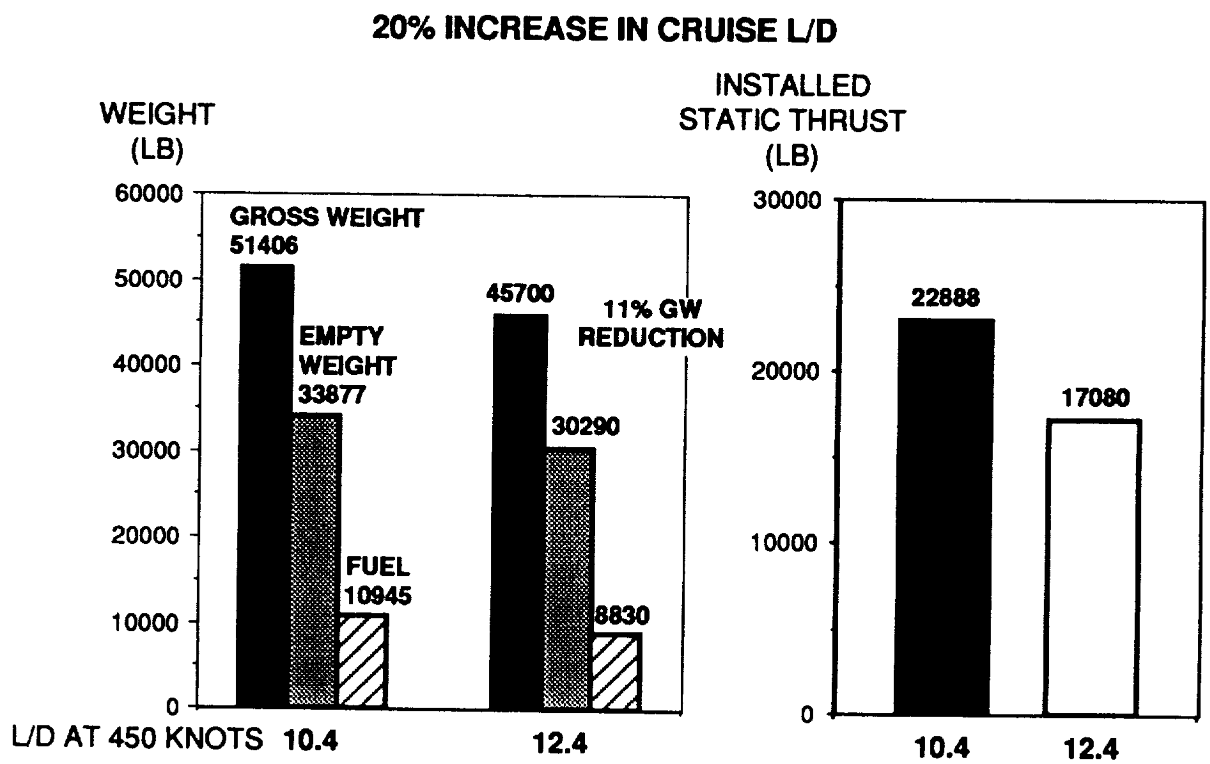

(b) Military Folding Tiltrotor

Figure 67. Sensitivity to Lift / Drag Ratio

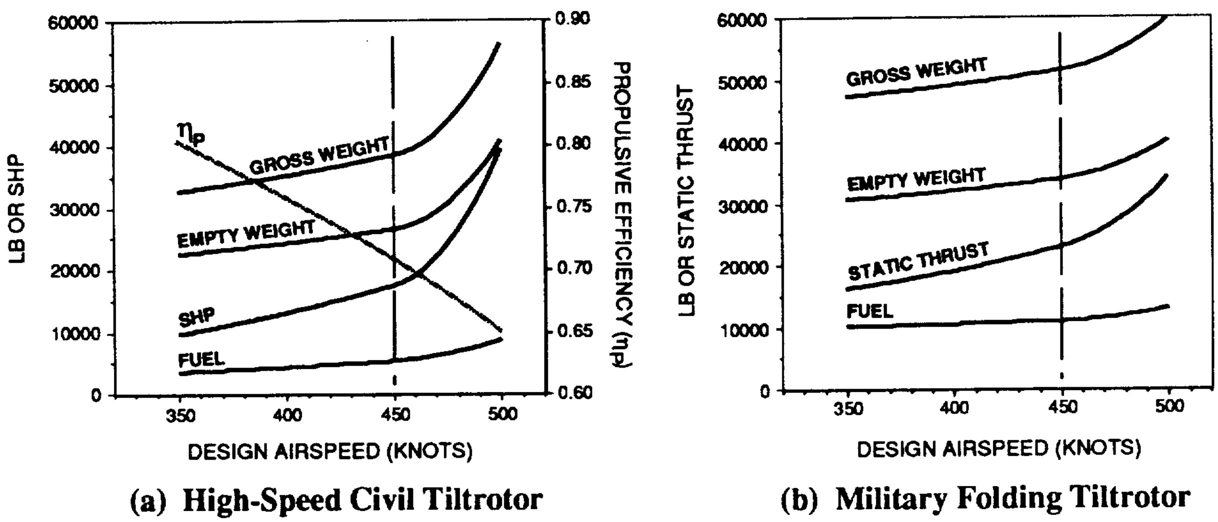

Figure 68. Sensitivity to Design Speed

speed, penalizing the size more than if they had been optimized for 500 knots. Likewise, the 350-knot design could take advantage of thicker wing sections, saving some wing weight, which would allow an optimum 350-knot design to be somewhat lighter than shown. Nevertheless, the trend is quite clear and the different sensitivity shown by the two different concepts is also quite clear. The high-speed tiltrotor is encroaching on fundamental Mach limitations for prop-rotor cruise efficiency, forcing it to much higher power requirements and substantially higher gross weights at the 500-knot design speed. Conversely, the folding tiltrotor growth is much less severe without the prop-rotor limitations. Furthermore, the folding tiltrotor's wing could be more easily redesigned to minimize drag divergence at 500 knots since it is unconstrained by the need to satisfy whirl flutter stability boundaries in high-speed cruise.

The comparison between the two concepts' sensitivity to speed is more readily seen on a relative scale as shown in Figure 69. At 500 knots the high-speed tiltrotor empty weight is over 50% greater than its 450-knot empty weight, whereas the folding tiltrotor's empty weight fraction increased by only 18% from its 450-knot value. The figure also shows that relative production costs (based on a 200-aircraft buy) track very closely with the empty weight trends.

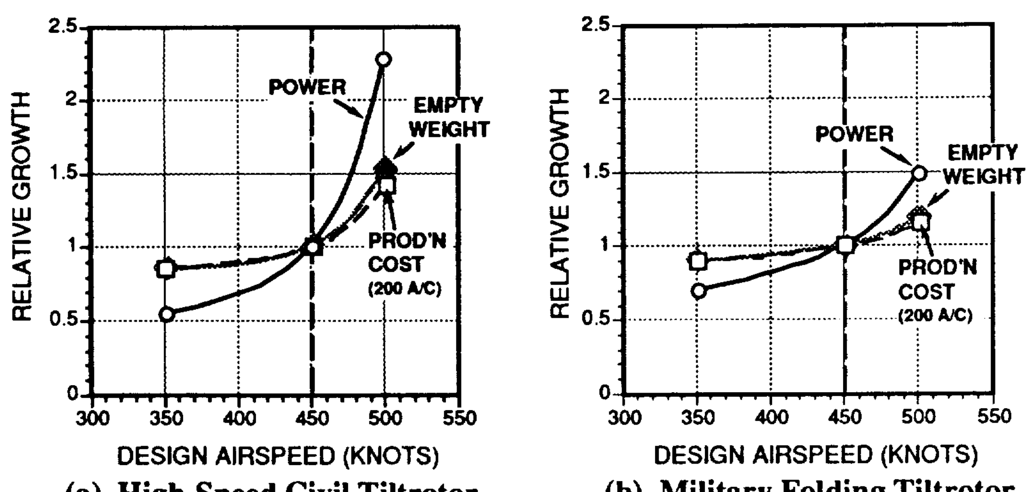

Figure 69. Relative Gross Weight and Cost Sensitivity to Design Speed

Technology Sensitivity

An assessment was made of year 2000 level capability in selected technology areas. These projections were then factored back into the VASCOMP sizing program and the vehicles were resized to reflect the advanced-technology impact. Finally, all of the advanced-technology changes were incorporated in one aircraft to assess the combined impact. This case was also cost-evaluated in comparison to the baseline 1990 technology.

Structures and Materials - Many new horizons are opening for advanced materials and manufacturing methods, but the experience base to put these into production aircraft is limited. A general discussion on the topic of structures and materials is included in Appendix B, Volume II of this report, but several significant ongoing programs are noteworthy. The NASA Advanced Technology Composite Airframe Structures Program (ATCAS) will be making substantial inroads to development and testing of large-scale composite airframes through 1994. The TransCentury Composite Aircraft Primary Structure (TCAPS) program will be developing and testing new techniques for advanced sandwich construction through 1997. Air Force programs are also focusing on composite fuselage manufacturing technology and the use of high-strength/modulus graphite construction. In addition, the Advanced Rotorcraft Transmission (ART) program is currently examining new and different uses of materials and means of fabrication in the area of rotorcraft transmissions, Phase II of which will provide hardware and test stand demonstrations through 1997.

An assessment of the impact on these programs on future weight savings was made by the weights and technology groups. Table 12 shows the percentage improvements which could be obtained by the year 2000 relative to the weights used for sizing the 1990 baseline rotorcraft. Often such projections turn out to be optimistic for two reasons. First, the funding required to develop the materials and structures technology is insufficient, so the potential improvements are not realized in production. Secondly, the improvements which are realized in production are not seen as a reduction in the rotorcraft gross weight because the weight savings are applied to enhance other areas (e.g., NBC hardening, acoustic and vibration improvements, better accessibility for improved maintenance, survivability enhancements, or higher power-to-weight ratios for improved speed/maneuverability). Still, the projected possible weight improvements of Table 12

Table 12. Year 2000 Relative Weight Improvements

ITEM	RELATIVE YEAR 2000 WEIGHT IMPROVEMENT	COMMENT
Structure		
- Body	15%	- Improved composites, manufacturing methods, expanded database, lower knockdowns, hi-modulus
- Landing Gear	3%	
- Wing	14%	
- Tail	11%	
Propulsion		
- Engines	21.8%	- IHPTET Phase II
- Drive system	14.5%	- Load limiting features, advanced rotorcraft transmission
- Fuel system	5.5%	
Rotor Group	5.5%	- Advanced composites
Flight Controls	8%	- CPU advancement, FBW/FBO, composite actuator casings, hi-pressure hydraulics

were used to resize the aircraft in order to assess the aircraft sensitivity to weight improvements. The results are shown in Figure 70. The military folding tiltrotor showed a 10% gross weight reduction and the high-speed civil tiltrotor showed a 17% gross weight reduction. The civil tiltrotor's turboshaft engine benefited more from the IHPTET Phase II specific fuel consumption (SFC) objectives than did the folding tiltrotor's convertible engine, which was treated as a turbofan engine for this analysis. So results indicate about a 10% potential reduction in gross weight due to improvements in engine weight, structure weight, drive system, and flight controls weight, without the SFC improvements.

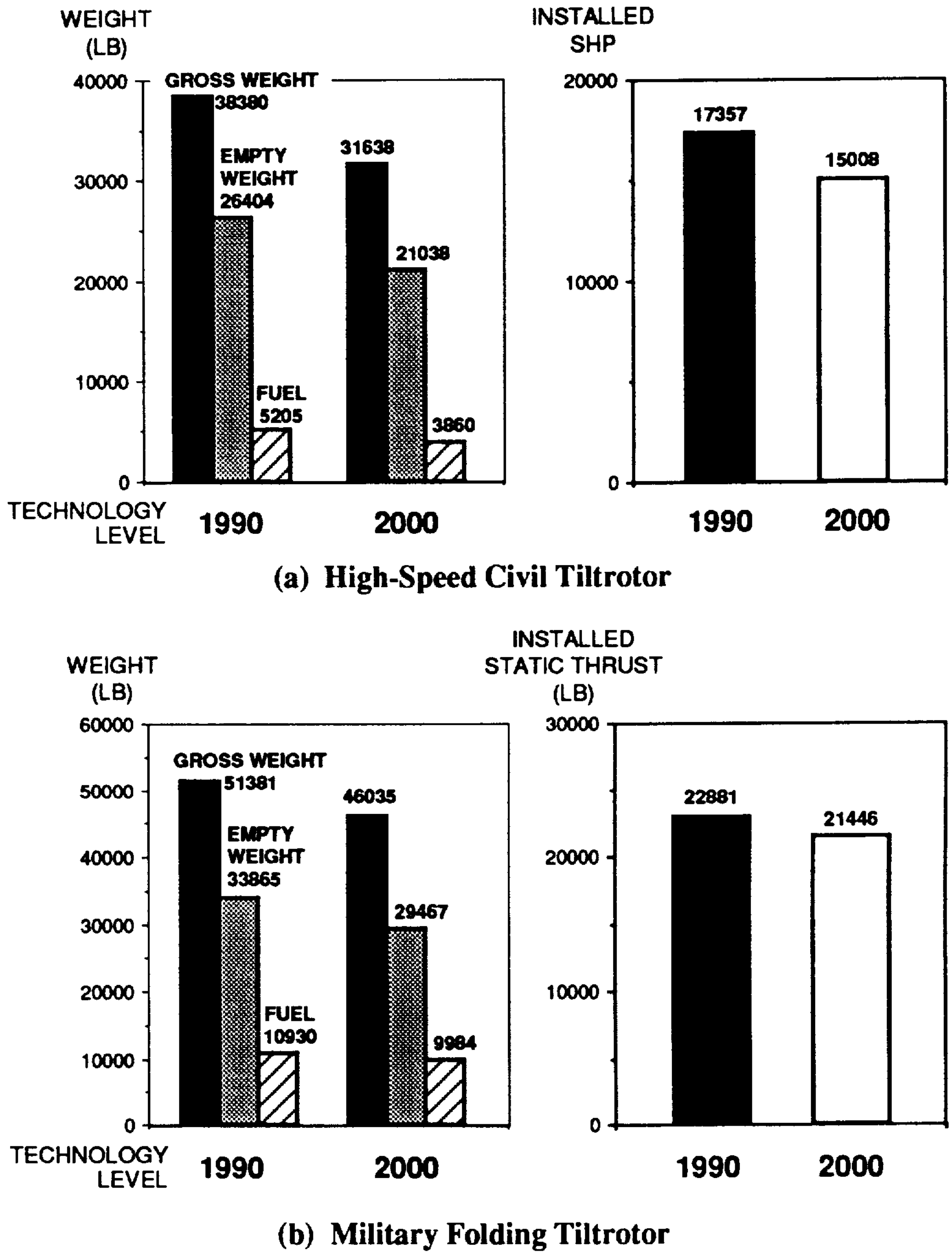

Figure 70. Sensitivity to Component Weight Improvements

Rotor System - Technology improvements in the rotor system are seen to be most significant for the high-speed civil tiltrotor in order to achieve the projected cruise propulsive efficiency. The advanced swept-geometry blade poses design issues in the technical disciplines of aerodynamics, dynamics, loads, and structures. It is also very likely to require more accurate manufacturing tolerances to ensure that blade contours and properties are consistent between blades. This is anticipated because of the expected sensitivity of the blade in its high-Mach-number cruise environment. The improved cruise propulsive efficiency for the swept-blade geometry shown in Figure 50 was used to resize the civil tiltrotor, all other design variables remaining fixed. The improved propulsive efficiency gave a 16.5% reduction in shaft horsepower which drove a 7.3% reduction in gross weight (Figure 71).

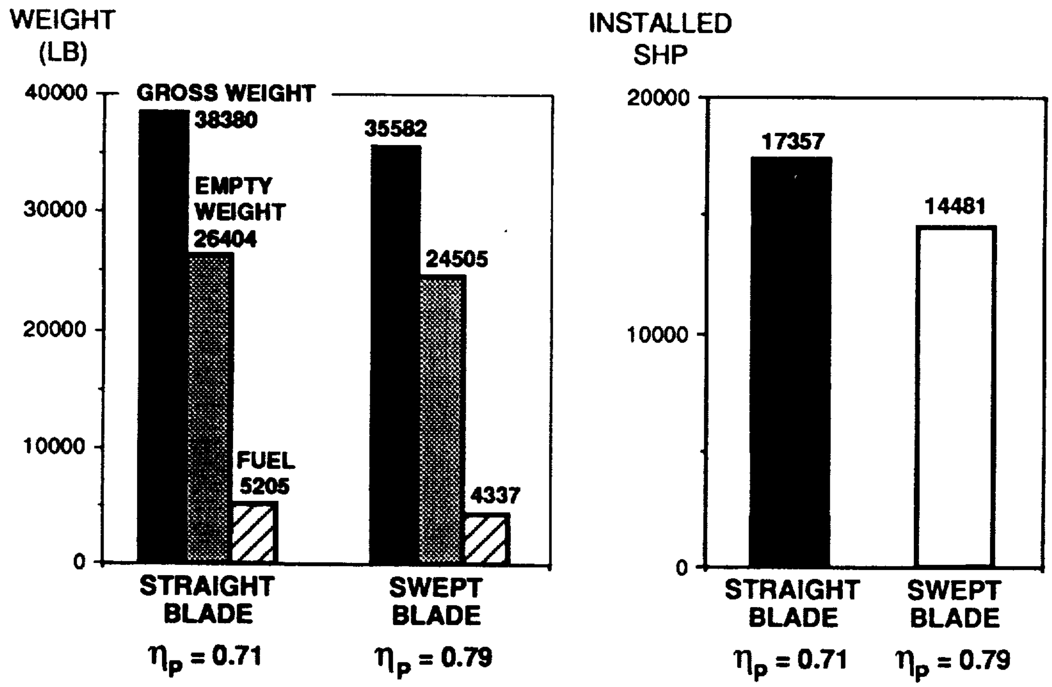

Figure 71. Civil Tiltrotor Sensitivity to Rotor Propulsive Efficiency

Propulsion System - The advanced engine characteristics were taken from the IHPTET Phase II objectives with respect to the IHPTET Phase I objectives. The turboshaft objectives were applied to the high-speed civil tiltrotor and the turbofan objectives were applied to the military folding tiltrotor. As shown below, the turbofan SFC objective improvement for Phase II is not as much as for the turboshaft SFC. Consequently, the concept sensitivity evaluation is not on the same percentage basis for the civil tiltrotor and for the military folding tiltrotor. Instead, the evaluation is based on technology improvements which are considered feasible by the year 2000.

	IHPTET	IHPTET	PHASE II PERFORMANCE
SHP/lb	Phase I	Phase II	Relative to Phase I
Turboshaft	+40%	+80%	+28% higher
Turbofan	+33%	+67%	+25% higher
SFC			
Turboshaft	-20%	-30%	12.5% lower
Turbofan	- 5%	-10%	5.3% lower

Figure 72 shows the results of resizing the civil tiltrotor and the military folding tiltrotor to the propulsion system improvements above. Both concepts experienced a 10% reduction in gross weight from the IHPTET Phase II technology. However, the folding tiltrotor's gross weight reduction was for less of a percentage improvement in the SFC, indicating it is more sensitive to fuel flow than is the civil tiltrotor.

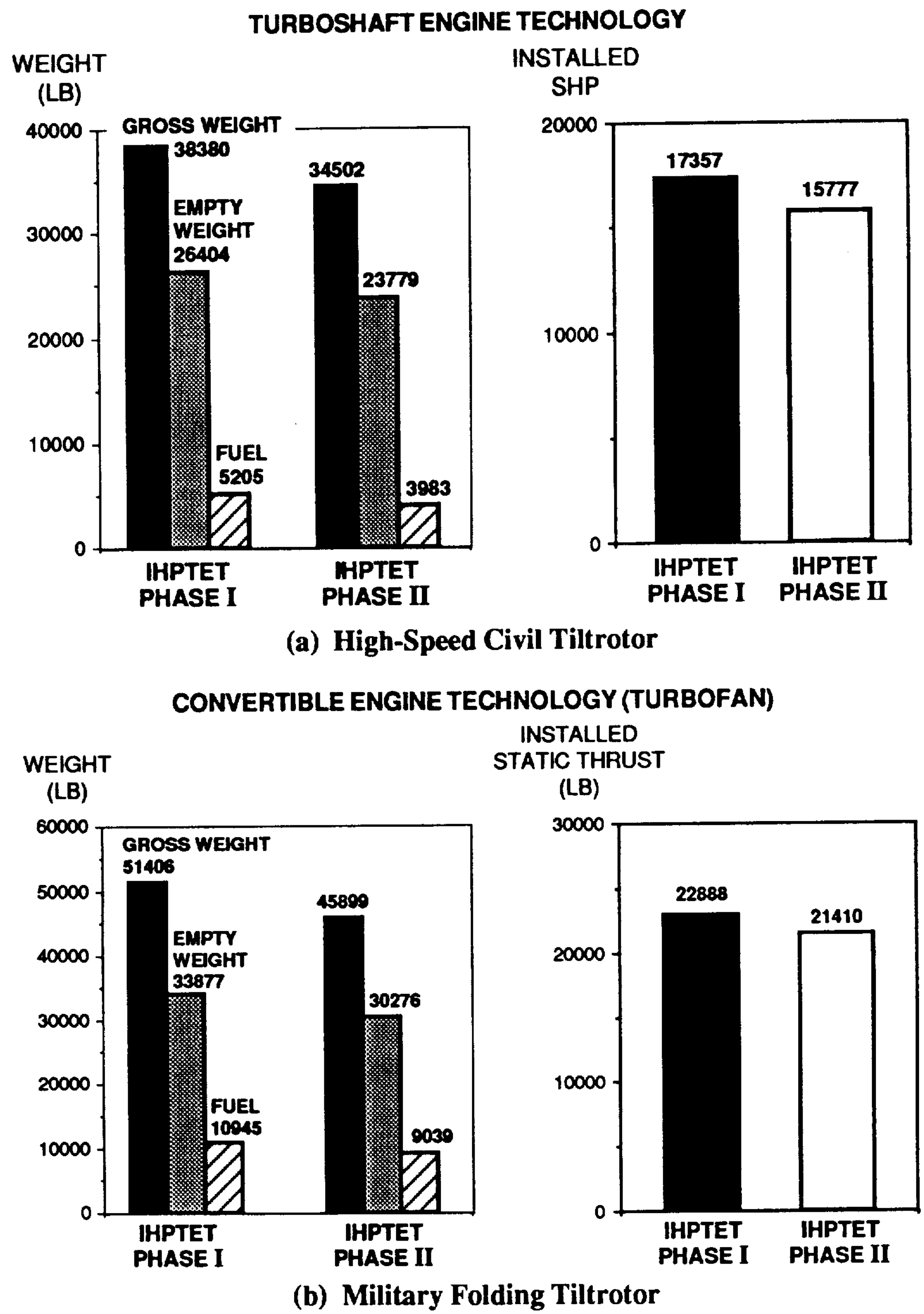

Figure 72. Sensitivity to Propulsion System Improvements

Combined - The advanced technologies described above were applied all together to assess the total net impact of technology improvements on the rotorcraft gross weight. The changes are summarized in Table 13 below. Figure 73 shows the results in bar chart form. Both the civil tiltrotor and the military folding tiltrotor showed 25% reductions in gross weight from the combined effect of year 2000 technology.

Table 13. Combined Effect of Advanced Technologies

	HIGH-SPEED CIVIL TILTROTOR		MILITARY FOLDING TILTROTOR	
TECHNOLOGY LEVEL:	1990	2000	1990	2000
Lift / Drag Ratio	9.16	10.8	10.4	11.7
Weight Improvements		Table 12		Table 12
Propulsive Efficiency	0.71	0.79	–	–
Engine Characteristics	IHPTET	Turboshaft	IHPTET	Turbofan
Design Gross Weight	38,380	28,609	51,381	38,720
Installed Power or Thrust	17,357	11,065	22,881	16,810

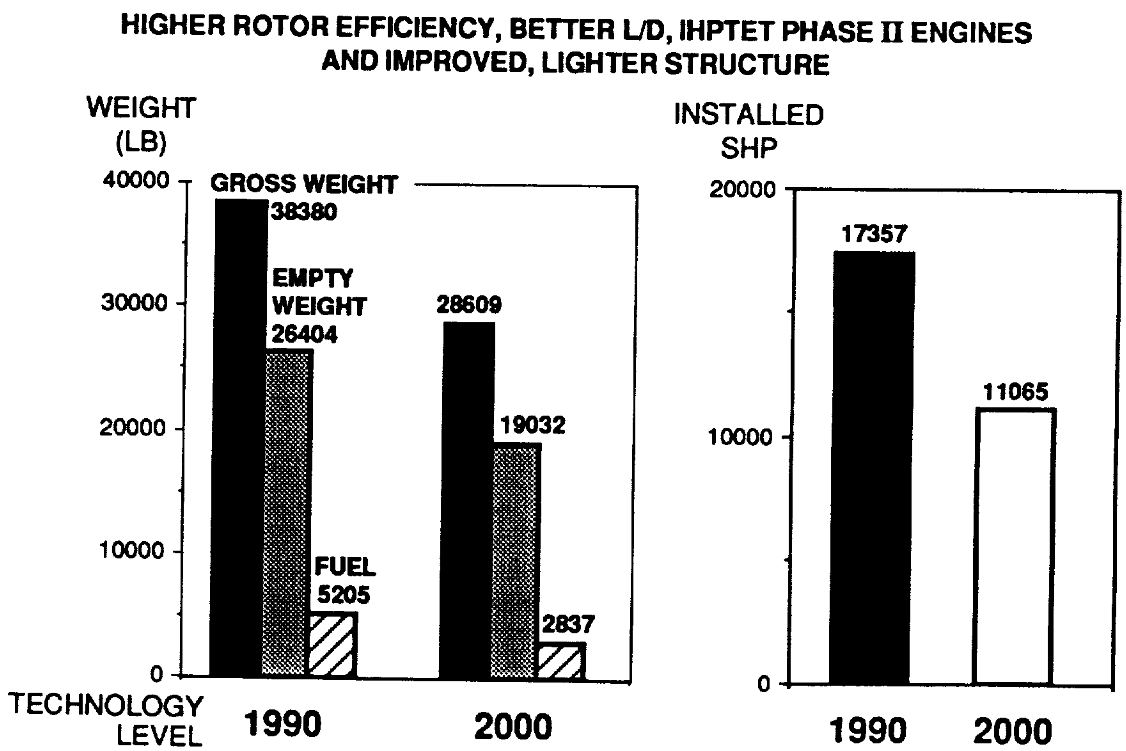

(a) High-Speed Civil Tiltrotor

Figure 73. Effect of Combined Year 2000 Technology

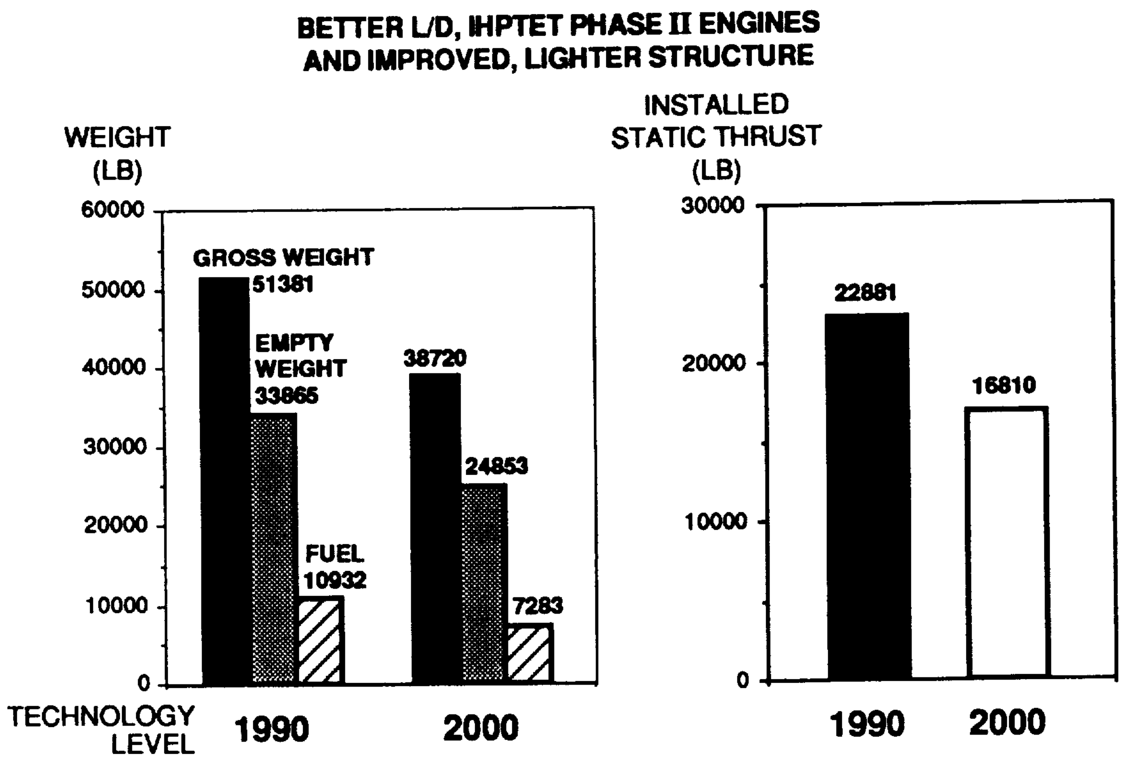

(b) Military Folding Tiltrotor

Figure 73. Effect of Combined Year 2000 Technology (Continued)

This is a tremendous potential reduction, which could represent savings in size, production costs, and operating costs over today's capabilities. The critical design issues must be addressed through concurrent engineering approaches to take advantage of every avenue in order to achieve the levels of performance and structural efficiency which have been projected here. Obviously, the magnitude of this projected benefit can only come to pass with substantial research and development effort to mature the technologies.

Aeroelasticity

The high-speed tiltrotor cruise speed of V_h = 450-ktas (knots true airspeed) , at 25,000-ft requires stability out to 621-knots, reference MIL-A-00870A(USAF). This specification requires that the aircraft have 3.0% damping at V_1 ($V_1 = 1.15V_h$) and the aircraft to be stable to $1.2V_1$ (450- ktas x 1.15 x 1.2 = 621-ktas).

Prop-rotor whirl flutter is the coupled motion of the rotor and the airframe. The aerodynamic forces on the rotor excite this motion, which can result in an instability at a high forward speed. The aeroelastic stability requirements of a tiltrotor drive the wing stiffness distribution, rather than bending moment criteria as for conventional fixed wing aircraft.

Few details are available at the conceptual design stage. The lack of detailed information and the lack of any database to correlate predictions of whirl flutter at such high speeds prevents accurate predictions. For this study, successive variations were made from a V-22 math model to approximate the high-speed civil tiltrotor configuration. Results from this approach showed a 19% drop in the stability speed due to the 30° forward swept wing, primarily from a 76% increase in the wing torsion participation in the symmetric wing bending mode. The thin airfoils and high solidity design of the high-speed prop-rotor drop the stability speed another 11%. These effects gave a new reference and a challenge which must be overcome by careful tailoring of the wing, pylon, and rotor structures to obtain a suitable set of frequencies and mode shapes.

A sensitivity of the whirl flutter stability speed to such parameters on blade in-plane frequency, blade kinematic coupling, blade and wing mode shapes, and the net torsional participation have indicated these as areas worth further investigation. More discussion of the study results is provided in Appendix B. A discussion of aeroelasticity as a critical technology is given in Section 3.

Relative Cost Assessment

Life-cycle cost (LCC) estimates were prepared for both the military folding tiltrotor and the high-speed civil tiltrotor. A general explaination of LCC can be found in Appendix A, Task I Cost Comparison. Estimates of LCC used commercially available models, supplemented with contractor-developed cost-estimating relationships for system test and evaluation (ST&E). Support investment costs (initial spares) and operating and support (O&S) costs were estimated using the Modular Life Cycle Costs Model (MLCCM). More description of the methodology is included in Appendix B.

Results for the military folding tiltrotor are shown in Figure 74. All figures have been normalized to the 1990 technology level, 450-knot baseline design. The O&S costs for the military folding tiltrotor were based on peacetime operations, averaging 400 flight hours per year. The 350-knot design speed saved 8% in LCC, whereas a 500-knot design speed cost 12% more in LCC. Development of year 2000 technologies showed a potential for a 19% decrease in LCC in constant 1990 dollars. Figure 75 shows the breakdown of recurring production costs by aircraft system. Increasing the design speed drives up the size, weight, and cost of the convertible engine. This in turn drives up the vehicle gross weight, requiring more fuel and more power to hover (Figure 72). The increased gross weight and hover power drive up the rotor weight and drive system weight. As shown in the figure, these weight and power increases are directly reflected in recurring-cost increases.

Results for the high-speed civil tiltrotor are shown in Figure 76. As for the folding tiltrotor, all figures were normalized to the 1990 technology level, 450-knot baseline design. The relative LCC comparisons for the high-speed civil tiltrotor exhibited more variation with design speed than the folding tiltrotor. This is primarily due to two factors. First, the rotor's cruise propulsive efficiency gets steadily worse at higher design speeds, compounding the airframe growth factor with design speed. Secondly, the civil tiltrotor O&S costs are based on 1976 flight hours per year, compounding the increase in mission fuel required as design speed and vehicle gross weight increased. Relative to the 450-knot baseline design, a 350-knot design speed yielded a 15% savings in LCC whereas a 500-knot design speed caused a 34% increase in LCC. The effect of year 2000 technology development projected a 14% decrease in LCC in constant 1990 dollars.

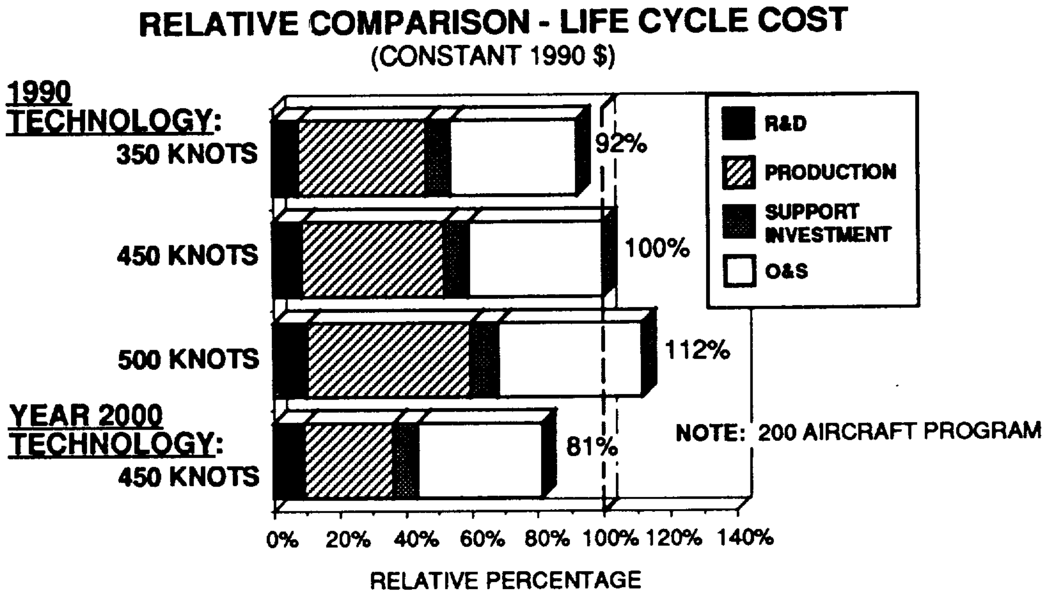

Figure 74. Military Folding Tiltrotor Life Cycle Costs

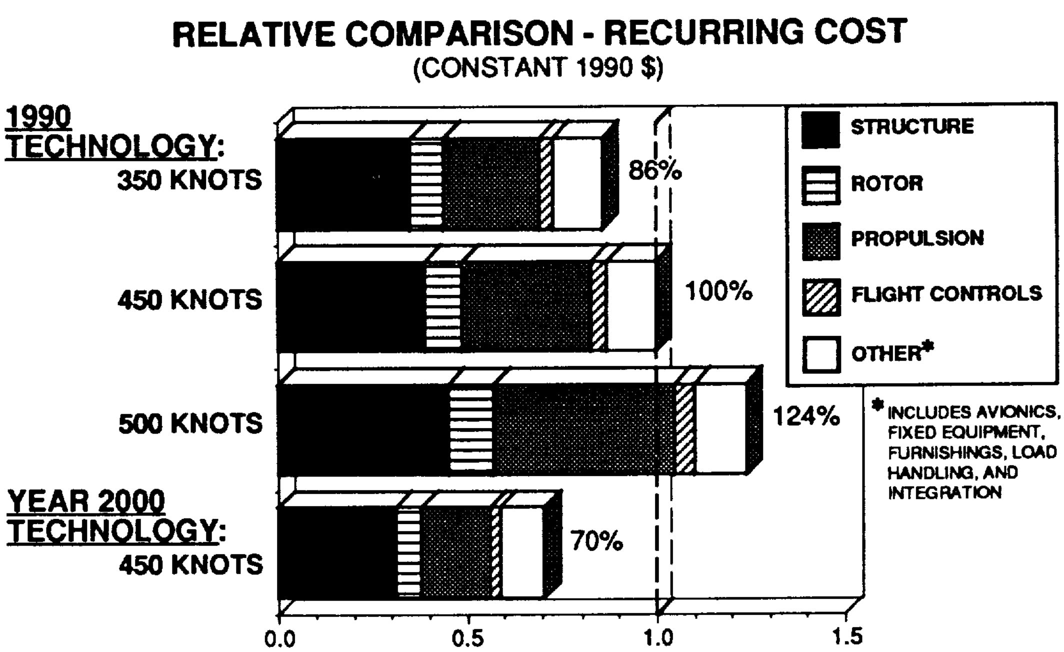

Figure 75. Military Folding Tiltrotor Recurring Costs

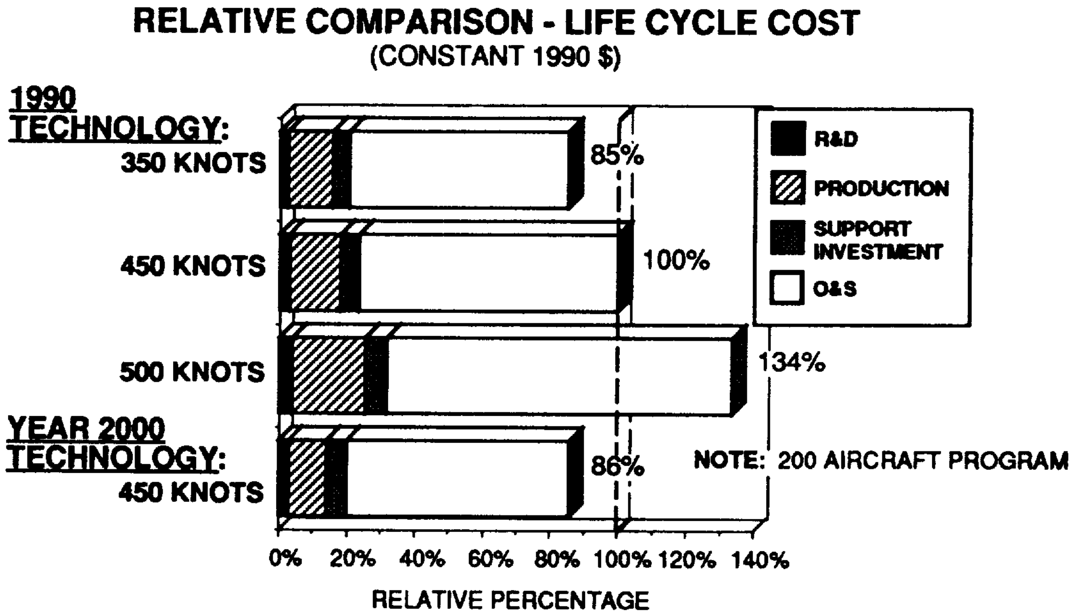

Figure 76. High-Speed Civil Tiltrotor Life Cycle Costs

Figure 77 shows the breakdown of recurring production costs by aircraft system for the high-speed civil tiltrotor. As for the folding tiltrotor, increasing the design speed drives up the size, weight, and power of the rotorcraft (Figure 68). These weight and power increases are directly reflected in recurring cost increases. But for the high-speed civil tiltrotor, they are driven to a much greater extent by the large power increases associated with increased design speeds over 450-knots.

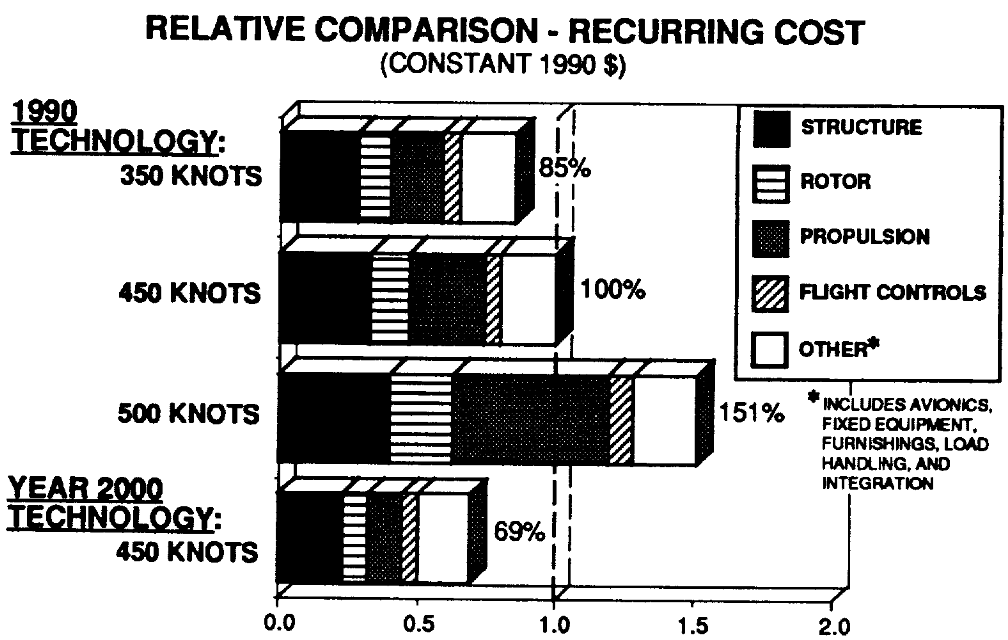

Figure 77. High-Speed Civil Tiltrotor Recurring Costs

Structures and Materials

The structures challenge for high-speed civil tiltrotors is to combine the attributes of several competing technologies such as materials, manufacturing, and design to cost into a single structural concept. The resulting concept must achieve its goal to maximize its structural performance at minimum cost and weight. Lightweight, minimum-gauge structure is required for VTOL characteristics. Manufacturing defects and impacts which occur in in-flight and service environments mandates that low-velocity damage tolerance be a part of the design. Military applications must provide for special features integrated into the structural design. Acquisition and operating costs determine the economic health of any concept.

The high-speed rotorcraft structures design will benefit from a series of aircraft systems currently in development. These include Advanced Technology Fighter or ATF, stealth bomber or B-2, Osprey tiltrotor or V-22, and Light Helicopter or LH. In addition, modular, semimonocoque composite structures have been demonstrated for VTOL aircraft in the Model 360 technology demonstrator as well as in the V-22. Both aircraft are undergoing flight envelope expansion into 200-knot (Model 360) to 350-knot (V-22) velocity ranges. The two different design approaches used throughout the Model 360 (honeycomb) and V-22 (stringer-stiffened skin) have identified that significantly different structures concepts can provide the same high level of structural efficiency which is required for high-speed VTOL aircraft.

The honeycomb sandwich design of the Model 360 has primary advantages in its use of a single major assembly jig for fabrication and the minimum use of fasteners throughout. The V-22 stringer-stiffened skin concept has as its advantages numerous tooling approaches developed in order to build large subassemblies and a part family design which reduces the number of required detail parts to lower costs. Aside from the overall structures concept, the following issues should be addressed for high-speed rotorcraft development.

Pressurized Fuselage - The high-speed rotorcraft's larger diameter cross sections, beyond those demonstrated in the Beech Starship, will require some additional development and validation which will culminate in tests. Critical details such as the wing-to-fuselage attachment have to be addressed in order for composites to be used in the pressurized fuselage application to insure that their in-service durability is as good as the metallics which composites will replace for improved structural efficiencies.

Forward-Swept Wing - The forward swept wing with high-mass, outboard nacelles offers the greatest structural challenge for high-speed rotorcraft. Composite structures which will optimize stiffness and bending-torsion coupling offer great potential for lighter structural weight. One possible approach would be to design a new wing which can be tuned to flight requirements by comformability by either a passive response (due to the composite skin layup) or active control (due to embedded motion actuators). This could include active flutter suppression, airfoil reshaping to reduce drag, and/or stiffness tailoring to control whirl flutter. Tailoring of composites by ply stacking sequence can produce some degree of bending-torsion coupling or bending-extensional coupling. These are, however, second-order effects when used in combination with the family of 0/±45/90 laminated composites because the coupling magnitudes are small. In order to increase the magnitude of the coupling effect, the in-plane properties of the laminates will be lowered. The solution lies in the use of nonorthotropic-based ply stacks in the initial design. The associated problems of failure criteria for nonorthotropic laminates and lack of design experience, including the availability of allowables for these composites, must be addressed.

The concept of a tailored-composite wing must result in a stable, conformal structure which acts in either a passive or actively controlled way to change its shape is an area for investigation. The overall goal would be to achieve the desired flutter boundaries with a lightweight structure and to reduce drag at all speeds. The potential benefit from such an achievement could be much greater than any single technology area. This area represents the single greatest challenge for the high-speed rotorcraft structure. The use of new materials in this application will probably overshadow the need to lower the cost of manufacture of this component because this design problem will push the state of the art in performance beyond the known limits.

Additional discussion on new materials and manufacturing methods is included in Appendix B.

SECTION 3 - ENABLING TECHNOLOGY PLAN

General Discussion

Task I of this study identified the two HSRC concepts which appear to have the greatest future potential. Task II further refined the designs of these concepts for their chosen missions and generated associated performance data, mass properties, and vehicle characteristics to more fully describe the conceptual design. This conceptual design process is the first step in the development roadmap shown in Figure 78. The Task III enabling technology plan identifies those technical areas needing further development to enable a low-risk, full-scale development of the selected concepts. It addresses the shaded steps of Figure 78.

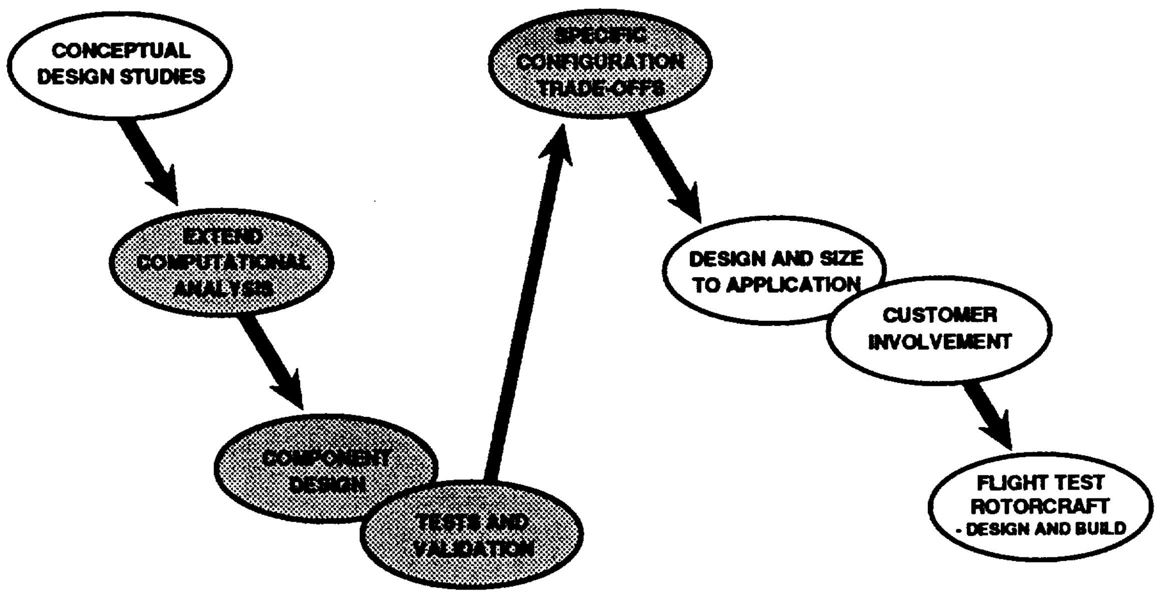

Figure 78. High-Speed Rotorcraft Development Roadmap

The enabling technology plan has been arranged according to design issues. These design issues are high payoff areas where risk-reduction programs could lead to substantial improvements in technology necessary to achieve the 450-knot design speed. The design issues require further development in the technical data base and analytical capability to prepare for a low-risk, full-scale development program. Solution of each of the critical design issues involves trades between various technical areas; i.e., a concurrent-engineering approach covering several technical disciplines. These design issues are outlined in Figures 79 and 80 for the high-speed civil tiltrotor and the military folding tiltrotor respectively.

The enabling technology plan developed for each design issue seeks to establish the analytical capability, associated data base, and validation of design methodologies which are the prerequisites to low-risk detailed design. Where practical, the needs of several technologies have been combined into a single wind tunnel test program, providing rotor performance data, acoustic data, and maybe blade and hub loads data, too. This approach avoids repetitive wind tunnel tests but

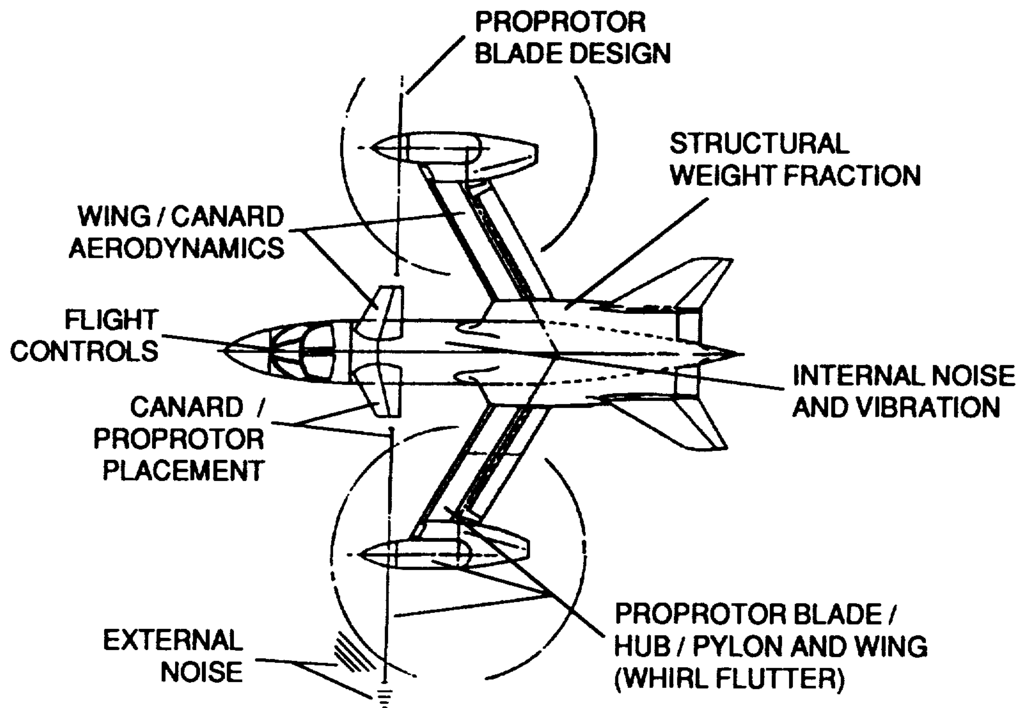

Figure 79. High-Speed Civil Tiltrotor Design Issues

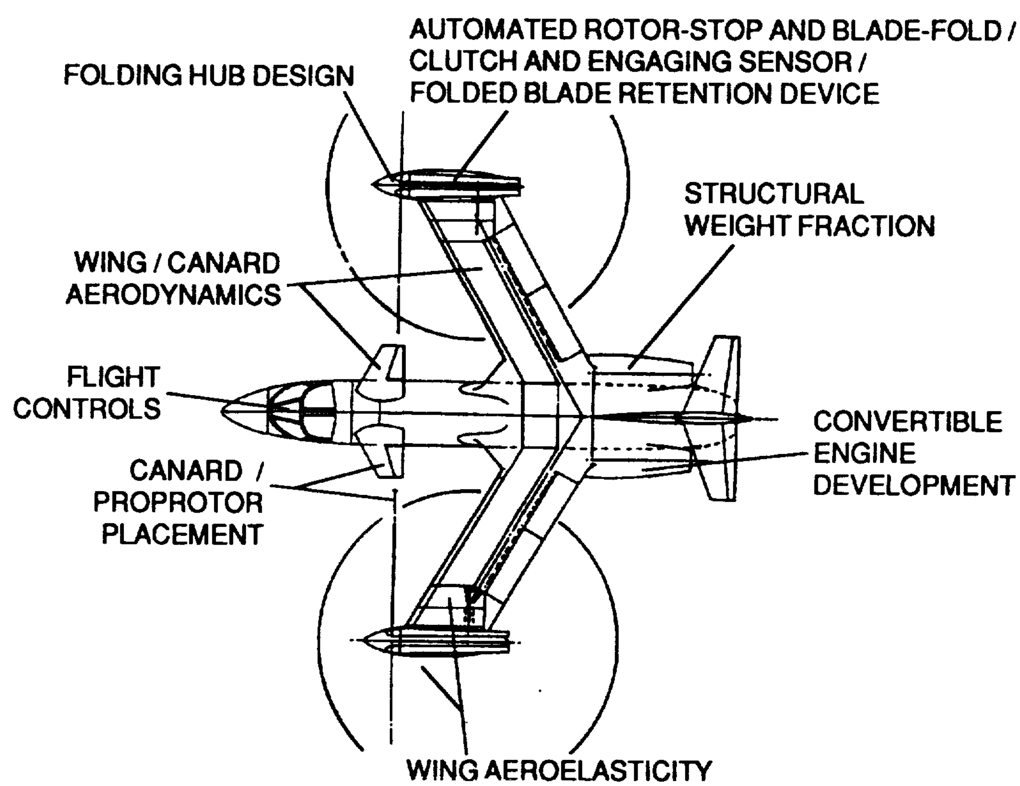

Figure 80. Military Folding Tiltrotor Design Issues

influences scheduling, so that one design issue's schedule affects another's. A summary of recommended wind tunnel tests is shown in Figure 81.

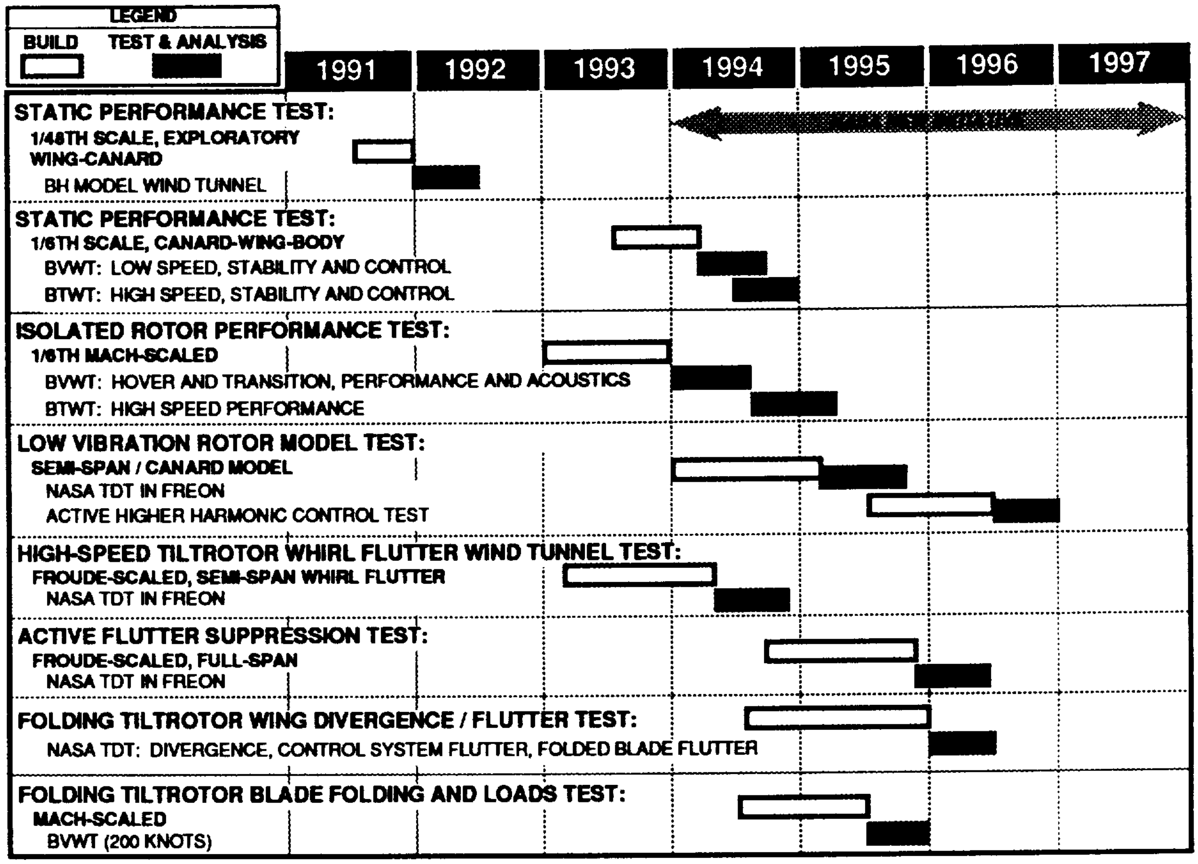

Figure 81. High-Speed Tiltrotor Enabling Technology Wind Tunnel Test Summary

The critical design issues required to achieve a 450-knot high-speed rotorcraft can be grouped as follows:

1) General design issues
   - Those which apply to more than one concept

2) Concept specific design issues
   a. Canard tiltrotor
   b. Folding tiltrotor

Critical Design Issues

High-Speed Civil Tiltrotor

The high-speed civil tiltrotor must achieve the 450-knot design speed with the lowest possible empty weight/gross weight fraction (EW/GW) at the lowest cost to build. Reductions in EW/GW, through either concept benefits or manufacturing/materials, will result in a higher payload fraction. Lower EW/GW values are often used by potential customers as an indication of airframe structural efficiency. The benefits of lower EW/GW are summarized in the table below.

Table 14. Benefits of Low Empty Weight / Gross Weight Ratio

Higher Useful Load	→	**Greater Range or More Passengers**
Lower Installed Power	→	**Lower Cost-to-Build**
Less Mission Fuel Required	→	**Lower Operating Costs**

The manufacturing cost-versus-marketing benefit is no doubt sensitive to design speed. The cost of a 450-knot design speed may exceed its value to the customer. While such a tradeoff was beyond the scope of this technology effort, it needs thorough investigation. Given a design speed, cost to build depends on many factors, but vehicle size and weight are primary indicators. Heavier aircraft take more material and more labor to build; they cost more. The key drivers of production cost are listed below. The first driver is determined by the customer's needs and budget constraints, but the other three drivers are certainly impacted by technology development.

- **Sustained manufacturing rate (no. of aircraft per month)**
- **Weight and size**
- **Installed power (thrust)**
- **Technical maturity of:**
  - Concept
  - Flight control system
  - Propulsion system
  - Manufacturing technology

The measures of effectiveness (MoE's) affecting aircraft competitiveness in a commercial market are performance, acquisition cost, and operating cost. Technologies must be reasonably mature for application in the commercial world (developing an immature technology for a new civil airframe would seriously escalate the nonrecurring cost). So technical maturity is a prerequisite, necessary for consideration of any concept or vehicle for application in the civil market, but insufficient to guarantee the concept's civil success.

The purpose of this technology plan is first of all to mature these necessary technology areas: speed capability, good-low speed and high-speed control, stability in all flight modes, and the lowest practical vibration and noise signatures in the basic, untreated design. The prerequisite design issues for the high-speed civil tiltrotor are shown in Table 15.

Military Folding Tiltrotor

The military folding tiltrotor can assuredly meet the required 450-knot airspeed in the clean cruise mode with folded blades and its turbofan propulsion. The areas of critical importance to the civil tiltrotor (whirl-mode stability and rotor propulsive efficiency) do not have the same importance for the folding tiltrotor, with its blades folded out of the way in high-speed cruise.

Table 15. Critical Design Issues for the High-Speed Civil Tiltrotor

DESIGN ISSUE	OBJECTIVE
Proprotor Blade Design	Improve high-speed efficiency
Proprotor Blade / Hub / Pylon and Wing	Avoid whirl flutter and other aeroelastic instabilities
Wing Structural Design	Avoid pure divergence throughout the flight envelope
Wing Aerodynamic Design	Efficient cruise L/D, and drag divergence avoidance
Wing / Canard Aerodynamics	Design and placement for cruise efficiency and stability
Flight Controls	Extend tiltrotor flight controls to high-speed operating regime
Canard / Proprotor	Placement to avoid unfavorable aerodynamic interactions or induced loads
Vibration	Levels which are acceptable for passenger comfort over the longest expected range
Noise - Internal	Levels which are acceptable for passenger comfort
Noise - External	Levels which are acceptable for VTOL vertiport operations near residential areas
Structural Weight Fraction	Minimum achievable

Also, operational fuel efficiency is of lesser importance for the military aircraft since there is not a direct price/cost relation to balance in the military application. However, many other factors are quite similar. Acquisition cost is most definitely a prime MoE for the military, and the EW/GW fraction is still a prime MoE for the same basic reasons as for the civil rotorcraft.

Military aircraft are usually on the "leading edge of technology" to ensure a combat advantage, whereas civil aircraft must wait until the technology is fairly mature and affordable (must balance cost to build versus the benefits). This leading-edge technology must be reasonably mature, but more often than not it requires further development and test verification during full-scale development. Thus, there is a difference between the fully matured technology required as a prerequisite for civil applications and the lower maturity level acceptable of leading-edge technologies applied in the early stages of new military aircraft development.

The critical design issues requiring further development for the military folding tiltrotor are shown in Table 16.

Any one of the technical issues shown will likely involve more than one technical discipline! For instance, developing an automated rotor-stop/blade-fold procedure involves 1) adjusting rotor blade pitch to a nonthrusting windmill state, 2) bringing turbofan thrust on line to maintain airspeed, 3) stopping the rotor by feathering the blades, 4) disconnecting the rotor drive system from engines, 5) final braking and indexing of the rotor, 6) folding the blades back along the nacelle, 7) locking down the blades after folding, and 8) control of the convertible engine thrust throughout the process to maintain airspeed and minimize longitudinal accelerations. To accomplish this requires knowledge of the blade aerodynamics, engine fuel control system, flight control system, hub/folding mechanism, rotor brake and indexing device, and blade lockdown device. This requires wind tunnel data to verify the blade loads and net longitudinal force (and moments) during stopping and folding; it requires engine response characteristics; and it requires an integrated simulation of the process for verification.

Several of these design issues are the same as for the high-speed civil tiltrotor. These are grouped as general design issues in the section which follows. Those which are specific to the concept are then treated under the heading of concept-specific design issues.

Table 16. Critical Design Issues for the Military Folding Tiltrotor

DESIGN ISSUE	OBJECTIVE
Convertible Engine Developement	**Develop VIGV / VEGV, or torque convertor, or variable pitch fan**
Hub Design	**Design mechanism for folding and deploying rotor blades in-flight**
Automated Rotor-Stop and Blade-Fold	**Develop procedure, including analysis and control laws**
Clutch and Engaging Sensor	**Develop operational system**
Folded Blade Retention Device	**Develop operational device**
Wing Structural Design	**Avoid pure divergence throughout the flight regime (high-speed turbofan mode)**
Wing Aerodynamic Design	**Efficient cruise L/D, and drag divergence avoidance**
Wing / Canard Aerodynamics	**Design and placement for cruise efficiency and stability**
Flight Controls	**Extend tiltrotor flight controls to high-speed turbofan powered cruise mode**
Maneuverability	**Wing / pylon design to satisfy required maneuver criteria (without washout or reversal)**
Aeroelasticity	**Design blade / hub / pylon and the forward swept wing to clear whirl flutter instabilities up thru 250 knots**
Structural Weight Fraction	**Minimum achievable**

Common Critical Technologies

There are several critical technologies that apply to design issues for both the high-speed civil tiltrotor and the military folding tiltrotor. These are listed in Table 17.

Table 17. Common Design Issues

- **Aerodynamics:** High-speed wing / canard design
- **Aeroelasticity:** Forward-swept wing structural design
- **Structures:** Materials and weights
- **Flight control laws**

The development of validated analyses and a wind tunnel data base will allow design tradeoffs such as showing the net effect of wing sweep angle on aircraft gross weight. These tradeoffs will then be able to accurately reflect the parameters' impact on the structural design, weight, and aerodynamic performance.

Aerodynamics: High-Speed Wing/Canard Design

Issue - There are many design compromises during an aircraft design. The wing/canard design tradeoffs for a military application, for example, may have to sacrifice cruise L/D by accepting less-than-optimum wing loadings, or go to relaxed static margins to achieve high maneuverability. Conversely, a civil version would tend to focus on maximum cruise efficiency to reduce fuel burn and still have far more maneuvering capability than it can use at high-speed. Whatever the constraints, the technology must be sufficiently developed that designers and analysts can make the tradeoffs wisely and with confidence. This may require the development/extension of analytical techniques to provide a more thorough model of tiltrotors with forward-swept-wing and canard arrangements. Some wind tunnel testing is also required to establish at least a minimum data base on tiltrotors with forward-swept-wing and canard arrangements.

Approach - Aerodynamic design of the wing and canard must satisfy several objectives:

1. It should provide the best possible L/D in high-speed cruise.
2. It should employ airfoils and planform which exhibit a suitably high drag-diver gence Mach number.
3. It must have acceptable static stability margins (including the destabilizing con tributions from wingtip rotors/nacelles); and
4. It must satisfy the specified maneuver and handling qualities characteristics.

Plan - The high-speed civil tiltrotor and the military folding tiltrotor are both three-control-surface designs. Cruise lift-to-drag ratio can therefore be maximized by an optimum combination of lift from the canard, wing, and tail. A four-step process is recommended to determine the best configuration, establish an appropriate data base, and validate analysis methodologies. These steps are shown in Figure 82.

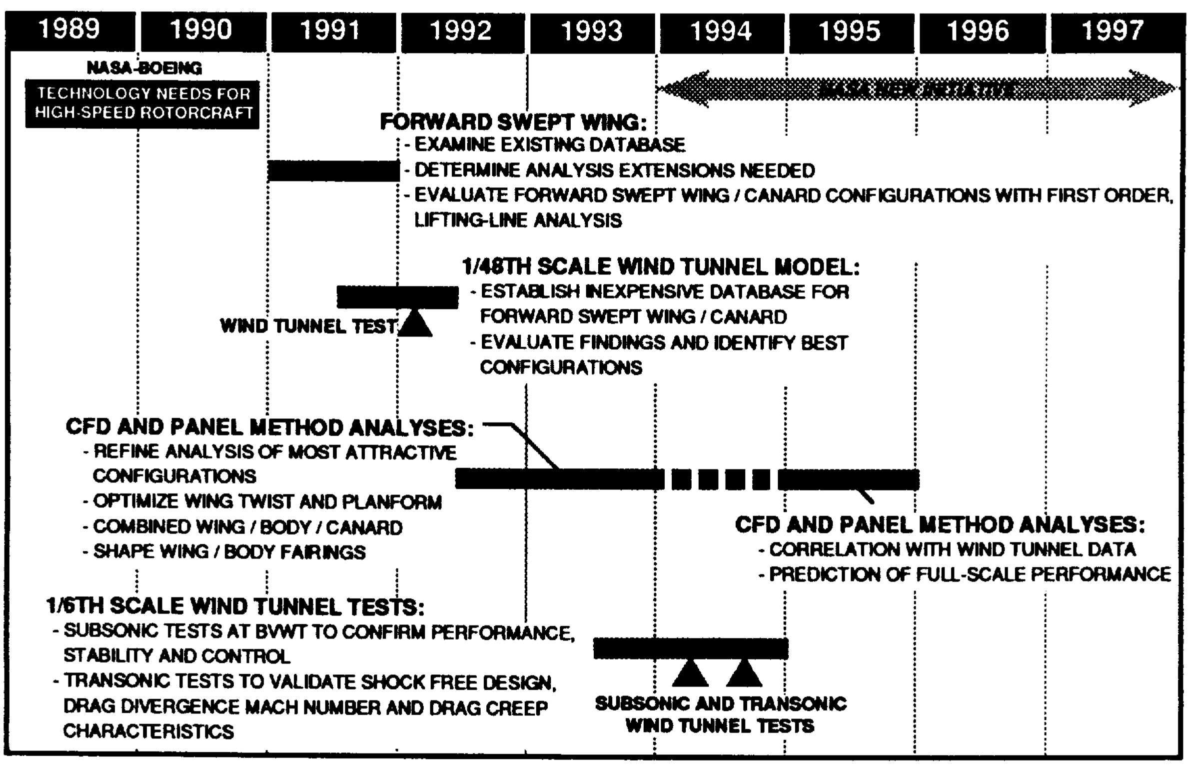

Figure 82. High-Speed Tiltrotor Aerodynamics Enabling Technology Plan

First: Examine the existing data base for forward-swept-wing and canard arrangements and evaluate the merits and pitfalls of the configuration. Then study the configuration with relatively simple analyses to tradeoff first-order effects on the tiltrotor designs, such as canard downwash on the wing or rotor, wing upwash on the canard and rotor, and the significance of wing sweep and the wing/canard relative locations on performance, stability, and control. Modified lifting-line analysis would serve this purpose well, requiring only a minimum of information consistent with conceptual design tradeoffs.

Second: Design and build a very small-scale wind tunnel model (1/48-scale) to establish a relatively inexpensive data base for various wing/canard configurations. Examine canard position and wing sweep effects on L/D and static stability. Choose the most promising wing/canard geometries from the fundamental analysis and the exploratory wind tunnel tests.

Third: Conduct more detailed analysis (CFD) on the most promising configurations and introduce configuration refinements such as optimum wing twist, planform geometry, and airfoil profiles. This step must also address details of the body contours, analyzing the combined canard-wing-body configuration. This will also refine the wing-body fairings to minimize interference velocities which would otherwise impact the Mdd.

Fourth: Conduct larger scale wind tunnel tests (1/6-scale) at subsonic and transonic speeds to confirm performance, stability, and control capability. Correlate predicted performance, stability and control with wind tunnel data.

Drag Divergence Mach Number

Total airframe drag-divergence Mach number (M_{dd}) primarily depends on the airfoil profile (shape and t/c), operating lift coefficient, supervelocities created by interference at junctures such as the wing-body and the wingtip-nacelle, aerodynamic interferences between the wing and canard, and the wing sweep angle. Fundamental tradeoffs need to be made between wing sweep and wing t/c for use in analysis of other areas like the wing structural weight.

Aeroelasticity: Forward-Swept-Wing Design

Issue - Tiltrotor aircraft must be designed to avoid a form of instability that involves the coupled flexible motions of the wing, pylon, and rotor. It is similar to propeller whirl flutter which occurred in turboprop transports in the 1960s. The tiltrotor version differs from that of the propeller by virtue of the tiltrotor's flapping and feathering degrees of freedom. The basic cause of tiltrotor instability is the same as that of propeller whirl flutter, in that destabilizing aerodynamic forces may be generated by precessional motion of the rotor on its pylon-wing support structure.

The V-22 has been designed to be free from whirl flutter to 397-knots, 15% above the 345-knot V_{dive} speed. It was achieved by rotor hub kinematics and wing stiffness design which together provide adequate positive damping. It was demonstrated by extensive analyses, aeroelastic wind tunnel tests, and flight tests.

Future tiltrotors must be concerned with this issue. Civil tiltrotors must by designed to be stable to a 20% margin above their high V_{dive} speed. This means that for a cruise speed goal of 450-knots, the dive speed must be 20% higher (540-knots) and the flutter boundary must be 20% higher than that, or 648-knots. Folding tiltrotors must be designed to be free of whirl flutter up to the 250-knot speed at which the rotors would be folded.

In addition to the whirl-flutter issue, these rotors must, as an individual rotor component, be aeroelastically stable to the same speed requirements. It is believed generally that if whirl stability is achieved, then the rotor itself would be individually stable.

For the folding tiltrotor above the 250-knot folding speed, the forward-swept wing is being propelled by jet thrust to very high airspeeds. An important stability issue of this configuration is divergence. It is possible with forward sweep for the accompanying noseup moment to statically diverge the wing torsion as airspeeds increase. This was addressed in recent years for the Air Force/Grumman X-29. It was necessary there to use tailored orientations of high-modulus composite fibers to reduce the wing's destabilizing pitch-up torsional response to outboard lift.

The common aeroelastic technology issue for the civil tiltrotor and the folding tiltrotor is whirl flutter up to the 250-knot fold speed. Above 250-knots the civil tiltrotor must cope with whirl flutter and wing static divergence/flutter up to 648-knots, and the folding tiltrotor must cope with wing static divergence/flutter up to 648-knots.

Approach - Wing design for tiltrotors must consider at least five specific design conditions. These are the jump takeoff condition, hard-landing conditions, in-flight maneuver requirements, the above-whirl-flutter aeroelastic instability prevention, and the above-wing-divergence prevention. These five design requirements are made more difficult by the forward-swept-wing configuration, thus requiring more torsion and bending stiffness than would normally be required.

Tailored-ply orientations of high-modulus composite fibers were used to reduce the X-29 wing's destabilizing pitch-up torsional response to outboard lift. A similar approach must be used with the forward-swept-wing designs of the civil tiltrotor and the folding tiltrotor. However, these rotorcraft configurations differ from the X-29 in that they have wingtip pylons which can generate destabilizing tip loads. Furthermore, the high-speed civil tiltrotor has both its engine nacelles and rotors at the wingtips. The rotor in particular can generate significant destabilizing loads due to changes in angle of attack. Thus, the tiltrotors' forward-swept wing must be designed to avoid pure divergence with sufficient margins throughout the flight envelope.

Plan - The issues of wing pure divergence and whirl flutter are common design problems for both the civil tiltrotor and the military folding tiltrotor. However, the emphasis for the civil tiltrotor is on whirl flutter while the emphasis for the military folding tiltrotor is on pure divergence. Thus, the technology plans are developed for each concept and presented in their respective sections.

Structures, Materials, and Weights

Issue - The structural weight fraction depends on many factors; some are concept/configuration-dependent and some are material/manufacturing-dependent. The high-speed rotorcraft concepts chosen by Boeing Helicopters gave the best capability and the lowest weight when compared to other concepts with the same technology advantages. They are believed to be the best concepts, but their specific configuration needs further optimization. For instance, the preceding sections described the steps needed to optimize the combination of wing sweep and t/c and the overall canard-wing-body design. These tradeoffs are normally dictated by the overriding performance and control requirements.

The body and wing structural design must integrate the structural design, the materials, and the manufacturing methods to satisfy the design requirements with the lowest weight and for the least cost to build.

Approach - Advanced weight-estimating techniques need to be developed for the conceptual design level to allow first-order tradeoffs of the primary airframe parameters on component weights. Tiltrotor wing weights are especially important here, since a forward-swept wing and a 450-knot cruise speed make it much more difficult to satisfy whirl-flutter stability and pure wing divergence boundaries. Fundamental analyses need to be developed which estimate wing weight as a function of basic parameters such as wing t/c, sweep, planform taper, spar size, and material properties. The analysis should also be able to estimate the weight improvements achievable with new design and manufacturing technology such as tailored-ply orientations, thermoplastic composites, and filament-wound components. Naturally, this methodology must cover the basic tiltrotor design requirements of jump takeoff, hard landing, pure divergence, and whirl flutter. Furthermore, it should be usable at the conceptual design level, where only basic geometry has been defined with virtually no structural definition. This practically eliminates the analysis programs typically used in detailed design, such as NASTRAN.

There are several structural/material technologies with the potential for high payoff which are essential in the high-speed rotorcraft enabling technology plan due to the VTOL requirement. These are:

1. The extensive use of fiber placement for the reduction of fasteners and parts.

2. The use of one-step manufacture and post-formable composites such as parts made from thermoplastic resins.

3. The use of braided structures and triaxial woven composites in near-net-shape forms to include frames and skins as well as complex shaped parts.

4. The use of 3-D reinforced structures such as those under development for the deep-sea submersibles program currently sponsored by DARPA and NAVSEA. This also applies to the thick-section composites work for primary structures application in landing gear and highly loaded parts.

5. The use of embedded sensors as previously described in the smart skins/structures section of Task II.

6. The use of new materials and processes such as metal matrix, high-hot-hardness steels, and carbon-carbon for exhaust ducts and engine areas.

7. The application of mathematical models and the use of shells in the design of more efficient structures which carry loads as a membrane, rather than in bending.

These are the prime candidate structural technologies which should be considered in the design of the high-speed rotorcraft. The most effective design exercise would be to apply these ideas in a prototyping experiment for new structures and materials concepts. Although producibility may not be adequately addressed by this approach, certainly the majority of structures design and analysis issues identified could be studied in enough detail to determine their relative worth as a high-risk/high-payoff candidate.

Plan - Figure 83 shows a plan for the multiyear development of an advanced wing weight-estimating technique. It must be evolved year by year to reflect new developments in materials and manufacturing technologies. This plan uses data from the composite wing section to validate the conceptual weight-estimating methodology (Figure 87).

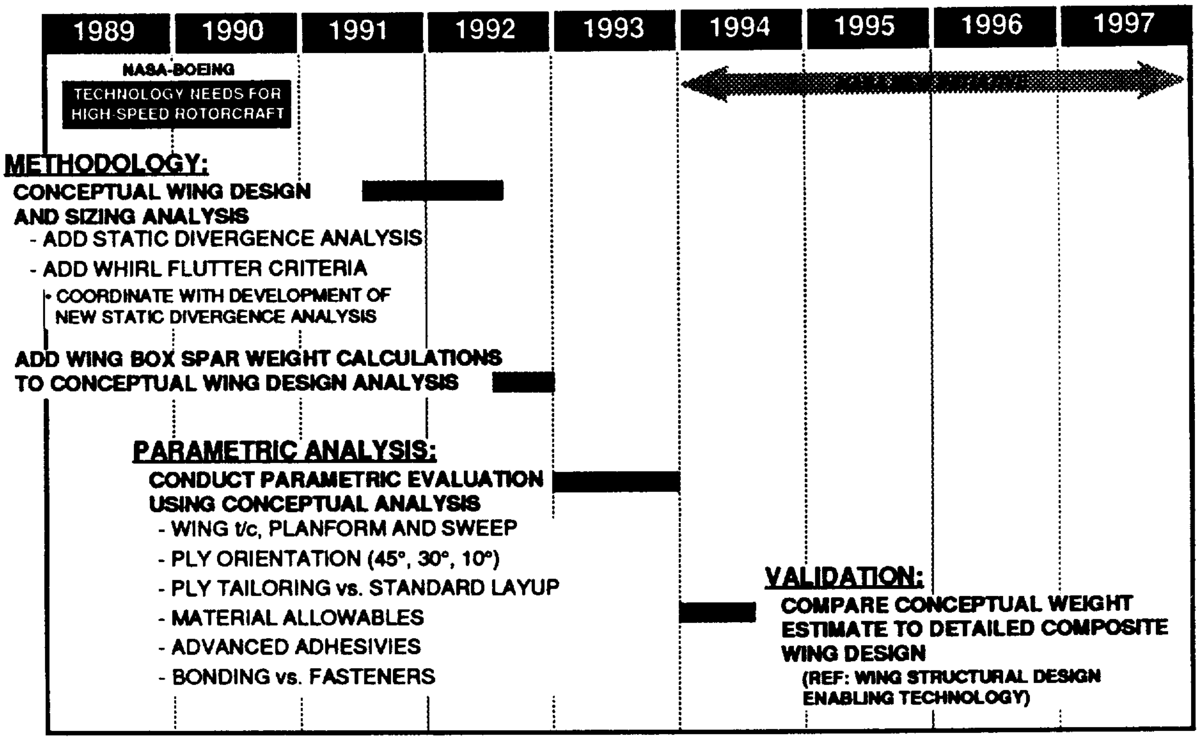

Figure 83. High-Speed Tiltrotor Wing Weight Estimation Development Plan

Figure 84 shows a plan for the multiyear development of advanced-structures design and application of new materials. The schedule for enabling technologies addresses three phases of effort to be pursued over the next 7 years. The high-payoff areas of new materials applied to the wing design are studied first after a determination of the loads and requirements for the forward-swept design is determined in year one. The materials screening and design concepts proceed in parallel for the next 2 years. The use of active control of the wing shape through a combination of tailored composites and intelligent structures is studied at the same time. The materials required for the active change in structural shaping would be studied at the same time. Laboratory bench demonstrations of the methods employed to actively reconfigure the structure would be performed as the final stage of the intelligent structure work. If the success of this effort is acceptable, then those features would be used in the larger-manufacturing plan. Wing fabrication and test would complete the first 5 years of the plan.

Fuselage design, manufacture, and test would comprise the last phase of the 7-year program. The issue of pressurization and damage tolerance for VTOL fuselage structure would be targeted for study and validation. Manufacture utilizing the same high-risk/high-payoff methods currently not in use by the aircraft industry would be given highest priority in the evolution of the design.

Flight Control Laws

Issue - Both the high-speed civil tiltrotor and the folding tiltrotor share the V-22-type tiltrotor flight control requirements in the helicopter mode, transition, and low-speed-rotor airplane mode. Each has some unique differences at higher speeds. These differences require significant modifications to the flight control laws for high-speed flight and need to be verified by flight simulators.

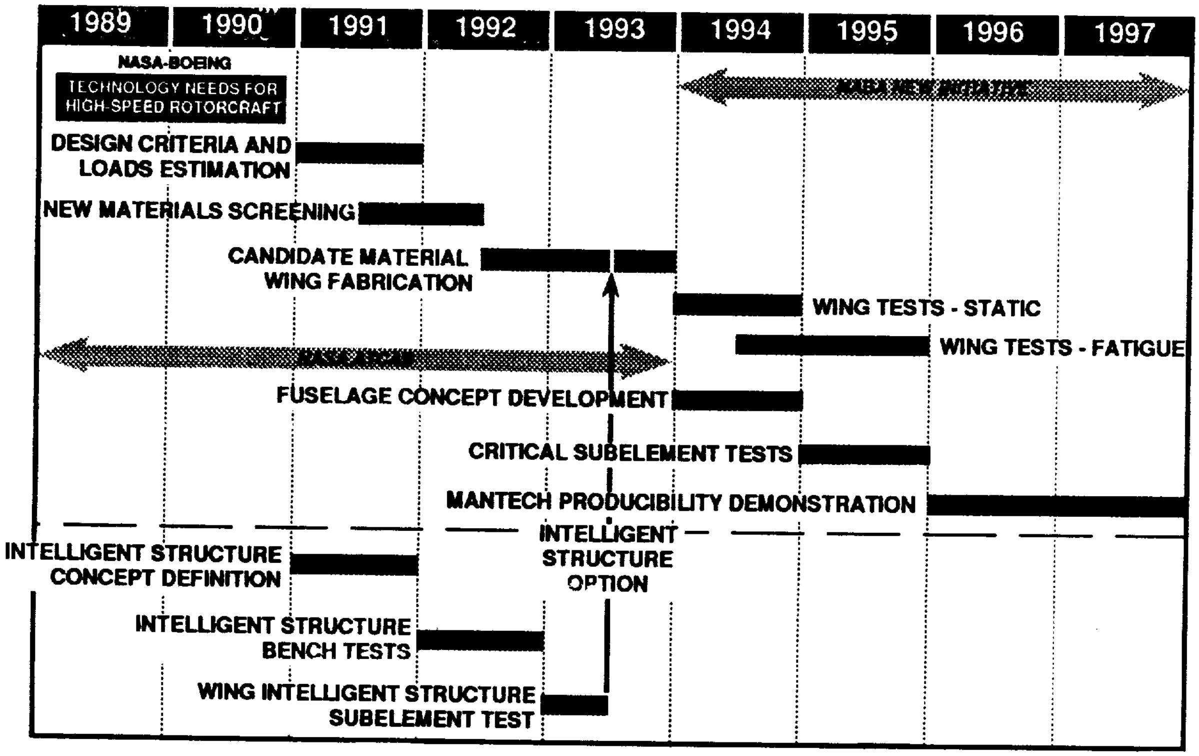

Figure 84. Structures and Materials Enabling Technology Plan

Approach - Develop control laws and procedures to handle the unique requirements of the civil tiltrotor and the military folding tiltrotor.

The civil tiltrotor, for instance, requires control laws and flight actuators to handle the higher collective-pitch sensitivity of a rotor operating at 450-knot cruise speeds. Blade local Mach numbers vary from 0.75 inboard to nearly 1.0 at the tip. This makes rotor thrust (and blade loads) very sensitive to small changes in angle of attack. Thus, controlling rotor thrust will require an accurate collective-pitch control with fine adjustments. It may also require sensors and feedback circuitry to restrict inadvertent blade and hub loads during high-speed flight.

Active aeroelastic controls should also be considered as an attractive technology with the potential to solve aeroelastic instabilities with a minimum impact on airplane structures. These civil tiltrotor controls need to be developed and then evaluated on a flight simulator to prove their effectiveness for load limiting, to fine-tune their sensitivity for pilots, and to assess their net impact on the aircraft handling qualities.

The folding tiltrotor has its own unique flight control needs. For example, the rotor-stop and blade-folding sequence outlined previously must be examined and automated. Its implementation in flight controls must be verified in a flight simulator. High-speed flight with turbofan thrust from the convertible engine poses a new flight regime for the tiltrotor ... no propeller!

Propulsion system thrust controls for the folding tiltrotor must also be verified, and the flight simulator can serve this purpose well. Other engine controls which can be verified on a simulator are thrust response to throttle control and overspeed protection. Engine thrust control in the turbofan mode can be through either VIGV control at fixed rpm or through varying rpm with fixed VIGV (0 degrees). The choice between these turbofan thrust controls affects the feedback loops which must be designed into the flight controls and FADEC. It also affects fuel consumption at partial power, which would directly impact loiter capability.

Plan - Plans were prepared for each concept and are presented in the respective section for concept-specific design issues.

High-Speed Civil Tiltrotor - Specific Design Issues

There are several design issues which are unique to the high-speed civil tiltrotor concept. Table 18 lists these and the paragraphs below discuss the issues and identify the associated critical technologies.

Table 18. Design Issues Unique to the High-Speed Civil Tiltrotor

■ Rotor aerodynamic design - Blade contours - Airfoils - Loads **■ Aeroelastic stability** - Hub type - Blade dynamics - Whirl flutter **■ Flight control laws / development**	**■ Acoustics** - External (good neighbor policy) • takeoff, approach, landing - Internal (passenger acceptance) • cruise: low frequency prop noise • takeoff / landing: prop + engine noise **■ Vibration** - Sources - Magnitudes - Solution approaches

Rotor Aerodynamic Design

Issue - Boeing Helicopters recommends that the design process be started by first defining the aerodynamically ideal rotor. In this case, that is a rotor with a combination of twist, planform, airfoils, and sweep which will achieve the best cruise propulsive efficiency while providing helicopter-like lift and control qualities in hover and low-speed flight. Multiple tradeoffs are required to achieve the optimum combination.

Approach - An ideal blade geometry for pure axial flight would be initially determined from aerodynamic requirements. This initial work would be done with a generic hub design, but without specifying blade structural properties. The ideal blade would be optimized for maximum propulsive efficiency in the critical high-speed-cruise condition, but would also be constrained by the hover requirements. The ideal contours would later be modified, compromised from the ideal geometry, as dictated by other technical areas such as stress, loads, and dynamics. This analysis can be done by both a lifting-line analysis using detailed airfoil data tables and by CFD codes which model the blade as a lifting surface. The CFD codes provide more accuracy in defining the local flow field, such as tip relief and describing the 3-D local flow along the outboard, swept portion of the blade. But the lifting-line analysis has the advantage of detailed airfoil tables and more precise definition of airfoil profile drag, including compressibility drag which must be carefully analyzed.

Rotor airfoil selection must be made to satisfy the cruise requirement for high drag-divergence Mach numbers but also deliver acceptable maximum-lift coefficients for hover. Thin airfoils give improved M_{dd} for cruise, but also lower C_{lmax}. The lower C_{lmax} requires more rotor solidity to satisfy hover lift requirements, which in turn can reduce cruise performance. The compromised rotor design must deliver the best possible propulsive efficiency in cruise with acceptable thrust margins in hover.

Rotor loads can be generated from the ideal rotor geometry described above in combination with blade elastic properties and a hub definition. Both the hub and the elastic properties will require their own tradeoffs, as well as iteration with the blade design, before deciding on a fixed geometry.

Plan - Figure 85 shows a schedule of all the required activities for high-speed rotor development. The top four bars correspond to the rotor aerodynamic design.

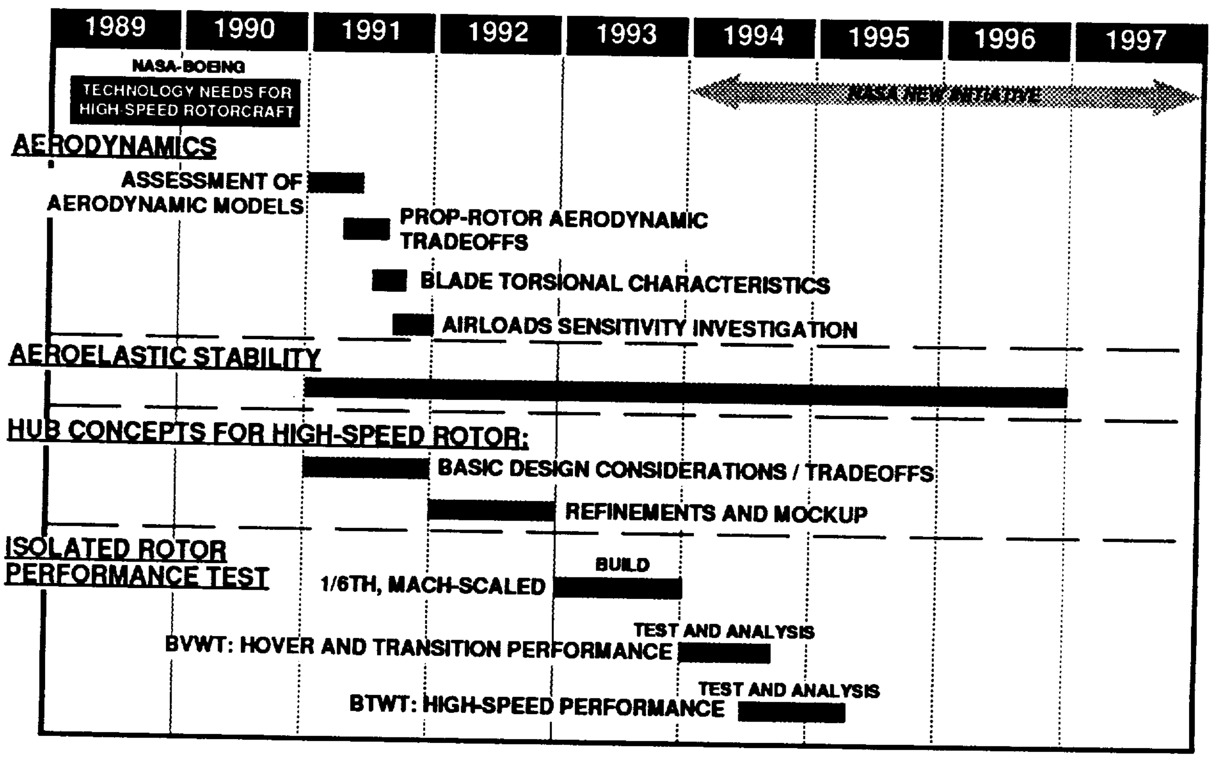

Figure 85. High-Speed Rotor Enabling Technology Plan

Aeroelastic Stability

Issue - As noted above, the NASA goal for a high-speed civil tiltrotor is to operate at 450-knots cruise speed. According to FAR Part XX, Interim Airworthiness Criteria for Powered-Lift Transport Category Aircraft, the dive speed is 20% higher or 540-knots, and the flutter boundary must be 20% higher than that or 648-knots. Whirl-flutter stability is the principal aeroelastic issue relative to achieving such high speeds. A second issue, which is really a subset of the first, is individual rotor blade stability. Three passive means to achieve this goal are; (1) rotor kinematic coupling for favorable blade aerodynamic damping, (2) mechanical damping within the blade structure such as an elastomer between the cuff and the flexure, and (3) wing stiffness and elastic coupling to raise frequency and minimize in-plane motion at the rotor hub. An active means is the use of rotor collective or cyclic control to provide favorable aerodynamic damping. These issues are addressed below:

Approach - Figure 86(a and b) shows the aeroelastic enabling technology. First, existing analyses would be used to determine the whirl-flutter boundaries. This would be done with the sharply forward-swept wings and the highly swept rotor blades of these new configurations. Then rotor kinematic coupling and wing stiffness variations would be explored. Deficiencies of the analysis would be identified.

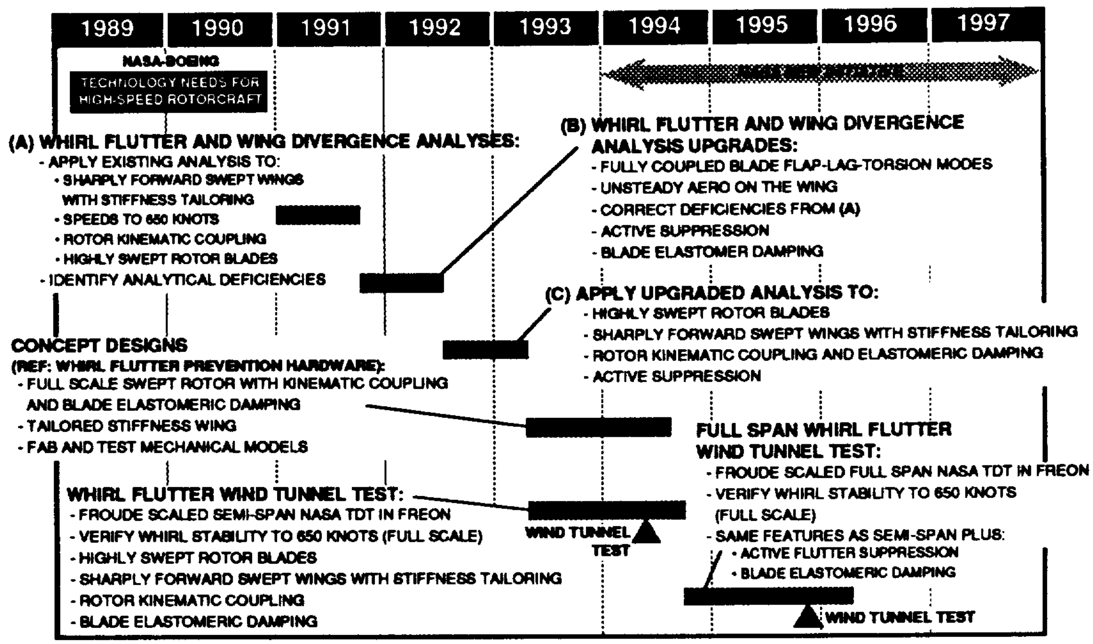

(a) Whirl Flutter Enabling Technology Plan

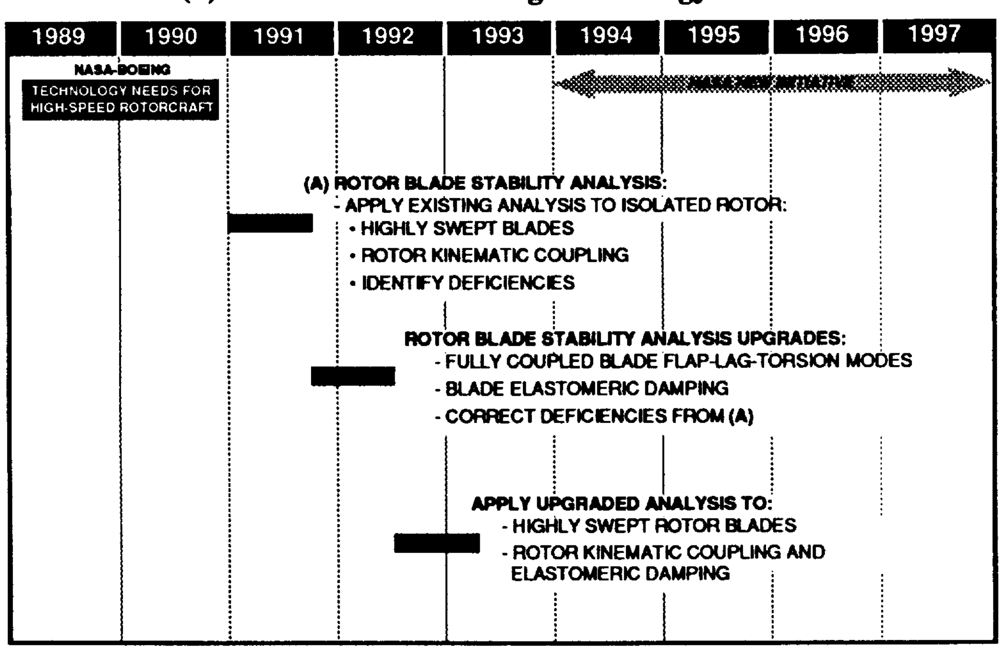

(b) Rotor Blade Stability Enabling Technology Plan

Figure 86. High-Speed Civil Tiltrotor Aeroelastics

Next, the analyses would be upgraded to include fully coupled blade flap-lag-torsion modes, to include conventional flutter unsteady aerodynamics on the wing, and to correct any deficiencies revealed by the first analysis above. A capability for active flutter suppression analysis would also be added to the analysis. Finally, the upgraded analysis would be used, the principal parameters rechecked and the active suppression system studied.

The analysis results would be reviewed and favorable ranges of rotor and wing parameters selected. Wind tunnel model predesign would be conducted and it would be decided whether to design specific new models or to modify existing V-22 model hardware.

A semispan model would then be designed and built. Bench tests and ground runs would be performed, and then at least one wind tunnel entry would be made. Whirl-flutter boundaries would be measured for the basic model and for parameter variations.

If the semispan tests were successful, then a full aircraft model test would be undertaken. This would follow a similar sequence of predesign and analysis, detail design, fabrication, bench test, and wind tunnel test. Tests would then verify the stability of the selected configuration and parameter variations around the base value.

As a subset of the whirl-flutter program, analyses of rotor-alone stability would be performed as well. These results would feed into the whirl-flutter work and would influence the design of the models and the wind tunnel test programs.

Full-Scale Whirl-Flutter Prevention Hardware

Figure 87 outlines a plan for research into practical means for achieving stability with full-scale hardware. It covers rotor design, wing design, and whirl-flutter suppression.

Rotor kinematic coupling recommendations from the analysis and wind tunnel testing of the aeroelastic enabling technology plan would now be studied for full-scale implementation. Layouts of full-scale rotors that would incorporate favorable coupling would be made. The possibility of incorporating supplementary elastomer damping into the hardware would be studied. Mechanical models of these designs could be made and tested.

Composite wing stiffness-tailored designs would be studied as well. Again from the recommendations of the enabling technology analysis and test work, layouts of full-scale design would be made. These would be analyzed and iterated until frequency and coupling goals were met by analysis.

In addition to the wing aeroelastic objectives of these designs, they would implement the other design requirements. These would include, as a minimum, the jump takeoff criteria, landing loads, and maneuver load requirements.

Whirl-flutter active suppression systems would also be studied.

Acoustics

Issues - External and internal noise must be addressed for a civil tiltrotor application. External noise has a direct and overriding influence on community acceptance of the vehicle and the vertiports which they must use. A "Good Neighbor Policy" must be adopted which strives to combine the best vehicle characteristics with practical takeoff and approach paths to minimize the noise impact on the community. Internal noise is, of course, important to the traveling passenger and will directly influence his/her willingness to use the service repeatedly.

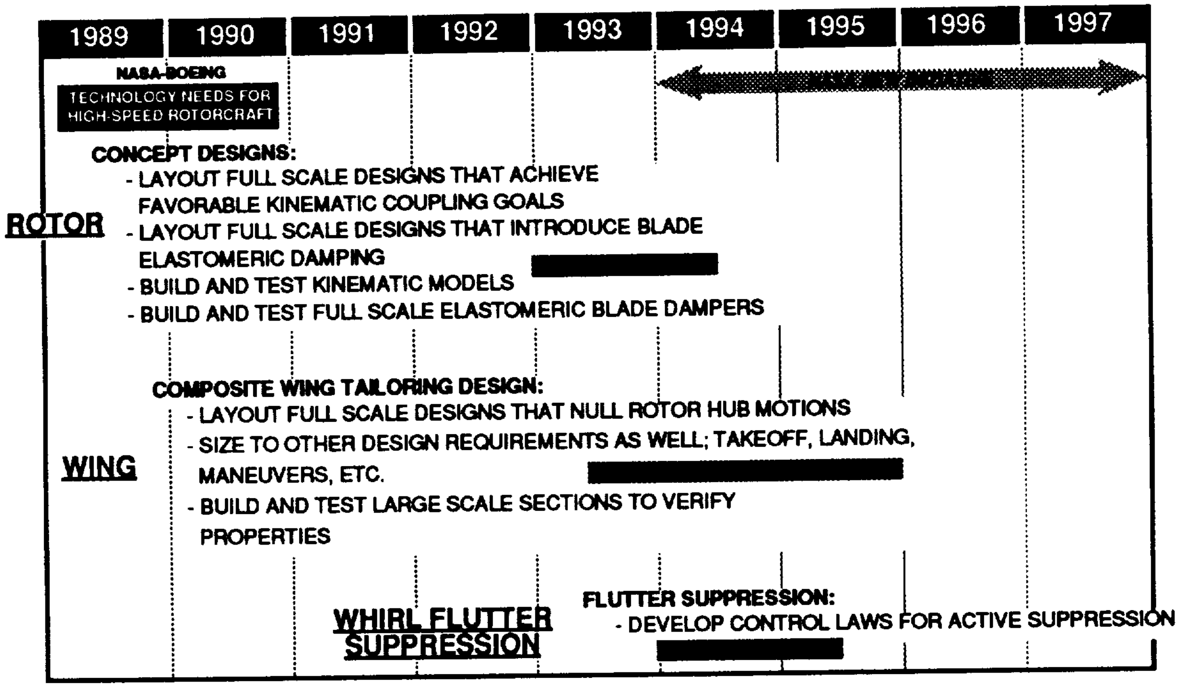

Figure 87. High-Speed Civil Tiltrotor Whirl Flutter Prevention Hardware Plan

The following two sections discuss the technology developments needed for acoustics. Figure 88 is a schedule of the recommended activities.

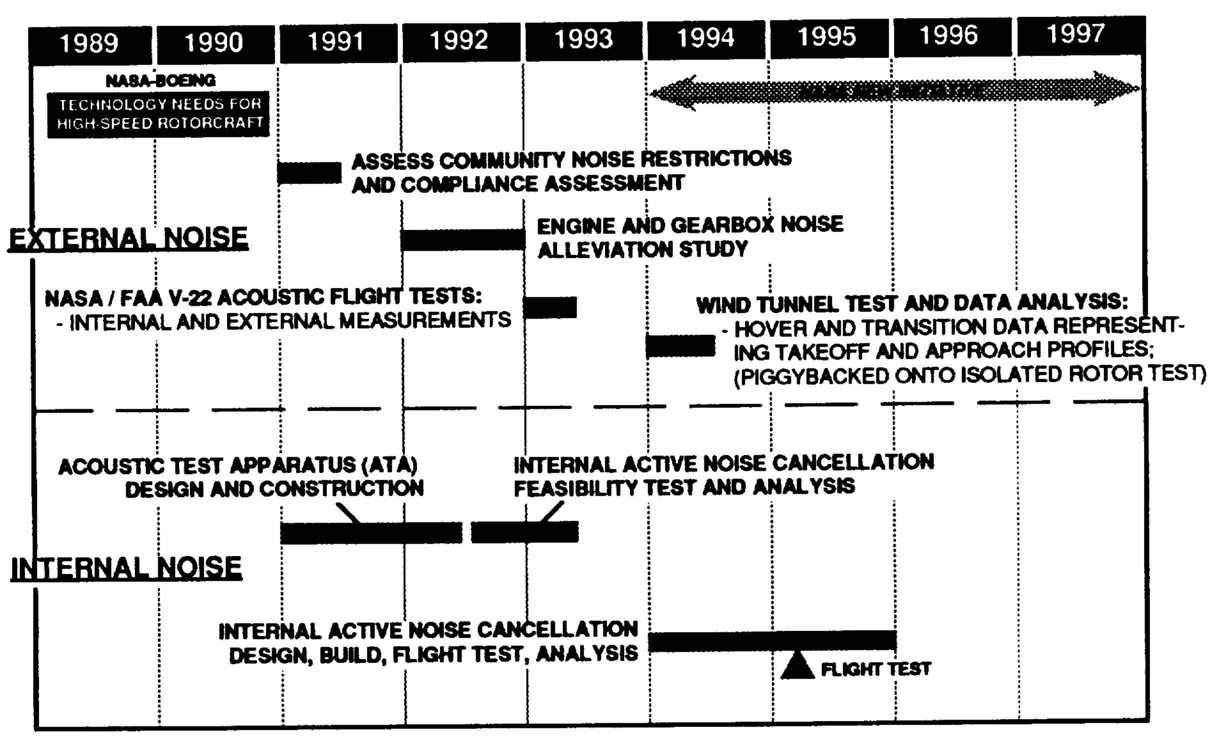

Figure 88. High-Speed Civil Tiltrotor Acoustics Enabling Technology Plan

External Noise

External noise must reflect a Good Neighbor Policy. Some of the many parameters which affect noise are listed below:

- Engine noise
- Rotor parameters
  - Airfoil contour, blade planform, rotational speed
- Flight condition
  - Helicopter mode, conversion, airplane mode
- Flight Path
  - Takeoff, climb, cruise, partial-power descent, loiter

Approach - Certification requirements for external noise of helicopters are covered in FAR-36, Part H, and ICAO Annex 16. However, the community criteria for airport planning, covered by FAR-150, Noise Control and Compatibility Planning for Airports, may impose more stringent local limits. Thus, a survey should be done to assess the restrictions which local community noise limitations might impose on civil tiltrotor operations. In a parallel activity, noise predictions for the high-speed civil tiltrotor would be used to develop noise footprints for several takeoff, approach, and landing trajectories. These footprints would be compared to the community noise limits to evaluate the degree of conformance or the limitations which noise constraints might impose.

As previously discussed in the civil tiltrotor noise section from Task II, engine noise can contribute a significant portion of the total aircraft noise. This is especially true for flyover noise, where the rotors are lightly loaded and have reduced tip speeds. In some direction, the engines also produced more noise than the rotors in predictions of 500-foot sideline hover noise. The engines still contributed heavily to the estimated departure and approach noise. Engine noise dominated while approaching the microphone, while rotor noise dominated overhead and after passing the microphone. The conclusion is that engine noise treatment is just as important as rotor noise reduction for civil tiltrotors.

Predicted external-noise levels must be verified by acoustic data from isolated rotor wind tunnel model tests. Acoustic data would be acquired piggybacked onto the test of another rotor model (performance or aeroelastic model) for a least-cost approach, such as the isolated rotor test shown in Figure 85. The acoustic data would be analyzed and corrected to full-scale free field. It would then be used to validate full-scale noise predictions. Improved data quality could be achieved by the addition of an acoustic lining for the wind tunnel (at least for the acoustic portion of the test). This approach would require separate runs for acoustics plus the cost of the liner, its installation, and removal.

Plan - Figure 88 is a schedule of activities, including full-scale flight test measurements on the V-22 and acoustic data from the advanced-geometry-rotor wind tunnel model test (coordinated with Figure 85).

Internal Noise

Approach - Internal noise on a tiltrotor is dominated by the low-frequency noise associated with the blade tips passing near the cabin. The noise is transmitted by exciting the body shell and so involves a structural response as well. The high-speed civil tiltrotor (and the military folding tiltrotor) has been intentionally designed with the blade tips outboard of the canard, giving a substantial 48-inch separation between the body and the blade tip. Predictions of internal noise for this spacing are considerably lower than those for rotors in proximity to the body. Still, acoustic treatment is required, but at less than half the weight penalty for treating a 12-inch prop-to-body spacing.

An internal acoustic goal of 78 dBA would require still more treatment and may justify active noise-cancellation technology. Static full-scale tests of this technology need to be done on a representative fuselage section (construction and materials similar to the full-scale design). Excitation from the blade tip passage could be simulated by loudspeakers and/or shakers external to the body section. Inside the body section an active cancellation controller would be used to drive a combination of internal airframe shakers and/or loudspeakers to cancel (minimize) the internal noise. This test would establish feasibility of the system and provide an inexpensive, ground-based facility for further acoustic work.

Plan - Figure 88 also shows a schedule for measurements of full-scale internal noise on the V-22, which would include calibration of analytic techniques. Two years are also devoted to the design and construction of a ground-based acoustic test apparatus for measurement and study of internal noise and its abatement. Once built and instrumented, this acoustic test apparatus would also be used to explore the feasibility of active noise cancellation.

Vibration

Issue - Another important issue for high-speed civil tiltrotors is vibration control. Vibration limits for helicopters qualified under military specifications have been steadily decreasing over the past 20 years, generally in keeping with technology improvements that have made it possible to meet them. Achieving lower vibration has also been aided indirectly by lower helicopter empty weights which have made it more feasible to add vibration treatment devices without degrading payloads. Specific vibration objectives have not yet been established for civil tiltrotors. But based on helicopter experience, a goal of 0.05g at cruise and 0.10g in maneuvers is needed for good pilot and passenger acceptance. Such levels should be achievable. The current MV-22 has demonstrated levels of 0.07g in the cockpit area with vibration treatment.

Approach - The technical challenge for a 450-knot tiltrotor is first to understand and deal with the sources of vibration in steady-state forward flight. From our extensive MV-22 experience, it is known that the major vibratory loads are in the rotor in-plane direction at 3P, the number-of-blades frequency. They are induced by two items: (1) the wing shadow interference as each blade passes the wing, and (2) the fuselage/canard interference as the rotor tip passes the fuselage/canard. These loads are partially isolated by the low bending frequencies of the wing, but partially transmitted to the fuselage by the higher frequency wing modes. Secondary, but still significant, excitation comes from rotor 3P vortices impacting the tail surfaces and exciting the fuselage starting at the aft end.

The rotor excitations due to wing and fuselage interference have been analyzed by CAMRAD and by C-60 assisted by the VSAERO 3-D potential code. They have been measured directly as shaft loads, and tail excitations have been measured with pressure instrumentation in wind tunnel tests. The analyses have given reasonable correlation with the tests.

For the high-speed tiltrotor, the wing interference excitation should be reduced by the sharply forward-swept wing, in that the rotor tip is longitudinally displaced farther forward and away from the wing than the MV-22. The proximity effect of the rotor tip near the fuselage is still present. In addition, a new interference is present by virtue of the forward canard. This aerodynamic surface, essential for flight pitch stability, will result in a rotor tip excitation to the blades passing near the canard, and will result in a new set of N-per-rev in-plane vibratory loads. In addition, the vortex excitation into the tail surfaces will still be present, but can be alleviated by improved tail design.

One approach which is in development by many researchers is optimization. The concept is that the structural response of the rotor blade to the aerodynamic excitation can be reduced by clever blade mass and stiffness distributions that will nearly null the transmitted vibratory root shears into the rotor hub. Our experience to date in this area is in having developed a helicopter rotor vibratory load reduction analytical optimizer and applying it to the design of a low-vibration model rotor. Wind tunnel tests of this rotor design have already demonstrated the success of the concept.

A second approach involving active control of vibration akin to helicopter rotor harmonic control should also be pursued. First, analyses would determine the collective and/or cyclic control inputs necessary to null the vibratory shears being fed into the rotor hub. Then concept studies of control arrangements to introduce these inputs would take place. A model version would be designed and implemented, and wind tunnel tests on the same semispan model would explore the concept. Note here an advantage for a 3-bladed rotor: swashplate HHC control of collective and cyclic fully control each blade without the need for individual blade control.

Plan - Figure 89 shows that rotor vibratory loads research for the high-speed tiltrotor should be pursued by analysis, wind tunnel test, and concept design studies. First, CAMRAD and C-60 load prediction methodology can be modified to include the canard interference. Then predictions of load magnitudes can be made. Next to be dealt with are means to control these loads.

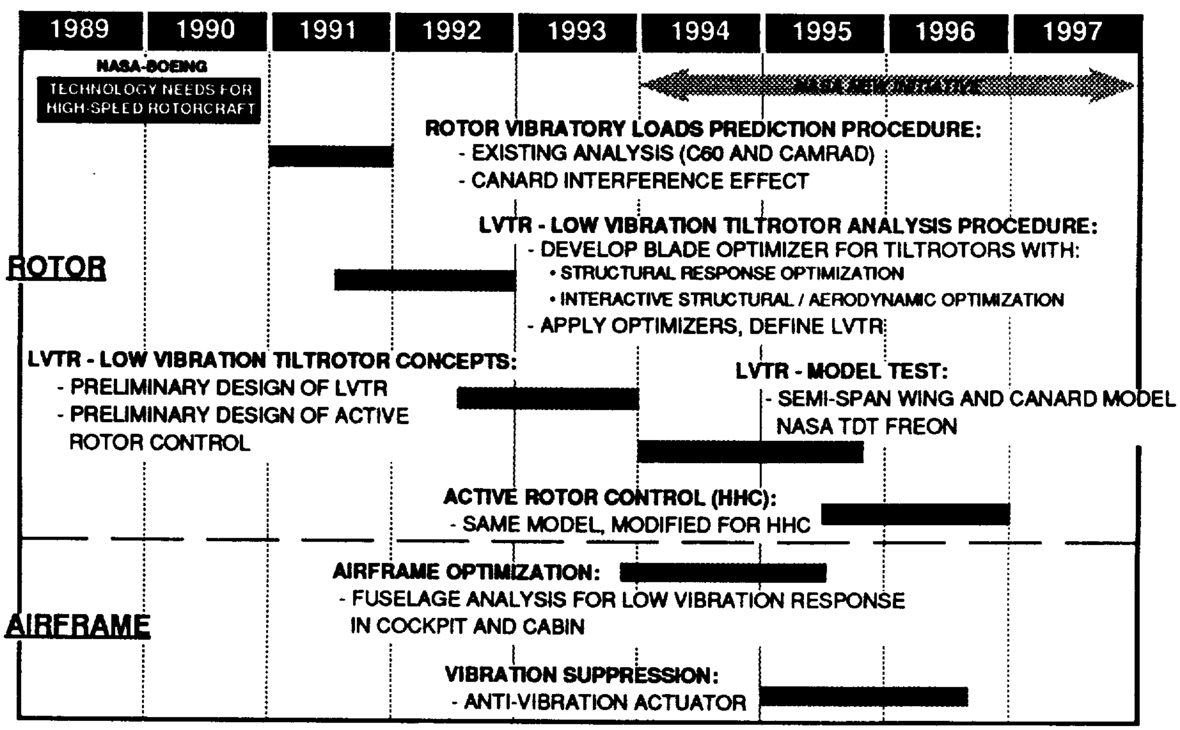

Figure 89. High-Speed Civil Tiltrotor Vibration Control Enabling Technology Plan

Figure 89 also shows the low-vibration rotor technology being developed for the high-speed tiltrotor. A similar analytical optimizer would first be developed. Then this would be applied to a preliminary tiltrotor design. In consort with rotor designers, the rotor structure would be iterated until a low-vibration tiltrotor (LVTR) was defined. A model would then be designed and built for testing in NASA's TDT tunnel on a semispan wing model, including the effect of canard interference.

In the lower part of Figure 89 are shown the airframe vibration control research efforts. First, airframe optimization would be undertaken using finite-element codes such as NASTRAN which now contain structural optimization routines. We could start with stick models of wing and fuselage and study vibration optimization. Later, the process could be repeated on more realistic models of a high-speed tiltrotor vehicle. A second effort would be a study of vibration suppressors in the fuselage. These would be similar to that already being flown successfully on the MV-22. The finite-element model would be excited by the rotor vibratory loads obtained above, and the suppressor located and sized to determine its practicality and effectiveness.

Flight Control Laws and Development

Issue - Both the high-speed civil tiltrotor and the folding tiltrotor share the V-22-type tiltrotor flight control requirements in the helicopter mode, transition, and low-speed-rotor airplane mode. In high-speed cruise, though, rotor controls for the high-speed civil tiltrotor must be tailored to the rotor's sensitivity in the high-Mach-number and high-dynamic-pressure environment. These differences require significant modifications to the flight control laws for high-speed flight and need to be verified by flight simulators.

Approach - At 450 knots, the high-speed civil tiltrotor's rotor must go to higher collective-pitch angles than the V-22 at 300-knots, driven by the combined effect of reduced tip speed and the 50% increase in airspeed. At this higher airspeed, the blade local Mach numbers vary from 0.75 inboard to nearly 1.00 at the tip, giving high dynamic pressures. Compounding this, compressibility effects drive up the airfoils' lift-curve slope. These combined factors make the rotor thrust (and blade loads) very sensitive to small changes in angle of attack. A 10% change in lift corresponds to only a 0.05-degree change in local angle of attack. Thus, controlling rotor thrust will require an accurate collective-pitch control with fine adjustments. It may also require sensors and feedback circuitry to restrict inadvertent blade and hub loads during high-speed flight.

Active aeroelastic controls should also be considered as an attractive technology with the potential to solve aeroelastic instabilities with a minimum impact on airplane structures. These civil tiltrotor controls need to be developed and then evaluated on a flight simulator to prove their effectiveness for load limiting, to fine-tune their sensitivity for pilots, and to assess their net impact on the aircraft handling qualities.

Plan - Figure 90 outlines the steps to develop the needed technology. Advanced control laws would be developed first. Loads limiting controls would be developed in 1993, following definition of the rotor and hub geometry. Studies of aeroservoelastic compensation would be conducted following the model rotor wind tunnel tests.

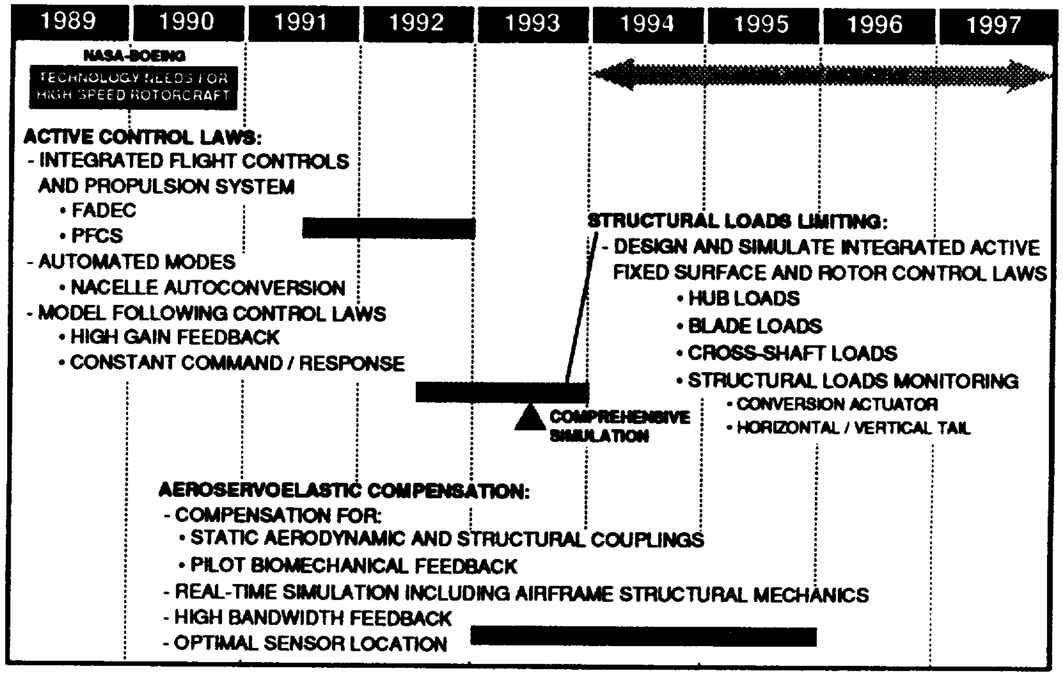

Figure 90. High-Speed Civil Tiltrotor Flight Control Laws Enabling Technology Plan

Military Folding Tiltrotor - Specific Design Issues

The folding tiltrotor concept, like the civil tiltrotor, has several specific design issues which must be resolved prior to full-scale development. These design issues involve many technical disciplines, and these disciplines must work in concert to achieve an integrated rotorcraft with helicopter-like hover performance and fixed-wing-like cruise performance. Several design issues pertaining to the folding tiltrotor were previously discussed in the section on Common Critical Technologies. Table 19 lists additional design issues which are specific to the military folding tiltrotor configuration.

Table 19. Design Issues Unique to the Military Folding Tiltrotor

■ **Convertible engine propulsion** - VIGV / VEGV versus variable pitch fan - Cruise thrust control - Residual thrust control (in shp mode) - Clutch and engaging sensor ■ **Hub design** - Stable low speed platform - Stable during slowing and stopping - In-flight blade folding mechanism - Folded blade retention device ■ **Aeroelasticity** - High-speed maneuvers - Wing static divergence	■ **Flight controls / handling qualities** - Multiple modes • helicopter mode • transition • turboprop airplane mode • automated stop / fold mode • turbofan airplane mode - Sensitivity with speed - Loads limiting features ■ **Automated stop / fold procedure** - Analysis - Integrated flight controls - Load limiting characteristics

Convertible Engine Propulsion

Issue - General Electric and Allison Gas Turbine Division were funded by NASA Lewis to perform an initial precursor study of convertible engine possibilities in 1989. Based on this data, the two most promising forms of convertible engines appear to be the variable-inlet guidevane/ variable-exit guidevane (VIGV/VEGV) and the torque-convertor concepts. Boeing Helicopters selected the VIGV/VEGV convertible engine configuration for the military folding tiltrotor in this study. Allison and General Electric are presently funded by NASA Lewis in a follow-on program to perform more detailed design studies of convertible engine configurations for high-speed rotorcraft.

Part of the Allison and General Electric effort will be to identify technology concerns. The paragraphs below address what Boeing Helicopters understands to be the technology concerns at this time. A detailed approach and technical plan will be forthcoming from the engine manufacturers' studies.

Concerns - One of the principal issues of the VIGV/VEGV configuration is operation in the turboshaft mode, with vanes closed. Some fan airflow is necessary even in this mode of operation to limit temperature rise in the fan. The technical issues are the windage losses, blade stresses, and noise associated with this mode of operation. The VIGV/VEGV configuration gives substantial shaft power for hover in turboshaft operation, but also results in considerable residual fan thrust. While this is undesirable for pure hover flight, it should give higher acceleration for rapid transitions to the airplane mode and improved STO operations. Methods to minimize hover residual thrust may need to be developed, depending on the vehicle's application.

Another technology concern to be considered is performance of the fan hub supercharging section. Losses can occur due to leakage from the fan hub supercharging section into the bypass fan airstream. Also, a bleed optimization system may need to be developed for the constant-speed turboshaft operation.

Propulsion system thrust controls for the folding tiltrotor must also be developed and verified. Maneuver capability includes accelerations and decelerations, which largely depend on engine response. The pilot's throttle control must now interface with both rotor controls while in hover and turboprop airplane mode, and with the high-bypass fan engine with VIGV/VEGV controls in the folded, turbofan airplane mode. The variable VIGV/VEGV is a requirement to control fan thrust at constant rpm when in the turboprop airplane mode. But in the turbofan mode this engine control could allow variable rpm at constant VIGV/VEGV settings, being fundamentally different from the constant-rpm rotor operation. The choice between these turbofan thrust controls affects the feedback loops which must be designed into the flight controls and FADEC. It also affects fuel consumption at partial power, which would directly impact loiter capability. These performance and control characteristics, and cost implications must be resolved.

The torque convertor configuration continues to offer a potential alternative convertible engine concept if development problems or performance shortfalls should arise in development of the VIGV/VEGV. In addition to the above concerns, the torque convertor concept lacks any large-scale development or demonstrator hardware to attest to its validity. A hardware development and demonstration program, similar to that of the convertible TF34, would need to be undertaken before giving it serious consideration. Size, weight, cost, and heat transfer are among the present uncertainties for this concept.

Plan - Figure 91 shows a general schedule of activities in preparation for a new engine development program go-ahead in about 1997.

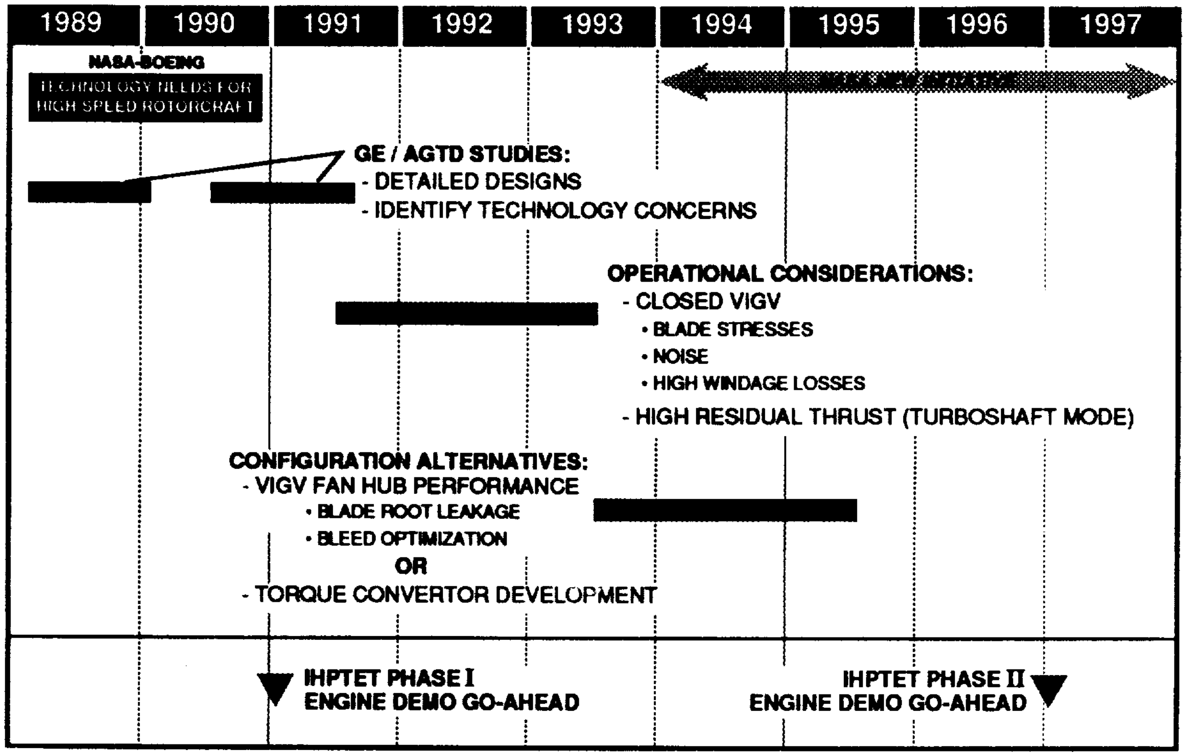

Figure 91. Folding Tiltrotor Convertible Engine Technology Plan

Hub Design

Issues - The hub design for the folding tiltrotor must provide a stable rotor system in the helicopter mode, during transition, and in the low-speed rotor airplane mode. It must provide a stable platform for the rotor during slowing/stopping and during spinup, avoiding large flapping/gimbaling excursions; and it must include the mechanism(s) for automatic in-flight blade folding. The hub must allow for a large range of collective pitch to accommodate:

- Low collective pitch
  (low thrust required by maneuvers and descents)
- Intermediate collective pitch
  (rotor airplane mode)
- High collective pitch
  (feathered blades during rotor stopping)

After these functions are achieved, the hub should be of relatively small diameter and the blade-folding joints must be carefully faired for aerodynamic drag reasons in high-speed cruise.

Approach - The folding tiltrotor hub design should be conducted in three parts: conceptual layouts, preliminary design and the detail design of a functional model. The design requirements would be established and conceptual layouts drawn which may satisfy them. This includes consideration of structural fatigue life, bearing life, blade attachment kinematics, controls requirements, and folding mechanisms. Several hub concepts would be examined. Their merits would be compared to one another and a final configuration would be selected. The selection criteria would include such factors as survivability, reliability, vibration factors (e.g., constant-velocity joint), functional requirements of feathering, stopping, folding, indexing, and control force and moment generation.

The second part, preliminary design, would include hub component design to satisfy predicted rotor hub loads, identify critical components, and establish margins of safety. Layouts would show close-tolerance parts and specify fits. Manufacturing technology will be integrally involved, drafting a manufacturing plan and proving any new manufacturing methods with a soft-tools approach. A critical design review (CDR) should be held at this point.

A functional mockup would be manufactured after the CDR to demonstrate form, fit, and function. CATIA solid modeling would be used to define all of the component parts' dimensions and tolerances.

Plan - Figure 92 shows the necessary activities to develop a hub design for the folding tiltrotor. Loads data would be extracted from wind tunnel tests which were shown in Figure 87. As with previous schedules, some of the activities must be scheduled around the wind tunnel test date to make use of the wind tunnel test data.

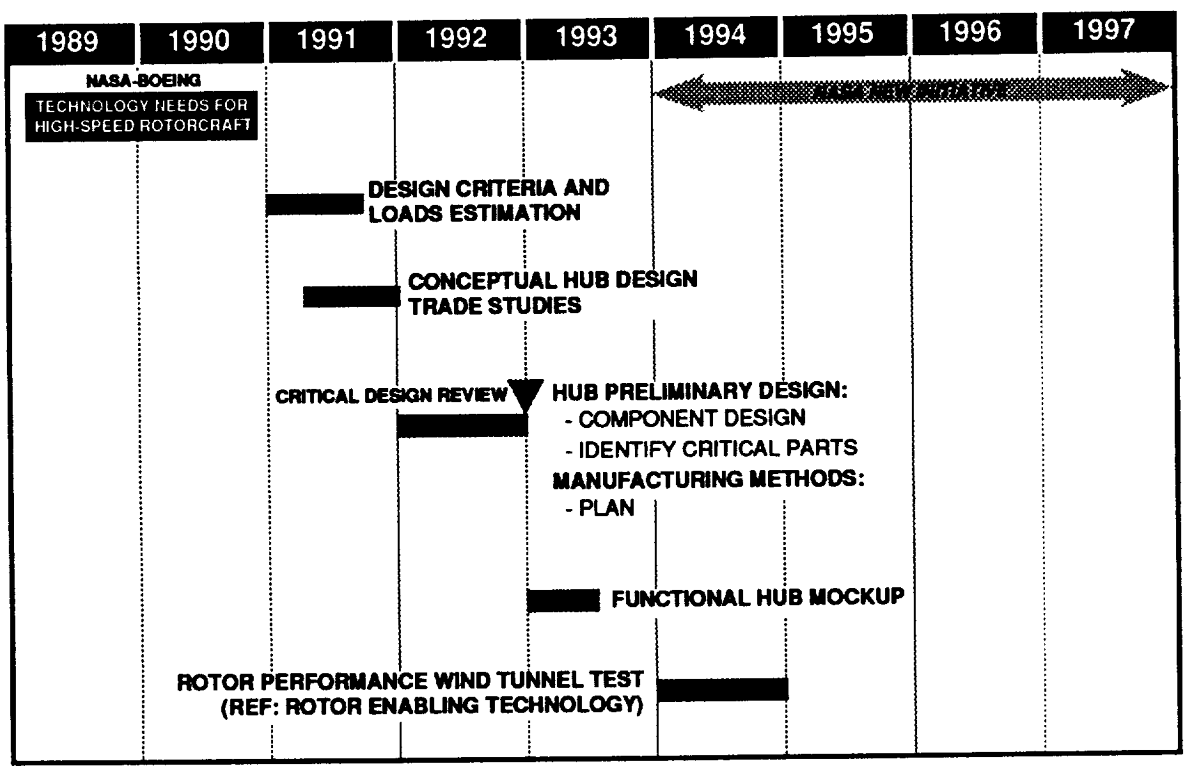

Figure 92. Folding Tiltrotor Hub Enabling Technology Plan

Automated Stop / Fold Procedure

Issue - An automated and reversible stop/fold procedure is a requirement for any practical, operational folding tiltrotor. The stop/fold sequence for the folding tiltrotor is described below:

1. Adjust shaft power and collective pitch to take the rotor from a propulsive state to a nonthrusting, zero torque, windmill state. Simultaneously adjust turbofan thrust from the convertible engine to maintain airspeed.
2. Declutch the rotor drive shafts from the engines.
3. Slow the rotor by feathering the blades. Adjust turbofan thrust to compensate for drag decrease during slowing/stopping.
4. Brake rotor to a stop and index blades to proper azimuth for folding.
5. Fold blades back over nacelle and lock into folded position. Adjust turbofan thrust to compensate for drag decrease after folding.

Approach - A prerequisite for accomplishing the above sequence is that each step be well understood, including associated loads and force and moment generation. Much of this work has already been accomplished through the studies and wind tunnel tests conducted on the folding-tiltrotor concept during the 1968 through 1973 time period. Test reports are available from this period which establish the feasibility of the process. They showed that slowing, stopping, and folding were readily achievable without exceeding blade loads typical of normal in-flight loads. However, it is necessary to design and test a specific hub (and blades) based on today's objective of a 450-knot cruise speed , a 250-knot folding speed, and using today's materials. These test data will provide the specific loads data necessary to determine an optimum set of control laws for automating the stop/fold sequence. Additional data would also be required to determine loads associated with off-design conditions, such as gusts or maneuvers during the stop and fold.

A folding-loads analysis must be developed which can predict and simulate the blade loads, hub loads, flapping and gimbal excursions, and net forces and moments during slowing, stopping, and folding. At the same time, flight control laws must be developed to control the sequence of events. Sensor requirements (types, positions, and sensitivities) will be determined at this stage. The feasibility of implementing loads-limiting features will also be addressed. A failure-mode-and-effects analysis should also be conducted on the whole system.

Finally, the folding-loads analysis and the flight control laws must be combined with a model of the convertible engine to create a comprehensive digital simulation of the entire process to validate the approach and to adjust gains in the flight control system. This comprehensive analysis is not envisioned as a real-time simulator, but rather a digital program to analyze the automated stop/fold process, and by which to further improve that automation.

Plan - Figure 93 shows a schedule of the cited activities, including a special wind tunnel test to define loads during stopping and folding. This would model the rotor and its folding sequence. It would verify the loads and blade dynamic deflections during the folding sequence.

Aeroelasticity

Issue - What were important whirl-flutter stability issues for the high-speed civil tiltrotor are no longer so important for the folding tiltrotor. The folding tiltrotor flies in the tiltrotor airplane mode only up to 250-knots, and the whirl-flutter issues are rather well understood up through this range as a result of the XV-15 and V-22 design, wind tunnel, and flight experience.

However, beyond 250-knots and up to its dive speed of 518-knots, there are at least two other aeroelastic issues for the folding tiltrotor in its high-speed turbofan airplane mode. These are:

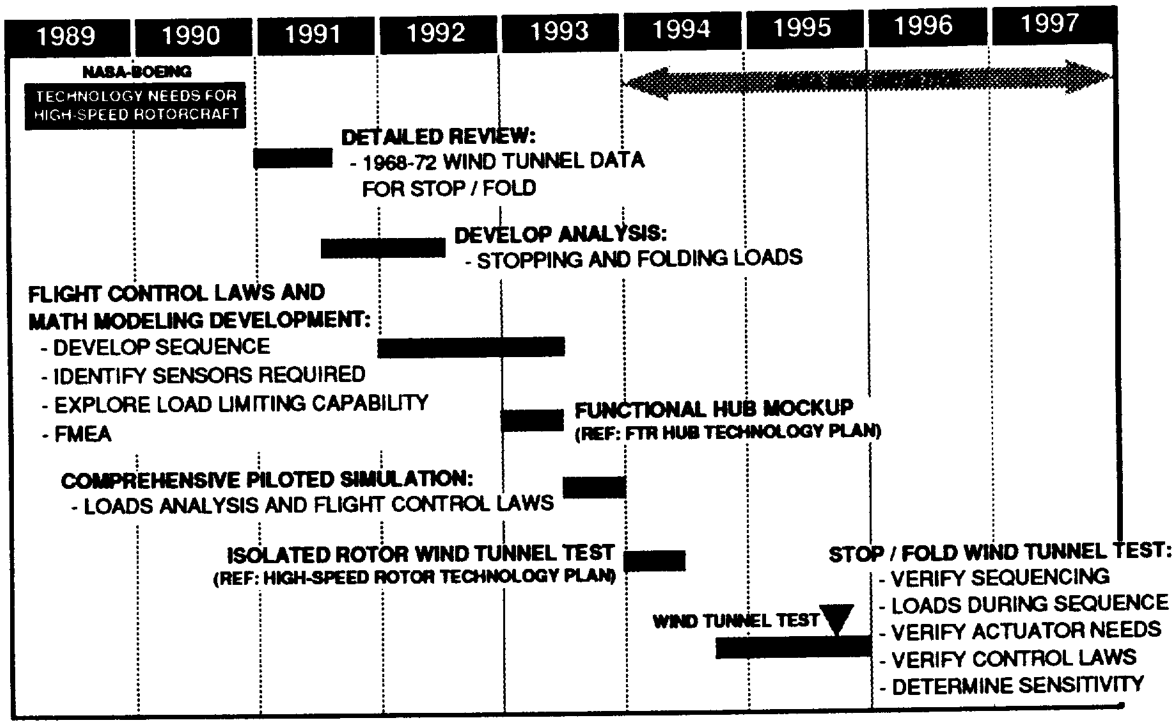

Figure 93. Folding Tiltrotor Stop / Fold Enabling Technology Plan

(1) wing static divergence, exacerbated by the forward-swept wing and its large-folded rotor pod, and (2) the class of aeroelastic phenomena which tends to neutralize airframe response to control inputs via structural deflections, such as aileron reversal. The latter could be especially important when designing for military maneuver requirements.

Approach - Wing static divergence of a forward-swept wing has been most recently addressed in the Grumman design of the X-29. Tailored-ply orientations of high-modulus composite fibers were used to reduce the wing's destabilizing pitch-up torsional response to outboard lift.

The folding tiltrotor would be subject to the same problem. It could be even more susceptible because its wingtip rotor pylons can generate additional destabilizing aerodynamic moments. Conventional wing flutter also must be considered and controlled for this configuration.

Existing industry codes such as NASTRAN or Boeing airplane flutter programs would first be used to predict divergence and flutter for the folding tiltrotor at high speeds, up to nearly 650-knots. If analytical deficiencies are revealed by these calculations, then a follow-on effort would try to correct the deficiencies. The upgraded analyses would be used to repeat the calculations and to define the wing stiffness required to prevent divergence and flutter.

A preliminary design of a full-scale wing that would meet these requirements would then be prepared. Next, a model of this wing would be designed and built, and a wind tunnel test conducted to verify the stability of the design.

Vibration control for the folding tiltrotor should fit within existing technology. The V-22 already covers the envelope conditions from helicopter to airplane flight that a folding tiltrotor would occupy. V-22 vibration meets military requirements with rotor pendulum vibration absorbers and an active hydraulic suppressor. Vibration-control technology developed under the civil tiltrotor enabling technology plan should be directly applicable to the folding tiltrotor as well.

Plan - Figure 94 is an enabling technology plan for the aeroelastic problems of the folding tilt-rotor.

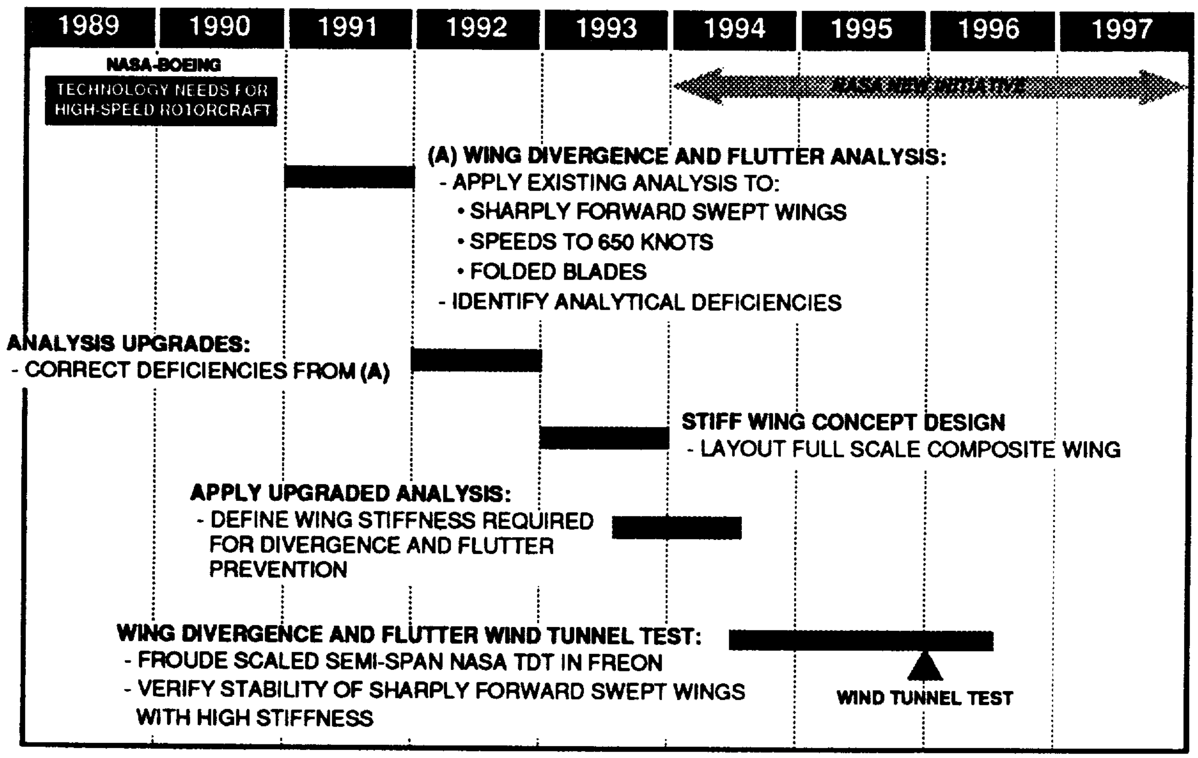

Figure 94. Folding Tiltrotor Aeroelastic Enabling Technology Plan

Flight Control Laws

Issue - The V-22 flight controls were designed to handle two flight regimes, helicopter mode and airplane mode, and the transition in between. The folding tiltrotor requires all of this for normal turboprop tiltrotor flight, but it also requires the integration of two more conditions. First, it must incorporate the automated stop/fold procedure developed previously, and second it must handle the high-speed turbofan airplane mode. This constitutes five distinct modes for the flight control system, each mode having its own set of unique requirements:

1. Helicopter mode
2. Transition
3. Turboprop airplane mode
4. Automatic stop/fold mode
5. Turbofan airplane mode

Approach - Operation in the first three modes is essentially the same as the V-22 flight control system and the fourth mode, automatic stop/fold, has been previously discussed. In the 250-450-knot turbofan airplane mode, the control system may require a change in control sensitivity to avoid over-sensitive vehicle responses. These would be similar to flight control changes implemented in many high-subsonic commercial aircraft. Also, the pilot's throttle control must now interface with a high-bypass fan engine with VIGV/VEGV controls. Or, as previously discussed, the throttle control may allow variable rpm for constant VIGV/VEGV settings. Also, aeroservoelastic compensation should be examined for high-speed flight as an attractive technology with potential to solve aeroelastic instabilities with a minimum impact on the airplane structure.

A flight simulation is recommended to verify the suitability of each of the five control modes and to allow pilot assessment of a smooth transition among them. Turbofan thrust response in the turbofan mode, through either VIGV control at fixed rpm or through varying rpm with fixed VIGV (0 degrees), can be examined on the simulator. Loads-limiting features of the control system can also be modeled and evaluated on the simulator for any flight mode.

Plan - Figure 95 outlines the steps to develop the needed technology. Advanced control laws would be developed first. Loads-limiting controls would be developed later, appropriate to measured loads data from the wind tunnel test program.

Figure 95 also shows a three-axis maneuver analysis which will recognize elastic wing and control deflections and will calculate loads. Data from the stop/fold wind tunnel test conducted under the automated stop/fold procedure would verify the loads and blade dynamic deflections during the folding sequence. This same model could be used in a high-speed test to obtain blade loads data and flutter tendencies when folded in high-speed cruise flight.

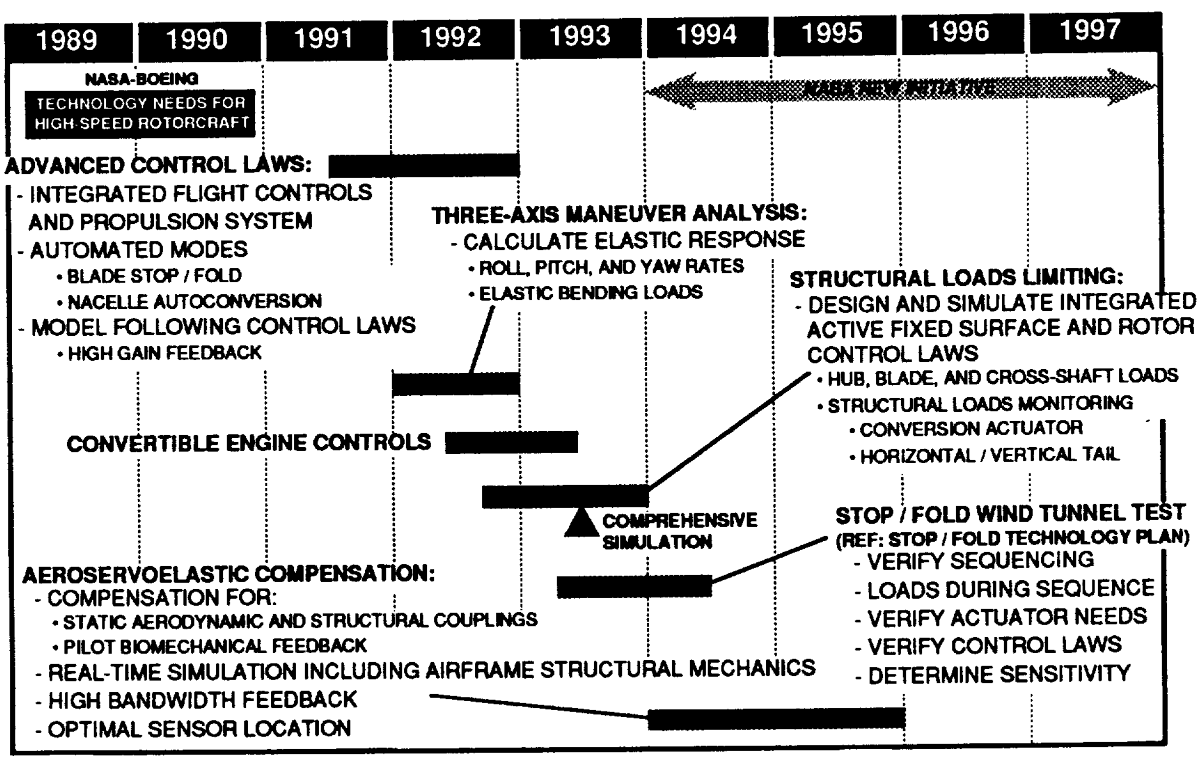

Figure 95. Folding Tiltrotor Flight Control Laws Enabling Technology Plan

CONCLUSIONS

Five candidate rotorcraft concepts out of a field of 20 were quantitatively evaluated to choose the two concepts which hold the most promise for achieving a 450-knot speed. The folding tiltrotor was the only low-disc-loading concept examined which had a realistic, near-term potential for speeds of 500-knots and greater. Furthermore, the folding tiltrotor had clearly superior survivability traits in the turbofan mode, making it ideally suited to military applications in either the transport or fighter/attack roles. The high-speed tiltrotor in a canard arrangement with an advanced-geometry rotor design was the lightest weight concept and the lowest cost concept. These attributes made it well suited to civil applications such as passenger service, light container cargo and public service. Conceptual designs were made for a military folding tiltrotor and a high-speed civil tiltrotor. The two high-speed tiltrotor concepts are a unique breed of powered-lift rotorcraft, challenging the helicopters' low-speed domain and the fixed wings' high-subsonic-speed domain.

Both of these 450-knot concepts are feasible with 1990 technology, but both were found to have risk areas requiring further technical development before entering a full-scale development program.

Estimates of the potential gains available with advanced technology were made for aerodynamics, structures, weights, aeroelasticity, and propulsion system technologies, to be representative of that achievable by the year 2000. Projected benefits of these advanced technologies on aircraft size, gross weight, and cost have enormous potential. The combined impact on the two high-speed rotorcraft was similar: 25% lower gross weight, 27% to 36% less installed power, and 30% lower recurring production costs. The truly long-term advantage is in energy savings and environmental impact: less raw material needs to be processed for manufacture, less energy used during manufacture, less fossil fuel used, and lower atmospheric emissions in flight. However, it will take a substantial investment in research over the next 5- to 10-years to make this potential become reality.

An enabling technology plan was prepared. Critical design issues are identified for each concept. Most of these issues involve more than one technical area and will require concurrent-engineering solutions. Some items are risk-reduction areas, a necessary step before entering full-scale preliminary design. Some items have not been previously explored in depth, such as: (1) low-disc-loading, high-speed rotor design with good propulsive efficiency, (2) design for whirl-flutter stability for 450-knot tiltrotors, (3) internal-noise levels on high-speed tiltrotors suitable for civil applications, and (4) production convertible engines and clutch design. Other items reflect a need for general technology improvement such as: (1) aggressive application of advanced materials and manufacturing methods to achieve lighter, cost-effective structure, and (2) external acoustics where today's technology has simply not kept pace with the high standards set for acceptance by local communities.

The conclusion is that 450-knot rotorcraft designs are feasible with 1990 technology, but would require at least a risk-reduction program conducted as a precursor to full-scale preliminary design. The individual improvements potentially available in several technology areas can have a tremendous synergistic effect on turn-of-the-century rotorcraft size and cost. The critical design issues identified in the enabling technology plan should be systematically pursued to achieve that potential.

REFERENCES

1. Wernicke, R. K., *Prediction of Tilt Rotor Outwash*, AIAA Paper 81-0013, AIAA 19th Aerospace Sciences Meeting 1981.

2. Jones, G. E., and Lucero, F. N., *Operational Suitability Tests (of XC-142A)*, USAF FTC-TR-67-28.

3. Schane, W. P., *Effects of Downwash Upon Man*, U.S. Army Aeromedical Research Unit Report No. 68-3, 1967.

4. Boyne, W. J. , and Lopez, D. S., *Vertical Flight, National Air and Space Museum, 1984; Rotary-Wing V/STOL: Development of the Tilt Rotor.*

5. Thomason, T. H., *The Bell Helicopter XV-3 and XV-15 Experimental Aircraft*, AIAA Paper 90-3265, 1990.

6. Schneider, J. J., *Advanced V/STOL Attack Aircraft Design/Operations Trade-off*, AIAA Paper 89-2116, 1989.

7. Schneider, J. J., *The History of V/STOL Aircraft*, Vertiflite, American Helicopter Society, Vol. 29, No's. 3 and 4, 1983.

8. Borst, H., *The Curtiss-Wright X-19 Experimental Aircraft - Lessons Learned*, AIAA Paper 90-3206, 1990.

9. Boeing Vertol Division, *Development of the U.S. Army VZ-2 Research Aircraft*, Technical Report R-219, August 1963.

10. Dausman, George E., *The LTV XC-142 Experimental Aircraft - Lessons Learned*, AIAA Paper 90-3204, 1990.

11. Nichols, J., *The Hiller X-18 Experimental Aircraft - Lessons Learned*, AIAA Paper 90-3203, 1990.

12. Phillips, Frederick C., *The Canadair CL-84 Experimental Aircraft - Lessons Learned*, AIAA Paper 90-3205, 1990.

13. *Interavia*, July, 1968, *The VC-400 Tilt-Wing V/STOL Transport.*

14. Cheeseman, I. C., *Circulation Control and its Application to Stopped Rotor Aircraft*, AIAA Paper 67-747, April 1967.

15. Deckert, W. H., and McCloud, J. L. III, *Considerations of the Stopped Rotor V/STOL Concept*, Journal of the American Helicopter Society, Vol. 13, No. 1, 1968.

16. Harned, M. S., Amer, K. B., and Sullivan, R. J., *Hot Cycle Rotor/Wing for High Speed City Center Transportation*, AIAA Paper 67-770, October 1967.

17. Krone, N. J., Jr., *X-Wing Experimental Aircraft - Lessons Learned*, AIAA Paper 90-3208, 1990.

18. Kisovec, A. V., *Convertiplane*, U. S. Patent No. 3,797,783, March 19, 1974.

19. Leoni, R. D., and Kaplita, T. T., *Research and Development of the Stowed Rotor V/STOL Concept*, SAE Paper 650194, April 1965.

20. Lockheed, *Composite Aircraft Program*, Report No. LR-20807, July 1967.

21. Fry, B. L., *Assessment of Commercial VTOL Aircraft with Rotor or Propeller Lift Systems*, AIAA Paper 67-411, June 1967.

22. Bell Helicopter Co., *The Trailing Rotor VTOL-Status and Projections*, USAF Systems Command "Beyond the Horizon" Report SCL-6-66-10, January 1967.

23. Fry, B. L., and Schneider, J. J., *Design Optimization of Stoppable-rotor V/STOL Aircraft Systems*, National Aerospace Electronics Conference, Dayton, Ohio, May 1969.

24. Fraga, D. E., and Liiva, J., *Design Studies and Model Tests of the Stowed-Tiltrotor Concept*, AIAA Paper 72-804, August 1972.

25. Bell Helicopter Co., *Large Scale Wind Tunnel Investigation of a Folding Tiltrotor*, Report D272-099-002, May 1972.

26. Isacco, V., *Telescopic Blade for Rotating Wing Aircraft*, U.S. Patent 2,713,393, 19 July 1955.

27. Tarcyznski, T. T., *Retractable Rotor Development*, American Helicopter Society Journal, January 1957.

28. Goldman, R. L., *Some Observations on the Dynamic Behavior of Extremely Flexible Rotor Blades*, AIAA (IAS) Paper 60-44, January, 1960.

29. Pruyn, R. R., and Swales, T. G., *Development of Rotor Blades with Extreme Chordwise and Spanwise Flexibility*, AHS National Forum, May 1964.

30. Kisovec, A. V., *Aircraft Propelling Assembly*, U.S. Patent 3,297,094, January 10, 1967.

31. Young, A. M., *Variable Diameter Propeller*, U.S. Patent 3,128,829, April 14, 1964.

32. *Aviation Week and Space Technology*, Page 66, 18 November, 1968.

33. Frandenburgh, E. A., *Application of a Variable Diameter Rotor System to Advanced VTOL Aircraft*, AHS National Forum, May 1975.

34. Frost, J.C.M., et al, *U.S. Patent 3,020,003*, February 6, 1962.

35. Murray, D., *The AVRO VZ-9 Experimental Aircraft - Lessons Learned*, AIAA Paper 90-3237, September 1990.

36. *Jane's All the World's Aircraft for 1988/89*, Sadleir VTOL Industries, Perth, Australia.

37. *Popular Mechanics*, July 1983, Technology Update, Page 123.

38. Schoen, A. H., et al; *User's Manual for VASCOMP II, The V/STOL Aircraft Sizing and Performance Computer Program*, Boeing Vertol Company, Report D8-0375, Volume II, 1980.

39. *International Standards and Recommended Practices - Environmental Protection*, Annex 16 to the Convention on International Civil Aviation, Volume I, 1988.

40. Heidmann, M. F., *Interim Prediction Method for Fan and Compressor Source Noise*, NASA TM X-71763, 1975.

APPENDIX A
SUBSTANTIATING DATA FOR TASK I

This appendix contains additional data which supplements the configuration information presented in Section 1 of the main body of this report. Data is also included here to substantiate both the preliminary qualitative evaluation and the final quantitative evaluation described in Section 1.

TABLE OF CONTENTS

LIST OF FIGURES

LIST OF TABLES

PAGE

Concept Comparisons

Conversion Sequence Differences

Lifting-Stoppable Rotors

The group of rotorcraft referred to as lifting-stoppable rotors include the disc-wing concepts (e.g., NASA's M-85 and Hughes Rotor-Wing), the Navy/DARPA X-wing, and the wing-extension concepts commonly referred to as the Rotafix. The disc-wing concept is shown in Figure A-1 as an example of this group. It was sized on the basis of an annular disc loading in order to meet the downwash criteria. This resulted in a 90-ft diameter rotor, an 11-psf disc loading, and a 21-psf wing loading. Low wing loadings are common to the group since it is generally a fall-out of sizing the rotor to satisfy hover requirements. The excessive wing area results in a low L/D in high-speed cruise, being most detrimental to the cruise efficiency. The conversion issues are:

- Conversion attitude
- Conversion dynamics and time
- Conversion roll control
- Maneuverability during conversion

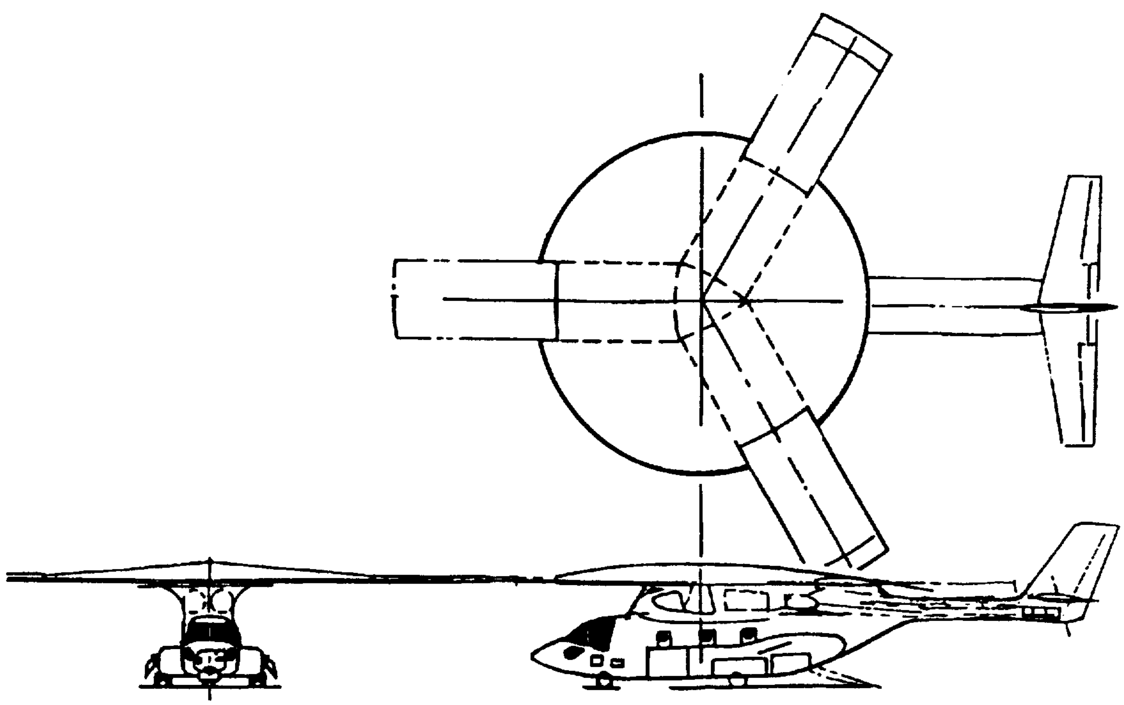

Figure A-1. Stopped / Lifting Wing Candidate Configuration - Disc Wing

Figure A-2 illustrates the conversion attitude variations of this group of concepts. Although the angles might be held to less than typical jet transport rotation angles, this is poor in comparison to the constant fuselage attitude capability of the tiltrotor concepts.

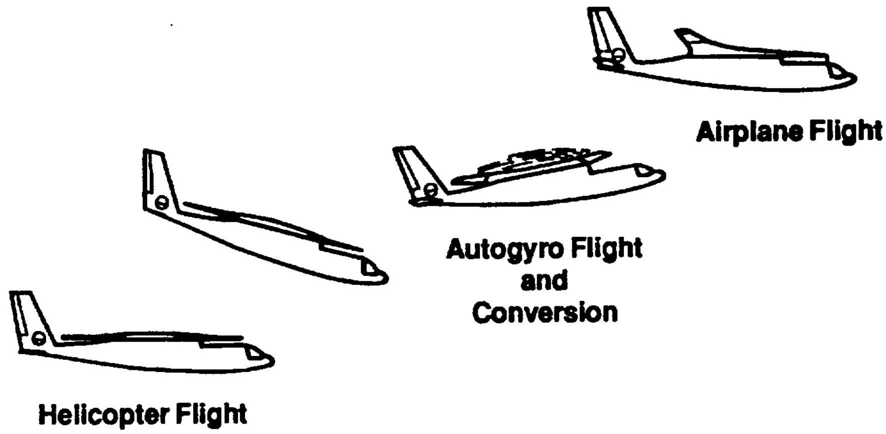

Figure A-2. Schematic Diagram of Disc-Wing Conversion Sequence

Trailed-Rotors

The Trailed-Rotor variant of the vertically stopped stowed rotor type is illustrated in Figure A-3. Rotor diameter is 38-ft for a disc loading of 22-psf. Although drawn for a 25° aft swept wing, the concept is probably only acceptable for small sweep angles due to the relationship of the tilt axis (at the C.G.) and the proper location on the M.A.C. If placed where stability requires, a very long overhang results as shown with severe weight, balance, and operational problems.

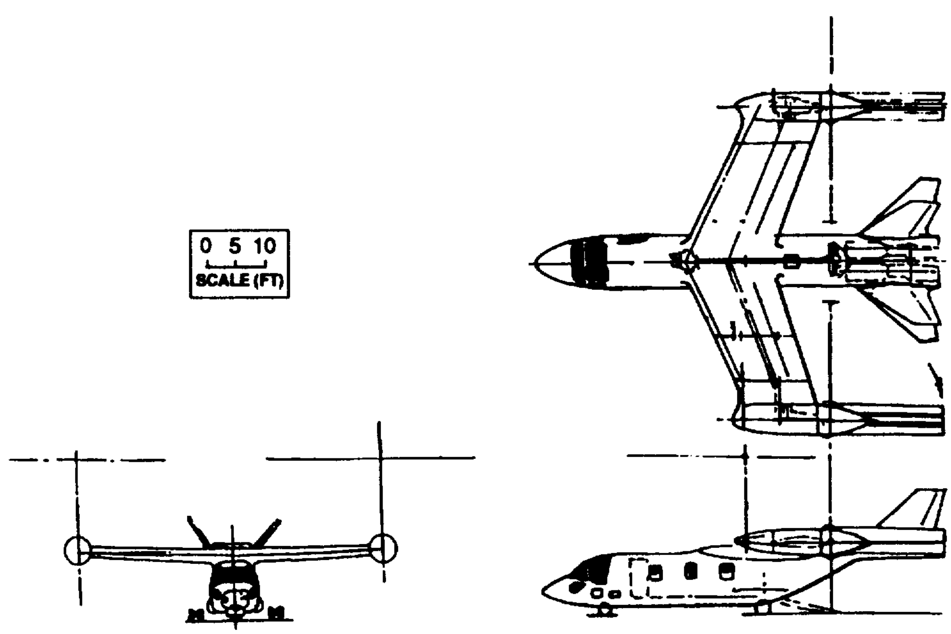

Figure A-3. Stopped / Stowed Rotor Candidate Configuration - Trailed Rotor

After early studies, it became obvious that the trailed rotor concept did not possess the characteristics desired for a high-speed variant of the tiltrotor. The trailed rotor could not utilize the tilting rotor for good takeoff acceleration and STOL capability nor could it operate in the efficient prop-rotor loiter mode. In those low speed regimes, it either operated as a helicopter (with about 15° forward tilt capability) or as a compound helicopter using very inefficient jet thrusting means. Figure A-4 illustrates the trailed-rotor conversion sequence. Therefore, both Bell and Boeing (and later Sikorsky) continued to explore and further develop folding tiltrotor configurations leading up to the 1970s series of U.S. Air Force and NASA studies and wind tunnel full-scale rotor and model tests.

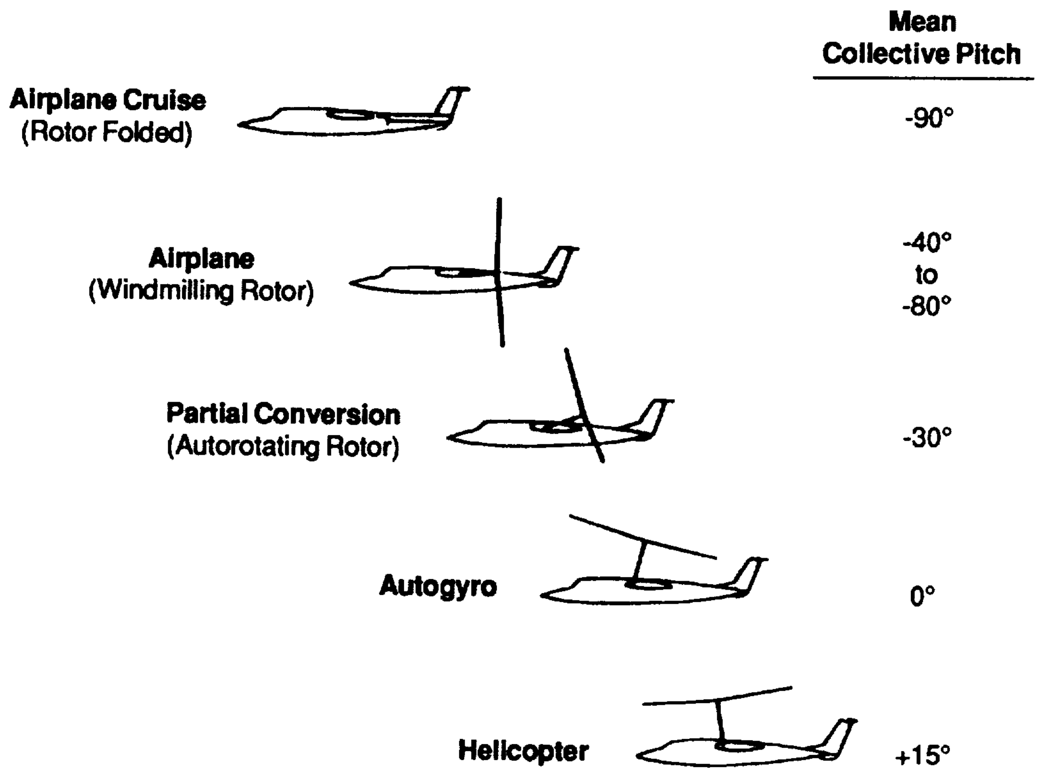

Figure A-4. Schematic Diagram of Trailing Rotor Conversion Sequence

Folding Tiltrotor

The folding tiltrotor, shown in Figure A-5, is essentially a tiltrotor during hovering and low speed flight. The rotors are used in the upright position for hovering and for vertical takeoff and landing. For transition to forward flight, the rotors are tilted through 90 degrees. The conversion corridor speed is of the order of 120- to 180-knots. Figure A-6 illustrates the conversion attitudes for the tiltrotor and folding tiltrotor. A smooth, continuously accelerating conversion is typical of this type of high-speed rotorcraft. When full wing lift is achieved, the forward thrust is transferred to the cruise fans and the rotors are feathered and stopped; the blades are then folded along the wingtip nacelles. The transition time from hover mode to prop-rotor mode is on the order of 15 to 30 seconds depending on the aircraft design criteria (transport or attack variant, e.q.) Boeing's early test programs demonstrated rotor stopping time to be on the order of 3 seconds. This was later confirmed by the Bell 25-ft folding rotor in the 40 x 80-ft tunnel to be 2 seconds for a smooth stop or start.[25] A design goal of about 3 seconds for blade folding was shown to be practical and within reasonable folding power limits by Boeing. Therefore, a total of six

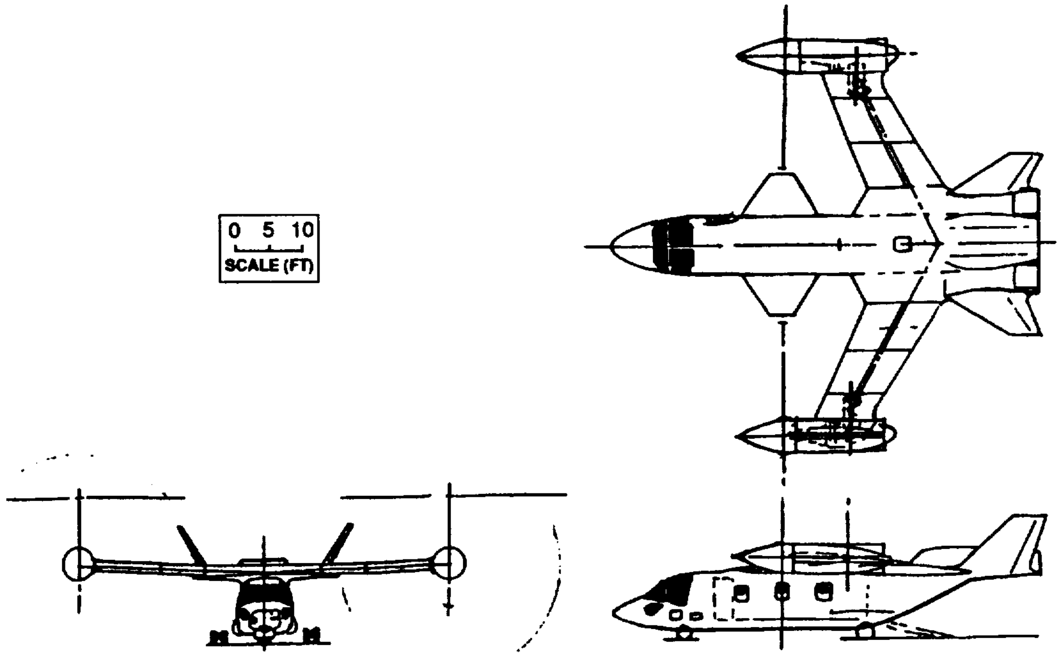

Figure A-5. Stopped / Stowed Rotor Candidate Configuration - Folding Tiltrotor

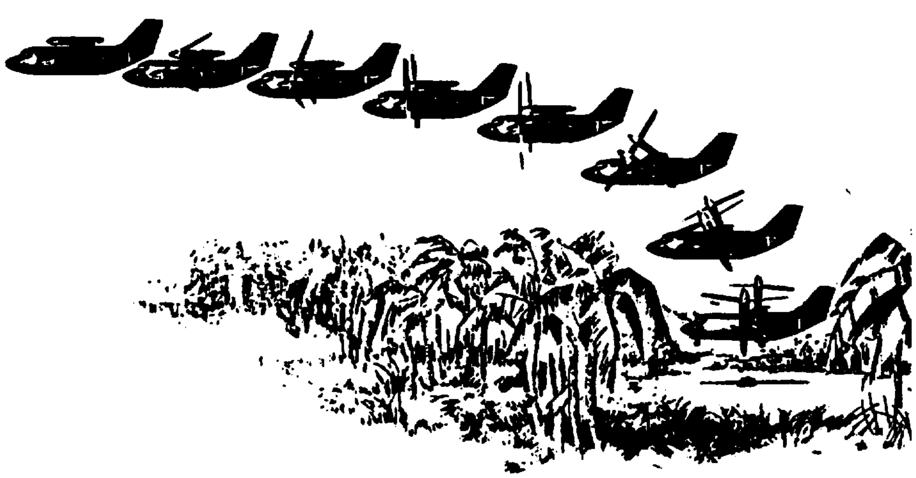

Figure A-6. Schematic Diagram of Folding Tiltrotor Conversion Sequence

seconds for the conversion sequence is a small portion of the take-off (or landing) time for a folding tiltrotor (16-28%) compared to any other rotorcraft. In addition, there is no loss in acceleration (or speed) during conversion. Maneuver capability is ample at any stage of conversion through the complementary forces available from the wing, tail and rotors. Even during the stop/start and folding modes the normal load factor capability inherent in the aircraft concept (about 3-4 g's) can be sustained by properly designed rotors without significant penalty. So the stop/fold process has little or no impact on maneuverability or survivability.

Studies and evaluations for the U.S. Air Force, NASA, and industry during the 1970s concluded that the folding tiltrotor concept was most attractive because it has the least risk associated with the conversion sequence (stopping and folding the rotors). Since the rotors are stopped and folded in a relatively constant aerodynamic environment, as opposed to the constantly changing one faced by horizontal stopping rotors, it faces fewer aerodynamic and dynamic design problems. The folding tiltrotor offers the greatest operational flexibility with good vertical takeoff capability and the forward rotor tilt for excellent acceleration, STOL performance, and climb-out capability.

Drive System Comparison

Schematics of the drive systems of all the configurations were developed for the evaluation and down select. Figure A-7 is an example of four arrangements. Major components, such as gear-boxes, high-torque clutches, and reel drives were counted and the comparisons displayed in Table A-1.

Table A-1. Drive System Comparison

CONCEPT			NUMBER OF SYSTEMS		
			HIGH-TORQUE FLUID CLUTCH	REEL DRIVES	TOTAL NUMBER OF GEARBOXES
TILTROTOR		V-22			6
		CONVENTIONAL			6
		CANARD			8
TILTPROP		X-19			12
		M300			17
TILTWING		2-PROP			6
		4-PROP			12
		TANDEM WING			14
STOPPABLE ROTOR	NON-LIFTING	BLOWN ROTOR	2		6
		UNBLOWN ROTOR	2		8
	LIFTING	LIFTING WING (DISC-WING, X-WING)	1		3
		WING EXTENSION	2		6
	STOWED	HORIZONTAL	1		7
		VERTICAL			9
VARIABLE DIAMETER	TELESCOPIC		1		3
	REELABLE		1	5	3
	FOLDABLE		1		6
	TILTABLE				8
BODY-MOUNTED ROTOR			1		3

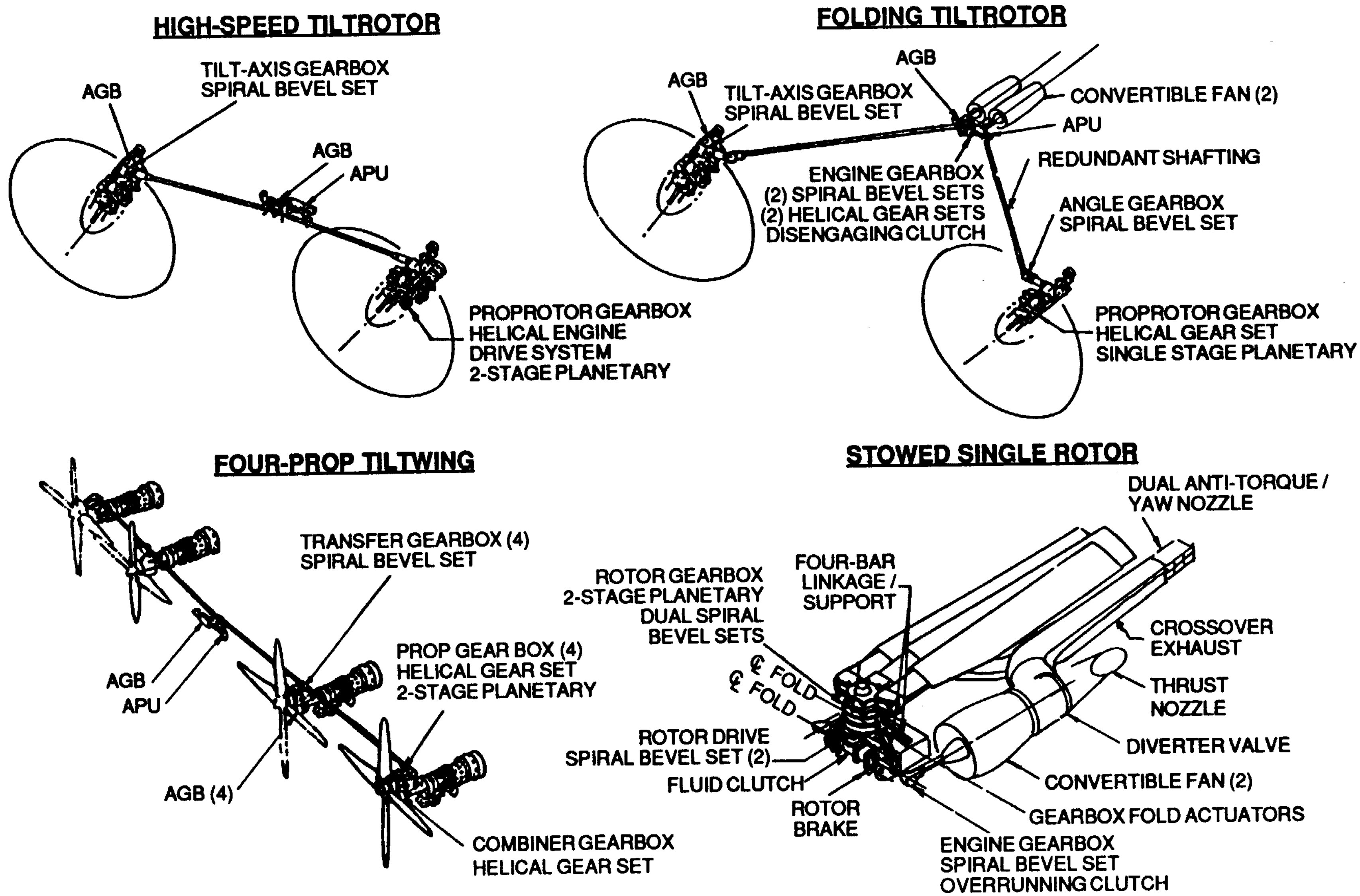

Figure A-7. Sample Drive System Schematics

Folding/Retraction Complexity

Another major discriminator for these kinds of aircraft is the number and variation of powered actuators required for the various folding and retraction schemes for the blades, closures, wings, and hub and transmissions. Figure A-8 summarizes the count for each configuration.

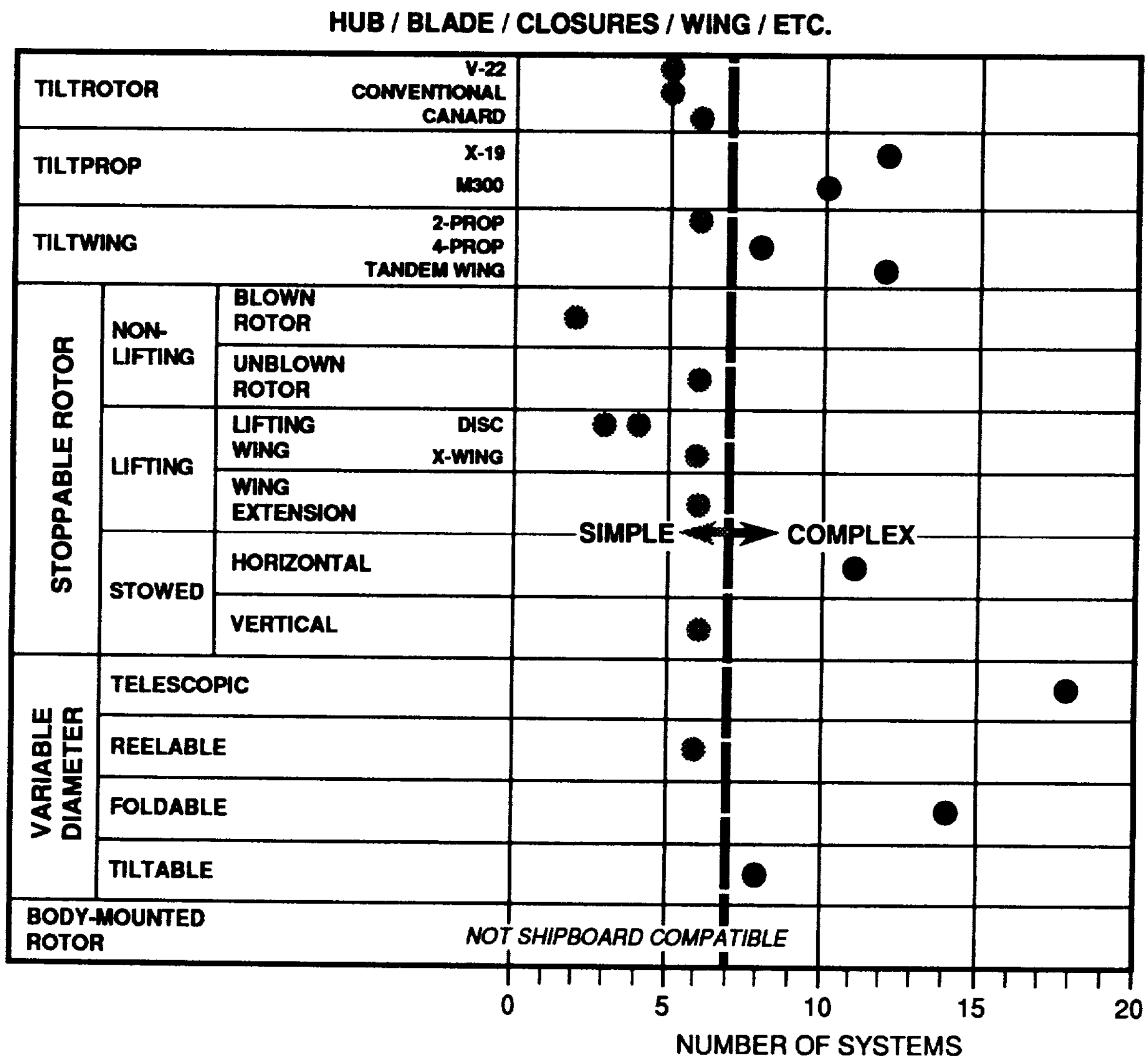

Figure A-8. Conversion, Folding and Retraction Systems

Aerodynamic Efficiency Comparison

Equivalent flat plate areas (f_e) were calculated for all of the configurations as summarized in Figure A-9. Significantly, "other" items such as empennage, fuselage, landing gear fairings, etc. totalled to about the same area. The major discriminator seen here is the effect of wing area. The dark triangles define the configurations having excessive wing area and therefore high drag.

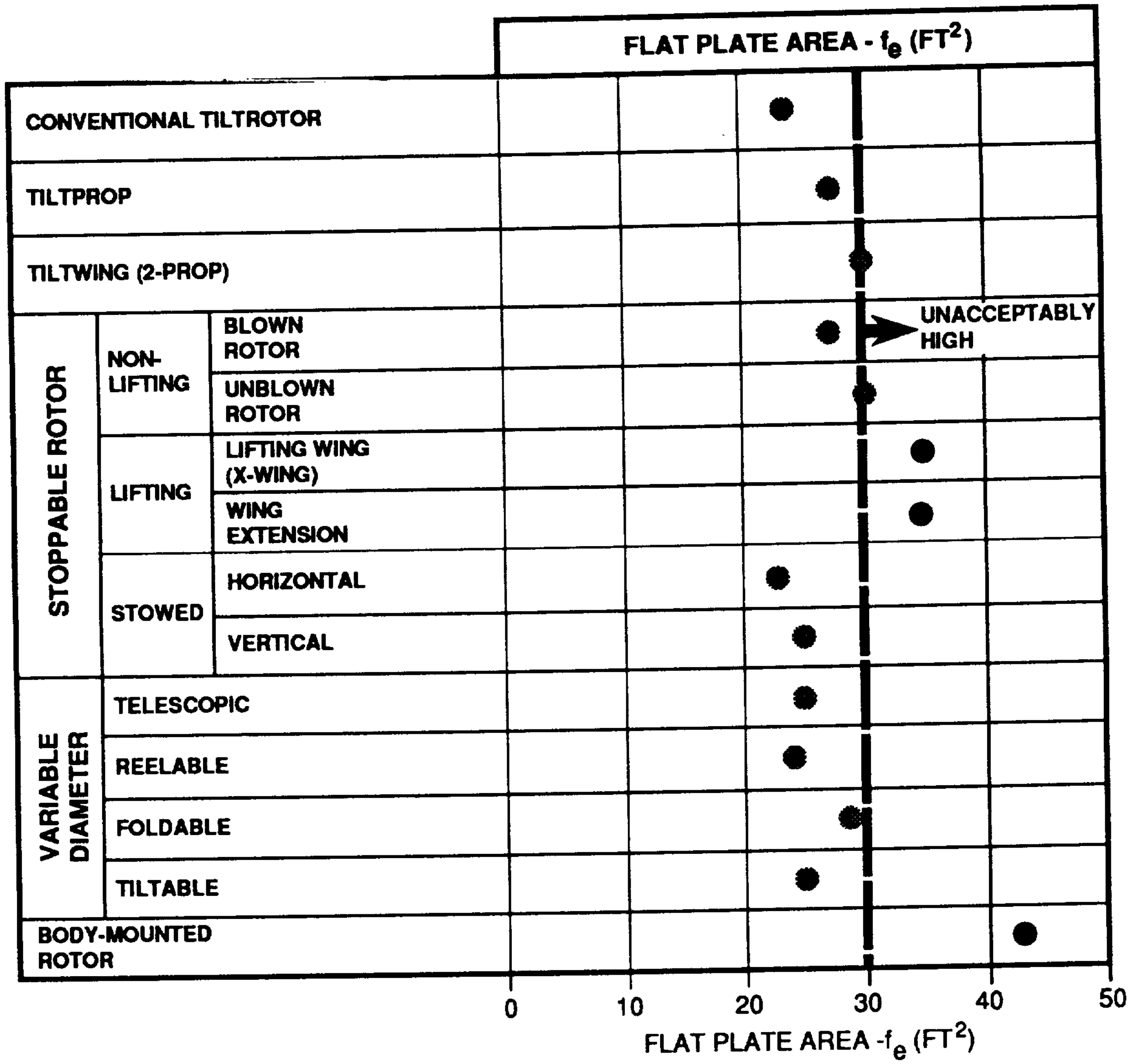

Figure A-9. Equivalent Flat Plate Area Comparison

While not of importance at lower speeds, the poor f_e's of these configurations cause poor L/D's at the higher speeds considered in this study. Figure A-10 is a sampling of preliminary estimates of L/D's for some of the candidate configurations, for the 50,000-lb first-cut gross weight.

Measures of Effectiveness

The term Measure of Effectiveness (MoE) is usually reserved for those terms which are meaningful to the user community (a military branch of service or civil market area). These kinds of terms might be exchange ratio, probability of kill, ton-miles/$, $/seat mi, or other measure of how well the vehicle does its intended function. MoE's may be qualitative or quantitative, but they always measure vehicle functionality from a user view.

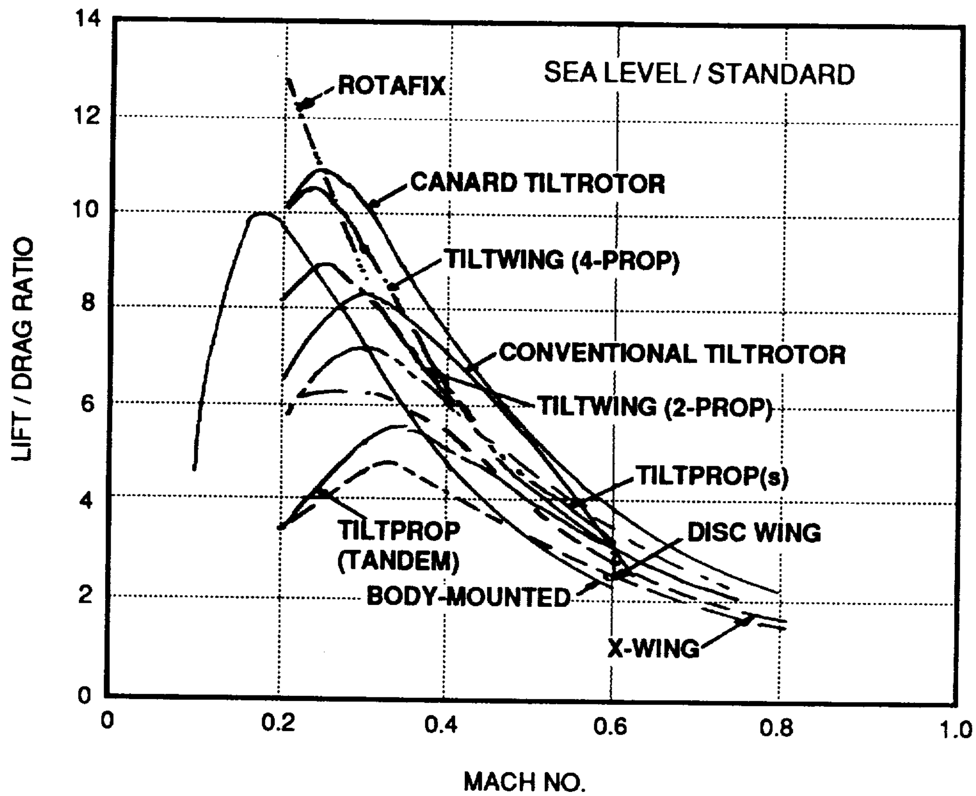

Figure A-10. Airplane L/D Comparison

The technical community most often uses some Measure of Performance (MoP) to compare one design or component to another design. These are invariably quantitative and usually do not relate directly to the mission. But they do describe the system, or vehicle, or subsystem in a way that can be compared in engineering terms. They allow identification and quantification of design improvements (which should eventually show up in an MoE). This distinction is indicated in Table A-2.

Table A-2. Hierarchy of Measures of Effectiveness

- **Military battlefield / civil market (measures of effectivenss)**
  - Exchange ratio
  - $ / seat-mile
  - Ton-miles / day / $
  - Competitive position
  - % succesful intercepts
- **Vehicle attributes (measures of performance)**
  - Speed
  - Maneuverability
  - Cost, direct operating cost
  - Availability
- **Design characteristics (parameters)**
  - Disc loading
  - HP / lb
  - Wing loading
  - Hub type

A specific list of MoEs and MoPs is given in Table A-3. This list is certainly not exhaustive, but does include those terms which are believed to be important in this study. All the MoEs relate to the users view of how well the vehicle performs its intended functions. Some of the MoEs are more qualitative, such as agility, ride quality and ease of conversion, while others are quantitative, such as range, spotting factor, and all of the cost MoEs. In contrast, the MoP's are all quantitative. The list was assembled for comparisons between concepts performing the same mission. The list of key discriminators used in the concepts comparative evaluation was mostly taken from Table A-3.

Table A-3. Example List of Measures of Effectiveness and Measures of Performance

MEASURES OF EFFECTIVENESS	MEASURES OF PERFORMANCE
- Exchange Ratio	- Hover Factor - GW / (Lb/Hr)
- Productivity - P x V/EW	- Range Factor - GW x (NMI./Lb)
- Range	- Dash Speed
- Maximum Payload (Short Hops)	- Noise
- STOL Overload Capability	- Vibration Index
- Spotting Factor	- Maneuverability Index
- Survivability	- Specific Power
- Agility	- STOL Performance
- Ride Quality	- Installed SHP/GW
- Ease of Conversion	- Growth Factor - GW/(FUL + PL)
- Safety	- EW/GW
- Dispatch Reliability	- Subsystems:
- $ Per Ton-Miles	• Rotor: Figure of Merit, Lb-Lift/SHP, Cruise Prop. Efficiency
- $ Per Seat-Miles	• Airframe: L/D
- DOC	• Engine: SFC, Lb-Thrust/SHP
- Life Cycle Cost	• Component Weight
	• Component Cost

Examples applicable to a cargo aircraft might be the productivity MoE, a ton-miles/$ MoE, or the Hover Factor or Range Factor MoPs. While gross weight GW is often used as an indicator of the best aircraft solution for a given mission, this is really because GW is so indicative of other things like relative size and relative cost. Other things being equal (technology level, materials, manufacturing technique, complexity, etc.) the lowest GW vehicle will probably be the lowest cost too. For this reason GW was used during the parametric sizing study to choose the best combination of wing loading and disc loading for a given concept (lighter is better). Once sized however, comparative ranking between vehicles was mostly determined by other MoEs such as Life Cycle Cost and MoPs such as Range Factor and dash speed potential.

An example of a case where GW itself would be a prime MoE is when it is necessary to constrain it for shipboard compatibility or for offshore oil rig load limits.

Subsystem MoPs are also useful when trying to assess the performance level of a particular rotorcraft element. Examples of these include the airframe L/D and the prop-rotor cruise efficiency. We don't have to convert them into an MoE to know that these improvements result in less power required. This translates into lower engine weight and drive system weight for a lighter vehicle (read smaller and cheaper).

Evaluation of High-Speed Aircraft Afterbody Shapes

The selected five configurations were designed with some common attributes as dictated by the chosen sizing mission. The baseline designs all had a cargo type fuselage with a rear loading ramp integrated into the fuselage afterbody. The configurations were partially selected for their compatibility with ship-board folding requirements. However, weight penalties associated with wing folding and automatic blade folding required for shipboard compatibility were excluded in this initial sizing study.

Helicopter type rear ramp designs such as those found on the CH-46, CH-47, Model 360, and CH-53D/E are inadequate for high-speed cruise conditions. The beaver tail of the V-22 is shown in three view in Figure A-11, including a rear quarter picture. It performs well up to the 300-knot design speed. But it cannot provide low drag up to 0.7 Mach number, corresponding to the 450-knot required cruise speed. However, a low drag afterbody is necessary to achieve a light weight (remember to read small and cheap) high-speed vehicle.

(a) Three-Quarter Rear-View of V-22 Ramp

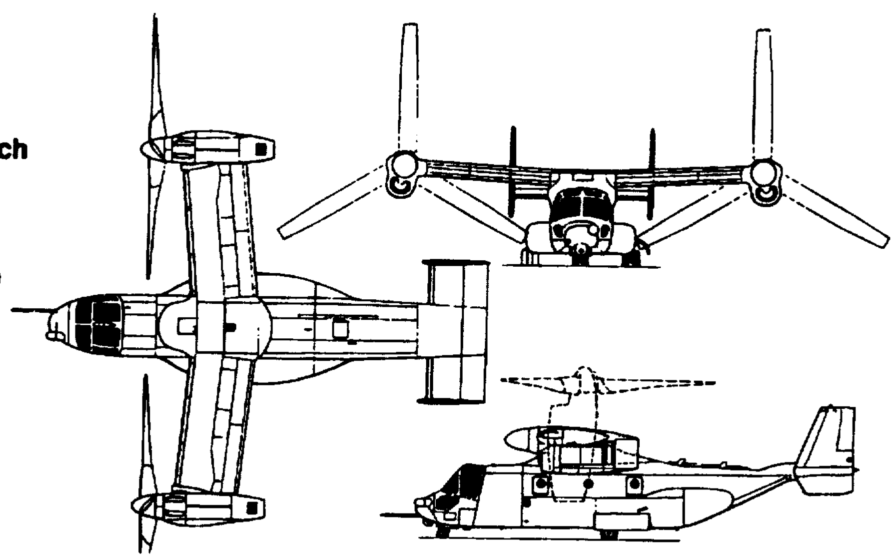

(b) Three-View of V-22

Figure A-11. Bell Boeing V-22 Osprey

A review of some high-speed fixed wing cargo aircraft showed that the afterbody closure must be more gradual and more rounded than those found on helicopters. Most of the aircraft surveyed employed a rear ramp which extended only part way up the afterbody in the closed position. The upper portion of the afterbodies had some form of clamshell doors opening sideways to provide a fully open cabin height for loading/unloading. Examples of these aircraft are shown in Figures A-12 through A-17. The weight penalty of extra doors, actuators, and stiffening structure around the large aft opening must be traded off against improvements in separation drag and base drag on the body. Large separated regions on the afterbody could also contribute to reduced tail effectiveness and poor low speed handling qualities. Current military transport aircraft have been through this detailed tradeoff prior to reaching production. The lessons learned are partially seen in the resulting configurations.

Figure A-12. Artist's Rendition for 1969 USAF/Boeing Folding Tiltrotor Study

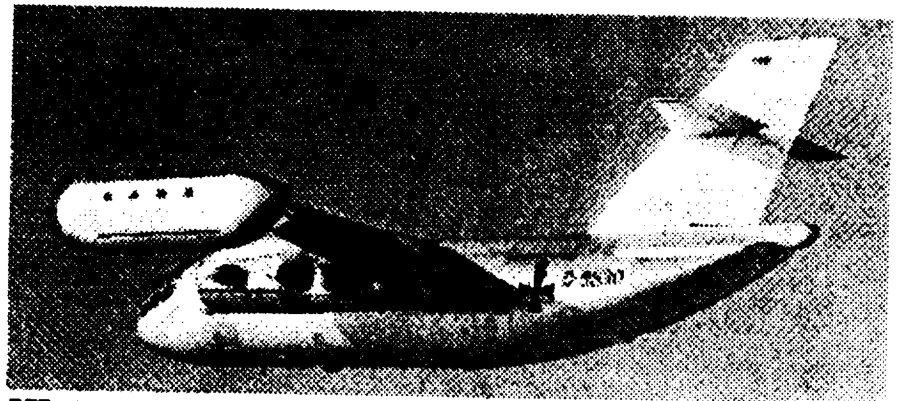

REF: 1967-68 JANE'S ALL THE WORLD'S AIRCRAFT

(a) Do 31E In-Flight Photo

(2) Bristol Siddeley Pegasus Vectored-Thrust Turbofan Engines **(15,500 lb thrust each) +**
(8) R-R R.B. 162 Lift-Jets **(4,400 lb thrust each)**

Maximum Takeoff Weight **= 60,600 lb**

Estimated Cruising Speed (at 20,000 ft) **= 400 mph**

Payload **= 6,600 - 11,000 lb (or 36 troops)**

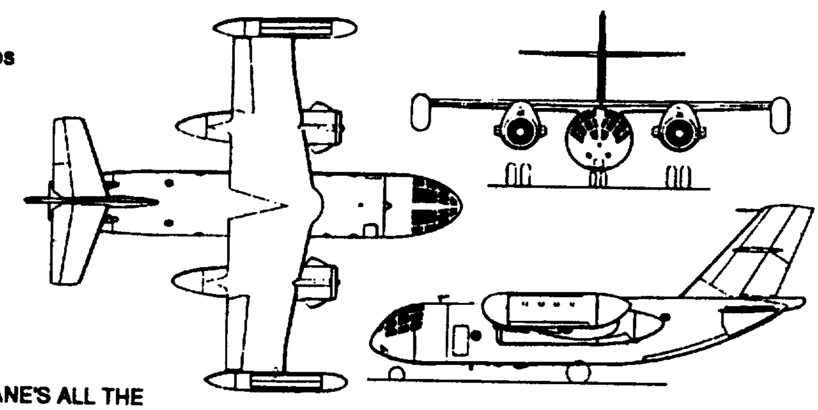

REF: 1967-68 JANE'S ALL THE WORLD'S AIRCRAFT

(b) Three-View of Do 31E

Figure A-13. Dornier Do 31 E V/STOL Experimental Transport

(2) Rolls-Royce R.B. 168 Turbofan Engines **(12,444 lb thrust each) +**
(14) Rolls-Royce R.B. 162 Lift-Jets **(5,900 lb thrust each)**

Design Vertical Takeoff Weight **= 83,000 lb**

Est. Max. Cruising Speed **= 530 mph**

Payload **= 10,800 lb**

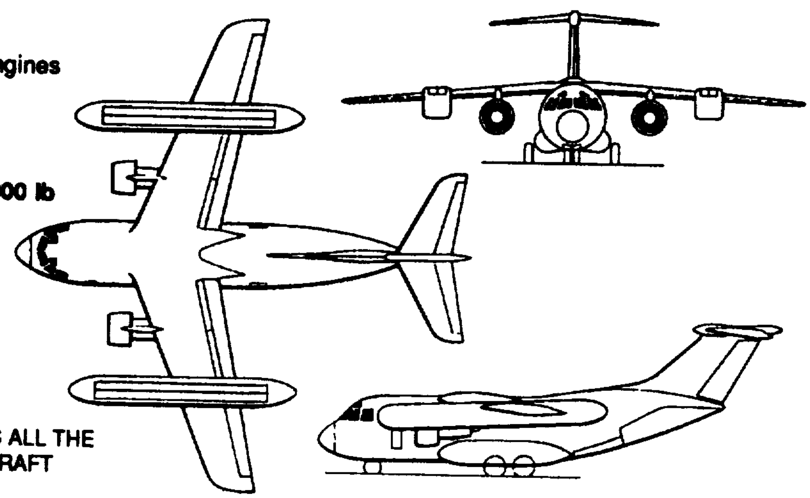

REF: 1967-68 JANE'S ALL THE WORLD'S AIRCRAFT

Figure A-14. Dornier Do 131A V/STOL Experimental Transport

(2) Rolls-Royce Dart Turboprops
(2,105 eshp each)
Maximum Speed = **258 mph**
Maximum Takeoff Weight = **43,500 lb**
Maximum Payload = **12,420 lb**

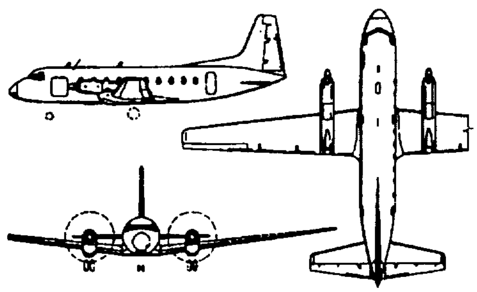

REF: 1963-64 JANE'S ALL THE WORLD'S AIRCRAFT

(a) HS 748 Andover (Sr. 2) Without Rear Ramp

(2) Rolls-Royce Dart Turboprops
(3,245 eshp each)
Maximum Speed = **305 mph**
Maximum Takeoff Weight = **50,000 lb**
Maximum Payload = **15,099 lb**

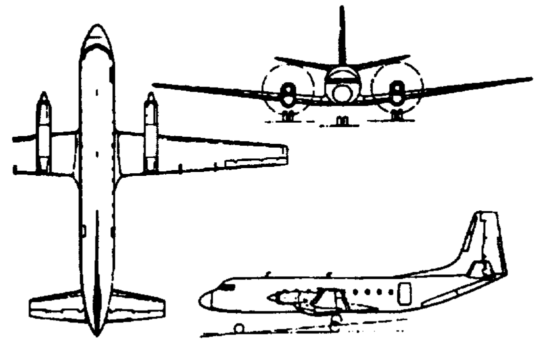

REF: 1963-64 JANE'S ALL THE WORLD'S AIRCRAFT

(b) HS 748MF Andover C Mk 1 With Rear Ramp

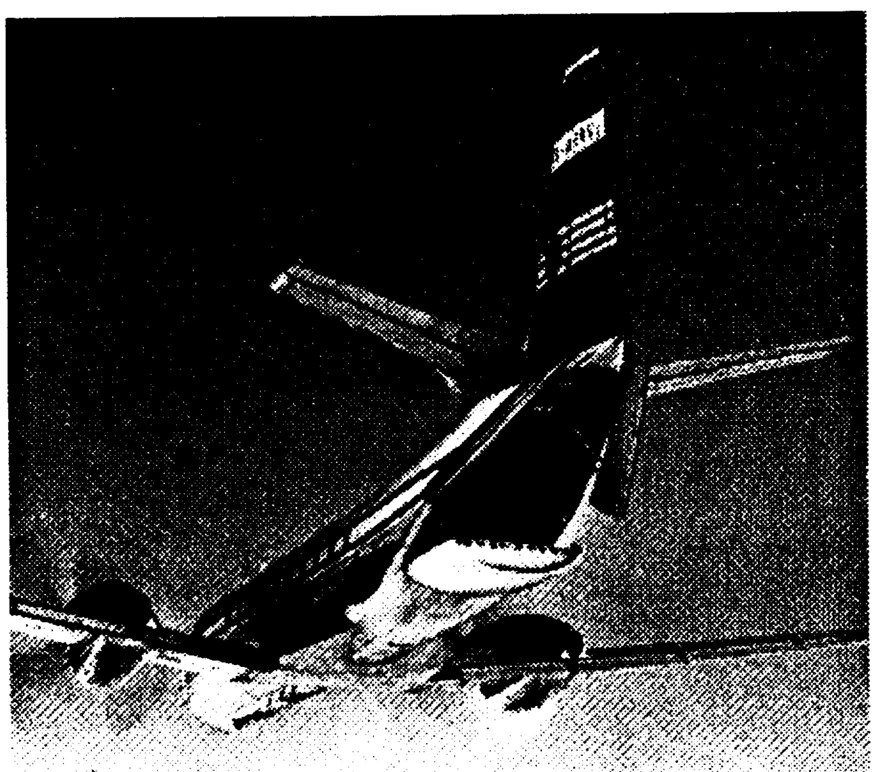

REF: 1964-65 JANE'S ALL THE WORLD'S AIRCRAFT

(c) HS 748MF In-Flight Photo / Ramp Detail

Figure A-15. Hawker Siddeley HS 748 Andover Transport

REF: USAF MAC HISTORY BOOKLET FEB'89

REF: AAR BROOKS & PERKINS CONTAINER BROCHURE

(a) C-141B Afterbody and Ramp Details

(4) P&W TF33-P-7 Turbofans (21,000 lb thrust each)
Maximum Ramp Weight = 344,900 lb
Maximum Cruising Speed = 569 mph
Payload = 89,152 lb

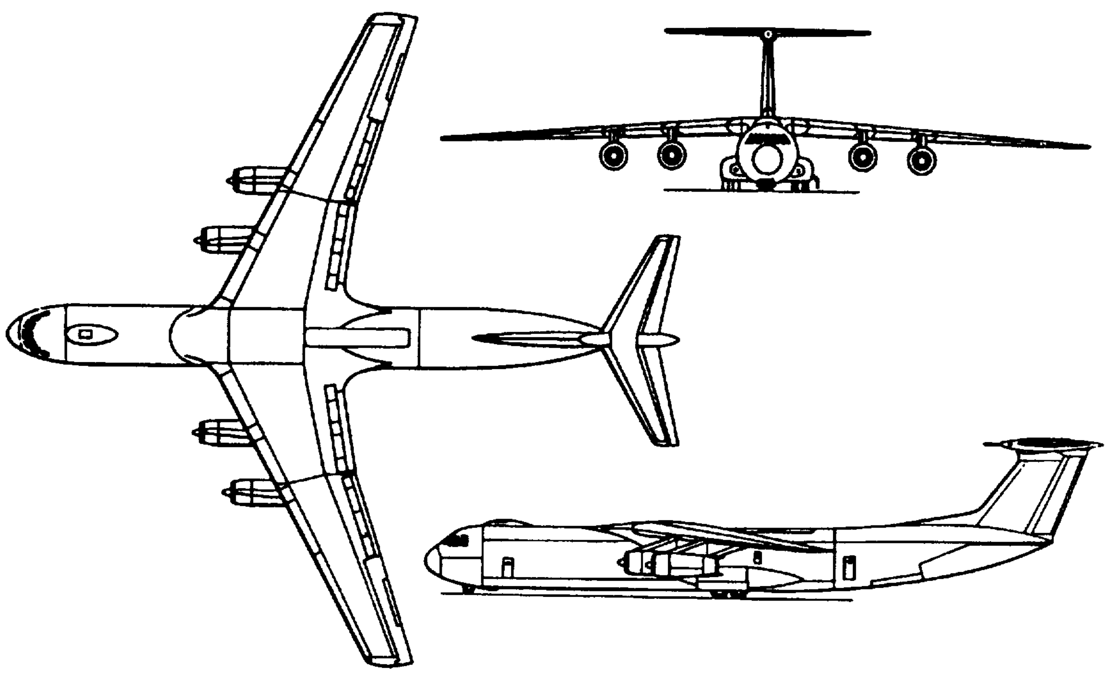

REF: 1978-79 JANE'S ALL THE WORLD'S AIRCRAFT

(b) C-141B Three-View

Figure A-16. Lockheed C-141B Starlifter

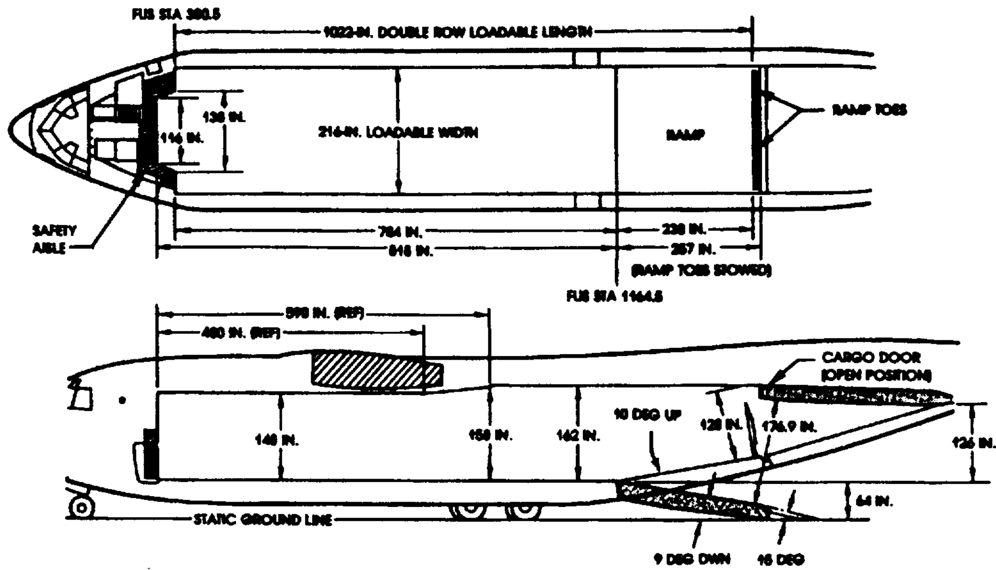

REF: McDONNELL DOUGLAS C-17 BROCHURE

(a) C-17 Cargo Compartment

(4) P&W F117-PW-100 Turbofans **(37,000 lb thrust each)**
Maximum Takeoff Weight = **580,000 lb**
Normal Cruising Speed (at high altitude) = **Mach 0.77**
Maximum Payload (2.25g load factor) = **172,200 lb**

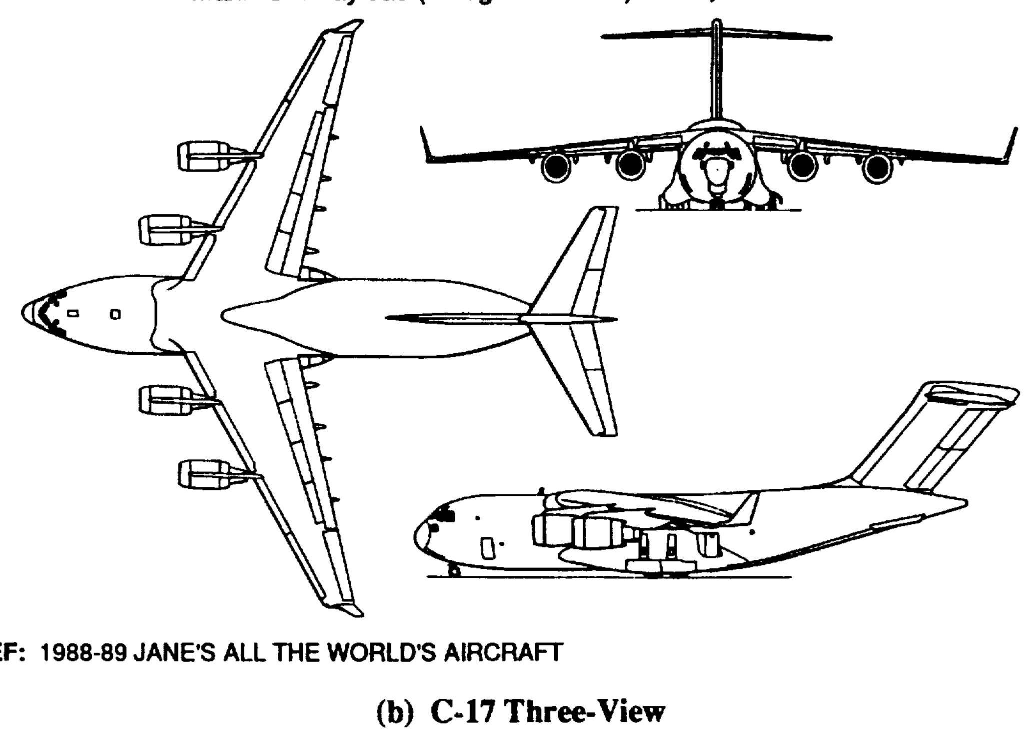

REF: 1988-89 JANE'S ALL THE WORLD'S AIRCRAFT

(b) C-17 Three-View

Figure A-17. McDonnell Douglas C-17

Technology Assessment

Weights

A review of past performance on the all composite Bell-Boeing V-22 Osprey and the Boeing Model 360 all composite tandem helicopter gave a good indication of progress in the area of weights for both primary structure and for rotor blades and hubs. Boeing involvement in other programs such as ADOCS, IHPTET, and ART (Advanced Rotorcraft Transmissions) gave the weight group specific knowledge and a substantial data base for estimation of future weight savings. Table A-4 shows the projected weight savings estimate in each of the major weight groups for both 1990 technology and year 2000 technology.

Table A-4. Component Weight Technology Factors

	RELATIVE BASELINE	TECHNOLOGY ADVANCEMENT	TECHNOLOGY FACTOR (%) 1990	2000
Structure				
Body	Metal	Advanced Composite Materials (ACM)	12	25
Landing Gear	Metal	ACM	2	5
Wing	Metal	ACM	12	25
Tail Surfaces	Metal	ACM	15	25
Flight Controls				
Fly-by-Wire / Fly-by-Light	Mechanical / Hydraulic	Digital / Optical	8	15
Hydro-Mechanical Rotor Controls	Metal	ACM Swashplate	8	15
Equipment				
Electrical	1970's	Digit. Cntl'd Pwr. Distrib. High Speed Generators Lightweight Battery	8	15
Crew Seats	Metal	ACM	8	15
Armor Protection	Metal	ACM	10	30
Mission Equipment	Separate	Integrated Digital Avionics	15	35
MEP Installation	Metal	Multiplexing, Composites	10	25
Rotor Group				
Tilt Rotor	Metal (XV-15)	ACM	10	15
Tilt Wing	Metal	ACM	10	15
Propulsion				
Engines	1970's	IHPTET Objectives	I	II
Engine Controls	1970's	Digital / Electronic Fuel Control	5	13
Fuel System	1970's	Bladder Material	5	10
Drive System				
Transmission	1970's	Advanced Rotorcraft Transmission (ART)	10	23
Main Rotor Shaft	Metal	ACM	8	15
Cross Shaft	Metal	Composite Shaft and Couplings	8	15

In addition to these weight improvements there are specific concept related weight penalties to consider. Wing weights for all of the tiltrotor concepts were generated from a Boeing Helicopter developed tiltrotor wing weight trend. (The tiltwing wing weight was estimated using standard VASCOMP wing weight trends with an appropriate multiplier.) This methodology accounts for both the wing strength and stiffness requirements. Strength requirements are dictated by the wing bending moments imposed by the VTO jump takeoff, in both vertical bending and wing torsion. The wing box spar stiffness requirement is dictated by the aeroelastic stability boundary, which is modeled in terms of the wing/pylon system frequency-to-rotor rotational frequency ratio. Linear spanwise variations of box spar thickness ratio and chord dimensions are accounted for. The methodology also accounts for the spanwise variation of jump takeoff bending moments, tapering the material thickness along the wingspan as allowed by the spar dimensions and loads. Spanwise variations of spar web and cover material thicknesses are then determined as the greater of strength or stiffness requirements.

Material property can also be varied in terms of the resultant E and G properties for a given percentage layup of unidirectional (longitudinal) and +/- 45 degree plies of composite material. As 45 degree plies are added to a unidirectional material, one trades off a loss in effective E against a gain in effective G. The wing weight is sensitive to this ply layup, requiring more material thickness if the ply layup is not in favor of the most critical loading direction. The optimum combination of these plies has been found to vary substantially with wing aspect ratio. Wing aspect ratios above 6 have been shown to require mostly unidirectional material (only about 23% of 45 degree plies) while wing aspect ratios down around 4 required about equal amounts of uni and 45 degree plies (45% of 45 degree plies.)

The rotor group also required specific weight penalties associated with the rotor concept geometry and complexity. Weight penalties for each of the 5 selected concepts are shown below. These multipliers were applied to the rotor group technology factors in Table A-4.

CONCEPT DESCRIPTION	ROTOR SYSTEM MULTIPLICATIVE WEIGHT PENALTY
Conventional tiltrotor	1.00
Canard Tiltrotor with advanced geometry rotor system	1.08
Canard Tiltrotor with variable diameter rotor system	1.26
Canard Tiltrotor with folding rotor system	1.20
Tilt Wing	1.00

Examples of the rotor group and wing group weight trends are presented in Figures A-18 and A-19. The wing group trend line is the standard VASCOMP wing weight trend for a metal wing with a 0.90 factor applied to correct it for composite materials. It can be used as an alternate method for wing weight prediction for tiltrotor aircraft. It accurately predicts the weight of conventional metal fabricated wings, including tiltwings. Adjustments must be made to the trend relief term R_m when analyzing tiltrotor configurations due to the large weight concentrations at the wingtips. R_m for metal tiltrotor aircraft is 1.4. Weight penalties and reductions are applied to the resulting basic wing weight as required to account for wing fold, composite material, or specific application requirements.

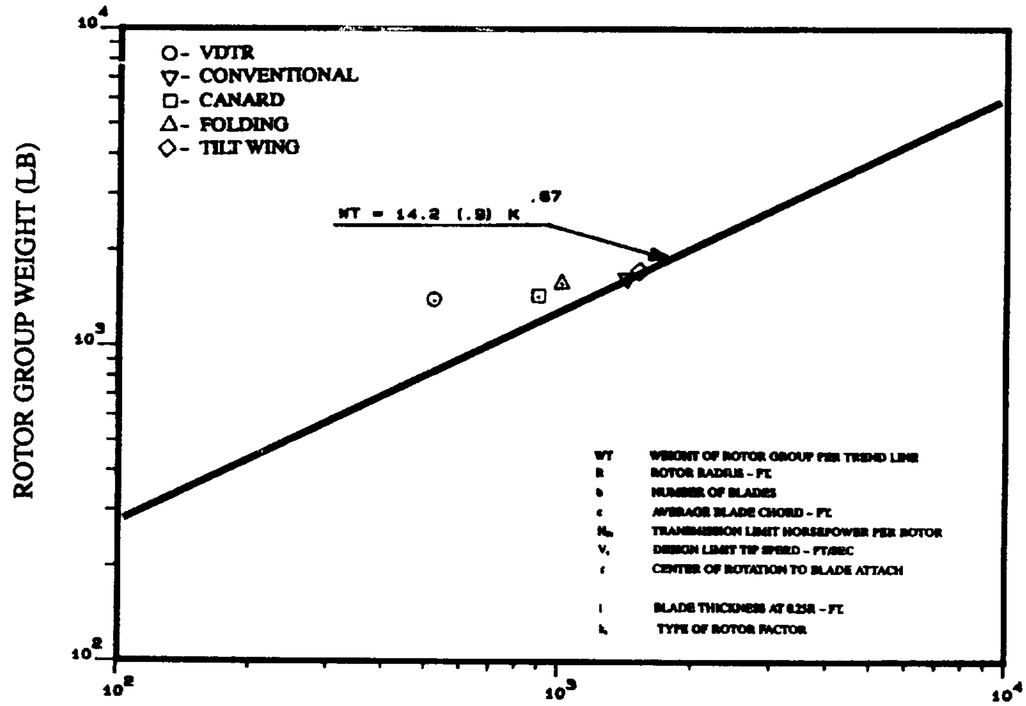

$$K = r^{.25}\sqrt{\frac{H_R}{100}}\cdot\frac{V_t}{100}\cdot\frac{(R\cdot b\cdot c)\cdot k_r}{10}$$

Figure A-18. Rotor Group Weight

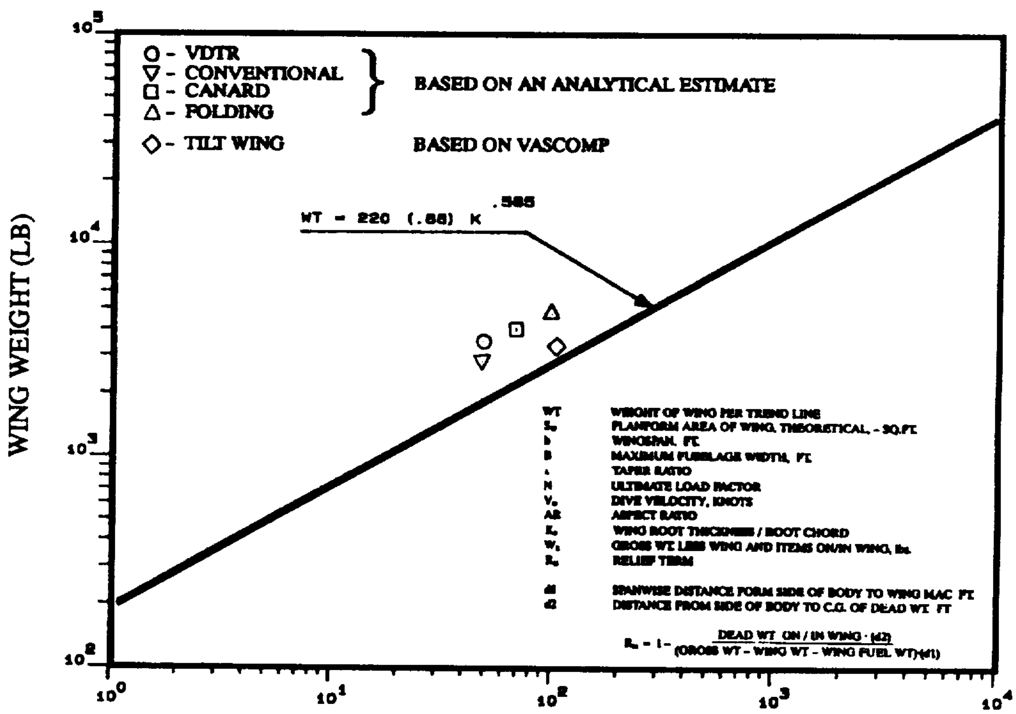

$$K = \frac{R_w W_x}{10^4}\cdot\frac{S_w}{100}\cdot \text{Log}\,\frac{b}{B}\sqrt{\frac{1+\lambda}{2\cdot K_R}}\sqrt{N}\cdot \text{Log}\ V_D\cdot \text{Log AR}$$

Figure A-19. Wing Group Weight

Aerodynamics

The aerodynamic analysis required for the five concepts can be summarized in the categories of airframe aerodynamics and rotor aerodynamics.

Airframe Aerodynamics

The primary airframe aerodynamic characteristics influence aircraft sizing through parasite drag, drag due to lift and compressibility drag.

Parasite Drag - The basic parasite drag of the concepts differed primarily because of the different wing and nacelle layouts. The basic fuselage and sponson geometry was unaltered between the various designs apart from the engine mounting. The primary distinctive characteristics of the five designs are:

> *Canard Tiltrotor:* This configuration has a smaller empennage than the conventional tilt-rotor, but has the added canard surface. The nacelles are small because only the rotor transmission was enclosed. Wing-nacelle interference drag was relatively low due to the small nacelle size and the tip mount. The wing sweep allowed a more blended approach to the wing-body fairing.
>
> *Folding Tiltrotor:* The general layout was identical to the canard tiltrotor. Body mounted convertible engines resulted in larger wetted area for the larger fan diameter and air inlet.
>
> *Conventional Tiltrotor:* The empennage was larger than the forward swept designs. The nacelles were large because the engine was enclosed as well as the transmission. Wing-nacelle interference was moderate. The large nacelle size caused high interference drag, but the tip mount produced only one junction.
>
> *Tiltwing:* The empennage was larger than the forward swept designs. The nacelles were large because the engine was enclosed as well as the transmission. Wing-nacelle interference was high. The large nacelle size caused high interference drag, and the mid-wing mount produced two junctions.
>
> *Variable Diameter Tiltrotor:* The general layout was identical to the canard tiltrotor.

Drag Due to Lift - The standard methodologies were used to determine values of the Oswald efficiency factor for each configuration. The major differences were due to differing end-plating effects, described below:

> *Canard Tiltrotor:* The end-plating effect for this configuration was moderate due to the slim nacelles located at the wing tip.
>
> *Folding Tiltrotor:* Same effect as the canard tiltrotor.
>
> *Conventional Tiltrotor:* The end-plating effect for this configuration was high due to the large nacelles located at the wing tip.
>
> *Tiltwing:* The end-plating effect for this configuration was negligible as the nacelles were mounted at the mid-span position.
>
> *Variable Diameter Tiltrotor:* Same effect as the canard tiltrotor.

Compressibility Drag - The compressibility drag was a very important driver in determining wing section geometry, particularly thickness/chord ratio, t/c. The challenge was to choose a high value of t/c for structural reasons, while keeping close to the boundary for drag divergence at the design Mach number. The test and theory data for wing drag divergence shows a gain of 0.06 Mach in drag divergence by changing from the V-22 wing airfoil to a 20% thick Boeing TR38 advanced airfoil. A further 0.05 Mach can be gained by reducing the thickness to 15%. A review of the speed and altitude requirements for the vehicles indicated that the vehicles would need to have airfoils in the 18% to 14% t/c range in order to avoid severe compressibility effects. The influence of airfoil t/c and lift coefficient on drag divergence Mach number is shown in Figure A-20. The compressible drag increment used in VASCOMP was derived from the TR38 2-D characteristics and then corrected to 3-D. Figure A-21 shows the resulting drag rise curves.

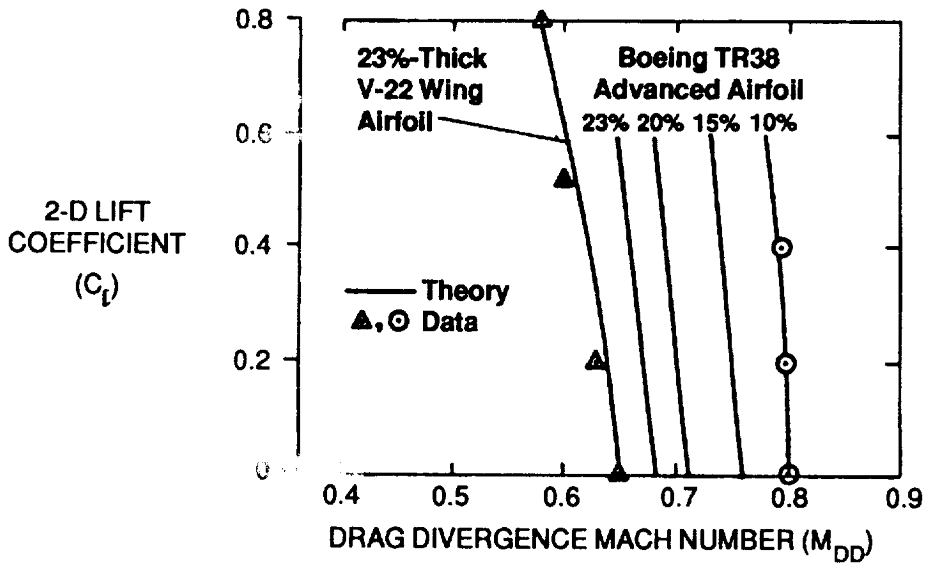

Figure A-20. Effect of Airfoil Thickness Ratio on Drag Divergence Mach Number

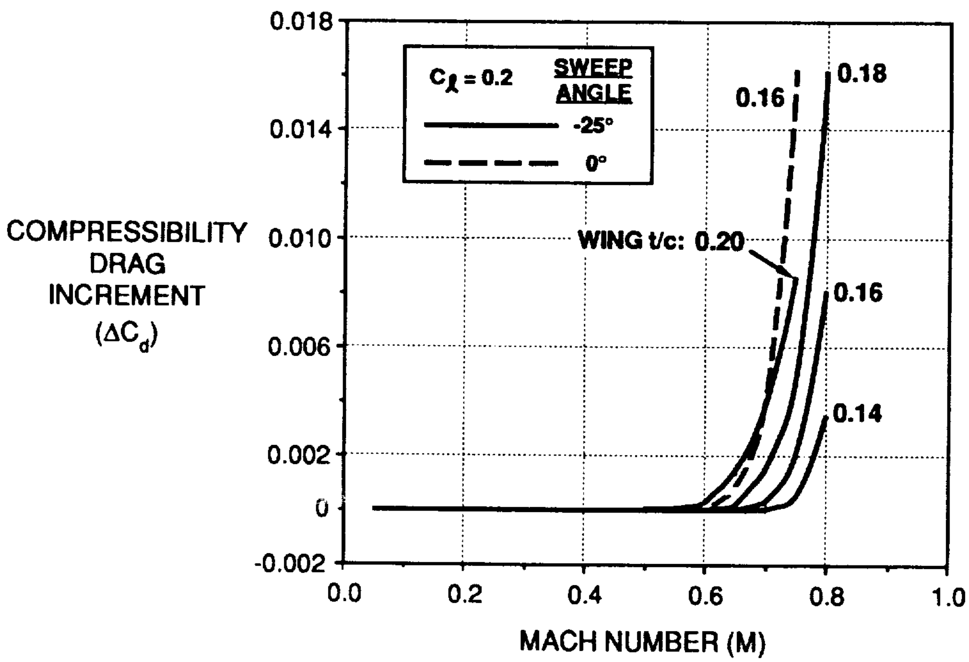

Figure A-21. Compressibility Drag Increments

Canard Tiltrotor: (16% wing t/c, -25° wing sweep) The wing sweep allowed a thicker wing to be used than the straight wing tiltrotor and tiltwing designs.

Folding Tiltrotor: (15% wing t/c, -25° wing sweep) The wing sweep allowed a thicker wing to be used than the straight wing designs. The turbofan engine characteristics drove the design to optimize at a much higher design altitude than the other designs. This had the effect of forcing up the design Mach number, as the speed of sound decreased with increasing altitude. The difference between sizing at 15,000-ft and 25,000-ft is a delta Mach number of 0.03. This requirement drove down the optimum t/c to 15%.

Conventional Tiltrotor: (14% wing t/c, -6° wing sweep) The lack of sweep forced the t/c down to 14%. Above this value the design gross weight increased rapidly, and above 16% a valid sizing solution for this configuration could not be obtained. The 14% t/c drove up the wing weight considerably due to the unique requirements of the tiltrotor concept.

Tiltwing: (15% wing t/c, 0° wing sweep) The straight wing required a thinner t/c than the swept designs.

Variable Diameter Tiltrotor: (16% wing t/c, -25° wing sweep) The wing design was very similar to the canard tiltrotor.

Rotor Aerodynamics

Each vehicle concept had a different rotor design. The blade twist was determined by the cruise condition. Fortunately, this results in an almost linear twist of close to 35°, which performs adequately in hover. The aircraft propulsion systems were all sized for cruise, which made them considerably oversized for hover. This rendered hover performance of little consequence, except for verifying its adequacy. Should OEI performance become an issue, however, hover would be of prime importance. Figure A-22 shows the 450-knot blade twist, a 35° linear twist, and the V-22 twist for comparison. Also shown are the efficiencies of the various rotors. The unique features of each rotor are described below.

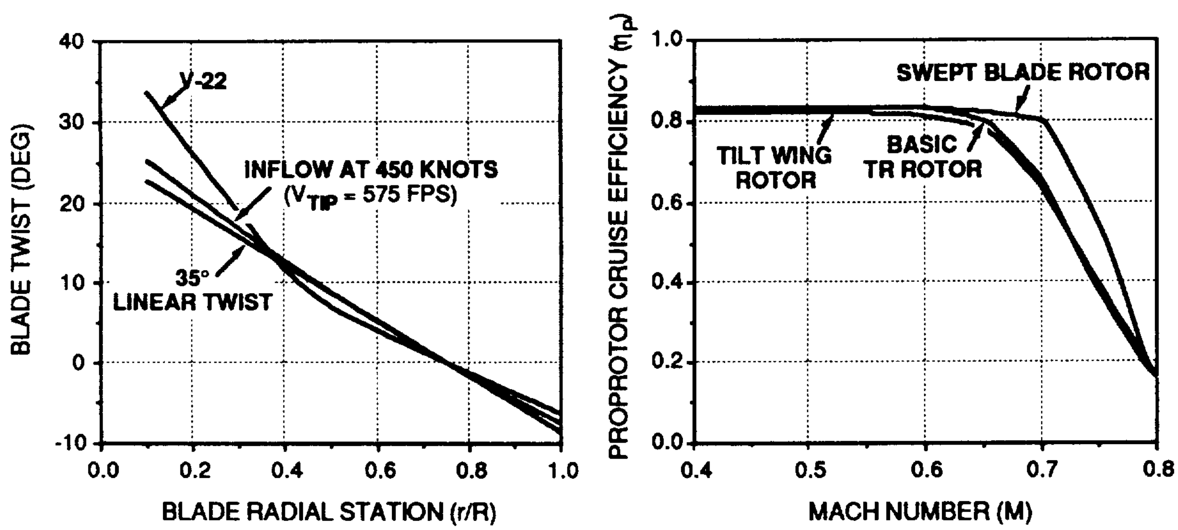

Figure A-22. High-Speed Rotor Twist and Propulsive Efficiency

Canard Tiltrotor: This configuration had a swept blade rotor, somewhat like a large propfan propulsor. Estimates of the performance of such a rotor were fairly elementary in Task I, as were the estimates of the dynamic characteristics. Nevertheless, a consider able improvement over straight blades should be possible, as shown in Figure A-22.

Folding Tiltrotor: The primary requirement for this configuration will be adequate hover performance and foldability, where some performance may have to be sacrificed in order to have the blade fold to a low drag configuration.

Conventional Tiltrotor: This rotor system used unswept rotor blades and current technology rotor airfoils. Figure A-22 shows that the rotor efficiency drops off starting at Mach 0.65. As a result the aircraft sizing condition occurred well into the region where compressibility effects had reduced rotor efficiency. The curve shown is by no means an optimum or a maximum achievable efficiency.

Tiltwing: This rotor was similar in nature to that of the tiltrotor. The efficiency was slightly lower, as the higher solidity and disc loading, and consequently lower blade aspect ratio, increased the tip losses.

Variable Diameter Tiltrotor: This rotor system was mechanically complex. The concept was for the outboard part of the blade to slide along a spar in order to vary rotor diameter. The cruise diameter was 75% of the hover diameter. The ratio was chosen as a result of choosing the desired hover and cruise tip speeds, and then requiring that the rotor rpm remain constant. This simplified the design considerably. This rotor performed similarly to the standard tiltrotor in terms of efficiency.

The ability to arbitrarily choose diameter ratio is not an easy thing to do if one also wishes to choose cruise tip speed independently. There will inevitably be a problem with the rpm ratio between hover and cruise.

Propulsion

Turboshaft engines were used with all of the concepts except the folding tiltrotor which required a convertible engine. Engine lapse rate and sfc characteristics with speed, altitude and part power were based on a growth version of the GE38 core engine. The absolute weight and fuel flow values were adjusted to IHPTET Phase I for the baseline 1990 technology and to IHPTET Phase II for the year 2000 technology. These adjusted SFC and weight values for the turboshaft engines are shown in Figure A-23 against historical trends for a number of other engines, including the MTDE. Note that the 1990 and year 2000 technology levels are actually initial full-scale preliminary design dates. In Figure A-23 these technology levels are plotted in terms of their IOC dates, which are year 2001 and year 2011 respectively. The 1990 technology turboshaft engine weight is very consistent with the historical trend, while the year 2000 technology turboshaft engine weight represents a distinct improvement. The 1990 technology turboshaft SFC value is substantially better than the historical trend, although not quite as good as the demonstrator MTDE design goal. The year 2000 technology turboshaft SFC is a substantial improvement, simply reflecting the difference between IHPTET Phase I goals and IHPTET Phase II goals.

The convertible engine characteristics were based on a variable inlet guidevane/ variable exit guidevane configuration with a high bypass ratio of 6.0 and a 1.75 overall pressure ratio. A thrust-to-horsepower ratio of 1.47 was used for the 1990 technology convertible. SFC values were adjusted

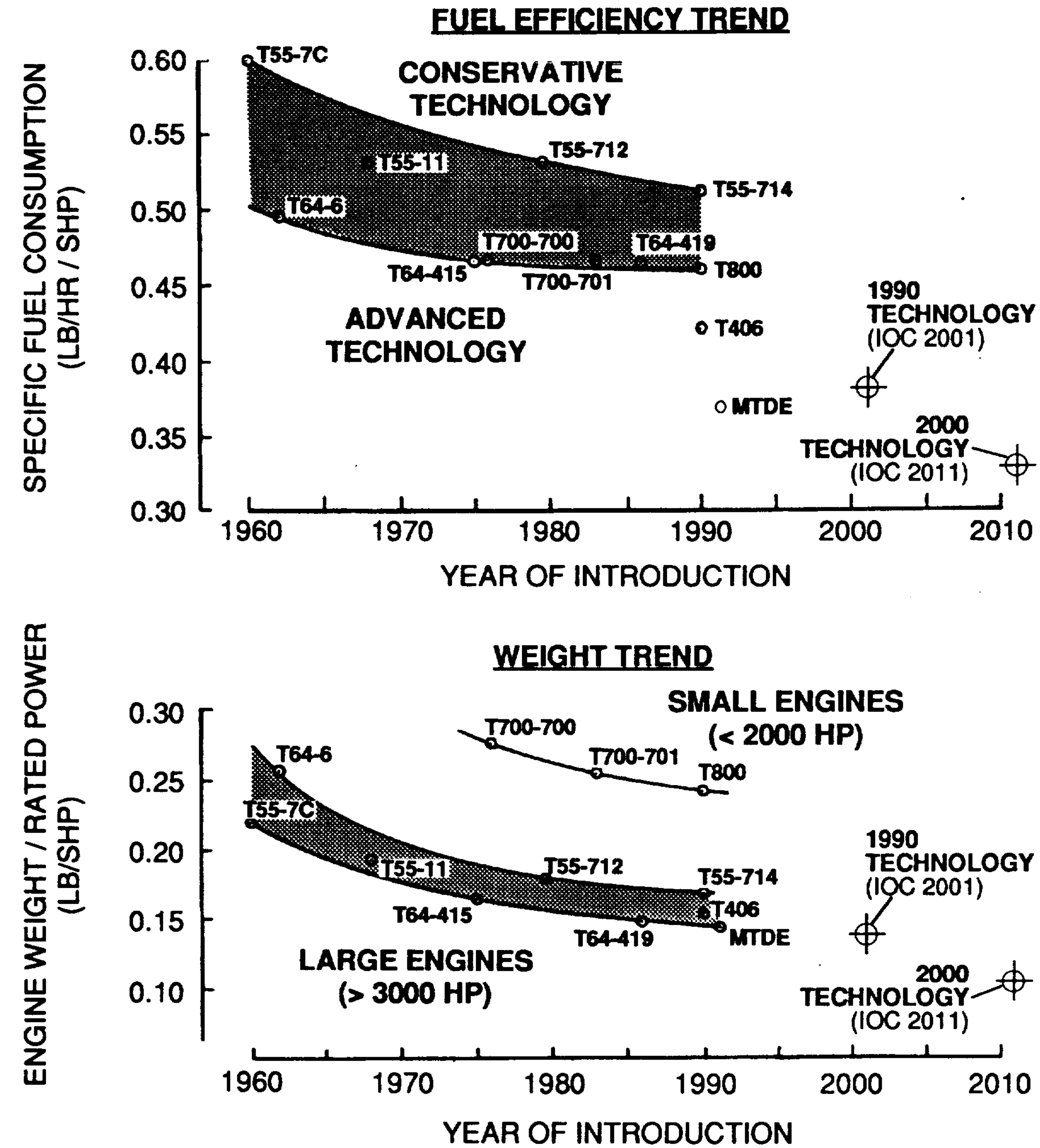

Figure A-23. Turboshaft Engine Fuel Efficiency and Weight Trends

to reflect the IHPTET goals as explained above. However, there is a difference between IHPTET goals for turboshaft engines and turbofan engines as shown in Table A-5. Convertible engine performance was based on the turbofan goals. The convertible engine weight trend is shown in Figure A-24 compared to the turboshaft engine weight trend. While the convertible engine is quite a bit heavier (about 80% heavier), it includes the cruise propulsive fan, VIGV/VEGV, controls, power takeoff shaft and gears, and clutch for decoupling the rotor drive system. This comparison points out a truer picture of the weight penalty associated with any concept requiring a convertible engine for cruise flight versus a concept which can utilize a pure turboshaft engine.

Table A-5. IHPTET Performance and Weight Goals

	PHASE I	PHASE II
Turboshaft Engines:		
SFC change	-20%	-30%
SHP/weight change	+40%	+80%
Turbofan Engines:		
SFC change	- 5%	-10%
SHP/weight change	+33%	+67%

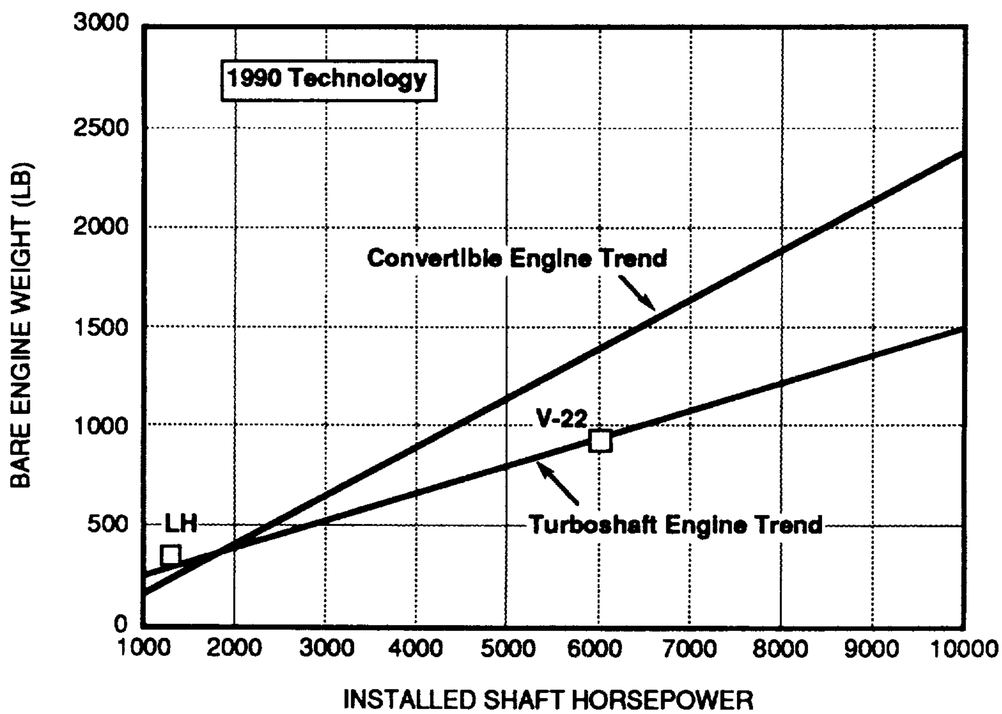

Figure A-24. Convertible Engine Weight Trend

The turboshaft and convertible engines were rubberized for these sizing studies. Adjustments to the SFC to reflect IHPTET goals were made in VASCOMP II runs by applying a fixed multiplier to the SFC as provided for in the standard VASCOMP input deck.

Survivability Considerations

To ensure survivability on the battlefield, an aircraft designer must consider the balance between susceptibility and vulnerability. Susceptibility is a measure of the likelihood of that aircraft being hit by any of the anticipated threats. Vulnerability is a measure of the ability of the anticipated threats to reduce the effectiveness of the weapons system when it is hit. The threats that should be considered include small arms, anti-aircraft artillery (AAA), guided missiles, lasers, nuclear weapons and chemicals.

Threats

Small arms, rifles and machine guns smaller than 14.5mm carried by foot soldiers, can be quiet effective against aircraft. The large number of small arms on the battlefield demands that all equipment should provide some form of protection against them.

AAA weapons are generally 23mm to 73mm in diameter and are designed to destroy aircraft or missiles. Most AAA weapons use some combination of visual and radar targeting systems. Since all radar systems emit radiation to locate and identify targets, aircraft equipped with radar warning receivers can identify that the weapon is operating and have a limited indication (usually by a quadrant) of where the threat is located and whether it has detected the aircraft. This can give the aircraft a distinct advantage.

Guided missiles use radar or infrared (IR) radiation to guide the missile to the target. These radar systems work essentially the same way as the AAA radar. The IR missiles have detectors that operate in the infrared frequency range and home in on heat emissions and hot surfaces of the aircraft.

Missiles can have a devastating effect on air assets, causing high rates of attrition. Tactics that can be used to avoid missiles involve flying higher and faster to "outrun" the missile or flying low and slow to avoid being seen. Some of the smaller missiles can be outrun, but the larger ones can catch any aircraft short of the SR-71. The performance envelope of the high-speed rotorcraft makes them highly susceptible to missiles, being too slow to outrun them yet too fast to avoid being seen.

Battlefield lasers are being developed that can damage electro optical sensors and perhaps aircraft structure. These lasers acquire and engage targets the same ways that small arms and AAA do.

All weapon systems that are essential to maintain a war fighting capability after the use of nuclear weapons should consider nuclear weapons effects. While clearly not a desirable weapon to use on a strategic level, there is a growing community that feels that a "limited" tactical nuclear war is possible. The weapons are available and the nuclear hardness of our weapon systems should be addressed, if only to discourage the use of tactical nuclear weapons by our enemies. While there are longer range surface-to-air missiles that can carry a nuclear warhead, it is very unlikely that a nuclear weapon will be targeted for any rotorcraft. Chances are great that any nuclear encounter for these concepts will be the result of being in the wrong place at the wrong time.

The same is true for chemical and biological (CB) weapons. The development and use of chemical weapons by smaller nations is reason for concern in the design of future battlefield assets. It emphasizes the low cost of these weapons and their effectiveness as a deterrent on the battlefield. Chemical weapons can cause tremendous reductions in the effectiveness of a weapon system if it is not protected and easy to decontaminate. Some of the chemicals will degrade unprotected structure. Assets that cannot be rapidly decontaminated present additional hazards to the crew and ground support personnel.

The likelihood of encountering CB threats is considerably less than for small arms, AAA, or missiles yet considerably greater than the chances of encountering a nuclear threat. The chemical experts are quick to point out that chemical weapons have been used as weapons quite recently while the last time a nuclear weapon was used against an enemy was in 1945.

Concept Ranking

In this study, a relative ranking was developed of the survivability of the high-speed rotorcraft concepts through an evaluation of some of the key survivability factors. Susceptibility can be evaluated by considering the signatures of the aircraft which allow the threats to detect, identify, target and hit that aircraft. Vulnerability can be evaluated for each of the major threats to the aircraft. Eight areas were evaluated for relative survivability of the high-speed rotorcraft concepts. These were:

- Radar Signature
- Infrared (IR) Signature
- Visual Signature
- Acoustic Signature
- Ballistic Vulnerability
- Laser Vulnerability
- Nuclear Vulnerability
- Chemical-Biological Protection
- Crashworthiness

Crashworthiness, although often considered separately from survivability, is a key element and plays an important role in how an aircraft system(s) maintains a high state of readiness.

Radar Signature

There are two aspects of the reflected radar signal that a radar system can exploit, the magnitude of the reflected signal or the Doppler shift of the signal due to the relative velocity of the target. The Doppler shift is used by some radars to separate the moving target from the background reflections. A filtering process is used to isolate "dynamic" signal to identify objects in the field of view whose velocity is above a certain limit. This dynamic component will include the rotating blades and may include the body of the aircraft if the aircraft speed is sufficient. But, this type of radar will not detect a rotorcraft on the ground if the rotors are not moving. Other radars will look for higher than average reflected signals or signals that change (magnitude or direction) with time.

The evaluation of the radar signature for this study considered both the static and the dynamic characteristics of aircraft. Additional signature evaluation complexity has been introduced by the existence of vastly different hover and cruise modes in the high-speed rotorcraft concepts. Static and dynamic returns are different in both configurations as during transition or any intermediate stop position.

Rotor body interaction (RBI) is a term that is used to describe the increased return signal that can be a result of various bounce modes of reflection between the rotor and the body (fuselage) of the rotorcraft. RBI is configuration dependent. RBI returns have been demonstrated in rotorcraft test bodies to rival main rotor blade returns in magnitude with significant azimuthal influence. The static, dynamic and RBI sources of radar signature are graphically shown in Figure A-25.

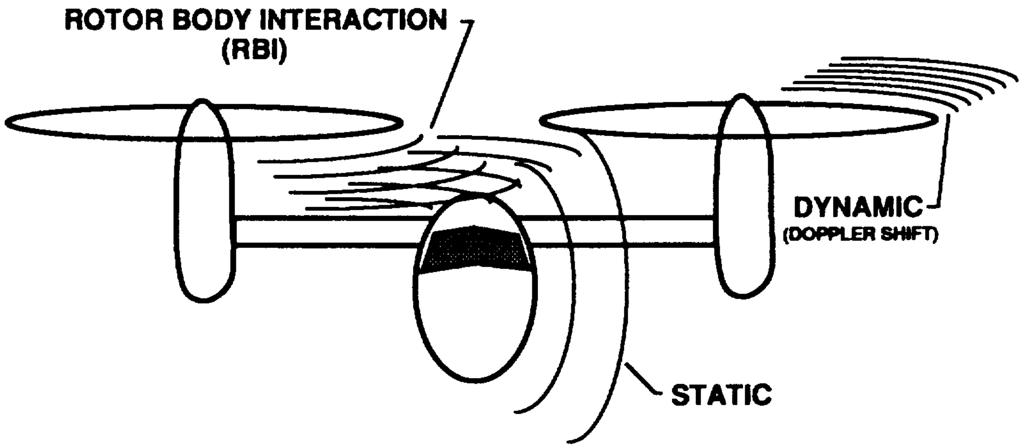

Figure A-25. Radar Signature Sources

The static signature requirement is usually determines shaping, orientation, and alignment options used to assess the signature. As no signature requirements (levels and processing techniques) for static and dynamic levels are provided in this program, the sector average approach was used for static. This approach averages s (in square meters or dbsm) over X number of degrees (i.e. 30, 60, 180 deg.). Dynamic data processing for a pulsed Doppler threat (dBsm/#HZ) was assumed. This resulted in a cross range image on the blade at the time of blade flash.

In summary, the folding tiltrotor and the variable diameter rotor scored slightly lower for hover signature. The poor static signature of the tiltwing in hover is offset by the lowered RBI. All configurations are expected to have comparable signatures in the cruise mode with the exception of the folding tiltrotor which has significantly reduced signature when the blades are stowed and slightly worse signature when unstowed.

Radar Signature Scores:

	TILTROTOR	CANARD TILTROTOR	VARIABLE DIAMETER	FOLDING TILTROTOR	TILT WING
HOVER	3.0	3.0	2.3	2.3	3.0
CRUISE	3.0	3.0	3.0	4.0	3.0
OVERALL	6.0	6.0	5.3	6.3	6.0

IR Signature

The IR signature is a combination of the engine exhaust temperature effects and the "hot metal" or skin temperature effects. Most rotorcraft incorporate heat exchangers into the propulsion system to reduce the engine exhaust temperatures. This was assumed for each of the turboshaft concepts. With the heat suppressors, the IR signatures will be similar for all of the turboshaft concepts. The tiltwing required significantly higher power than the others and was therefore scored 1/2 point lower. The folding tiltrotor had a naturally cool 6:1 bypass ratio fan driven by its convertible engine. However, it also had a mixing chamber for cruise and a combined core-exhaust suppressor for the hover mode.

IR Signature Scores:

	TILTROTOR	CANARD TILTROTOR	VARIABLE DIAMETER	FOLDING TILTROTOR	TILT WING
HOVER	3.0	3.0	3.0	3.0	2.5
CRUISE	3.0	3.0	3.0	4.0	2.5
OVERALL	6.0	6.0	6.0	7.0	5.0

Visual Signature

The aircraft's visual signature is an indication of the ability for someone to spot the aircraft using eyes or TV. Significant factors are flicker, RPM, contrast and size. Assuming that all concepts would have similar low reflectance paint, the visual signature is primarily a function of size. The body size of these concepts is very similar. The tiltwing has significantly greater presented area for the forward and aft viewing aspects when in the hover and conversion mode.

The ability to detect the rotor is a function of the disc diameter, contrast (assumed equal for this study) and the frequency of the blades presentation. The frequency effect is commonly known as flicker. The eye is drawn to light sources that "flash" or "flicker" at low frequencies. If the image of the rotor appears constant with time it will not be as noticeable as an image that flickers. It can be stated that higher frequencies of flicker are less noticeable than lower. This means that a faster rotation or more blades can reduce the flicker effect. The tiltwing will have the lowest flicker in hover. The folding tiltrotor has no flicker in cruise with the rotors stowed. The variable diameter tiltrotor was designed to have a smaller rotor diameter in cruise giving it a modest advantage.

Visual signatures were considered for hover and cruise for both body (size) and flicker.

Visual Scores:

	TILTROTOR	CANARD TILTROTOR	VARIABLE DIAMETER	FOLDING TILTROTOR	TILT WING
HOVER	3.0	3.0	3.0	3.0	3.0
CRUISE	3.0	3.0	3.3	4.0	3.5
OVERALL	6.0	6.0	6.3	7.0	6.5

Acoustic Signature

For military applications, quieter is better but the advantage of low acoustic signature is questionable. While there are acoustic detectors, these are generally used to direct artillery fire, which has a relatively long time of flight and a corresponding low probability of hit for aircraft. While infantry may be warned of the approach of aircraft by hearing them, there is considerable background noise from combat vehicles and weapons that can mask the aircraft noise. For covert operations it is imperative to avoid detection, so the value of a low acoustic signature is very high. The acoustic signature was not quantitatively evaluated in Task I.

Ballistic Vulnerability

It is not practical to armor an aircraft. Armor is too heavy and is only good for the threat and impact velocity designed. While considerable ballistic tolerance can be built into many of the critical systems, in this study the most survivable concepts are the ones that have redundancy and separation of critical components.

Redundancy means more than having two components. To be truly redundant, each individual component must be capable of performing the tasks of the other component. Separation is required to assure that both components performing the same function are not damaged at the same time. For armor piercing (AP) rounds, the required separation is not very much. High explosive (HE) rounds require considerably more separation. A rule of thumb used for preliminary design is that critical component pairs must have at least 18" separation or be isolated from each other by shielding material to be considered redundant. Transmissions and fuel tanks are examples of shielding materials.

An aircraft is considered vulnerable if a hit on that aircraft can cause the loss of that aircraft either through destruction (attrition) of the aircraft and major damage (forced landing) or loss of mission essential functions for that aircraft (mission abort). For this study it has been assumed that every concept would have the same mission equipment and the same basic vulnerability for mission aborts. For the same reason flight controls, hydraulics, and electrical systems were not considered for the concept evaluations.

The ballistic rankings were based on areas on the aircraft that could result in attrition of that aircraft either through failure to sustain flight back to a safe landing zone or inability to land safely upon return. Traditionally, the criteria for survival for rotorcraft has been to sustain 30 minutes flight after a hit.

For this program it was assumed that every concept has the same one engine inoperative (OEI) capability and therefore could complete the mission if one engine was lost. For comparative evaluations, this assumption does not have a great affect on the results and it avoids confusion over the relative size and vulnerability of the individual engines of each concept. With this assumption the only vulnerability consideration for the engines is the separation between them, to avoid killing both engines with one shot. The canard versions have inboard engines which increases the chances of killing both engines. Some form of shielding may be required for safety in these concepts. The conventional tiltrotor and the tiltwing have more separation with wing-mounted outboard engines.

Another advantage to having the engines located on the wings is the potential to survive either a cross shaft failure or a one engine inoperative condition. This would require better engine speed control to assure adequate synchronization of the rotors. If the cross shaft is required to control the individual rotor speeds, then the shaft integrity must be maintained for controlled flight.

These aircraft will need to carry significant amounts of fuel in the wings. The dynamic response of a fuel tank that is penetrated by a high velocity or an explosive projectile can cause the wing structure to fail. All of these concepts will require considerable effort and probably additional weight to make the wing/fuel system ballistically tolerant. The tiltwing will be more critical and more difficult to protect because of the large presented area of the wing in hover and the change in fuel tank position and fuel location between hover and cruise. While this will be cause for concern in the development of the tiltwing concept, fuel protection is required on all of the concepts and adequate protection can be developed for all of them.

The assumption was made that the basic flight controls, ailerons, flaps, rudder, elevator and even the rotor controls are equivalent. There are not anticipated differences that significantly affect the vulnerability of the aircraft. There is one exception to this, the conversion mechanism. For each of the tiltrotors, the conversion mechanism will be located at the end of the wing. These mechanisms will be subject to jamming or severance. A jam would make it impossible to convert. This could make a hovering aircraft more vulnerable because of limited speed and range or unable to return to base if the base was not nearby. A jammed conversion mechanism could cause the aircraft to be destroyed in landing if it is jammed in the cruise mode. It is possible to design the folding tiltrotor to land with the blades designed for higher speed landing. The tilting wing provides automatic synchronization between the rotors, allowing the use of one, larger, ballistically tolerant mechanism or several smaller, redundant systems. The conversion mechanism for the tiltwing should be located in the fuselage, allowing greater flexibility in the design of attachment points and redundant structure while providing better shielding for the mechanism at the same time.

The rotors of each of these concepts will have similar blade area for the same gross weight. This means that the chord on the smaller diameter tiltwing blades will be considerably longer than the others. These blades will probably be more ballistically tolerant, although the other blades will have adequate hardness.

The folding mechanism on the folding tiltrotor may be vulnerable to jamming or separation (loss of control). Like the conversion mechanism, this may not cause a problem if the aircraft can land with the blades stowed.

The variable diameter tiltrotor will be vulnerable to jamming and separation also. A jam could cause an imbalance in the rotors to prevent conversion. The sliding fit of the blades will cause considerable jamming problems for all threats, even small arms due to damage and distortion of the blade or the blade mechanism as the projectile passes through it. Larger threats may be able to separate the blade mechanism causing a rotor imbalance and loss of the aircraft. A summary of key differences in ballistic vulnerability are listed below.

Engine Separation - Tiltrotor and Tiltwing have less chance of killing both engines from a single shot and the drive shafts are less critical.

Fuel - Tiltwing has much higher exposure of wing fuel tanks in hover than other configurations.

Controls - Tiltwing conversion mechanism is less exposed and therefore more survivable.

Rotor - Tiltwing has a larger chord, giving higher survivability. The folding mechanism of the folding tiltrotor could jam and the blade retracting mechanism could jam on the variable diameter tiltrotor.

Ballistic Hover Scores:

	TILTROTOR	CANARD TILTROTOR	VARIABLE DIAMETER	FOLDING TILTROTOR	TILT WING
ENGINES	4.0	3.0	3.0	3.0	4.0
DRIVES	4.0	2.0	2.0	2.0	4.0
FUEL	3.0	3.0	3.0	3.0	1.0
CONTROLS	3.0	3.0	3.0	3.0	5.0
ROTOR	3.0	3.0	1.0	2.5	3.5
OVERALL	3.4	2.8	2.4	2.7	3.5

Ballistic Cruise Scores:

	TILTROTOR	CANARD TILTROTOR	VARIABLE DIAMETER	FOLDING TILTROTOR	TILT WING
ENGINES	4.0	3.0	3.0	3.0	4.0
DRIVES	4.0	2.0	2.0	2.0	4.0
FUEL	3.0	3.0	3.0	3.0	3.0
CONTROLS	3.0	3.0	3.0	3.0	5.0
ROTOR	3.0	3.0	1.0	2.5	3.5
OVERALL	3.4	2.8	2.4	2.7	3.9

Total Ballistic Scores:

	TILTROTOR	CANARD TILTROTOR	VARIABLE DIAMETER	FOLDING TILTROTOR	TILT WING
HOVER	3.4	2.8	2.4	2.7	3.5
CRUISE	3.4	2.8	2.4	2.7	3.9
OVERALL	6.8	5.6	4.8	5.4	7.4

Laser Vulnerability

Battlefield lasers with new capabilities are being developed at a rapid pace. A large number of low energy lasers that are used for range finding and target designation have some capability to limit the usefulness of electro-optic (EO) sensors and direct vision, particularly at night. In the future, lasers can be expected that will have enough power to damage sensors and canopies and perhaps weaken structure.

The assumption that each concept will employ the same mission equipment eliminates any potential differences for low energy laser vulnerability. The protection techniques employed for high energy laser protection would be very similar for all of the concepts. Therefore the laser vulnerability was assumed equal for all of the concepts.

Nuclear Vulnerability

Figure A-26 shows the five threats to aircraft from a nuclear explosion. The nuclear effects that were considered for evaluation of the concepts were the blast (shock wave) and gust. Other nuclear effects do not have significantly different effects from one concept to the next.

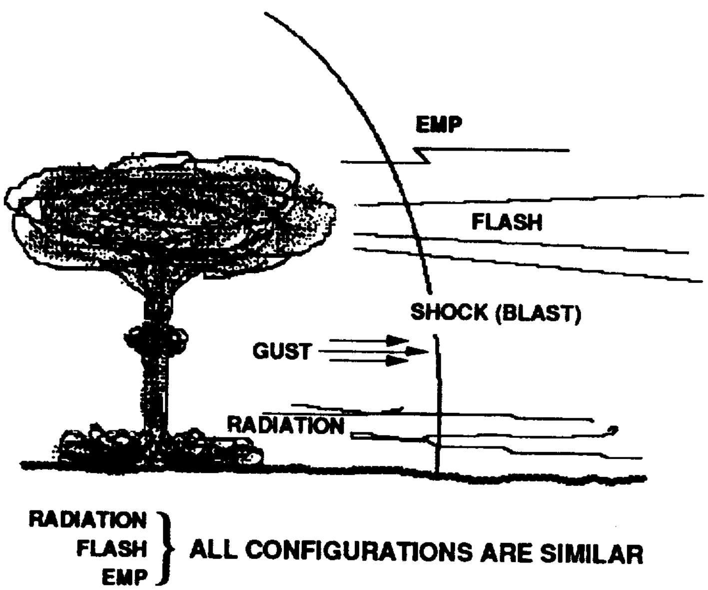

Figure A-26. Nuclear Effects

The blast effect is caused by the interaction of the shock from the nuclear blast with the skins of the aircraft. The pressure wave is reflected from the skin, causing a very sharp and short duration pressure pulse on the skin that can rupture the skins and possibly damage stringers and frames. The effects of this on the different concepts will be similar except for blasts directly forward and aft of the tiltwing in hover, where the wing presents a very large relatively perpendicular face to the blast. The full impact cannot be assessed without a detailed analysis that is outside the scope of this contract. Because of the unknowns and the angular dependance of this problem, a low penalty was added to the tiltwing in hover.

A sharp aerodynamic gust follows the shock wave of a nuclear blast. This gust affects the aircraft in the same manner as a zero rise time atmospheric gust would. The effect has a longer duration than the blast, producing flapping and bending in the blades and the structure. As was true for the blast, the response of the fuselage will be similar for each of the concepts except the tiltwing in hover.

The rotors will also respond similarly for each of the concepts except for the folding tiltrotor and the variable diameter tiltrotor. When the blades are stowed in cruise, they may be more vulnerable to sideward gusts, depending on the design of blade lock-down devices. This fact is offset by the lower vulnerability to blasts that are not from the side and the ability to land in the airplane mode with the blades stowed. It is believed these factors are offsetting and the overall vulnerability is probably the same or marginally better than the other concepts. The increased bending deflections due to the gust may cause problems for blades of the variable diameter concept from all directions in both hover and cruise.

Nuclear Scores:

	TILTROTOR	CANARD TILTROTOR	VARIABLE DIAMETER	FOLDING TILTROTOR	TILT WING
HOVER	3.0	3.0	2.5	3.0	2.5
CRUISE	3.0	3.0	2.5	3.0	3.0
OVERALL	6.0	6.0	5.0	6.0	5.5

Chemical-Biological

There are no significant differences between the concepts for CB protection except that the sliding mechanism of the variable diameter rotor will be very difficult to seal and decontaminate.

C-B Scores:

	TILTROTOR	CANARD TILTROTOR	VARIABLE DIAMETER	FOLDING TILTROTOR	TILT WING
HOVER	3.0	3.0	1.5	3.0	3.0
CRUISE	3.0	3.0	1.5	3.0	3.0
OVERALL	6.0	6.0	3.0	6.0	6.0

Crashworthiness

The important factors for crashworthiness are underfloor structure, space retention, large mass placement and retention and crashworthy seats as indicated in Figure A-27. Since these factors are similar for each of the concepts, there were not major differences to allow a relative ranking.

Survivability Relative Ranking

Relative rankings have been developed for radar, IR, and visual signatures and for ballistic, nuclear and CB vulnerability. It is difficult to rank the relative importance of each of these areas without a defined mission and threat, however some assumptions have been made. The speed range of these concepts will make them quite vulnerable to missiles, making the IR and radar signatures somewhat more important than the visual signature. The likelihood of encountering

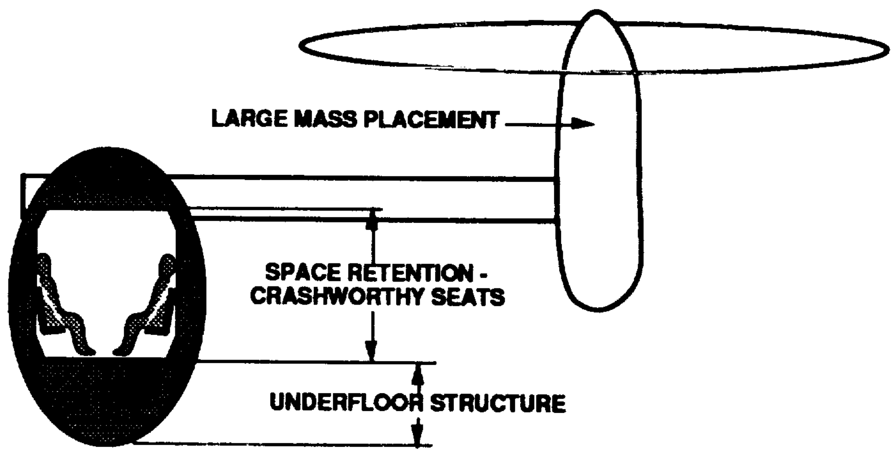

Figure A-27. Crashworthiness Considerations

ballistic threats is higher than CB threats. The likelihood of encountering a nuclear threat is considerably less than either the CB or the ballistic. These assumptions led to the following weighting factors for the total survivability comparison;

AREA	WEIGHTING FACTOR
Radar	2
IR	2
Visual	1
Ballistic	2
Nuclear	0.5
C-B	1

Weighted Scores:

	TILTROTOR	CANARD TILTROTOR	VARIABLE DIAMETER	FOLDING TILTROTOR	TILT WING
RADAR (x2)	12.0	12.0	10.6	12.6	12.0
IR (x2)	12.0	12.0	12.0	14.0	10.0
VISUAL (x1)	6.0	6.0	6.3	7.0	6.5
BALLISTIC (x2)	13.6	7.2	9.6	10.8	14.8
NUCLEAR (x0.5)	3.0	3.0	2.5	3.0	2.8
C-B (x1)	6.0	6.0	3.0	6.0	6.0
TOTAL	52.6	46.2	44.0	53.4	52.1

Reliability and Maintainability

Maintainability of the five candidate rotorcraft concepts was evaluated on the six factors described in Table A-6. The relative importance of these factors was reflected by the number of potential points assigned to each, for a total perfect score of 100.

Table A-6. Maintainability Factors

Factor	POINTS
Access - One sided, good view/access, no special tools	25
Location - Large components located to allow access to smaller ones - High failure rate parts accessible	15
Structure - Eliminate special installation sequence - Replaceable abrasion surfaces - Horizontal surfaces are walking surfaces	10
Lubrication - Precluded where possible	10
Ease of maintenance - Overall vehicle quality	25
Complexity - Complex structures/designs require a maintainability analysis to ensure satisfaction of requirements	15
	100

Judgements were based on the basic concept and configuration layout. A discussion of some of the considerations follows. Fuselage buried engines were judged to be less accessible for major maintenance, but the midwing gearbox location was considered more accessible. Engines mounted over the fuselage tail area were judged to make maintenance more difficult. The midwing mounting of the tiltwing tilt mechanism was previously considered favorable from a survivability standpoint, but was penalized from maintenance considerations due to its inaccessibility with the wing in a down position. Likewise, the variable diameter tiltrotor was penalized for poor access to the rotor blade retraction mechanism when the blades are in a retracted position. From a maintenance perspective these mechanisms must be accessible for any position within their designed capability for the mechanics trying to service an airframe. The variable diameter tiltrotor was also penalized for the complexity of the hub and blade mechanism required for blade retraction. These maintainability factors were scored for each concept, and summed for a total maintainability score.

Reliability was also evaluated for each concept. Figure A-28 shows the percentage contribution of various aircraft systems to total reliability. Out of these, only the rotor group, the propulsion system, and the flight controls were considered to be distinctly different between the five rotorcraft concepts. These systems were evaluated by considering the concepts' drive system components and other distinguishing features which contribute to system reliability. The evaluator then put the scores into a relative ranking.

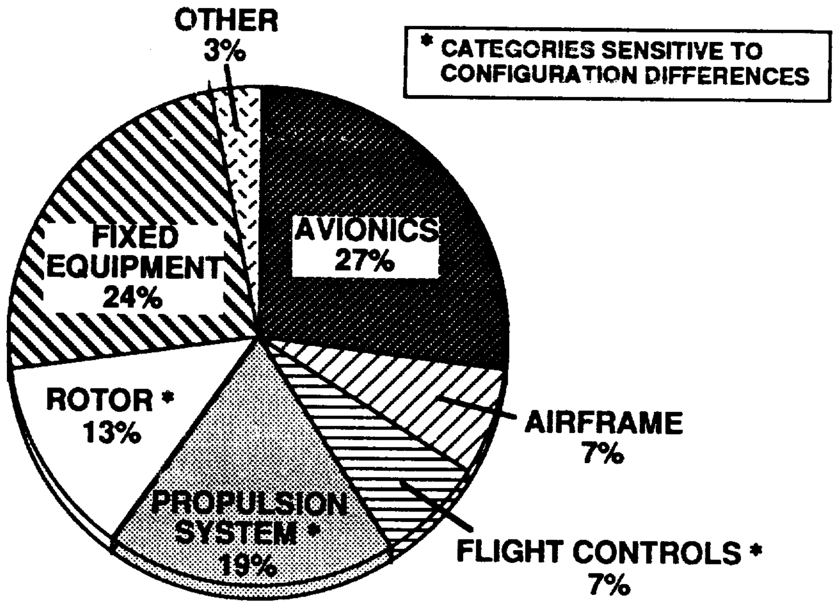

Figure A-28. Reliability Areas

An average R&M score was calculated by taking the numeric average of the reliability score and the maintainability score. These were then normalized again by dividing all the averaged scores by the highest average score, giving 100% as the highest averaged rating. The reliability, maintainability, and averaged R&M scores are shown below:

	RELIABILITY	MAINTAINABILITY	AVERAGE OF R&M
Conventional Tiltrotor	93%	100%	100%
Canard Tiltrotor	84%	83%	86%
Variable Diameter Tiltrotor	80%	77%	81%
Folding Tiltrotor	73%	77%	78%
Tiltwing	100%	90%	98%

Task I Cost Comparison

Life Cycle Cost (LCC) estimates were made for each of the five concepts in order to obtain comparative cost data. A parametric approach was chosen for the initial estimate. This methodology offers several advantages for programs in the concept development phase of the life cycle. The primary consideration is availability of data. In preliminary design, the majority of data generated is for relatively top level parameters; mission gross weight, fuel system capacity, wing area, fuel consumption and fuselage volume are typically available. Another concern impacting operating and support costs is the lack of definition about maintenance concepts, logistics support and aircraft basing. An approach which addresses these subjects indirectly, i.e., parametrics, is required.

Over 100 discrete parameters were evaluated for each of the concepts. The technical and performance data which served as the foundation of the estimates were derived from the baseline 1990 optimum configurations. These configurations were selected on the basis of gross weight, not cost. However, the correlation between weight and cost has been demonstrated to be very high and, therefore, qualifies weight as a legitimate discriminator for conceptual design.

Figure A-29 provides a synopsis of the LCC elements in their relative proportion to one another. The Research and Development phase includes costs accrued under conceptual and preliminary design and full-scale development for the airframe, engines and avionics. It constitutes 10-20% of the life cycle cost and varies upward with the number of new technologies, materials and production processes being explored. The airframe cost estimating relationships were developed from a data base of 18 aircraft and provide for engineering labor, tooling labor, manufacturing/quality control labor, materials and other direct charges. Cost estimating relationships for avionics research, development, test and evaluation were developed from a 10 aircraft data base. This included labor and materials for brassboards, breadboards and prototype hardware from the start of full-scale development of the avionics suite through completion of flight test, including spares, maintenance and engineering support. Cost estimating relationships for engine development were developed from a data base of 13 turbojet and turbofan engines. Engine pressure ratio, thrust-to-weight ratio, turbine inlet temperature and a technology factor were the primary independent variables.

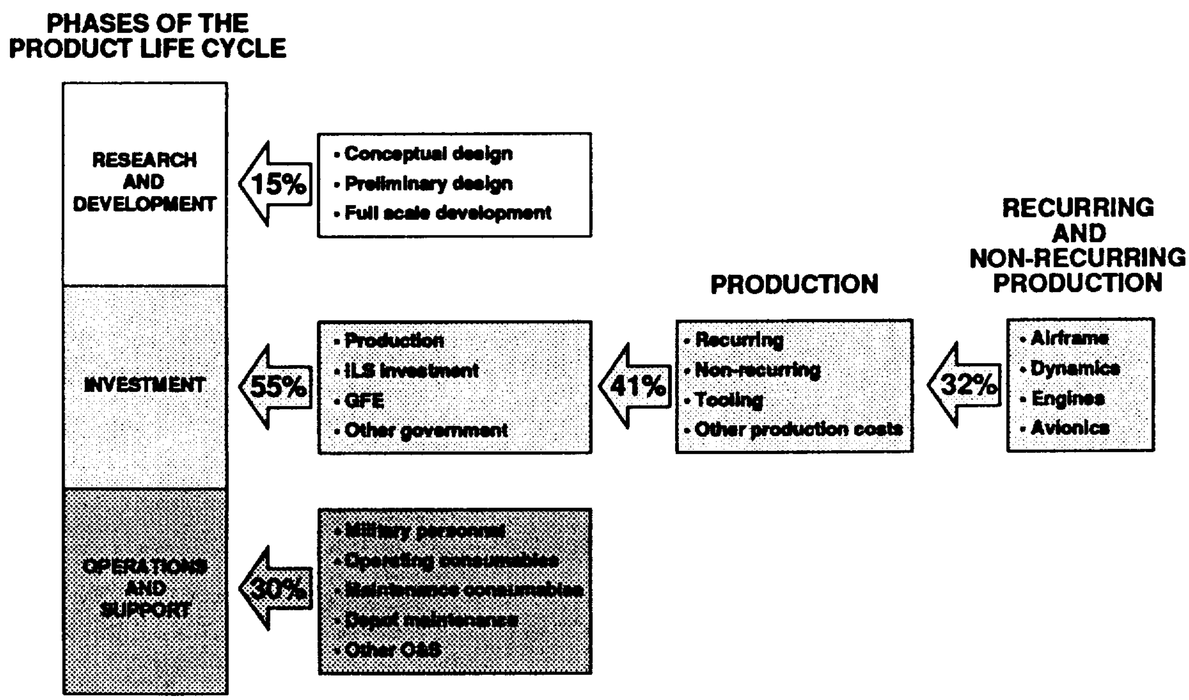

Figure A-29. Components of Rotorcraft Life Cycle Cost

The investment phase of the aircraft life cycle is the largest in terms of outlays. Production costs, support equipment and initial spares investment and trainings costs account for the majority of expenditures in this area. Investment costs constitute 50-60% of the LCC. The airframe cost estimating relationships discretely estimate subsystem unit production costs, raw material, sustaining engineering, quality control and final assembly. In addition, parametric estimates for training, data, support equipment, initial spares, engine spares, unit activation and war reserve materials were included. Facilities and modifications (ECPs) costs were not estimated.

Operating and support costs comprise 30-35% of the LCC and include indirect and direct personnel, operating and maintenance consumables, depot maintenance and supply, replenishment and other spares and personnel acquisition and training.

The results of the LCC analysis are depicted in Figure A-30. The conventional tiltrotor design was designated as the baseline aircraft. The LCC of the remaining designs were normalized by the baseline cost. The aircraft with the highest gross weight had the highest LCC, that was the

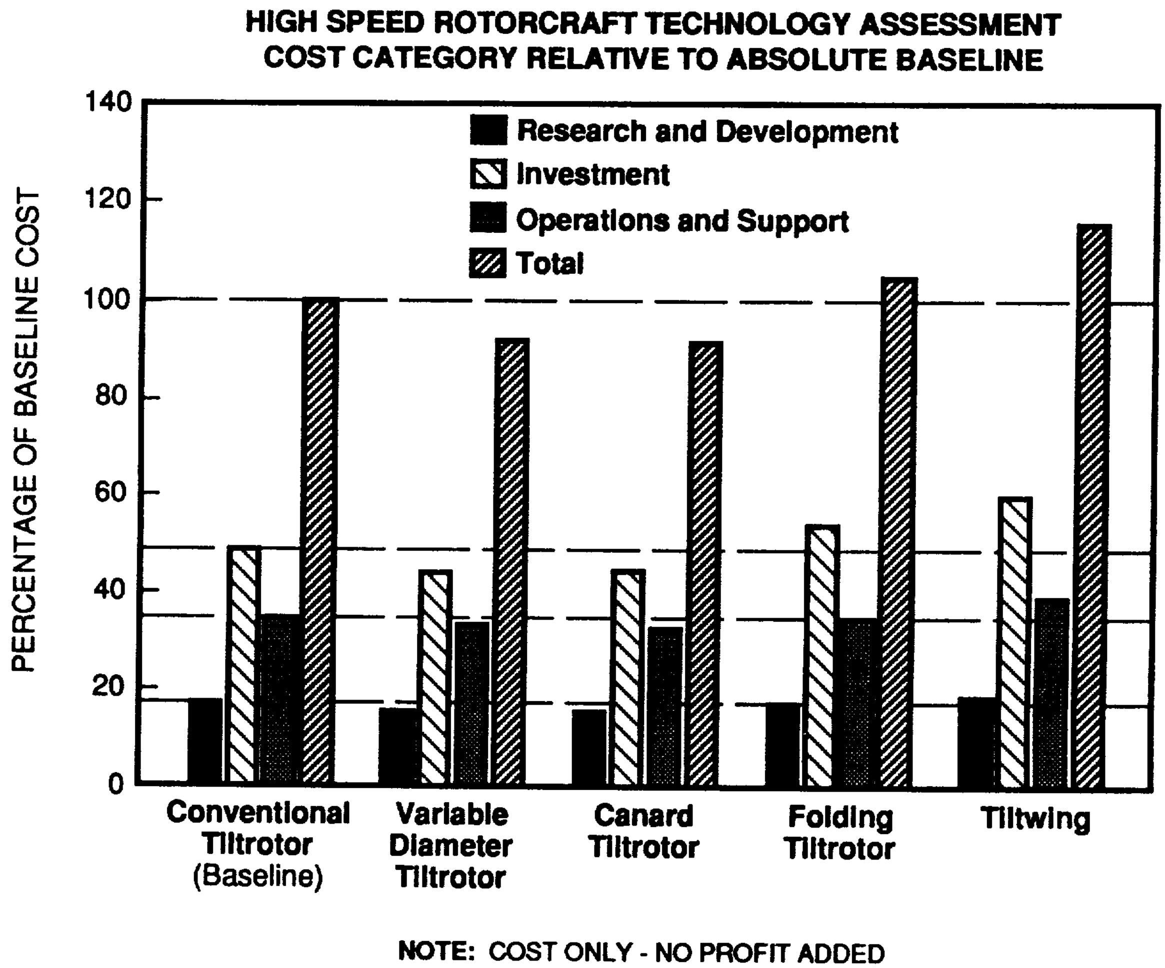

Figure A-30. Life Cycle Cost Evaluation

tiltwing concept. Conversely, those with the lowest gross weight had the lowest LCC, that was the canard tiltrotor and the variable diameter tiltrotor. With the conventional tiltrotor as the reference, the following observations were made:

> ***Variable Diameter Tiltrotor and Canard Tiltrotor*** - The takeoff GW was about 10,000 pounds less than the conventional tiltrotor. Wing area and tail area were substantially less. Nacelle wetted area was much less since the engines for these two configurations are body mounted versus nacelle mounts for the conventional tiltrotor. Installed power was 30% and 36% less, respectively than for the conventional tiltrotor. O&S costs were driven down by a 32% reduction in fuel consumption and by reduction in spares costs inherent of lighter weight and lower power.

Folding Tiltrotor - The folding tiltrotor has nearly the same gross weight as the conventional tiltrotor. A 25% increase in wing area, higher fuselage density due to the fuselage mounted engines and the added weight of the convertible engines contributed to the increase in investment costs.

Tiltwing - The tiltwing has a 6% higher takeoff GW and a 27% higher installed power than the conventional tiltrotor. A larger fuel system, 54% larger tail, higher takeoff GW, and over 50% more wing area drove the investment costs. The higher installed power and 20% higher fuel consumption were major drivers of the increased O&S costs.

APPENDIX B
SUPPLEMENTAL DATA FOR TASK II

This appendix contains data which supplements the limited presentation of the technical data and performance for the High-Speed Civil Tiltrotor and the Military Folding Tiltrotor in Section 2 of the main body of this report. General discussions are also included on rotor downwash characteristics, flight control systems, materials and manufacturing methods, and details of the life cycle cost analysis.

TABLE OF CONTENTS

PAGE

TABLE OF CONTENTS (continued)

LIST OF FIGURES

LIST OF FIGURES (continued)

PAGE

LIST OF TABLES

PAGE

APPENDIX B
SUPPLEMENTAL DATA FOR TASK II

Mass Properties Summary

The component weights, weight empty, and mission design gross weight of the high-speed civil tiltrotor and military folding tiltrotor aircraft are presented in MIL-STD-1374 format in Figure B-1. Aircraft balance, based on fuel loading and burn off, is presented in helicopter and airplane modes in Figures B-2 and B-3. Longitudinal (x) and vertical (z), reference datums are identified on the aircraft profiles. The lateral reference datum (y) is on the centerline of the aircraft. A summary of the aircraft mass moments of inertia is presented in Table B-1 and B-2.

	CIVIL TILT ROTOR	
WING		1660
ROTOR		2290
TAIL		542
HORIZONTAL	338	
VERTICAL	204	
BODY		4048
BASIC		
SECONDARY		
ALIGHTING GEAR GROUP		1380
ENGINE SECTION AND AIR INDUCTION		630
PROPULSION GROUP		6919
ENGINE INST'L	2520	
EXHAUST SYSTEM		
COOLING		
CONTROLS	428	
STARTING		
PROPELLER INST'L		
LUBRICATING		
FUEL	397	
DRIVE	3574	
FLIGHT CONTROLS		2018
TILT MECHANISM		960
AUX. POWER PLANT		
INSTRUMENTS		
HYDR. & PNEUMATIC		
ELECTRICAL GROUP		
AVIONICS GROUP		
ARMAMENT GROUP		4800
FURN. & EQUIP. GROUP		(INCLUDES 800 LB OF AVIONICS)
ACCOM. FOR PERSON.		
MISC. EQUIPMENT		
FURNISHINGS		
EMERG. EQUIPMENT		
AIR CONDITIONING		
ANTI-ICING GROUP		
LOAD AND HANDLING GP.		
MISC.		1167
WEIGHT EMPTY		26414 LB
CREW (3)		510
TRAPPED LIQUIDS		65
ENGINE OIL		50
PASS. SERVICE ITEMS		115
PAYLOAD		6000
FUEL		5226
GROSS WEIGHT		38380 LB

	FOLDING TILT ROTOR	
WING		4019
ROTOR		3152
TAIL		712
HORIZONTAL	495	
VERTICAL	217	
BODY		4286
BASIC		
SECONDARY		
ALIGHTING GEAR GROUP		1511
ENGINE SECTION AND AIR INDUCTION		937
PROPULSION GROUP		9746
ENGINE INST'L	3747	
EXHAUST SYSTEM		
COOLING		
CONTROLS	749	
STARTING		
PROPELLER INST'L		
LUBRICATING		
FUEL	1560	
DRIVE	3690	
FLIGHT CONTROLS		2328
TILT MECHANISM		1286
AUX. POWER PLANT		
INSTRUMENTS		
HYDR. & PNEUMATIC		
ELECTRICAL GROUP		
AVIONICS GROUP		
ARMAMENT GROUP		4500
FURN. & EQUIP. GROUP		(INCLUDES 1500 LB OF AVIONICS)
ACCOM. FOR PERSON.		
MISC. EQUIPMENT		
FURNISHINGS		
EMERG. EQUIPMENT		
AIR CONDITIONING		
ANTI-ICING GROUP		
LOAD AND HANDLING GP.		
OTHER (ARMOR & MISSION KIT)		1400
WEIGHT EMPTY		33877 LB
CREW (2)		470
TRAPPED LIQUIDS		64
ENGINE OIL		54
PAYLOAD		6000
FUEL		10945
GROSS WEIGHT		51406 LB

Figure B-1. MIL-STD-1374 Weight Summaries

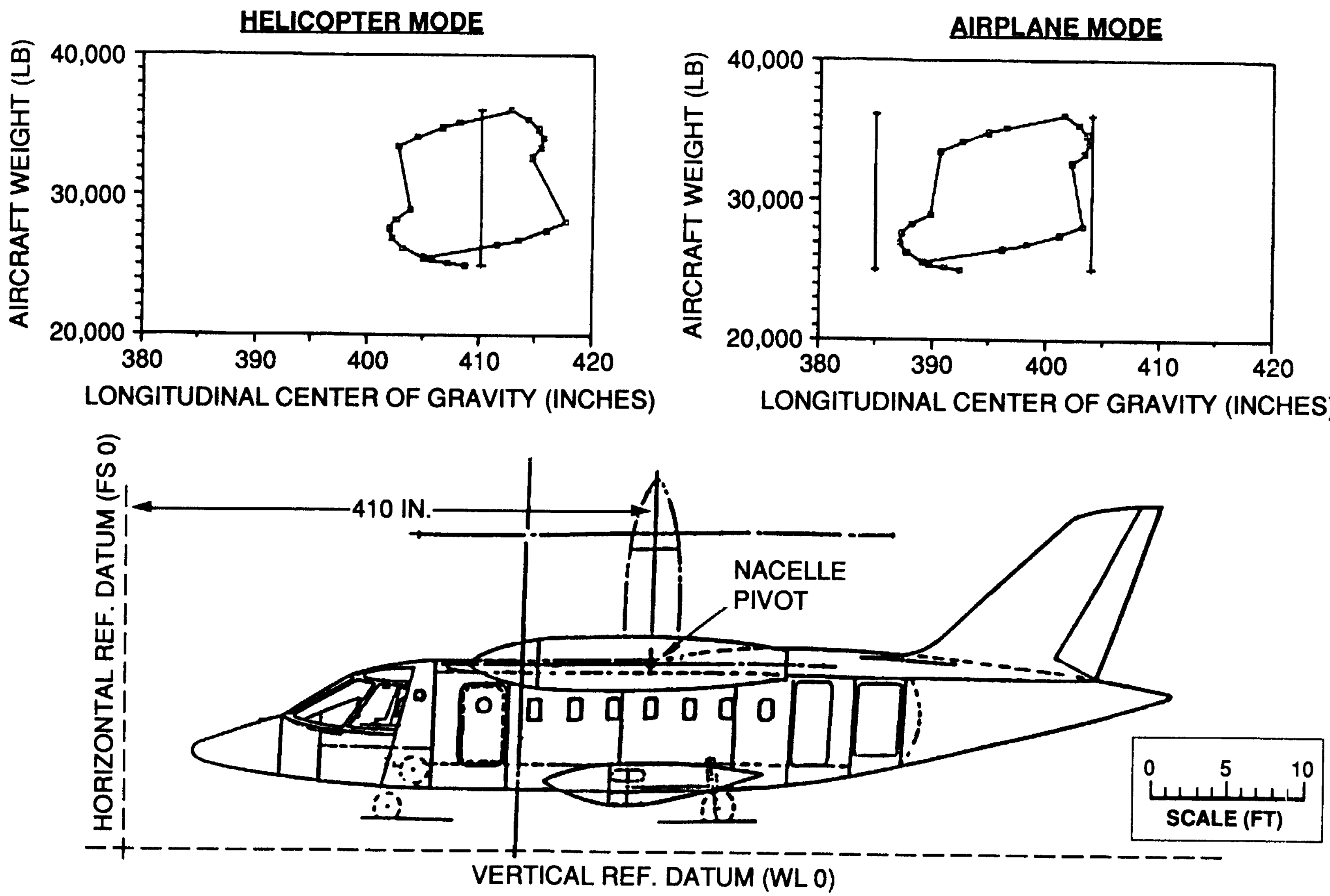

Figure B-2. Civil Tiltrotor Weight and CG Diagram

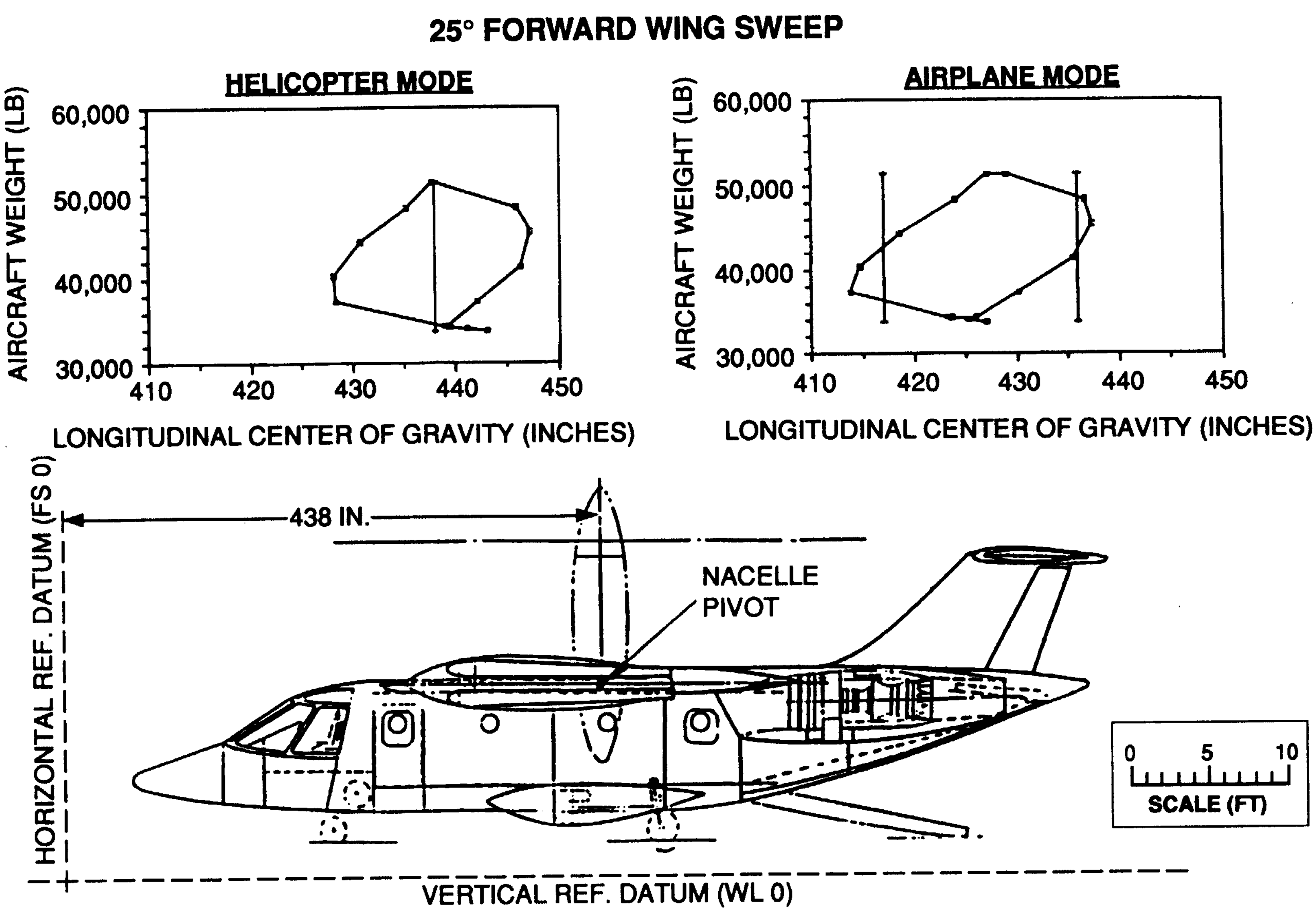

Figure B-3. Foding Tiltrotor Weight and CG Diagram

Table B-1. Civil Tiltrotor Mass Properties

CONFIGURATION	MISSION GW (LB)	BALANCE (IN.) F.S.	B.L.	W.L.	MOMENTS OF INERTIA (SLUG-FT^2) I_{XX} (ROLL)	I_{YY} (PITCH)	I_{ZZ} (YAW)
HELICOPTER MODE - NACELLES VERTICAL - LANDING GEAR DOWN	38380	410.0	0	122.4	224069	97550	261238
AIRPLANE MODE - NACELLES HORIZONTAL - LANDING GEAR UP	38380	401.0	0	110.8	210012	89344	267083

Table B-2. Military Folding Tiltrotor Mass Properties

CONFIGURATION	MISSION GW (LB)	BALANCE (IN.) F.S.	B.L.	W.L.	MOMENTS OF INERTIA (SLUG-FT^2) I_{XX} (ROLL)	I_{YY} (PITCH)	I_{ZZ} (YAW)
HELICOPTER MODE - NACELLES VERTICAL - LANDING GEAR DOWN	51406	438.0	0	136.0	310211	151082	414473
AIRPLANE MODE - NACELLES HORIZONTAL - LANDING GEAR UP - BLADES - NORMAL	51406	426.4	0	129.9	299538	149116	423178
BLADES - FOLDED	51406	427.6	0	129.9	299538	147625	418946

Weight trade studies leading to the selection of the military configuration was accomplished using the VASCOMP program. The program divides the weight empty into three groups: propulsion, structures and flight controls. Weight trends are programmed for each group which compute their respective weights. These are then combined with weight input values of fixed useful load, fixed equipment and payload to determine the weight of the fuel available for a given gross weight and payload.

The weight trends were developed at Boeing from statistical and semianalytical data of existing aircraft. They combine geometric, design and structural parameters into an accurate weight prediction tool. Examples of the weight trends and their associated component weight technology factors for the 1990 and 2000 year time frame are included in the main text. Contract specified "fixed weights" are defined in Table B-3. A summary of wetted areas and frontal areas for the two configurations is shown in Table B-4.

Downwash Characteristics

The high-speed civil tiltrotor and the military folding tiltrotor have similar geometry and both have 25-psf disc loadings in hover. Thus, their downwash characteristic are similar in character,

Table B-3. High-Speed Rotorcraft Fixed Weights

	MILITARY TRANSPORT (LB)	CIVIL TRANSPORT (LB)
Payload	6000	6000
Fixed Equipment	3000	4000
Mission Kit	1000	–
Avionics	1500	800
Armor	400	–
Fixed Useful Load	470	625

GW = STRUCTURE + PROPULSION + CONTROLS + FIXED EQUIPMENT*
+ FIXED USEFUL LOAD* + FUEL + PAYLOAD*

* CONTRACT SPECIFIED

Table B-4. Wetted Areas and Frontal Areas

	HIGH-SPEED CIVIL TILTROTOR		MILITARY FOLDING TILTROTOR	
	THEOR. AREA OR FRONTAL AREA (FT^2)	EXPOSED WETTED AREA (FT^2)	THEOR. AREA OR FRONTAL AREA (FT^2)	EXPOSED WETTED AREA (FT^2)
WING	384	602	570	1060
CANARD	84	136	80	130
HORIZONTAL TAIL			125	240
VERTICAL TAIL			120	245
V-TAILS	165	306		
FUSELAGE - LENGTH	63 FT		60.5 FT	
- MAX. DIAM.	9.08 FT		8 FT	
- AREAS	64.8	1336 ①	50	1140
LANDING GEAR FAIRINGS	4.5 EACH	168	5.5 EACH	200
TIP PODS, PYLONS AND SPINNERS	10.6 EACH	340	11.3 EACH	340
ENGINE NACELLES		166		255
TOTAL WETTED AREA		3046		3610

① INCLUDES VEHUDIE AND BODY FLAP

but are different in magnitude due to their different rotor diameters. Figure B-4 shows the typical hover downwash environment for a tiltrotor. The region under the fuselage is subject to unsteady flow with substantial mixing between the two rotor downwash fields and interaction with the underside of the fuselage and wing. The outboard regions to either side of the wing typically exhibit steady flow patterns with predictable outwash velocity profiles. A steady, predictable flow is also characteristic of the fore and aft regions where the dual rotor downwash patterns join together, increasing the total outwash momentum.

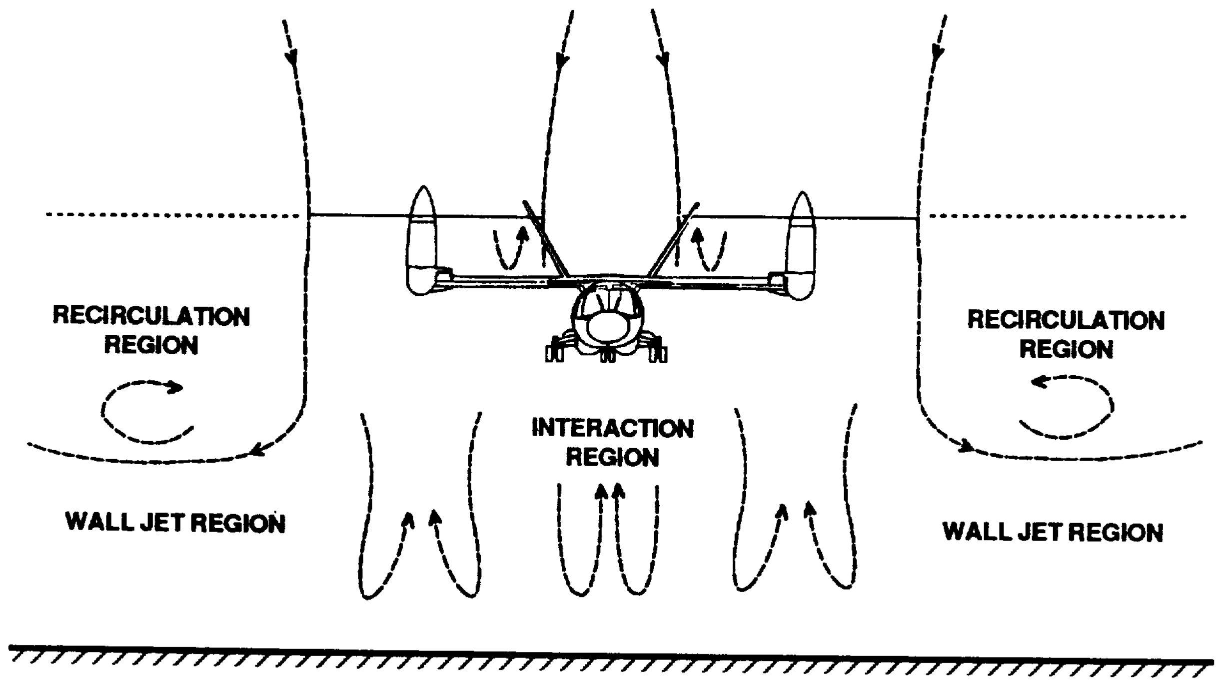

Figure B-4. Tiltrotor Hover Downwash Environment in Ground Effect

The method of Reference B-1 was used to estimate the outwash velocities. The method's prediction was correlated with flight test measured data for the CH-53E and for the XV-15 taken from Reference B-2. Results from this correlation are shown in Figure B-5. The agreement is quite good for these two aircraft, both at a 25-foot wheel height hover.

Figure B-6 shows predicted outwash to the front of the high-speed civil tiltrotor at a 25-foot wheel height. The top plot shows the maximum dynamic pressure and the maximum velocity along the ground, both dropping off with increasing longitudinal distance from the rotors' centerline of rotation. The bottom plots show the wall jet profile, outwash velocity as a function of height above ground, at selected distances from the rotor centerline; 60-ft, 100-ft, 140-ft, and 180-ft. At 60-ft in front of the rotors the wall jet has a peak velocity of about 46 knots, but drops below 20 knots above 8-ft. At 140-ft in front of the rotors the wall jet peak velocity has dropped down to only 20-knots, but has become much thicker. Figure B-7 shows similar predictions for outwash to the side of the high-speed civil tiltrotor. The total momentum in the sideward direction is seen to be less than in the forward direction. This is evidenced by the lower overall height of the sideward profile, although the peak velocity is somewhat higher.

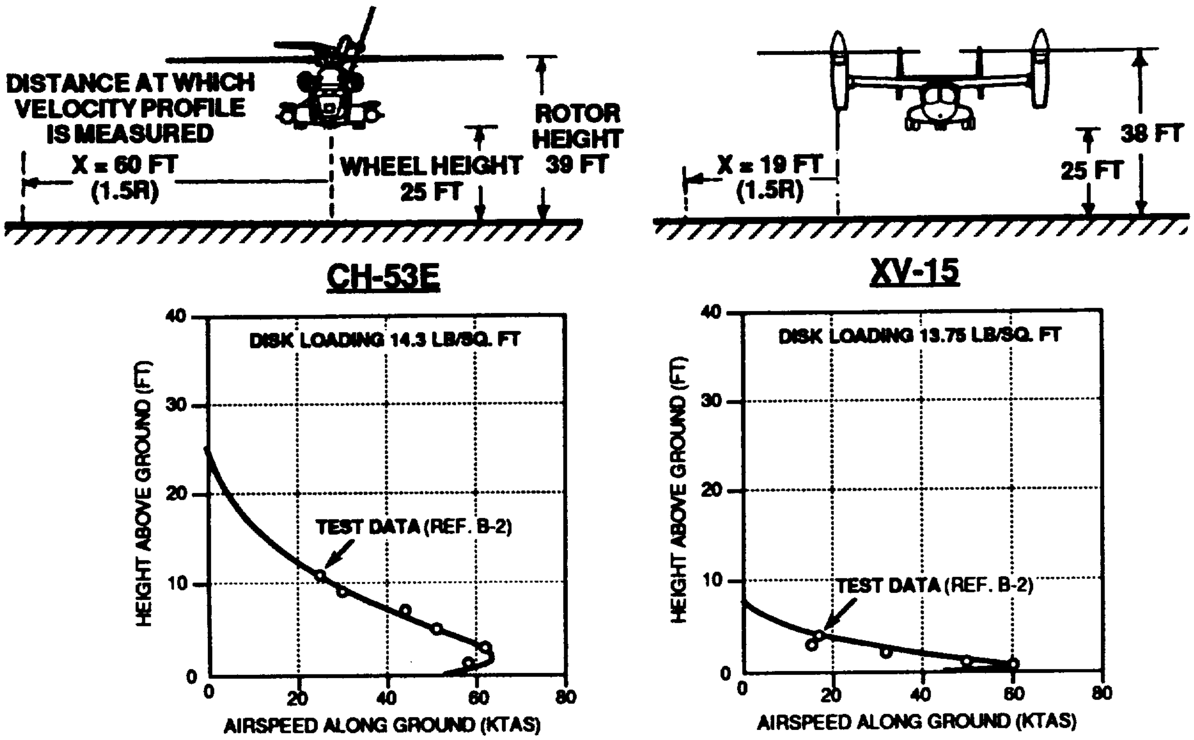

Figure B-5. Comparison of Outwash Calculations with Flight Test Measured Data

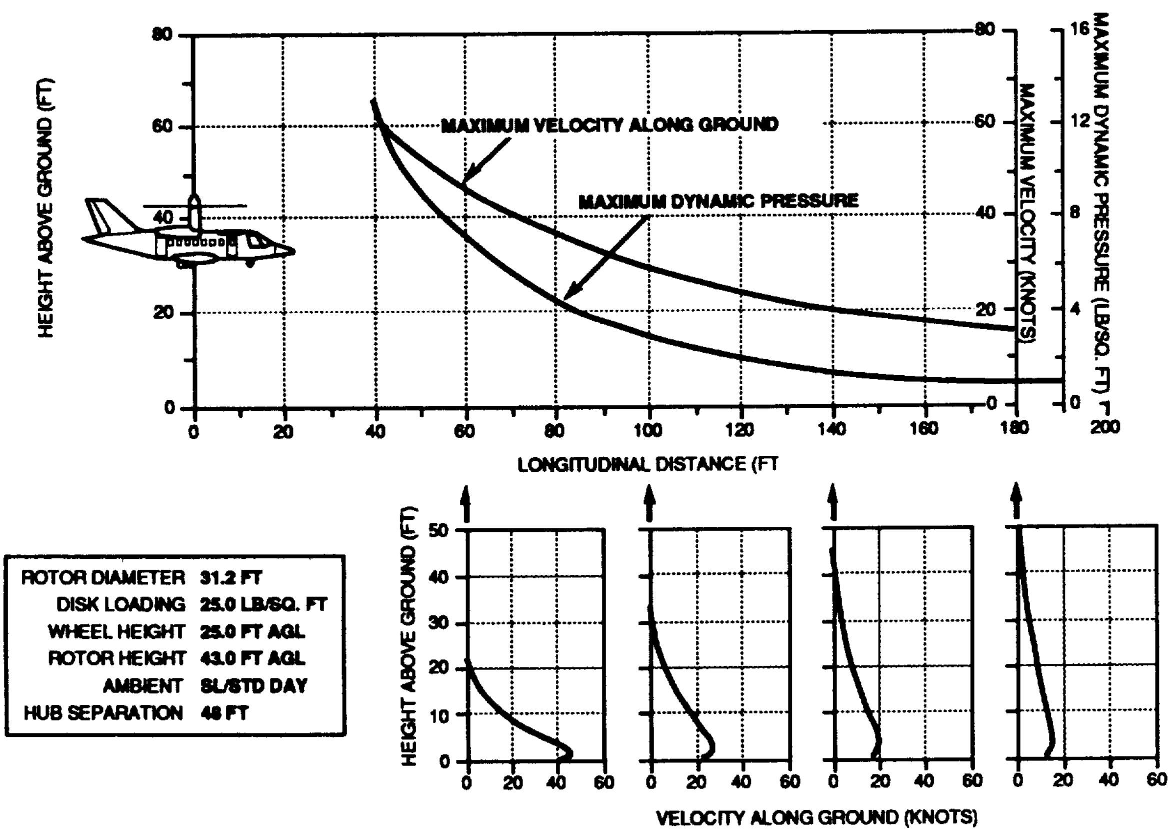

Figure B-6. Outwash Ahead of Aircraft Nose for Civil Tiltrotor

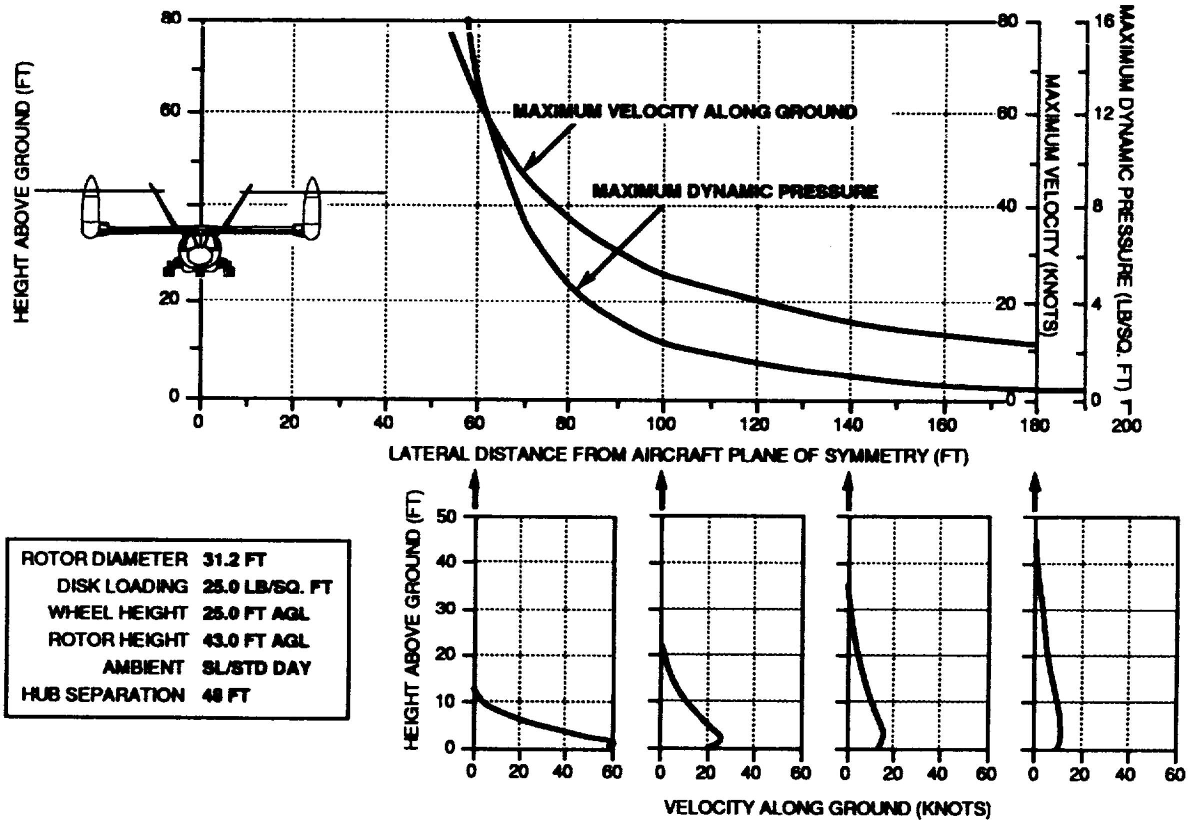

Figure B-7. Outwash Along Side of Aircraft for Civil Tiltrotor

Outwash characteristics for the military folding tiltrotor are shown in Figure B-8 in the forward direction and in Figure B-9 in the sideward direction. This rotor disc loading is the same as that of the civil tiltrotor, but the magnitude of the outwash velocities are much higher. There are two reasons for this. First, the military folding tiltrotor is larger and heavier, producing more rotor wake momentum. Secondly, the military folding tiltrotor is of larger diameter so a fixed distance from the centerline of rotation is actually closer to the rotor than in the case of the smaller civil tiltrotor. Comparison to the civil tiltrotor plots will confirm this effect.

VASCOMP Sizing Runs

Many VASCOMP sizing runs were made to conduct parametric trade-offs of wing loading, disc loading, wing thickness ratio and cruise altitude against vehicle gross weight. A printout from the VASCOMP II sizing run for each of the two selected optimum configurations is included for reference. A description of the VASCOMP II V/STOL sizing and performance computer analysis may be found in Reference B-3.

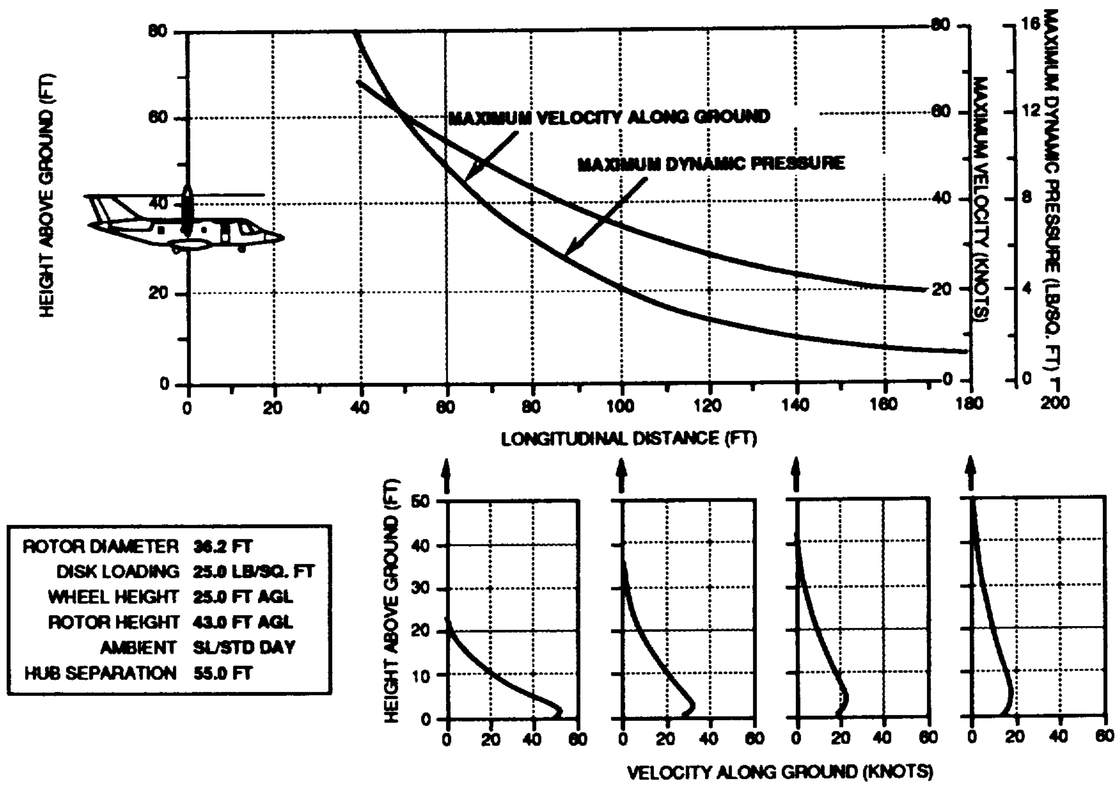

Figure B-8. Outwash Ahead of Aircraft Nose for Military Folding Tiltrotor

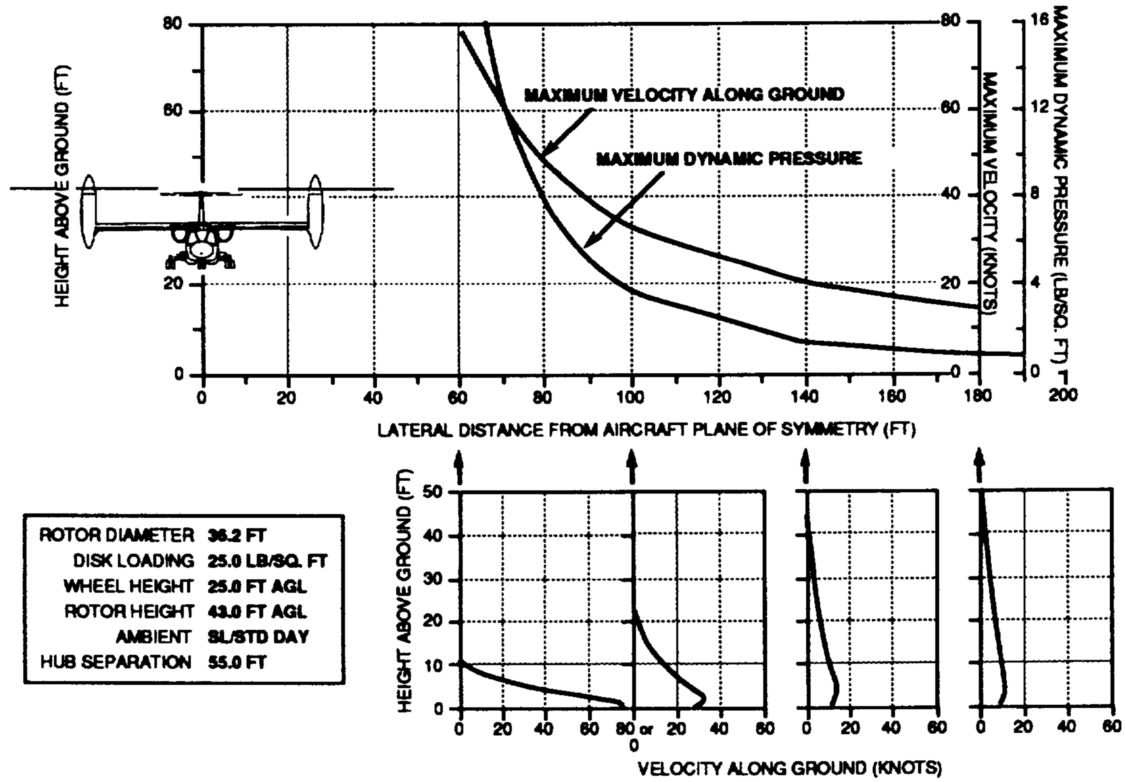

Figure B-9. Outwash Along Side of Aircraft for Military Folding Tiltrotor

Figures B-10 through B-12 show VASCOMP output for the high-speed civil tiltrotor. Figure B-10 shows the final size, the geometric properties and the weight breakdown. Figure B-11 shows the propulsion system installed power, transmission rating, transmission efficiency, accessory power allowance in cruise, and effective flat plate area. Figure B-12 shows the mission performance for each leg of the NASA specified civil transport mission. The second leg of the mission, 180-knot cruise for 30 seconds, is an allowance for conversion from the helicopter mode to the airplane mode.

```
          CTRS CIVIL BASELINE  W/S - 100  W/A - 25    Vmax=450 @ MRP 25000 ft 25k  PAGE   2

                                   V A S C O M P  II
             V/STOL AIRCRAFT SIZING & PERFORMANCE COMPUTER PROGRAM  B-93

S I Z E   D A T A  THIS RUN CONVERGED IN  6 ITERATIONS
                                  GROSS WEIGHT -  38380. LBS
       FUSELAGE
          LF             LENGTH                              63.0     FT
          WF             WIDTH                            [illegible] FT
          SF             WETTED AREA                       1305.      SQFT
       WING
          AR             ASPECT RATIO                       6.07
          SW             AREA                             [illegible] SQFT
          B              SPAN                             [illegible] FT
          CBARW          GEOM. MEAN CHORD                 [illegible] FT
          LAMBDA C/4     QUARTER CHORD SWEEP              -30.0      DEG
          LAMBDA         TAPER RATIO                        1.000
          (T/C)R         ROOT THICKNESS                     0.160
          (T/C)T         TIP THICKNESS                      0.160
          WG/SW          WING LOADING                     100.0      LB/SQFT
          C BAR / D      MEAN CHORD / PROP. DIA.            0.254
       HOR. TAIL
          ARHT           ASPECT RATIO                       2.30
          SHT            AREA                               81.5     SQFT
          BHT            SPAN                               13.7     FT
          CBARHT         MEAN CHORD                       [illegible] FT
          (T/C)HT        THICKNESS / CHORD                  0.120
          LTH            MOMENT ARM                         10.0     FT
          VBARH          VOLUME COEF.                       0.267
       VERT. TAIL
          ARVT           ASPECT RATIO                       1.25
          SVT            AREA                               79.3     SQFT
          BVT            SPAN                               10.0     FT
          CBARVT         MEAN CHORD                       [illegible] FT
          (T/C)VT        THICKNESS / CHORD                  0.090
          LTV            MOMENT ARM                         28.0     FT
          VBARV          VOLUME COEF.                       0.120
       PRIMARY ENG. NACELLE
          LN             LENGTH                             14.0     FT
          DBARN          MEAN DIAMETER                       4.7     FT
          SN             WETTED AREA                       409.7     SQFT
       LIFT ENG. NACELLE
                         NO LIFT PROPULSION SELECTED
       PROPELLER
          D              DIAMETER                           31.3     FT
          SIGMA R/P      SOLIDITY                           0.167
          WG/A           DISC LOADING                       25.0     LB/SQFT
          CT/SIGMA       THRUST COEFF. / SOLIDITY           0.128
          NR             NO. OF PROPELLERS                  2.000
          NO. BLADES     NO. OF BLADES/PROP                 4.000
          SR             BLADE CUTOUT / RADIUS RATIO        0.090
          F              TIPSPEED                          750.0     FT/SEC

          CTRS CIVIL BASELINE  W/S - 100  W/A - 25    Vmax=450 @ MRP 25000 ft 25k  PAGE   3

                                   V A S C O M P  II
             V/STOL AIRCRAFT SIZING & PERFORMANCE COMPUTER PROGRAM  B-93
W E I G H T S   D A T A    IN LBS
          NMLF           MANEUVER LOAD FACTOR               2.500
          GLF            GUST LOAD     FACTOR             [illegible]
          ULF            ULTIMATE LOAD FACTOR               3.750
       STRUCTURES GROUP
          K8   WW        WING                              1660.
          K9   WHT       HOR. TAIL                        [illegible]
          K10  WVT       VERT. TAIL                       [illegible]
          K11  WB        FUSELAGE                         [illegible]
          K12  WLG       LANDING GEAR                      1380.
          K13  WLES      LIFT ENGINE SECTION                  0.
          K14  WPES      PRIMARY ENGINE SECTION             630.
               WTREAT    PRIMARY ENGINE ACOUSTIC TREAT.       0.
          DELTA WST      STRUCTURE WEIGHT INCREMENT        1167.
          WST            TOTAL STRUCTURE WEIGHT            9427.
       PROPULSION GROUP
          K2   WR/P      ROTOR OR PROP                     2230.
          K3   WDS       DRIVE SYSTEM                      3571.
          K4   WEL       LIFT ENGINES                         0.
          K5   WEP       PRIMARY ENGINES                   2520.
          K6   WLEI      LIFT ENGINE INSTALLATION             0.
          K7   WPEI      PRIMARY ENGINE INSTALLATION        428.
          K21  WFS       FUEL SYSTEM                        397.
          DELTA WP       PROPULSION GROUP WEIGHT INCREMENT   60.
          WP             TOTAL PROPULSION GROUP WEIGHT     9205.
       FLIGHT CONTROLS GROUP
          K15  WCC       COCKPIT CONTROLS                   107.
          K16  WUC       UPPER   CONTROLS                 [illegible]
          K17  WH        HYDRAULICS                         450.
          K18  WFW       FIXED WING CONTROLS              [illegible]
          K19  WSAS      SAS                                400.
          K20  WTM       TILT MECHANISM                     960.
          DELTA WFC      CONTROL WEIGHT INCREMENT             0.
          WFC            TOTAL CONTROL WEIGHT              2978.
       WFE               WEIGHT OF FIXED EQUIPMENT         4800.
       WE                WEIGHT EMPTY                     26414.
       WFUL              FIXED USEFUL LOAD                  740.
       OWE               OPERATING WEIGHT EMPTY           27154.
       WPL               PAYLOAD                           6000.
       (WF)A             FUEL                              5226.          (WF)W            5226.
       WG                GROSS WEIGHT                     38380.
```

Figure B-10. VASCOMP II Sizing and Weight Data Output for Civil Tiltrotor

```
    CTRS CIVIL BASELINE  W/S = 100  W/A = 25    Vmax=450 @ MRP 25000 ft 25k  PAGE   4

                                   V A S C O M P  II
        V/STOL AIRCRAFT SIZING & PERFORMANCE COMPUTER PROGRAM  B-93

P R O P U L S I O N   D A T A
        PRIMARY PROPULSION CYCLE NO.     8.888
                 TURBOSHAFT ENGINE

             2.  ENGINES

          BHP*P            MAX. STANDARD S.L. STATIC H.P.          17357.     H.P.     POWER LOADING = 0.4522

          ENGINE SIZED FOR CRUISE AT VC = 450. KNOTS,
          HC = 25000. FT, TEMPERATURE =  -3.13 DEG F.

        ACCESSORY HORSEPOWER EXTRACTED =  300.00  H.P.

        NO LIFT ENGINE CYCLE SELECTED

        POWER REQUIRED TO HOVER IS WITHIN 1 PERCENT OF
        CRUISE POWER REQUIRED AT DESIGN CONDITIONS

        XMSN SIZED AT  100. PERCENT OF ROTOR HOVER POWER REQUIRED
        AT H=     0. FT,TEMP= 86.02 DEG.F., 79.8  PERCENT HOVER RPM

        XMSN RATED AT      8535.5 HP

        TRANSMISSION EFFICIENCY = 0.9800


    CTRS CIVIL BASELINE  W/S = 100  W/A = 25    Vmax=450 @ MRP 25000 ft 25k  PAGE   5

                                   V A S C O M P  II
        V/STOL AIRCRAFT SIZING & PERFORMANCE COMPUTER PROGRAM  B-93

A E R O D Y N A M I C S   D A T A
          FE               TOTAL EFFECTIVE FLATPLATE AREA          11.797     SQFT
          SWET             TOTAL WETTED AREA                        2733.     SQFT
          CBARF            MEAN SKIN FRICTION COEFF.            0.004317

D R A G   B R E A K D O W N         IN  SQFT
          FEW              WING FE                                -0.055
          FEF              FUSELAGE FE                             7.576
          FEVT             VERT. TAIL FE                           0.000
          FEHT             HOR.  TAIL FE                           0.000
          FEN              PRIMARY ENG. NACELLE FE                 0.000
          FELN             LIFT ENG. NACELLE FE                    0.000
          DELTA FE         INCREMENTAL FE                          4.276

A E R O D Y N A M I C   C O E F F .
          A5                                                     0.03088
          A6                                                     1.42442
          A7                                                     0.06365
          CL ALPHA         3-D LIFT SLOPE                        4.44036      PER RADIAN
```

Figure B-11. VASCOMP II Propulsion and Aerodynamic Data Output for Civil Tiltrotor

CTRS CIVIL BASELINE W/S = 100 W/A = 25 Vmax=450 @ MRP 25000 ft 25k PAGE 6

V A S C O M P II
V/STOL AIRCRAFT SIZING & PERFORMANCE COMPUTER PROGRAM B-93
MISSION PERFORMANCE DATA

TAKEOFF, HOVER, OR LAND AT T/W = 1.090 FOR 0.017 HRS.
VERTICAL RATE OF CLIMB = 0.0 FT/MIN TEMPERATURE = 86.0 DEG.F

TIME (HRS)	RANGE (N.M.)	FUEL USED (LBS)	WEIGHT (LBS.)	PRES. ALT. (FT)	TAS (KTS)	TURB. TEMP. (R)	ENG. CODE	PETF OR PEMP	LETF	THRUST TO WEIGHT	FM	BMP	CT	VTIP (FPS)
0.000 / 0.017	0.00 / 0.00	0.0 / 69.0	38380. / 38311.	0.	0.0	1785.1	P	0.304	0.000	1.090	0.758	8233. / 8228.	0.0214	750.

CAUTION, STATIC THRUST NOT INCLUDED IN PROP DECK, LOWEST ADVANCE RATIO USED

CRUISE AT 100.0 KNOTS TAS, LIMITED BY NORMAL ENGINE RATING TEMPERATURE = 86.0 DEG.F

TIME (HRS) / CL	RANGE (N.M.) / CD	FUEL USED (LBS) / L/D	WEIGHT (LBS.) / LIFT (LBS)	PRES. ALT. (FT) / DRAG (LBS)	TAS (KTS) / FUEL FLOW (LBS/HR)	TURB. TEMP. (R) / BMP	ENG. CODE	PETF OR PEMP / THRUST (LBS)	EAS / CP	MACH / CT	MACH DIV / J	SPEC. RANGE (NMPP) / VTIP (FPS)	ETAP PROP
0.017 / 0.956	0.00 / 0.0697	69.0 / 10.653	38311. / 38311.	0. / 3596.	100.0 / 2437.	1617.9 / 3633.	P	0.323 / 3920.	175.5 / 0.0026	0.265 / 0.0031	0.000 / 0.507	0.07387 / 600.0	0.609
0.027 / 0.956	1.00 / 0.0697	82.5 / 10.654	38298. / 38298.	0. / 3595.	100.0 / 2436.	1617.9 / 3632.	P	0.323 / 3918.	175.5 / 0.0026	0.265 / 0.0031	0.000 / 0.507	0.07388 / 600.0	0.609

CLIMB TO 25000. FT. WITH MAXIMUM R/C AT NORMAL ENGINE RATING

TIME (HRS) / CL	RANGE (N.M.) / CD	FUEL USED (LBS) / L/D	WEIGHT (LBS.) / LIFT (LBS)	PRES. ALT. (FT) / DRAG (LBS)	TAS (KTS) / FUEL FLOW (LBS/HR)	TURB. TEMP. (R) / BMP	ENG. CODE	PETF OR PEMP / THRUST (LBS)	EAS / CP	MACH / CT	MACH DIV / J	GAMMA (DEG) / VTIP (FPS)	THETA -P (DEG) / ETAP	R/C (FPM)
0.027 / 1.293	1.00 / 0.1485	82.5 / 8.860	38298. / 38085.	0. / 4328.	134.3 / 3004.	1679.9 / 5244.	P	0.374 / 9645.	150.4 / 0.0030	0.227 / 0.0072	0.000 / 0.434	6.3 / 600.0	20.0 / 0.834	1719.
0.071 / 1.305	8.44 / 0.1502	229.2 / 8.690	38152. / 37932.	5000. / 4365.	165.3 / 2892.	1671.6 / 5542.	P	0.385 / 9868.	149.4 / 0.0046	0.248 / 0.0084	0.000 / 0.465	6.2 / 600.0	20.0 / 0.847	1795.
0.117 / 1.318	16.07 / 0.1537	362.5 / 8.575	38018. / 37818.	10000. / 4409.	177.6 / 2615.	1675.4 / 5829.	P	0.472 / 9990.	148.5 / 0.0057	0.271 / 0.0098	0.000 / 0.500	6.0 / 600.0	20.0 / 0.850	1880.
0.161 / 1.322	23.31 / 0.1524	487.3 / 8.672	37893. / 37685.	15000. / 4346.	191.9 / 4123.	1938.8 / 9789.	P	0.964 / 11596.	148.8 / 0.0113	0.298 / 0.0148	0.000 / 0.548	5.9 / 600.0	20.0 / 0.712	2013.
0.203 / 1.322	31.82 / 0.1555	658.0 / 8.460	37722. / 37520.	20000. / 4424.	208.3 / 3455.	1930.1 / 8302.	C	1.000 / 9853.	147.7 / 0.0113	0.329 / 0.0149	0.000 / 0.588	5.9 / 600.0	20.0 / 0.775	2105.
0.241 / 1.324	39.73 / 0.1560	789.8 / 8.338	37590. / 37451.	25000. / 4492.	227.1 / 2760.	1861.6 / 6745.	C	1.000 / 6339.	147.4 / 0.0109	0.366 / 0.0151	0.000 / 0.639	4.9 / 600.0	19.0 / 0.879	1979.

CRUISE AT 450.0 KNOTS TAS, LIMITED BY NORMAL ENGINE RATING TEMPERATURE = -3.1 DEG.F

TIME (HRS) / CL	RANGE (N.M.) / CD	FUEL USED (LBS) / L/D	WEIGHT (LBS.) / LIFT (LBS)	PRES. ALT. (FT) / DRAG (LBS)	TAS (KTS) / FUEL FLOW (LBS/HR)	TURB. TEMP. (R) / BMP	ENG. CODE	PETF OR PEMP / THRUST (LBS)	EAS / CP	MACH / CT	MACH DIV / J	SPEC. RANGE (NMPP) / VTIP (FPS)	ETAP PROP
0.241 / 0.338	39.73 / 0.0345	789.8 / 9.158	37590. / 37590.	25000. / 4104.	450.0 / 3196.	1835.8 / 8335.	P	0.997 / 4296.	292.2 / 0.0137	0.735 / 0.0077	0.000 / 1.267	0.14086 / 600.0	0.712
0.373 / 0.333	100.00 / 0.0339	1211.4 / 9.165	37168. / 37168.	25000. / 4082.	450.0 / 3197.	1839.4 / 8351.	P	0.997 / 4233.	292.2 / 0.0136	0.735 / 0.0076	0.000 / 1.267	0.14301 / 600.0	0.711
0.597 / 0.326	200.00 / 0.0324	1913.5 / 9.013	36466. / 36466.	25000. / 4046.	450.0 / 3112.	1822.5 / 8331.	P	0.976 / 4197.	292.2 / 0.0135	0.735 / 0.0076	0.000 / 1.267	0.14461 / 600.0	0.710
0.819 / 0.322	300.00 / 0.0321	2605.1 / 8.920	35775. / 35775.	25000. / 4011.	450.0 / 3082.	1815.8 / 8278.	P	0.963 / 4162.	292.2 / 0.0134	0.735 / 0.0075	0.000 / 1.267	0.14602 / 600.0	0.709
1.042 / 0.318	400.00 / 0.0358	3290.0 / 8.824	35090. / 35090.	25000. / 3977.	450.0 / 3057.	1810.4 / 8222.	P	0.953 / 4127.	292.2 / 0.0133	0.735 / 0.0075	0.000 / 1.267	0.14722 / 600.0	0.708
1.264 / 0.316	500.00 / 0.0355	3968.2 / 8.728	34411. / 34411.	25000. / 3943.	450.0 / 3034.	1806.0 / 8169.	P	0.951 / 4094.	292.2 / 0.0132	0.735 / 0.0075	0.000 / 1.267	0.14821 / 600.0	0.707
1.486 / 0.385	600.00 / 0.0355	4641.9 / 8.637	33736. / 33736.	25000. / 3911.	450.0 / 3021.	1802.7 / 8117.	P	0.950 / 4061.	292.2 / 0.0132	0.735 / 0.0075	0.000 / 1.267	0.14896 / 600.0	0.705

TRANSFER ALTITUDE TO 0. FT.

TIME (HRS)	RANGE (N.M.)	FUEL USED (LBS)	WEIGHT (LBS.)	PRES. ALT. (FT)
1.486	600.00 / 600.00	4641.9 / 4641.0	33736. / 33738.	25000. / 0.

TAKEOFF, HOVER, OR LAND AT T/W = 1.090 FOR 0.017 HRS.
VERTICAL RATE OF CLIMB = 0.0 FT/MIN TEMPERATURE = 86.0 DEG.F

TIME (HRS)	RANGE (N.M.)	FUEL USED (LBS)	WEIGHT (LBS.)	PRES. ALT. (FT)	TAS (KTS)	TURB. TEMP. (R)	ENG. CODE	PETF OR PEMP	LETF	THRUST TO WEIGHT	FM	BMP	CT	VTIP (FPS)
1.486 / 1.503	600.00 / 600.00	4641.0 / 4703.2	33738. / 33677.	0.	0.0	1729.9 / 1725.8	P	0.357 / 0.351	0.000	1.090	0.815 / 0.815	6326. / 6300.	0.0188 / 0.0188	750.

CAUTION, STATIC THRUST NOT INCLUDED IN PROP DECK, LOWEST ADVANCE RATIO USED

MISSION FUEL REQUIRED = 4703.20
RESERVE FUEL REQUIRED = 522.58
TOTAL FUEL REQUIRED = 5225.78

****

END OF SUCCESSFUL CASE

****

Figure B-12. VASCOMP II Mission Performance Output for Civil Tiltrotor

Figures B-13 through B-15 show VASCOMP output for the military folding tiltrotor in the same order as described above for the civil tiltrotor. Figure B-15 shows mission performance for each leg out and back of the NASA specified military transport mission.

```
FTR CASE 1  W/S = 90    W/A = 25    Vmax=450 @ MRP 25000 ft                PAGE  2

                                  V A S C O M P  II
          V/STOL AIRCRAFT SIZING & PERFORMANCE COMPUTER PROGRAM  B-93

S I Z E   D A T A   THIS RUN CONVERGED IN  4 ITERATIONS
                                GROSS WEIGHT =  51406. LBS
      FUSELAGE
         LF              LENGTH                                60.5    FT
         WF              WIDTH                                  8.0    FT
         SF              WETTED AREA                          1600.    SQFT
      WING
         AR              ASPECT RATIO                          5.33
         SW              AREA                                 571.2    SQFT
         B               SPAN                                  55.2    FT
         CBARW           GEOM. MEAN CHORD                      10.4    FT
         LAMBDA C/4      QUARTER CHORD SWEEP                  -30.0    DEG
         LAMBDA          TAPER RATIO                          0.900
         (T/C)R          ROOT THICKNESS                       0.150
         (T/C)T          TIP  THICKNESS                       0.150
         WG/SW           WING LOADING                          90.0    LB/SQFT
         C BAR / D       MEAN CHORD / PROP. DIA.              0.286
      HOR. TAIL
         ARHT            ASPECT RATIO                          3.60
         SHT             AREA                                 167.4    SQFT
         BHT             SPAN                                  24.5    FT
         CBARHT          MEAN CHORD                             7.5    FT
         (T/C)HT         THICKNESS / CHORD                    0.120
         LTH             MOMENT ARM                            20.4    FT
         VBARH           VOLUME COEF.                         0.577
      VERT. TAIL
         ARVT            ASPECT RATIO                          0.84
         SVT             AREA                                  73.1    SQFT
         BVT             SPAN                                   7.8    FT
         CBARVT          MEAN CHORD                             9.0    FT
         (T/C)VT         THICKNESS / CHORD                    0.090
         LTV             MOMENT ARM                            25.0    FT
         VBARV           VOLUME COEF.                         0.058
      PRIMARY ENG. NACELLE
         LN              LENGTH                                 0.0    FT
         DBARN           MEAN DIAMETER                          0.0    FT
         SN              WETTED AREA                            0.0    SQFT
      LIFT ENG. NACELLE
                         NO LIFT PROPULSION SELECTED
      PROPELLER
         D               DIAMETER                              36.2    FT
         SIGMA R/P       SOLIDITY                             0.122
         WG/A            DISC LOADING                          25.0    LB/SQFT
         CT/SIGMA        THRUST COEFF. / SOLIDITY             0.146
         NR              NO. OF PROPELLERS                    2.000
         NO. BLADES      NO. OF BLADES/PROP                   4.000
         SR              BLADE CUTOUT / RADIUS RATIO          0.090
         P               TIPSPEED                               0.0    FT/SEC

FTR CASE 1  W/S = 90    W/A = 25    Vmax=450 @ MRP 25000 ft                PAGE  3

                                  V A S C O M P  II
          V/STOL AIRCRAFT SIZING & PERFORMANCE COMPUTER PROGRAM  B-93
W E I G H T S   D A T A    IN LBS
         EMLF            MANEUVER LOAD FACTOR                 3.680
         GLF             GUST LOAD     FACTOR                 2.202
         ULF             ULTIMATE LOAD FACTOR                 5.520
      STRUCTURES GROUP
         K8  WW          WING                                 4019.
         K9  WHT         HOR. TAIL                             495.
         K10 WVT         VERT. TAIL                            217.
         K11 WB          FUSELAGE                             4296.
         K12 WLG         LANDING GEAR                         1511.
         K13 WLES        LIFT ENGINE SECTION                     0.
         K14 WPES        PRIMARY ENGINE SECTION                937.
             WPEAT       PRIMARY ENGINE ACOUSTIC TREAT.          0.
         DELTA WST       STRUCTURE WEIGHT INCREMENT           1400.
         WST             TOTAL STRUCTURE WEIGHT              12865.
      PROPULSION GROUP
         K2  WR/P        ROTOR OR PROP                        3077.
         K3  WDS         DRIVE SYSTEM                         3690.
         K4  WEL         LIFT ENGINES                            0.
         K5  WEP         PRIMARY ENGINES                      3747.
         K6  WLEI        LIFT ENGINE INSTALLATION                0.
         K7  WPEI        PRIMARY ENGINE INSTALLATION           749.
         K21 WFS         FUEL SYSTEM                          1560.
         DELTA WP        PROPULSION GROUP WEIGHT INCREMENT      75.
         WP              TOTAL PROPULSION GROUP WEIGHT       12898.
      FLIGHT CONTROLS GROUP
         K15 WCC         COCKPIT CONTROLS                      120.
         K16 WUC         UPPER   CONTROLS                      735.
         K17 WH          HYDRAULICS                            506.
         K18 WFW         FIXED WING CONTROLS                   568.
         K19 WSAS        SAS                                   400.
         K20 WTM         TILT MECHANISM                       1285.
         DELTA WFC       CONTROL WEIGHT INCREMENT                0.
         WFC             TOTAL CONTROL WEIGHT                 3613.
      WFE                WEIGHT OF FIXED EQUIPMENT            4500.
      WE                 WEIGHT EMPTY                        33877.
      WFUL               FIXED USEFUL LOAD                     584.
      OWE                OPERATING WEIGHT EMPTY              34461.
      WPL                PAYLOAD                              6000.
      (WF)A              FUEL                                10945.          (WF)W               10945.
      WG                 GROSS WEIGHT                        51406.
```

Figure B-13. VASCOMP II Sizing and Weight Data Output for Military Folding Tiltrotor

```
FTR CASE .  W/S = 90    W/A = 25    Vmax=450 @ MRP 25000 ft              PAGE   4

                                      V A S C O M P  II
      V/STOL AIRCRAFT SIZING & PERFORMANCE COMPUTER PROGRAM  B-93
P R O P U L S I O N  D A T A
    PRIMARY PROPULSION CYCLE NO.   10.111
            TURBOJET  ENGINE

        2.  ENGINES

      T*P          MAX. STANDARD S.L. STATIC THRUST        [illegible]    LB.    RATED T/W = 0.4452
      BHP*P        MAX. STANDARD S.L. STATIC S.P.          15570.    H.P.   POWER LOADING = 0.3029

      ENGINE SIZED FOR CRUISE AT VC = 450. KNOTS,
      HC = 25000. FT, TEMPERATURE =  -3.13 DEG F.

    ACCESSORY HORSEPOWER EXTRACTED =  300.00  H.P.

    NO LIFT ENGINE CYCLE SELECTED

    XMSN SIZED AT  100. PERCENT OF ROTOR HOVER POWER REQUIRED
    AT H=    0. FT,TEMP= [illegible] DEG.F.,100.0 PERCENT HOVER RPM

    XMSN RATED AT    10391.2 HP

    TRANSMISSION EFFICIENCY = 0.9000

FTR CASE 1  W/S = 90    W/A = 25    Vmax=450 @ MRP 25000 ft              PAGE   5

                                      V A S C O M P  II
      V/STOL AIRCRAFT SIZING & PERFORMANCE COMPUTER PROGRAM  B-93
A E R O D Y N A M I C S  D A T A
         FE          TOTAL EFFECTIVE FLATPLATE AREA            13.789    SQFT
         SWET        TOTAL WETTED AREA                         [illegible]  SQFT
         CBARF       MEAN SKIN FRICTION COEFF.               0.004396
D R A G  B R E A K D O W N       IN  SQFT
         [illegible] WING FE                                   -0.077
         [illegible] FUSELAGE FE                               [illegible]
         [illegible] VERT. TAIL FE                             [illegible]
         [illegible] HOR. TAIL FE                              [illegible]
         [illegible] PRIMARY ENG. NACELLE FE                   [illegible]
         [illegible] LIFT ENG. NACELLE FE                      [illegible]
         DELTA FE    INCREMENTAL FE                            [illegible]
A E R O D Y N A M I C  C O E F F .
         [illegible]                                           0.02428
         [illegible]                                           [illegible]
         [illegible]                                           [illegible]
         CL ALPHA    3-D LIFT SLOPE                            4.24120   PER RADIAN
```

Figure B-14. VASCOMP II Propulsion and Aerodynamic Data Output for Military Folding Tiltrotor

```
FTR CASE 1  W/S = 90    W/A = 25    Vmax=450 @ MRP 25000 ft              PAGE   6

                                      V A S C O M P  II
      V/STOL AIRCRAFT SIZING & PERFORMANCE COMPUTER PROGRAM  B-93
    MISSION PERFORMANCE DATA

TAKEOFF, HOVER, OR LAND AT  T/W = [illegible] FOR  0.017 MIN.
VERTICAL RATE OF CLIMB =    0.0 FT/MIN     TEMPERATURE =  86.0 DEG.F
[illegible]
CRUISE AT   200.0  KNOTS TAS, LIMITED BY  NORMAL   ENGINE RATING       TEMPERATURE =  86.0 DEG.F
[illegible]
CLIMB  TO 25000.  FT. WITH   MAXIMUM R/C  AT  NORMAL   ENGINE RATING
[illegible]                                                              2303.
[illegible]                                                              2150.
[illegible]                                                              1963.
[illegible]                                                              1765.
[illegible]                                                              1532.
[illegible]                                                              1206.
CRUISE AT   450.0  KNOTS TAS, LIMITED BY  NORMAL   ENGINE RATING       TEMPERATURE =  -3.1 DEG.F
 TIME     RANGE    FUEL     WEIGHT   PRES.    TAS     TURB.  ENG.  PCT   EAS    MACH   MACH   SPEC.    STAB
 (HRS)    (N.M.)   USED     (LBS.)   ALT.     (KTS)   TEMP.  CODE  OF           DIV    RANGE    PROP
                   (LBS)             (FT)             (R)          PRMP                 (NMPP)
 CL       CD       L/D      LIFT     DRAG     FUEL FLOW  BHP       THRUST CP     CT     J      VTIP
                            (LBS)    (LBS)    (LBS/HR)             (LBS)                       (FPS)
[illegible]                                                                              1.000
[illegible]                                                                              1.000
[illegible]                                                                              1.000
 0.778    300.00   3269.5   40136.   25000.   450.0  1010.0  P     0.952  292.2  0.725  0.000  0.12043  1.000
```

Figure B-15. VASCOMP II Mission Performance Output for for Military Folding Tiltrotor (Sheet 1 of 2)

ORIGINAL PAGE IS
OF POOR QUALITY

```
0.291     0.0206    10.196    40136.    4721.    3737.    0.    4721.  ****** ****** ******  790.3
[illegible]                                                                          1.000

TRANSFER ALTITUDE TO       0. FT.
 TIME,     RANGE,    FUEL USED,  WEIGHT    PRES. ALT.
 (HRS)     (N.M.)    (LBS)       (LBS.)    (FT)
[illegible]                                 25000.
CRUISE AT   200.0  KNOTS TAS, LIMITED BY  NORMAL  ENGINE RATING          TEMPERATURE -  86.0 DEG.F
 TIME,  RANGE,  FUEL USED,  WEIGHT  PRES. ALT.  TAS,  TURB. TEMP.  ENG. CODE  PCT OF POWER  EAS  MACH  MACH DIV  SPEC. RANGE  STAP FAIR
 CL     CD      L/D         LIFT,   DRAG,       FUEL FLOW  SHP    THRUST   CP   CT   J   VTIP,
[illegible]                      1542.  P  [illegible]                                1.000
[illegible]                      1542.  P  [illegible]                                1.000

TAKEOFF, HOVER, OR LAND AT  T/W = [illegible] FOR  0.250 HRS.   TEMPERATURE -  86.0 DEG.F
VERTICAL RATE OF CLIMB -  0.0 FT/MIN
 TIME,  RANGE,  FUEL USED,  WEIGHT  PRES. ALT.  TAS,  TURB. TEMP.  ENG. CODE  PCT OF POWER  LIFT  THRUST TO WEIGHT  FM  SHP  CT  VTIP,
[illegible]
LOITER  FOR  0.500 HRS.                          TEMPERATURE -  86.0 DEG.F
 TIME,  RANGE,  FUEL USED,  WEIGHT  PRES. ALT.  TAS,  TURB. TEMP.  ENG. CODE  PCT OF POWER  EAS  MACH  MACH DIV  FUEL FLOW (LB-HR)  STAP FAIR
 CL     CD      L/D         LIFT,   DRAG,       FUEL FLOW  SHP    THRUST   CP   CT   J   VTIP,   ETAP
[illegible]                      1500.  P  [illegible]
[illegible]                      1560.  P  [illegible]

CLIMB  TO 30000.  FT. WITH  MAXIMUM R/C  AT  NORMAL  ENGINE RATING
 TIME,  RANGE,  FUEL USED,  WEIGHT  PRES. ALT.  TAS,  TURB. TEMP.  ENG. CODE  PCT OF POWER  EAS  MACH  MACH DIV  GAMMA (DEG)  THETA (DEG)  R/C (FPM)
 CL     CD      L/D         LIFT,   DRAG,       FUEL FLOW  SHP    THRUST   CP   CT   J   VTIP,   ETAP
[illegible]                      1825.  T  [illegible]                 2909.
[illegible]                      1825.  T  [illegible]                 2757.
[illegible]                      1825.  T  [illegible]                 2554.
[illegible]                      1825.  T  [illegible]                 2344.
[illegible]                      1825.  T  [illegible]                 2101.
1.819     396.77    7691.9    43706.    25000.   [illegible]  1825.0  T  [illegible]   790.3   1.000   1750.
0.561     0.0442    12.699    43637.    3437.
[illegible]                      1707.  MI [illegible]                 1143.

CRUISE AT SPEED FOR 99 PER CENT BEST RANGE WITH HEADWIND OF   0.0 KNOTS      TEMPERATURE - -21.0 DEG.F
CRUISE-CLIMB AT CONSTANT W/DELTA = [illegible]
 TIME,  RANGE,  FUEL USED,  WEIGHT  PRES. ALT.  TAS,  TURB. TEMP.  ENG. CODE  PCT OF POWER  EAS  MACH  MACH DIV  SPEC. RANGE  STAP FAIR
 CL     CD      L/D         LIFT,   DRAG,       FUEL FLOW  SHP    THRUST   CP   CT   J   VTIP,
[illegible]                      1700.  P  [illegible]                 1.000
[illegible]                      1703.  P  [illegible]                 1.000
[illegible]                      1701.  P  [illegible]                 1.000
[illegible]                      1696.  P  [illegible]                 1.000
[illegible]                      1696.  P  [illegible]                 1.000

TRANSFER ALTITUDE TO       0. FT.
 TIME,     RANGE,    FUEL USED,  WEIGHT    PRES. ALT.
 (HRS)     (N.M.)    (LBS)       (LBS.)    (FT)
[illegible]                                 30000.
TAKEOFF, HOVER, OR LAND AT  T/W = [illegible] FOR  0.017 HRS.   TEMPERATURE -  86.0 DEG.F
VERTICAL RATE OF CLIMB -  0.0 FT/MIN
 TIME,  RANGE,  FUEL USED,  WEIGHT  PRES. ALT.  TAS,  TURB. TEMP.  ENG. CODE  PCT OF POWER  LIFT  THRUST TO WEIGHT  FM  SHP  CT  VTIP,
[illegible]

      MISSION FUEL REQUIRED = [illegible]
      TOTAL FUEL REQUIRED = [illegible]
******************************************************************************************

END OF SUCCESSFUL CASE

******************************************************************************************
```

Figure B-15. VASCOMP II Mission Performance Output for Military Folding Tiltrotor (Sheet 2 of 2)

Flight Control System

An assessment of the state-of-the-art technology for flight control of a high-speed tiltrotor aircraft indicates that an architecture similar to the developmental V-22 can be used. Modifications will be necessary in the areas of actuation, embedded software, electric and hydraulic power sources, and precise blade angle control. The use of fiber optic technology can be considered for implementation by the year 2000 time frame.

Flight Control Laws

A current technology high-speed rotorcraft would incorporate a digital fly-by-wire/light control system which offers a flexibility to the control law/handling qualities engineer unmatched by current mechanical control systems. The control laws designed for a high-speed rotorcraft would include features such as:

- Model following control laws
- High gain feedback to provide high levels of stability
- Automatic modes to reduce pilot workload
- Coupled flight director modes to provide IRF capability
- Structural load monitoring and alleviation
- Integrated flight control/propulsion controls to enhance maneuverability

Military Folding Tiltrotor

Model Following Control Laws - The inclusion of a "desired" aircraft command/response characteristic can be tailored to the flight condition or aircraft state. For instance, the V-22 control/response characteristics vary as the aircraft transitions from helicopter mode to airplane mode. During development, piloted simulation experiments can define the desirable characteristics for each flight regime and mission task element. Desirable features such as constant stick forge per "g" or maneuvering stability can be defined within this command model independent of the inherent characteristics of the airframe.

This feature of advanced control law concepts is especially applicable to the folding tiltrotor concept where the command/response features will dramatically vary as the rotorcraft transitions through the three flight conditions (helicopter, tiltrotor, and turbojet). This concept has been demonstrated in-flight on several programs including ADOCS and V-22. With proper simulation experiments to define requirements and refine the implementation, this portion of the control laws is considered low-risk.

High Gain Feedback - Relaxed stability design is often used to improve maneuverability. Good handling qualities characteristics of the airframe design are achieved through the use of highly reliable, high gain stability loops optimized for system stability and gust rejection. These loops dominate classical phugoid, dutch roll, spiral, and short period modes and provide desirable levels of stability without the penalties classically associated with larger stability surfaces.

In the region of flight where blade stow aerodynamics may induce undesirable flight characteristics or coupling tendencies, the high gain stabilization system will provide robust, tight flight path retention providing good handling qualities through the blade folding process.

Automatic Modes - Automatic switching within the digital control system is controlled by the control law logic. Complex algorithms are programmed to ensure that the pilot maintains proper control characteristics. This type of mode switching has been successfully demonstrated on ADOCS and V-22. It is a system requirement for a rotorcraft which flies through a wide range of flight conditions.

The automatic blade folding will be controlled by this logic. The logic to control the blade fold process can be defined to be a function of airspeed, altitude, maneuver or trim state, and even blade loads. Real time simulations will be required to define the details associated with the blade stow logic. This logic might be pilot initiated as long as specific condition were met; that is the aircraft was inside an approved conversion corridor. Once initiated, the folding sequence would be automatic unless stopped, or reversed, by the pilot. The digital computer allows for the design flexibility to accommodate each requirement.

Structural Loads Monitoring - High speed rotorcraft typically have flight envelope limits based on rotor or airframe loads limits. An active monitoring/limiting system allows pilot control to the boundaries of the operational flight envelope without unintentionally exceeding it. Several additional sensors may be required for this system depending on the selected configuration. For the military folding tiltrotor, the loads monitoring system may be interfaced with the blade folding system to restrict initiating blade folding at flight conditions which induce undesirable loads. In any case, for a military rotorcraft, loads monitoring and not limiting is suggested so the pilot retains the ability to overstress the airframe/rotor during periods where warranted.

Integrated Flight Control/Propulsion System - The advent of digital engine controls has enabled complex control laws to be defined which improve the integrated performance of the propulsion system and air vehicle. In addition to using this concept to provide control anticipation, control laws can be defined which provide decoupled responses using the propulsion system as an extra control device.

The integration of the fuel or engine control system and the flight control system is especially important for the folding tiltrotor where the engines will be required to convert from a turboshaft to a turbofan operation. During periods of transition, specific control law changes might be required to maintain a desired level of control margin and handling qualities.

Current technology systems such as the V-22 include interfaces between the FADEC and the FCS. Proposed systems such as the LH include numerous feed-forward compensation paths from the FCS to the FADEC. Other than in the area of engine conversion, the control law integration of the FCS and FADEC appears to be low-risk. The coordination of the FCS and FADEC during conversion however may be higher risk as the dynamics associated with this process are not well known.

High-Speed Civil Tiltrotor

The control laws for a civil tiltrotor are similar to those proposed above with the following exceptions:

Coupled Flight Director - A fully coupled flight director is included in the civil control system to provide the pilot the capability to fly missions in degraded visual environments without dramatically increasing workload. The flight director provides automatic modes such as:

- Way point to way point
- Automatic approach
- Automatic departure
- MLS/ILS Approach

There are no high risk areas associated with a commercial flight director.

Integrated Flight Control/Propulsion Systems - The FDC/FADEC interface for the commercial tiltrotor would be similar to that of the V-22. During high-speed flight, the engine/governor control laws are required to maintain thrust commands while the loads limiting system minimizes interconnect drive shaft and in-plane loads. In the helicopter mode used for low-speed flight, the control laws need to provide higher bandwidth for precise altitude control.

Structural Loads Limiting - In a civil application, active loads limiting is required to avoid inadvertent inputs which overstress dynamic components of the rotorcraft. In high-speed flight, a tiltrotor is especially susceptible to in-plane rotor loads which are proportional to pitch rate plus rate of flapping. An active loads suppression systems has been proposed

Automatic Modes - In a civil tiltrotor, automatic nacelle conversion is included to reduce pilot workload through the conversion corridor. Such a system provides protection from stalling the aircraft at the low-speed portion of the corridor and protection from overstressing the aircraft in the high-speed portion of the corridor. An autoconversion system has been developed for the V-22, so these control laws are felt to be low-risk.

System Architecture

The military and the civil high-speed rotorcraft were determined to have compatible flight control characteristics. Configuration differences, due to the distinct mission requirements, will be reflected in the details of control laws, actuator dynamics and level of component redundancy.

The high-speed tiltrotor Flight Control System (FCS) consist of primary and secondary devices and of electronic sensing and computing devices which in combination with the aircraft control surfaces enable the crew to control the flight path of the aircraft. The proposed implementation of this concept is presented in Figure B-16. This configuration provides Primary Flight Control System (PFCS) functions necessary for the safe operation of the aircraft, as well as Automatic Flight Control System (AFCS) functions required to effectively accomplish the respective missions. It is a fly-by-wire implementation, employing triplex in-line monitored sensors and computers, and is two-fail/operative with respect to sensing, computing, and flight-critical PFCS functions.

The level of redundancy due to the flight safety requirements would be designed to satisfy the applicable military and civilian specification for development, manufacturing and testing, emphasizing flight critical components.

A flight control system conceptual architecture for a high-speed tiltrotor is presented in Figure B-17. The state-of-the-art technology for the configuration shown has been assessed to be suitable for both the civilian and military aircraft. Special components, only necessary for the folding tiltrotor, are shown in shaded areas.

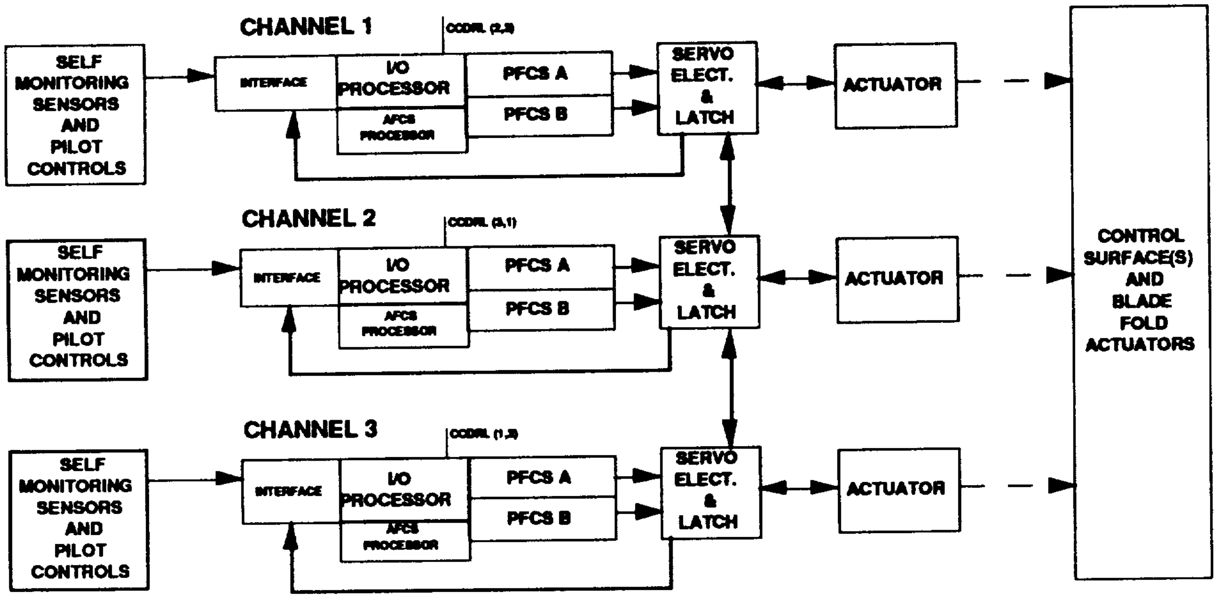

Figure B-16. High-Speed Civil Tiltrotor Flight Control System Schematic

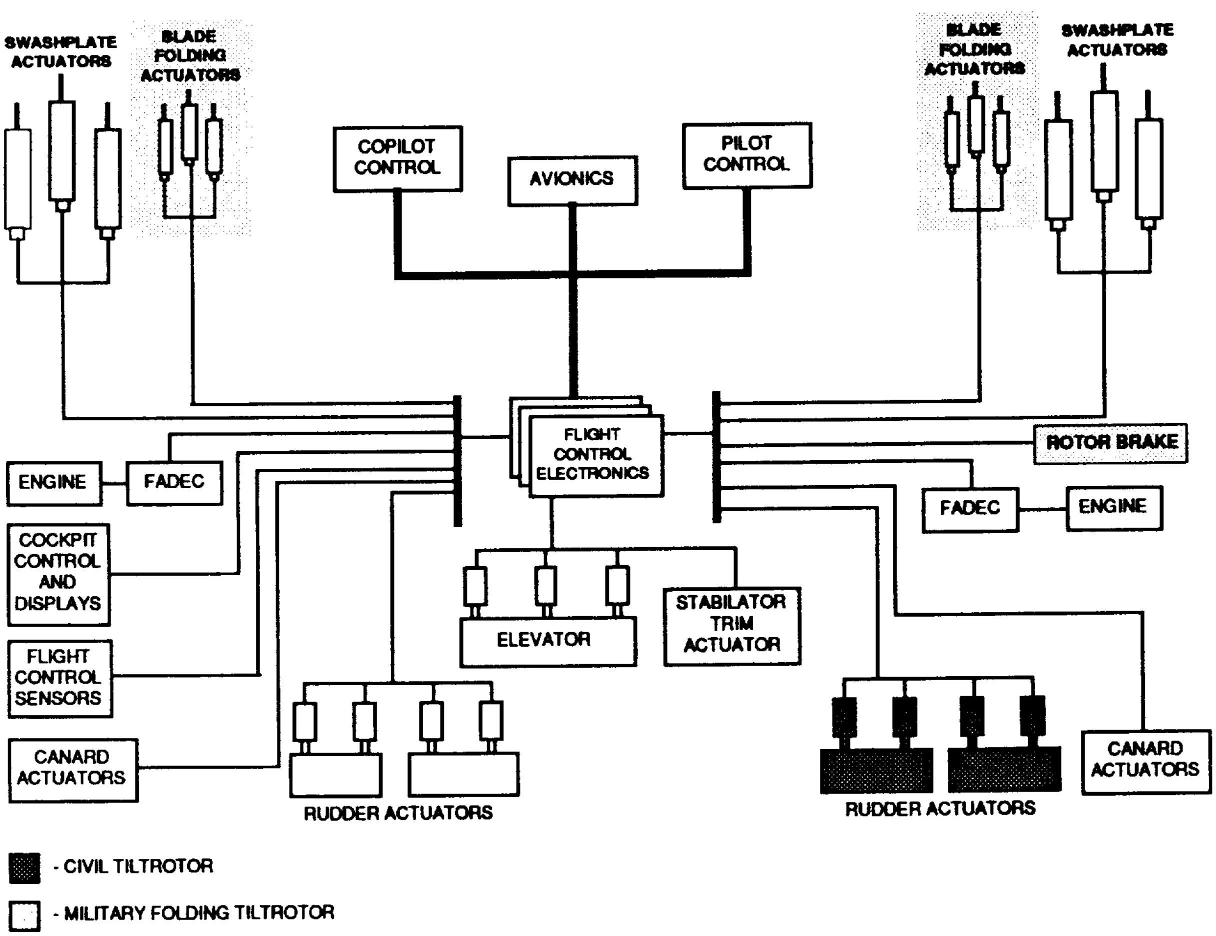

Figure B-17. Flight Control System Elements

Folding Tiltrotor

The folding tiltrotor aircraft requires the following automated additional capabilities:

1. Rotor slowdown,
2. Rotor stopping,
3. Blade folding and unfolding, and
4. Uninterrupted electrical and hydraulic power while stopping rotor

These functions are required to be performed in flight and during moderate levels of aircraft motion (i.e. maneuvers). Due to the flight critical issues of rotor slowdown, rotor stopping and blade folding functions, it is proposed that these processes have a two-fail/operate capability. These functions can be incorporated in the FCCs, or in electronic hardware units.

The system will be designed so that rotor slowdown can only be initiated by the pilot through a cockpit control panel. The sequence will require rotor blade feathering, convertible engine VIGV thrust control, rotor slowdown, rotor stop at a predetermined position through the use of a rotor brake, and blade folding and locking. The process will be reversible at any point during the conversion.

The kinematics of the swashplate due to rotor actuator displacement will be designed such that blade feathering is possible. Based on previous research performed on in-flight blade folding, unacceptable blade vibration or swashplate loads are not expected. However, wind tunnel testing of the nacelle and the rotor system needs to be performed to assess the load envelope for the blade folding sequence. The aircraft maneuver envelope for the blade stow transition also needs to be determined. If a condition of structural instability through the blade folding sequence is found, an adaptive control design can be implemented to stabilize blade pitching while transitioning.

Electric and Hydraulic Power - The typical rotorcraft approach to obtain electric and hydraulic power is to attach electric generators and hydraulic pumps onto the rotating system. In the event of engine failure(s), the rotating system will continue to be used for power generation until a backup system is engaged (e.g., an APU). Since the rotating system will be stopped on the folding tiltrotor configuration, the generator needs to be connected directly to the engine(s) to continue to have power while cruising at high speeds after blade folding.

Technology Risk Areas

The concept of a high-speed tiltrotor aircraft exhibits a flight control challenge in the areas of blade angle control sensitivity, dynamic control of differential balance of rotor blades, stability, and control of the rotor loads and vibration while spinning down and folding.

The resolution of the actuator feedback currently implemented on similar swashplate actuators cannot be utilized to accurately control differential rotor loads, blade flapping or blade angle on a high-speed rotorcraft. The large stroke of these actuators (about 19-inches), and the low resolution needed for their accurate control, less than 0.254-mm (0.01-inches), represents a problem due to the signal-to-noise ratio requirements. However, this area of risk can be resolved using current technology.

Areas of research related to flight controls encompass fiber optic technology, development of faster computers, development of software tools for code development, and improved testing techniques. For the military vehicle, wind tunnel research is needed to establish the maneuvering envelope while folding the blades during flight.

The development of the fiber optic technology, applied to flight controls and avionic systems for future generation aircraft is appropriate because of the large protection it provides against threats from lightning, EMI and EMP. Civil and military aircraft can benefit from this technology. The current level of technology does not permit full use of optics in flight critical areas because of unacceptable reliability, size, weight and cost.

The other area of technology that needs to continue to evolve is software development. Software generation costs are very high, and continue to increase. Software engineering practices need to address the issues of manufacturing costs and improvement of software estimation techniques for embedded code. Continued research and development related to software design testing maintenance, emphasizing flight critical computing, is also needed.

Research on the fault tolerant design area is needed to better understand and generate analytical tools to estimate the level of performability and safety of digital systems. The British government is currently investing heavily in the research of safety-critical software . Since the use of digital fly-by-wire technology in flight-critical control systems is becoming the state-of-the-art approach, research on developing the technology, for industry, is essential.

High-Speed Rotor System

Variable Diameter Considerations

The 450-knot variable diameter tiltrotor is caught in a design incompatibility. A 450-knot proprotor design requires thin airfoils to avoid drag divergence in cruise. This means about a 12% inboard airfoil and an 8% tip airfoil. But these thin sections are virtually incompatible with the dimensional requirements of the "double-structure" retractable blade and its screwjack system as depicted in Figure B-18.

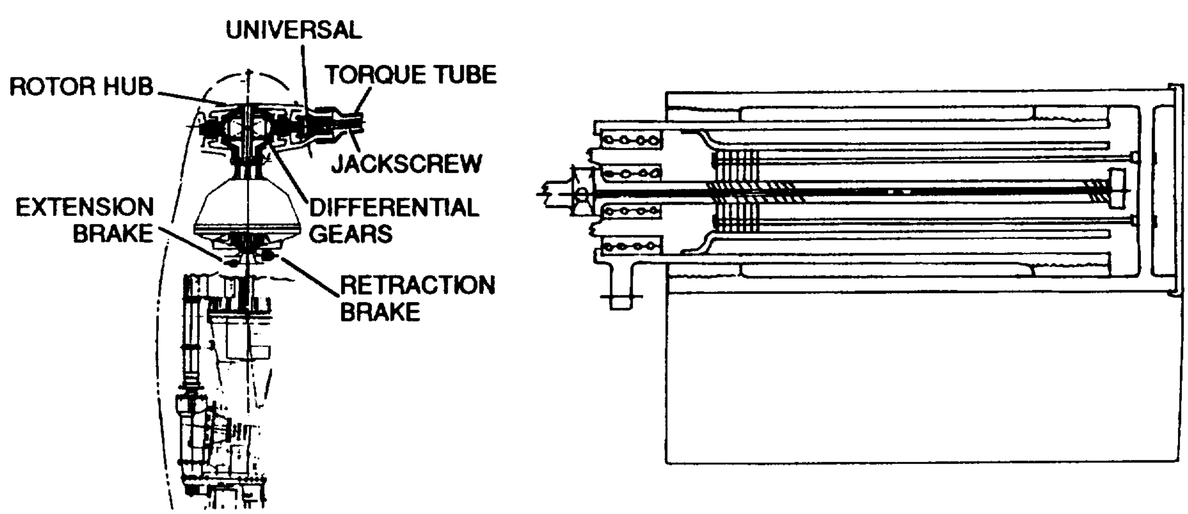

Figure B-18. Sample Arrangement for Variable Diameter Rotor

Time for retraction/extension is dependent on rotor rpm (shaft torque) to drive through hub gears to a jackscrew in the blade. Due to the low speed (300-400 rpm) of the rotor shaft, time to retract or extend the blades is in the range of 10-50 seconds (or more) depending on diameter, tip speed, and the details of the gear ratios, screw lead, number of threads, etc. This excessive time is not only important to the operational timing of assault aircraft launches or retrievals on carriers, but is questionable in any transition from the hover mode to fixed-wing flight. The typical tiltrotors continuous, smooth-flowing/high-acceleration transition and conversion must be interrupted when nearing 60° mast tilt to allow the rotor blade to retract (necessary for fuselage clearance) before continuing the transition; see Figure B-19. In addition, the increased power required resulting from the diameter reduction can increase the transmission rating (weight) or, conversely, result in a longer conversion time (at a higher speed).

This conversion-disconnect does not allow the low-speed conversion corridor and fast acceleration/deceleration that are major attributes of the tiltrotor.

Design requirements for a variable-diameter rotor using a geared jackscrew retraction system are not compatible with modern gimballed or flex beam/elastomeric rotor hub configurations. The concept is probably dependent on a rigid hub-to-shaft arrangement and is not very adaptable to elastomeric hinges in the flap/lag systems. Elastomeric bearing concepts severely increase in size (and weight) along with larger hub support structure. The rotor system complexity is increased drastically with reductions in reliability and increased maintenance actions for the internal (buried) gears, bearings, shafts, brakes, lubrication systems, actuators, etc.

As a consequence of these considerations, the variable diameter tiltrotor was dropped in favor of fixed diameter, advanced geometry swept blade design.

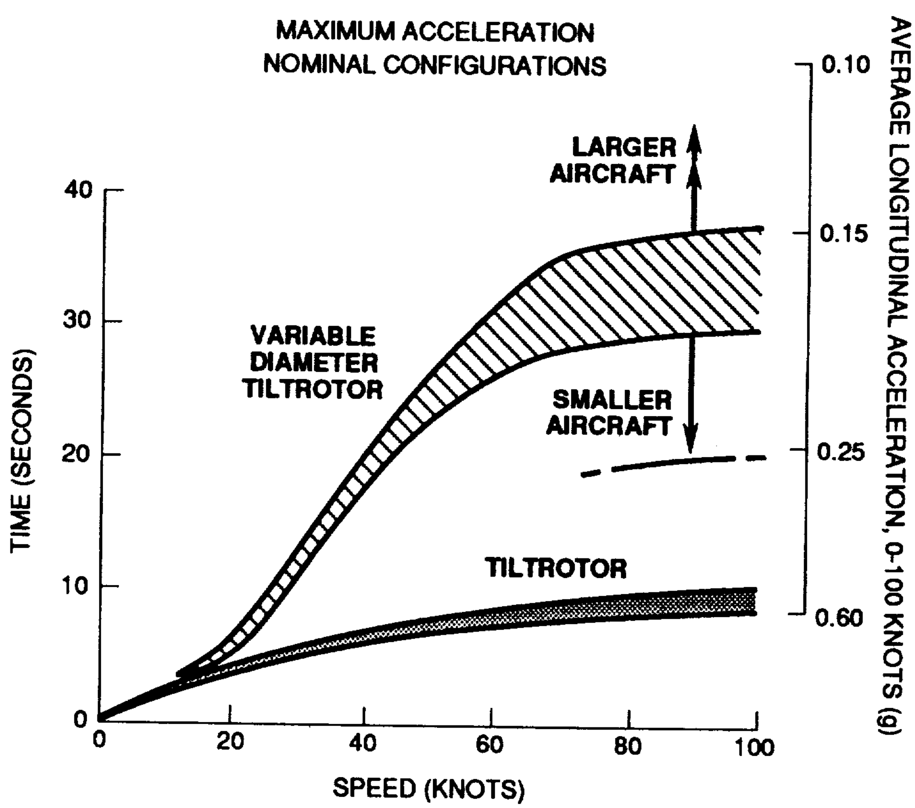

Figure B-19. Conversion Time Trends

Rotor Description

General design considerations for a high-speed prop-rotor were discussed in Section 2 of the main body of this report. The specific chord and twist distributions used to analyze rotor performance are shown in Figures B-20 and B-21. These apply to both the unswept, baseline 1990 technology level and to the advanced geometry year 2000 technology level rotors. However, the advanced geometry rotor blade incorporated a significant degree of blade sweep, see Figure 49 in the main text.

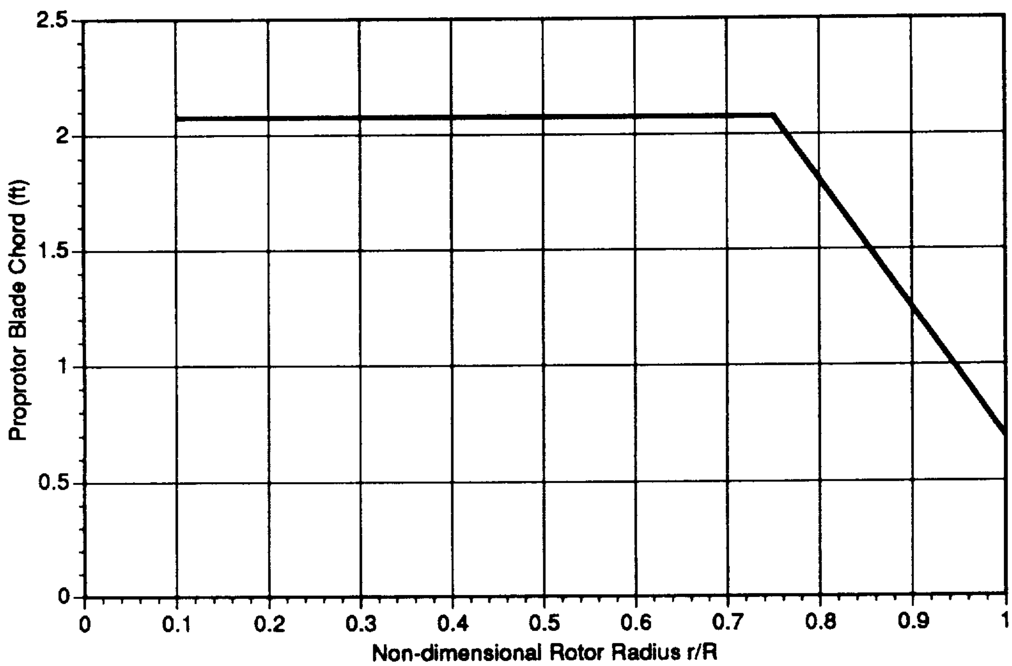

Figure B-20. High-Speed Civil Tiltrotor Blade Chord Distribution

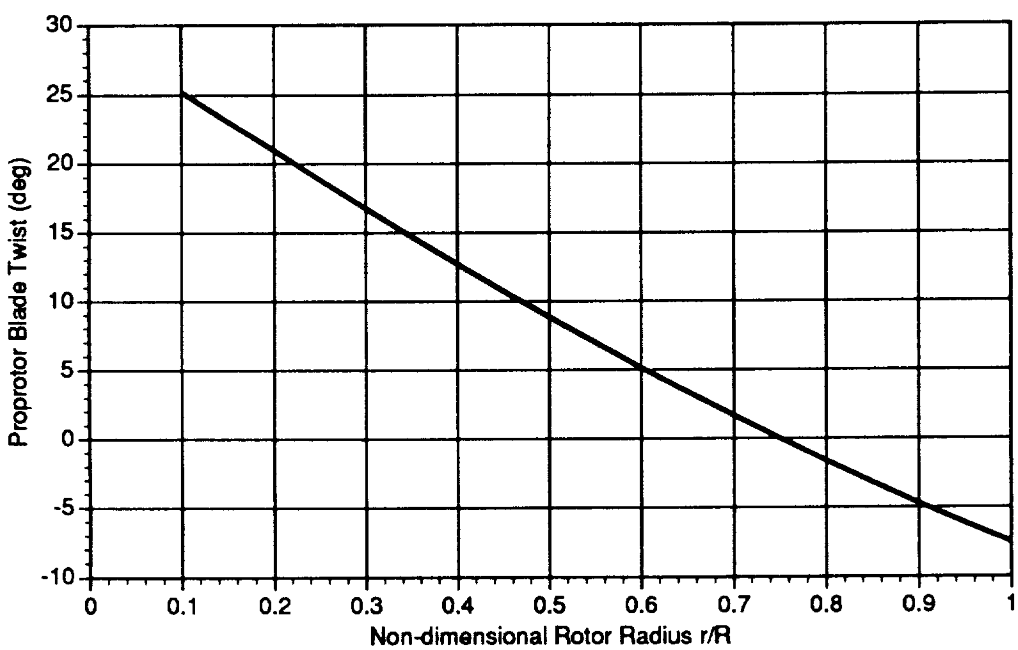

Figure B-21. High-Speed Civil Tiltrotor Blade Twist Distribution

Performance

Predicted hover figure of merit for the baseline rotor was shown in Figure 51 in the main text. A curve of rotor hover C_T versus C_P is shown in Figure B-22. Cruise propulsive efficiency for the baseline rotor and the advanced geometry rotor were shown in Figure 50 in the main text at the 450-knot cruise speed. A map of cruise propulsive versus airspeed for the baseline rotor is shown in Figure B-23 for several thrust coefficients.

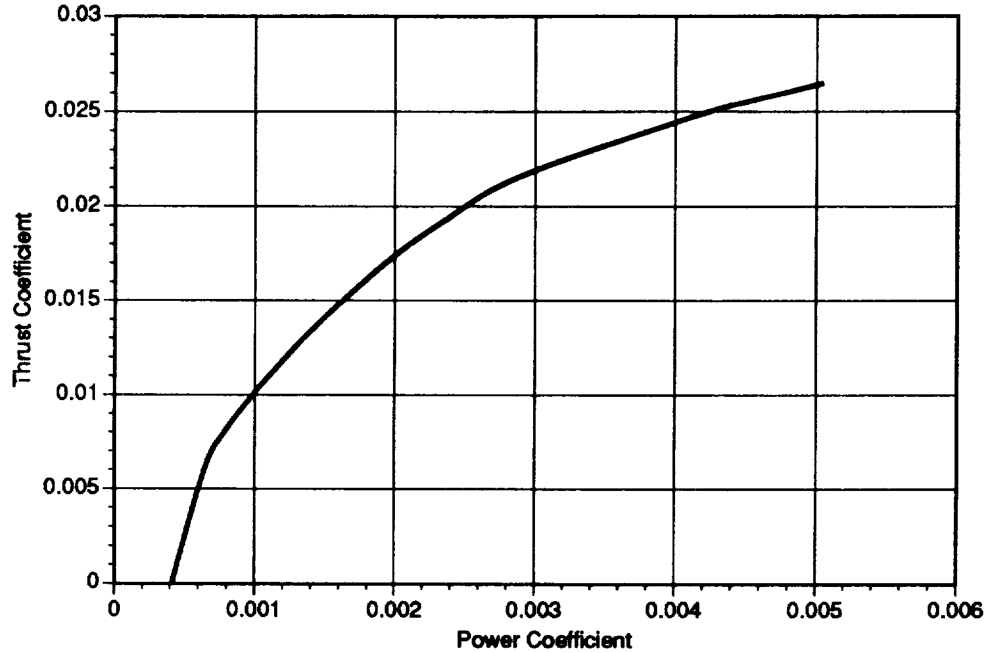

Figure B-22. High-Speed Civil Tiltrotor Hover C_T vs. C_P

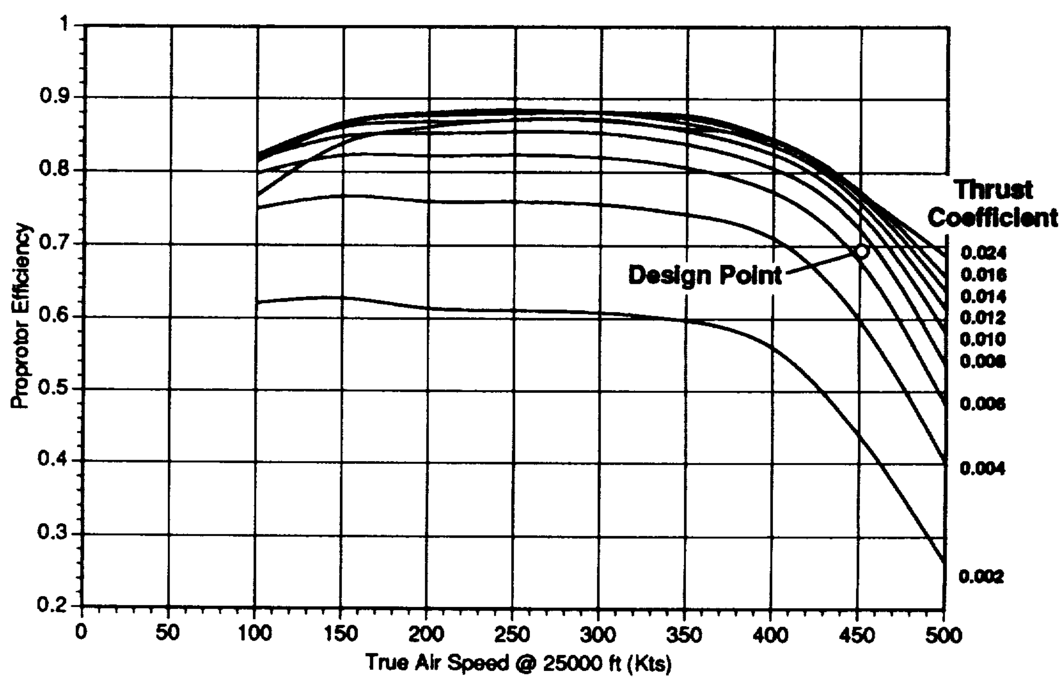

Figure B-23. Effect of Thrust Coefficient on Prop-Rotor Cruise Efficiency (Unswept Blade)

Autorotation

A commonly used measure of autorotation performance is the "equivalent hover time," the time that the stored kinetic energy of the rotor could supply the power necessary for hover before stalling. The equation for determining this equivalent time is the first equation on page 363 of Reference B-4. An alternative method is given by the second equation on the same page , being a slightly simpler calculation based on the maximum height to which the stored kinetic energy could lift the vehicle.

The first index has been calculated to be 0.30 seconds for the civil tiltrotor and 0.39 for the military folding tiltrotor. These can be compared with recommended values of 1.5-seconds for single engined helicopters and 0.8 seconds for twin engined helicopters.

The second index is calculated to be 14 for the civil tiltrotor and 16 for the military folding tiltrotor, where the recommended value for single engined helicopters is 60 and for twin engined helicopters, the recommended minimum is 25.

The above results indicate that pure autorotation behavior would not be acceptable by current standard for vehicles which are supported only by a rotor system. For these tiltrotor vehicles, however, the combination of wing lift and rotor thrust should provide a reasonable capability for autorotative descent and landing. Due to the lack of a significant amount of historical data on this type of vehicle, a program of batch and piloted simulations is recommended, the scope of which is beyond this current study. It is possible, however, to draw some conclusions from some simple calculations. The second autorotation index discussed above is proportional to rotor inertia, and inversely proportional to weight and disc loading. Assuming similar vehicles will have similar gross weights and rotor inertias, the primary variation is that due to disc loading. Figure B-24 shows how the index varies with disc loading assuming the rotor inertia and gross weight of the military folding tiltrotor.

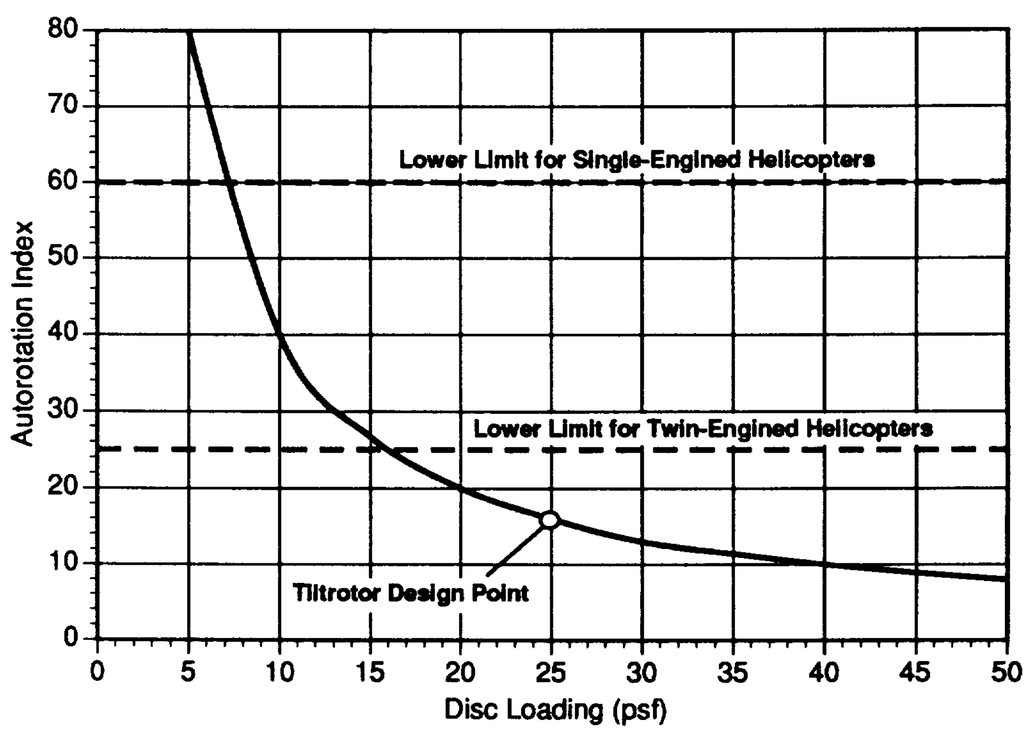

Figure B-24. Autorotation Index Variation with Disk Loading

The first observation that can be made is that conventional single-engined helicopters would be limited to disc loadings no higher than 7-psf and twins limited to no higher than 16-psf. The value for the tiltrotor is 64% of that recommended for twin engined helicopters. However, as noted above, the wing will provide a further cushion in autorotative flight. At higher disc loadings, however, the ability of the rotor to provide classical autorotative behavior decreases further. Typically vehicles designed to operate at 40-50-psf such as tilt wings have historically also been high wing loading, low aspect ratio vehicles, factors which also reduce the wing's ability to provide stable flight with all engines inoperative.

High-Speed Aeroelastic Stability

The aeroelastic study evaluated the effect of various design parameters on the aeroelastic stability of a high-speed rotorcraft. Most of the work focused on the civil tiltrotor configuration. Parameters studied included forward sweep of the wing, fuselage stiffness and mass properties, wing mass distribution, and rotor properties such as aerodynamic sweep, rotor radius, and airfoils. NASTRAN was used to calculate mode shapes for the different wing and fuselage configurations, and CAMRAD used these mode shapes to calculate the stability boundary.

The goal for this aircraft is to cruise 450-knots true airspeed (ktas). Using the V-22 design specification, this translates to a dive speed of 540-knots and a stability boundary of 621-knots. The analysis was conducted at 7,500-ft, being consistent with the V-22 reference. The 621-ktas flutter boundary equates to a 555-knot equivalent airspeed at 7,500-ft, or 415-keas at 25,000-ft.

NASTRAN Results

The baseline finite element model used for this study is the 42,000-lb gross weight V-22 fuselage model with an elastic line wing model. The frequencies of this elastic line wing model agree reasonably well with the frequencies calculated using the detailed wing model. For the swept wing configuration, the wing was swept forward to 30 degrees, with the nacelles at the same buttline and with the same wing/fuselage attachment point.

Wing

Sweeping the wing forward has a significant impact on the frequency placement of the fundamental wing modes. In general, the frequency of all wing modes dropped and there is more intermodal coupling due to the decreased frequency separation of the modes. The 30 degree sweep also increased the wing torsion motion in the first six wing modes. Specifically, the frequency of the symmetric wing beam mode (SWB) dropped 10.3% and had 76% more torsion in its mode shape. Similarly, the antisymmetric wing beam mode (AWB) dropped 19% and had 33% more torsion. These are two of the key modes for aeroelastic concerns and the changes in these modes caused by sweeping the wing will have a negative effect on the whirl flutter stability.

Civil Tiltrotor Fuselage

An elastic line fuselage model was developed to idealize the fuselage of the civil tiltrotor canard arrangement. This model had a lower gross weight than the V-22, and a scaled down sectional EI distribution. It also had a rigid connection between the fuselage and the wing, where the V-22 had a flexible stow ring attachment, and it incorporated the aft location of the wing/fuselage joint.

In general, this new fuselage model caused an increase in the frequency of the first six wing modes when compared to the frequencies calculated with the V-22 fuselage. A rigid wing/fuselage connection, a lower gross weight, and a less detailed model all contribute to these higher frequencies. The most significant change was the anti-symmetric wing chord mode increase from 3.46 hz for the V-22 to 5.39 hz due to the lack of stow joint flexibility. For both the unswept and swept wing configuration, there is more torsion of the wing for a flap detection, because of the aft mounted wing (the model with the unswept wing has 88% more torsion in the SWB mode than the baseline V-22 model).

Finally, a model was developed that idealized the civil tiltrotor wing and fuselage. The fuselage model was described above. The wing was modelled using the V-22 elastic line wing with the civil tiltrotor mass distribution and with the V-22 wing stiffness properties. This configuration had a gross weight of 36,711-lbs. Since the wing was now lighter, the calculated frequencies are higher than the previous configurations.

CAMRAD Results

Baseline

The CAMRAD analysis used the V-22 model with the NASTRAN modes discussed in the previous sections. The modes included in the stability analysis are the symmetric and antisymmetric wing beam, chord and torsion modes (SWB, SWC, SWT, AWB, AWC, AWT). The baseline model predicted the SWB mode to go unstable at 445-keas. Typical frequency and damping curves are shown in Figure B-25. The 445-keas instability is approximately 10% higher than the current V-22 stability prediction (402-keas). This increased flutter speed is attributable to a combination of using the elastic line wing model and a reduced number of airframe modes.

A series of step changes were made to transform the V-22 model to a model of the high-speed civil tiltrotor. The incremental effect of these changes are shown in Figure B-26 and are briefly discussed below.

V-22 with Swept Stick Wing

When the wing is swept forward to 30 degrees, the flutter speed drops to 360-keas (-19%). As discussed previously, the decrease in stability is caused by the combination of lower frequency of the mode, more torsion in the mode shape, and more coupling of the modes.

Swept Wing and Canard Stick Body

This configuration combines the canard fuselage and the civil tiltrotor forward swept wing. It showed a flutter speed of 344-keas, approximately the same as the configuration with the fuselage and the V-22 wing swept forward.

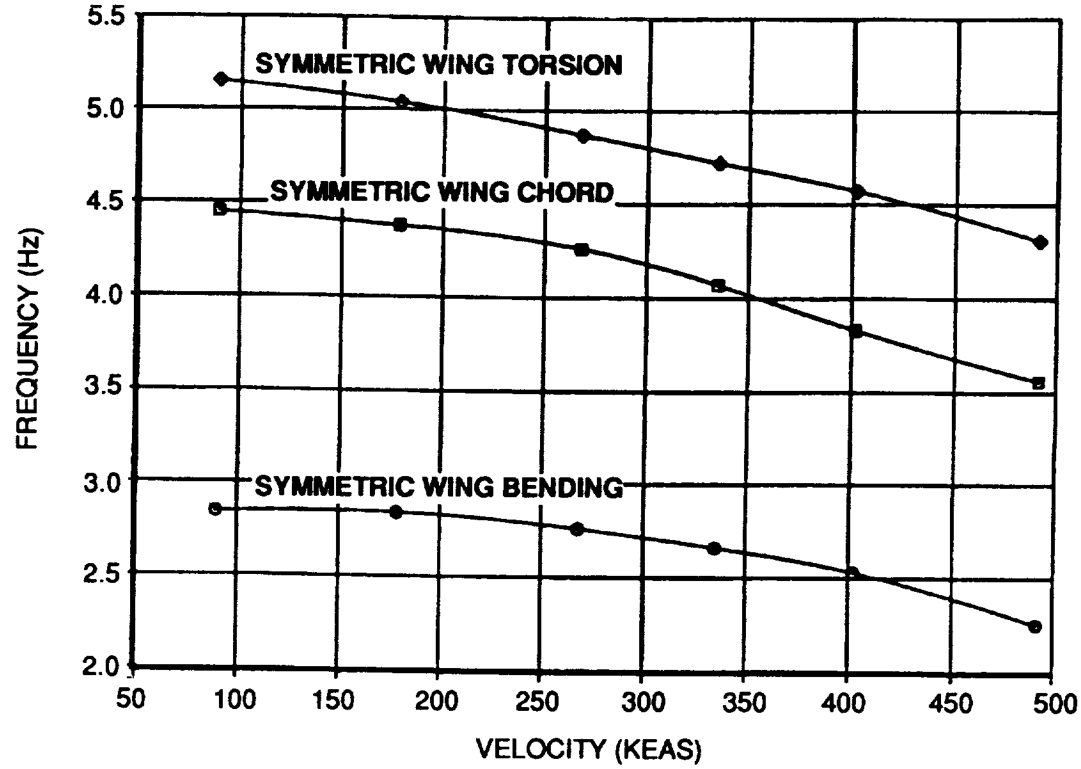

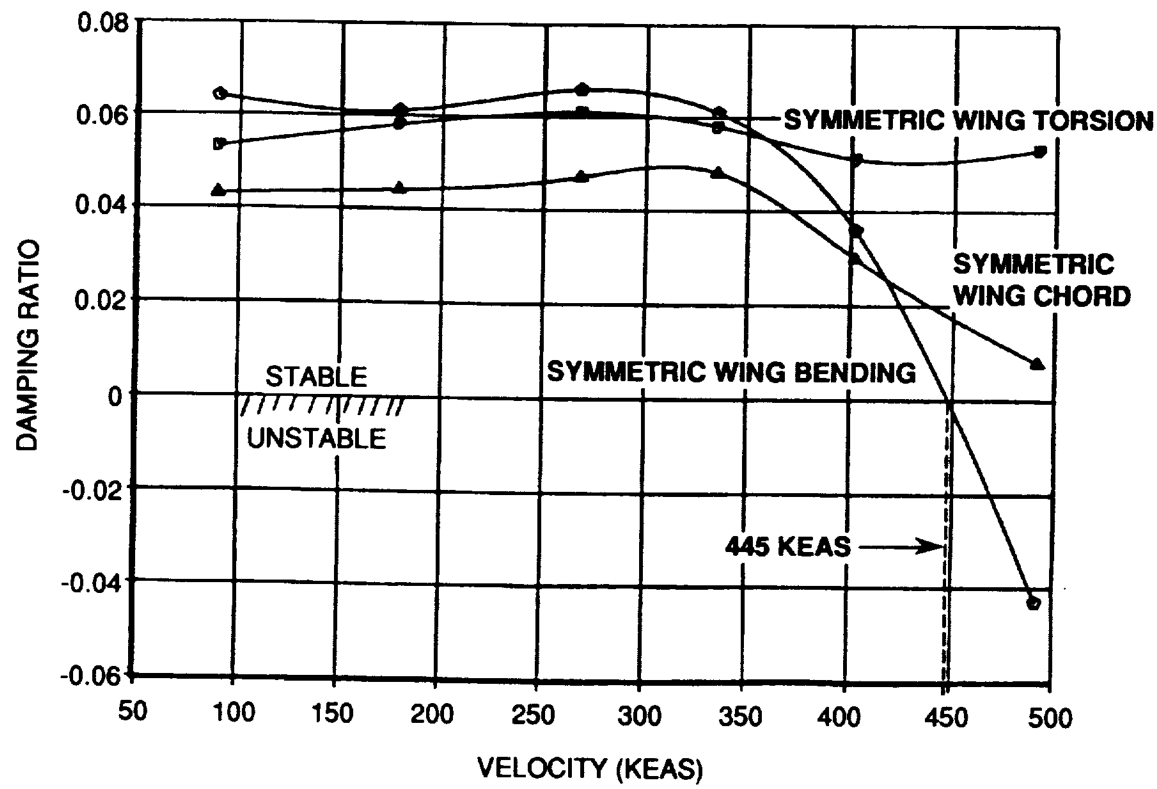

Figure B-25. High-Speed Civil Tiltrotor Baseline Aeroelastic Stability

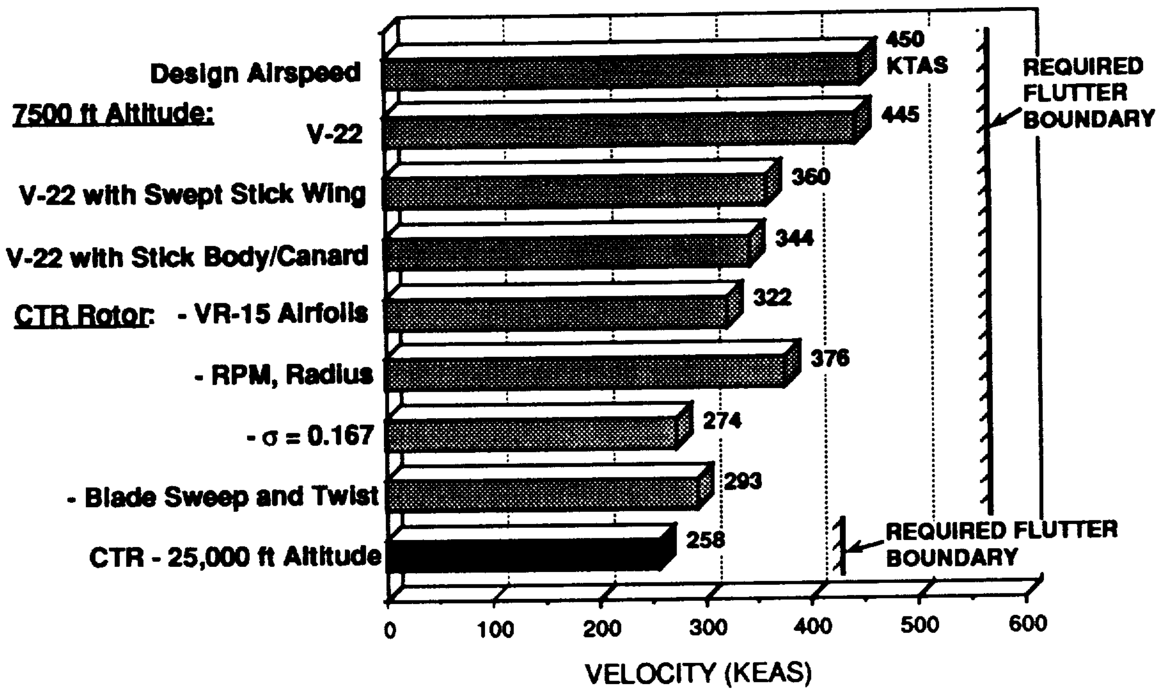

Figure B-26. High-Speed Civil Tiltrotor Whirl Flutter Boundary

Civil Tiltrotor Rotor System

This configuration combines the fuselage and wing with the rotor properties which are known at this time. No blade or rotor structural properties are available, so the V-22 rotor and blade structural properties (input blade modes) are used in the analysis. In actuality, the blade and rotor structural properties will have a significant effect on the aeroelastic characteristics of the aircraft, and should be included in future studies (at this time CAMRAD has no capability to analyze swept blades structurally - only aerodynamically). The properties changed were blade airfoil, mass, length and chord, aerodynamic sweep and twist, rotor rpm and solidity, and the number of blades. The changes were done incrementally to study the effect of each on the stability.

As shown in Figure B-26, parameters that dropped the flutter speed were VR-15 airfoils and increasing the rotor solidity (which includes increasing number of blades to four and increasing the blade chord). All of these changes increased the aerodynamic forces on the rotor which decreased the flutter speed. Parameters that increased the flutter speed were lower blade mass, the combination of rpm and smaller radius, and the combination of aerodynamic blade sweep and new twist. When all of the rotor changes were incorporated, the flutter speed dropped to 293-keas, approximately 15% lower than the flutter speed of this configuration with the V-22 rotor.

Increasing Flutter Speed

Stability for the final configuration was run at the design cruise altitude of 25,000-ft. The flutter speed at 25,000-ft was calculated to be 258-keas, with a requirement of 415-keas. Therefore the design did not meet the stability requirement at either 7,500-ft or at the design altitude of 25,000-ft.

As shown in Figure B-27, there are design parameters which can increase the flutter speed. Increasing the wing GJ four times increases the stability speed 9.3% to 282-keas, because there is now less pitch in the wing modes shapes. Another very powerful parameter is the inplane frequency of the rotor. A 5% increase in the inplane rotor frequency increased the stability 16% to 327-keas. However, this is not a simple inplane stiffening of the blade, because of the large twist of the blade and the large range of collective angles. Large stability gains are available by reducing the pitch in the wing mode shapes, which may be achievable by mode shape tailoring using advanced composite technology. A 50% reduction in the pitch in the wing mode shapes gave a whirl flutter stability increase of 32% to 432-keas. These preliminary estimates suggest that a combination of increased torsional stiffness, increased inplane rotor frequency, and reduced nacelle pitch can satisfy the whirl flutter stability requirement for a 450-knot high-speed tiltrotor. A more detailed design and analysis of the wing and rotor, backed by model scale tests, would be necessary to identify the specific combination of design parameters.

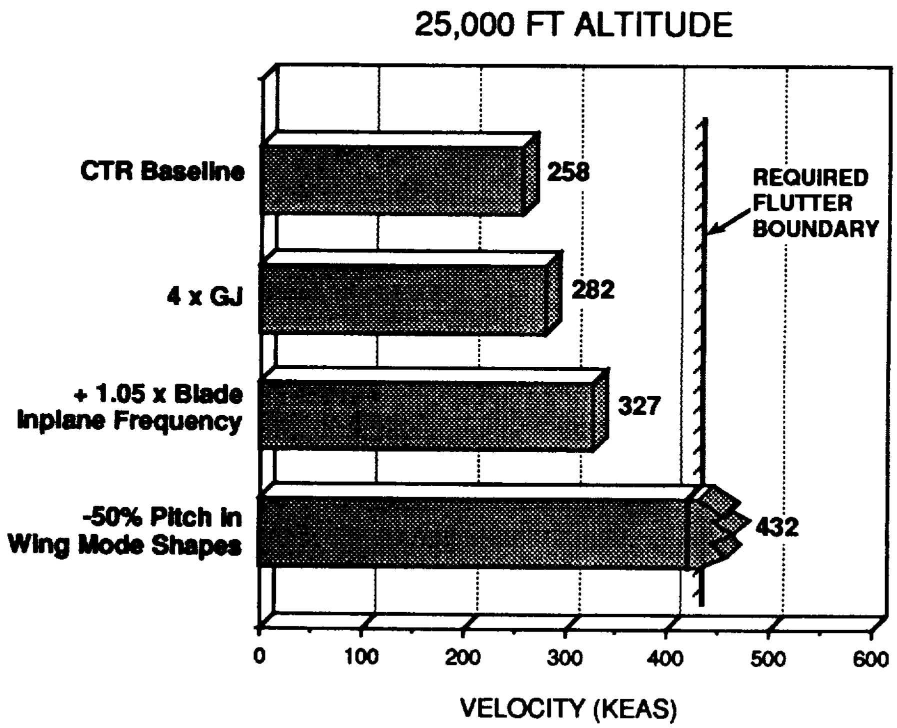

Figure B-27. High-Speed Civil Tiltrotor Whirl Flutter Improvement

Civil Tiltrotor General Performance

Hover Performance

The out-of-ground effect hover ceiling for the baseline rotor design is shown in Figure B-28 versus takeoff gross weight for both standard day and ISA + 15°C ambient conditions.

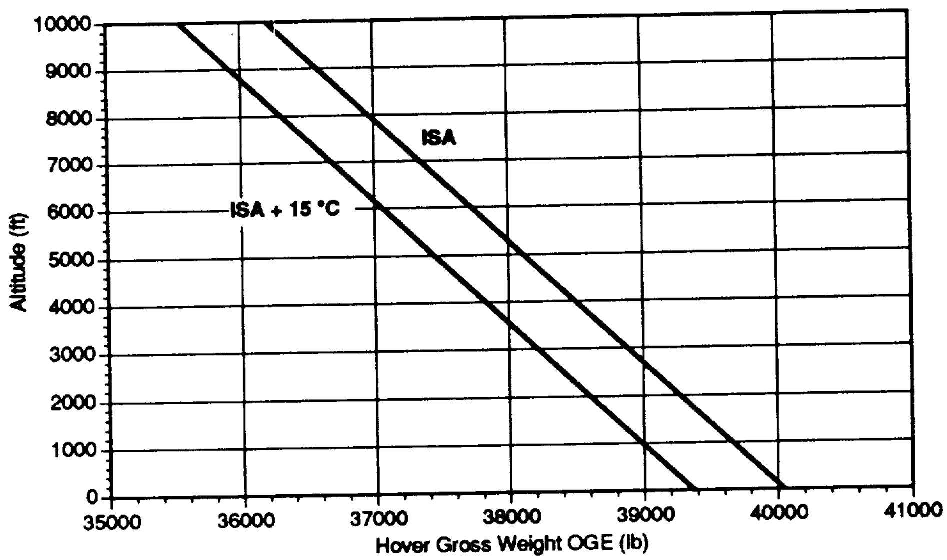

Figure B-28. Out-of-Ground Effect Hover Ceiling for Civil Tiltrotor

Conversion Envelope

The basic conversion envelope was presented in Section 2 of the main text. Figure 53 showed the power/transmission limits and stall/attitude limiting curves. Figure B-29 shows power required as a function of conversion speed and nacelle angle. The trends are similar to the now familiar V-22 performance, showing a fairly broad power bucket which allows efficient loiter over a range of airspeeds from 80-knots to 200-knots.

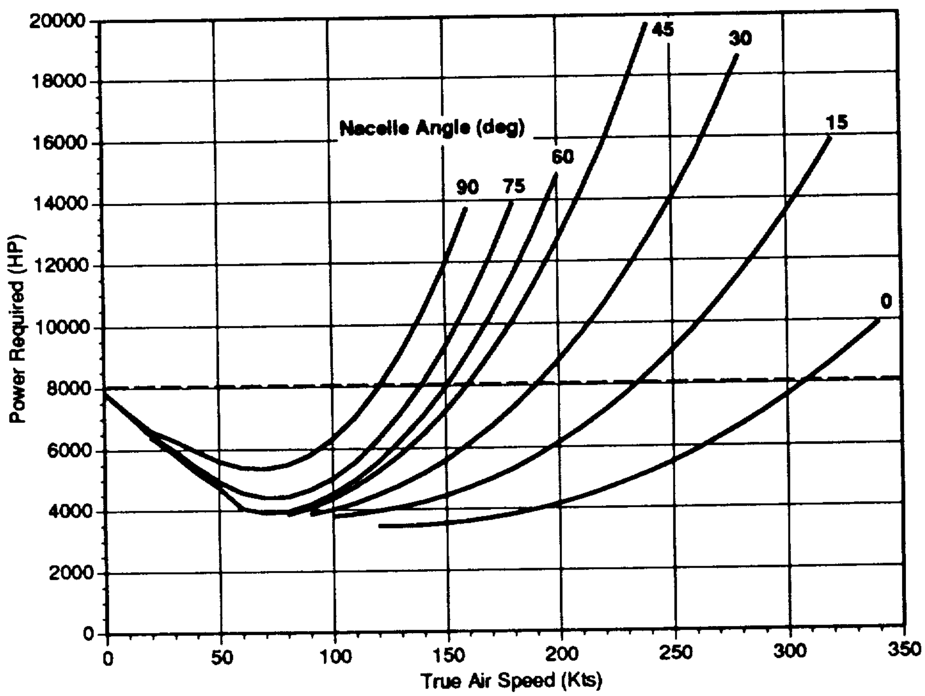

Figure B-29. High-Speed Civil Tiltrotor Conversion Power Required (Standard Day)

Cruise Performance

Basic airframe drag polars, lift-to-drag ratios, and specific range curves were shown in the main text, Figures 54 through 56 respectively. The parasite drag build-up for the civil tiltrotor is shown in Figure B-30 for a total f_e of 11.8-sq.ft Table B-5 shows the breakdown of drag coefficient for the cruise condition at 450-knots.

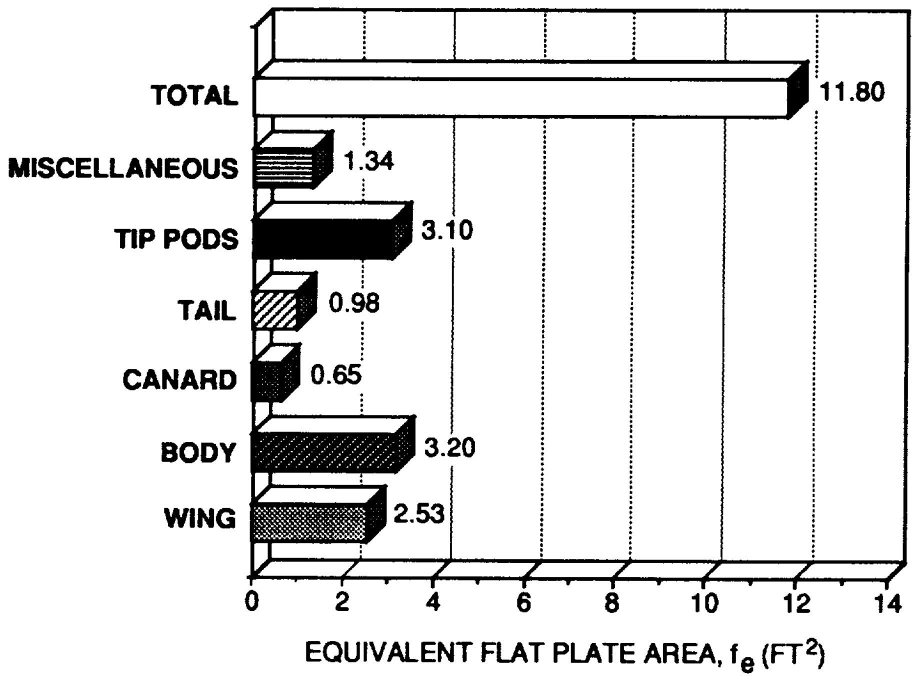

Figure B-30. Civil Tiltrotor Parasite Drag Build-Up

Table B-5. Civil Tiltrotor Cruise Drag Components

COMPONENT	DRAG COEFFICIENT (1g, 450-KTS, 25,000-FT)
Parasite Drag	0.03075
Induced Drag	0.00615
Compressible	0.0
Total	0.0369

The absolute power required versus airspeed is shown in Figure B-31 for altitudes of 0, 10,000, 20,000, and 25,000 feet. Figure B-32 shows the ratio of power required to power available as a function of airspeed and altitude, which is one indication of climb capability and altitude capability. Note that the transmission limits shown in Figure 52 would also apply to this figure, limiting the airspeed.

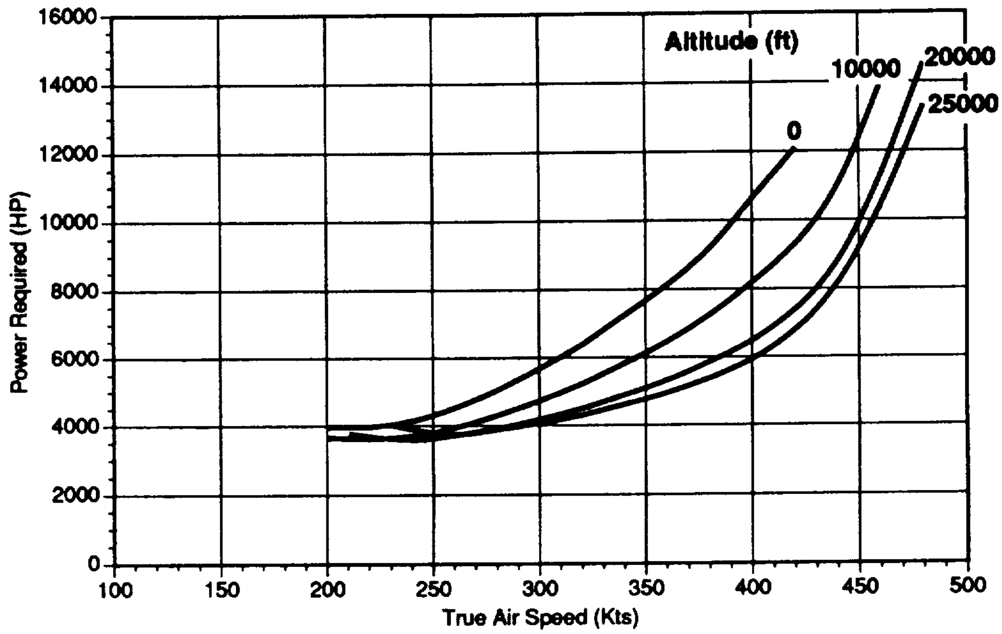

Figure B-31. High-Speed Civil Tiltrotor Power Required (Standard Day)

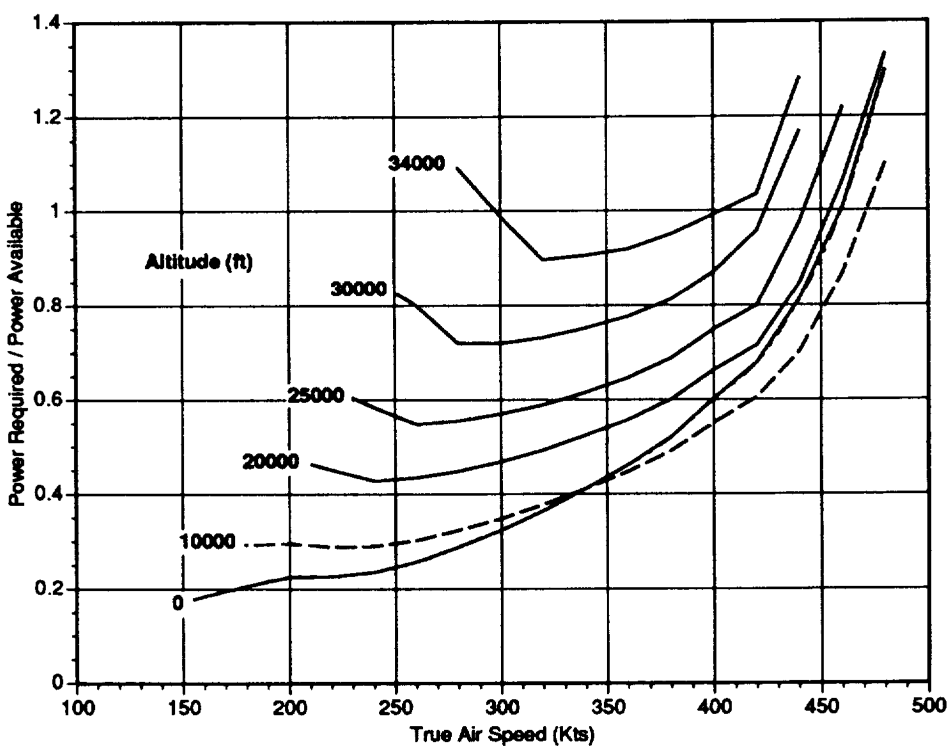

Figure B-32. High-Speed Civil Tiltrotor Power Fraction vs. Speed (Standard Day)

A flight envelope is shown in Figure B-33 for several normal load factors. Sustained maneuver performance is shown in Figure B-34 for both the helicopter mode and the airplane mode, as limited by the structural limit design load factors. The target maneuver capabilities of Figure 43 were met or exceeded.

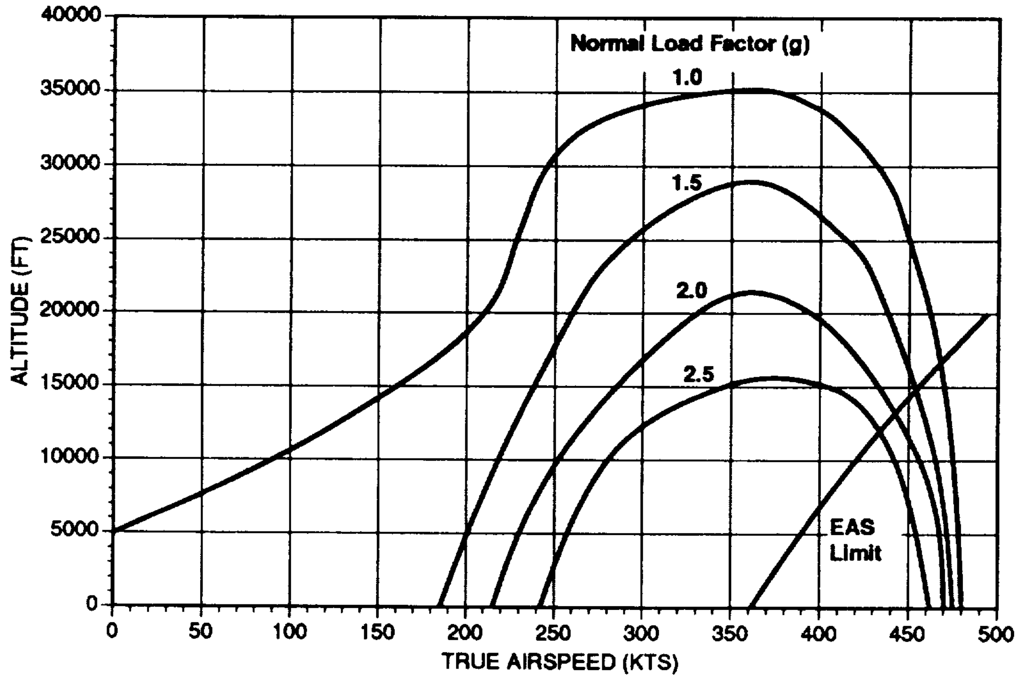

Figure B-33. High-Speed Civil Tiltrotor Flight Envelope (Standard Day)

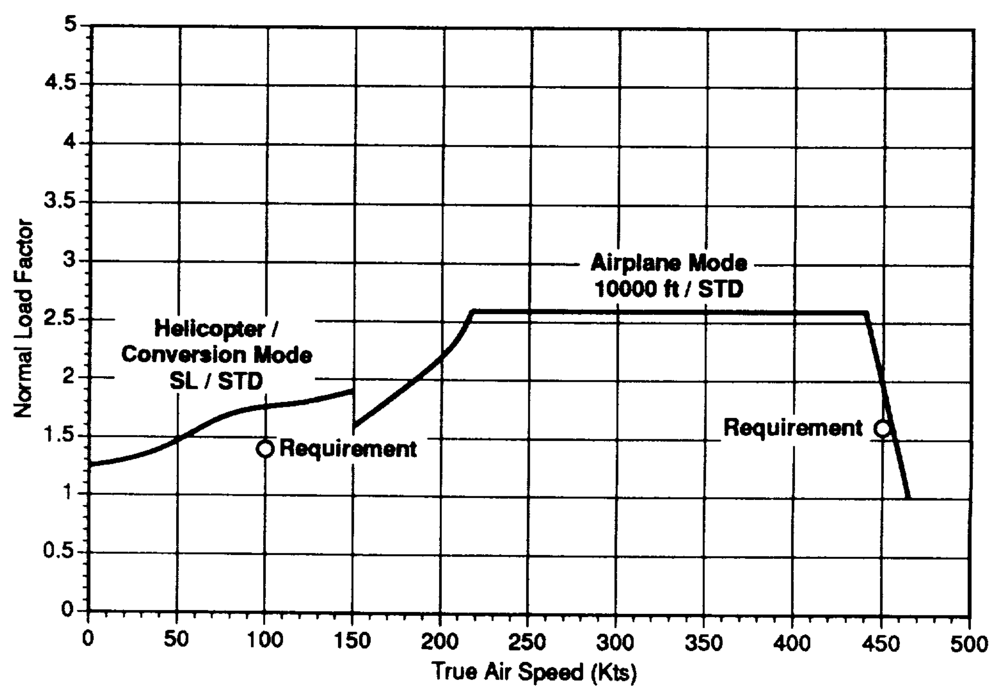

Figure B-34. High-Speed Civil Tiltrotor Sustained Maneuver Capability

The lift sharing between the canard, wing, rotor and body, and tail surfaces was estimated and is shown in Figure B-35 at the stall speed and at the 450-knot cruise speed for both forward and aft CG limits. These calculations were performed after the basic rotorcraft size had been fixed. They indicate a need to refine the design to decrease the amount of load carried by the canard in the cruise mode.

		LIFT / GW			
SPEED	CG	CANARD	ROTOR + BODY	WING	TAIL
Stall ($\delta_F = 0$)	Fwd (C_L)	18.9% (2.00)	9.7%	68.9% (1.60)	2.4% (0.30)
	Aft (C_L)	14.8% (1.58)	9.7%	68.9% (1.60)	6.6% (0.8)
450 Knots	Fwd (C_L)	28.0% (0.30)	1.6%	68.9% (0.16)	1.5% (0.02)
	Aft (C_L)	23.9% (0.25)	1.6%	68.9% (0.16)	5.6% (0.07)

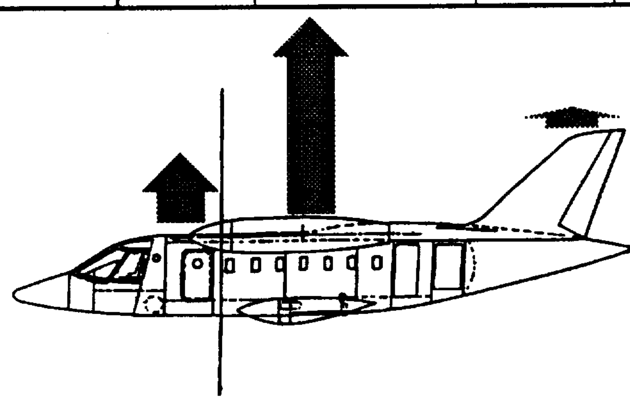

Figure B-35. Civil Tiltrotor Airplane Mode Lift Sharing

Rate of climb capability is shown in Figure B-36 for both standard day and ISA + 15°C ambient conditions.

Payload-Range Curves

Figure B-37 shows the payload-range curve for the high-speed civil tiltrotor. The design point of a 600-nm range with 30 passengers is just met. The rotorcraft could have an extended range capability by carrying additional fuel. This would be achieved for the basic design with STO operations, allowing higher takeoff gross weights. Or, a higher alternate VTO gross weight could be achieved by upgrading the transmission to accept more torque in hover. The engines would not have to be resized unless one needed to cruise at 450-knots at the alternate VTO gross weight. The 450-knot airspeed would be available sometime during the cruise phase as fuel was burned off.

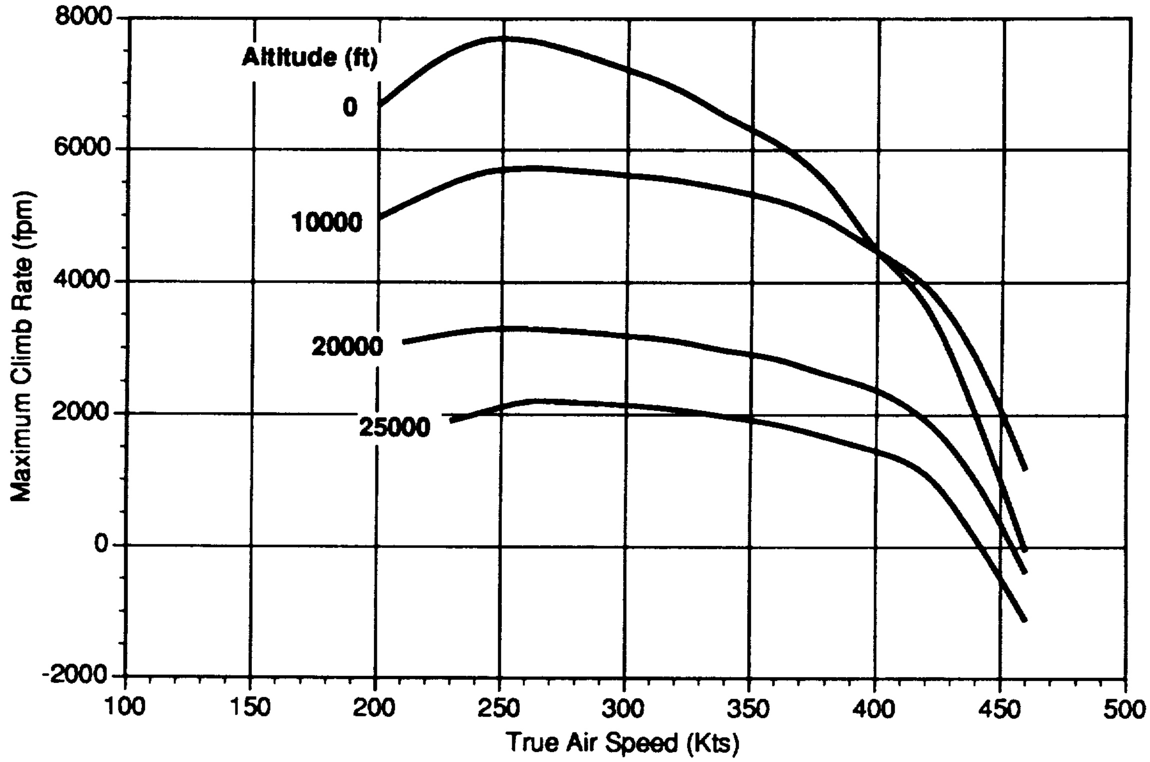

(a) Standard Day

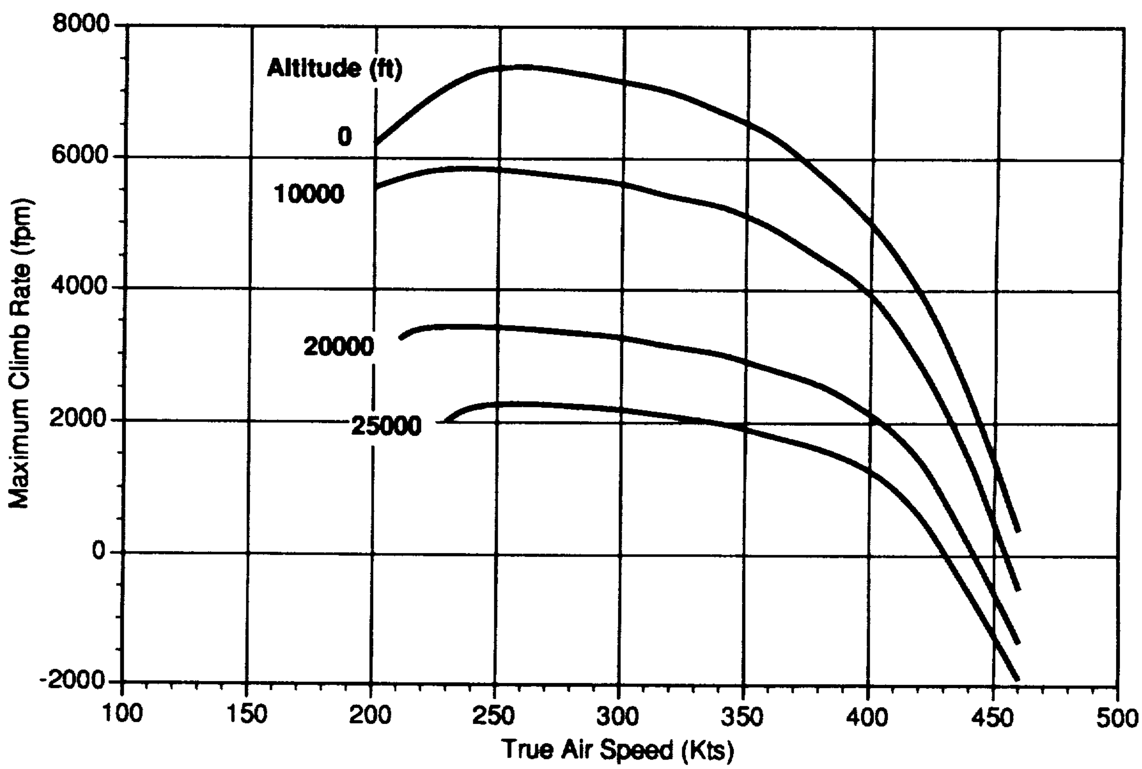

(b) ISA + 15°C Day

Figure B-36. High-Speed Civil Tiltrotor Maximum Rate-of-Climb Capability

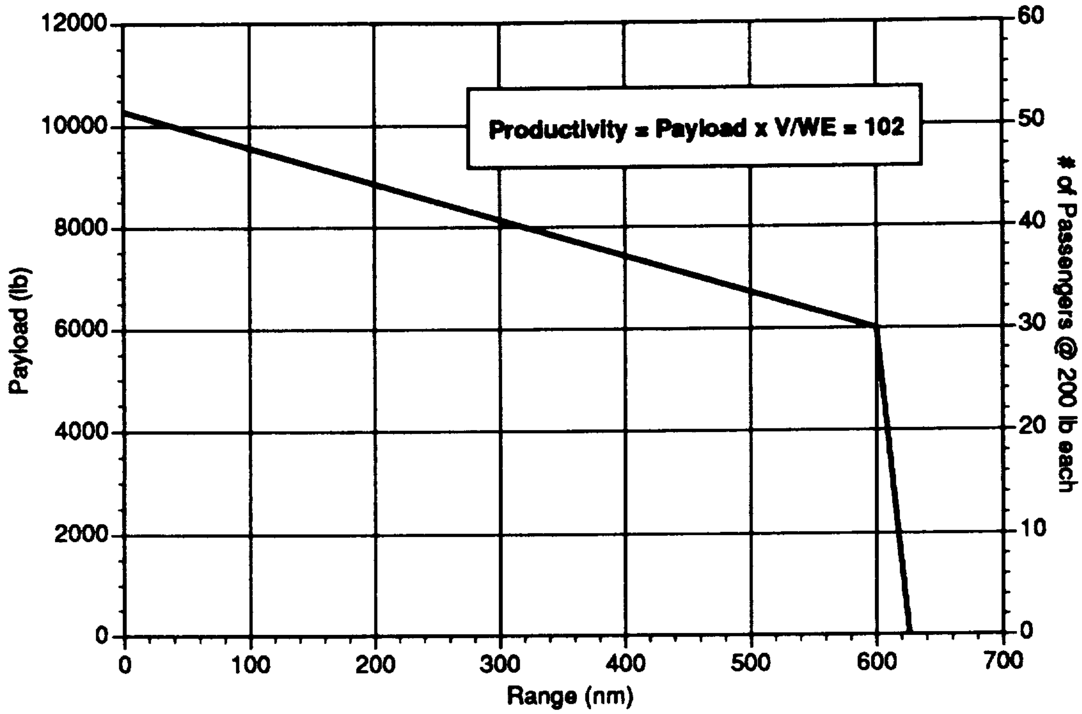

Figure B-37. High-Speed Civil Tiltrotor Payload-Range

Short Takeoff Performance

The tiltrotor has excellent short takeoff (STO) performance. Tiltrotor STO is accomplished with a ground roll followed by rotation to gain wing lift and then a climbout; see Figure B-38. This is quite similar to a fixed wing takeoff, except that the "prop" in this case is actually carrying about 75%-85% of the vehicle gross weight at lift-off.

The prop-rotor shaft is set at an angle of 60 degrees from the horizontal during the ground roll, thus providing 50% of the rotor thrust as a longitudinal propulsive force. This corresponds to about 0.4g longitudinal acceleration, depending of course on the gross weight. This nacelle angle,

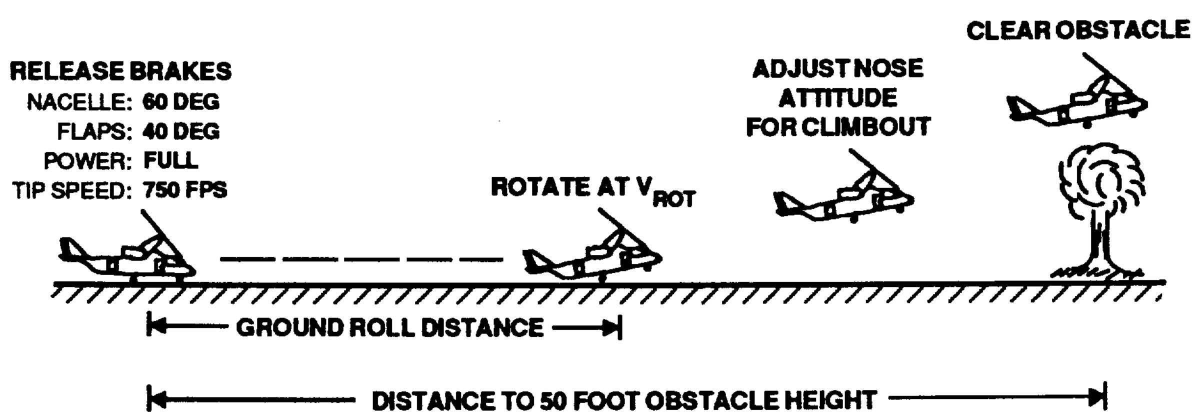

Figure B-38. Tiltrotor Rolling Takeoff Profile

and a 40-degree flap angle, were chosen for maximum climb rate after rotation, thereby giving a minimum takeoff distance to clear a 50-foot obstacle. At rotation speed the aircraft is pitched nose up to about 14 degrees developing the needed wing lift. But at the same time this rotates the prop-rotor from its 60-degree attitude up to a 74-degree attitude amplifying its "lift" force. Even at the 74-degree angle though, 27% of that prop-rotor thrust is still in the longitudinal direction. This maintains about a 0.22g longitudinal acceleration, depending on aircraft gross weight.

Figure B-39 shows the useful load increase as a function of ground distance. This useful load increase is shown as a percentage increase over the vehicle's VTO useful load (payload, fuel, and fixed useful load). An operator could achieve a 30% increase in useful load with only about 220 feet of ground roll and a total of 550 feet of clearway. Just this 30% useful load increase could be taken as:

- a 64% increase in fuel (range), or
- about 3000 pounds of cargo (in addition to the full passenger load), or
- about 30% more passengers (including the added weight for a stretched fuselage and the extra furnishings).

There are numerous operational situations where this kind of potential could be applied to enhance the utilization of a commercial (or military) tiltrotor. Some first hand operational experience would no doubt define these more clearly.

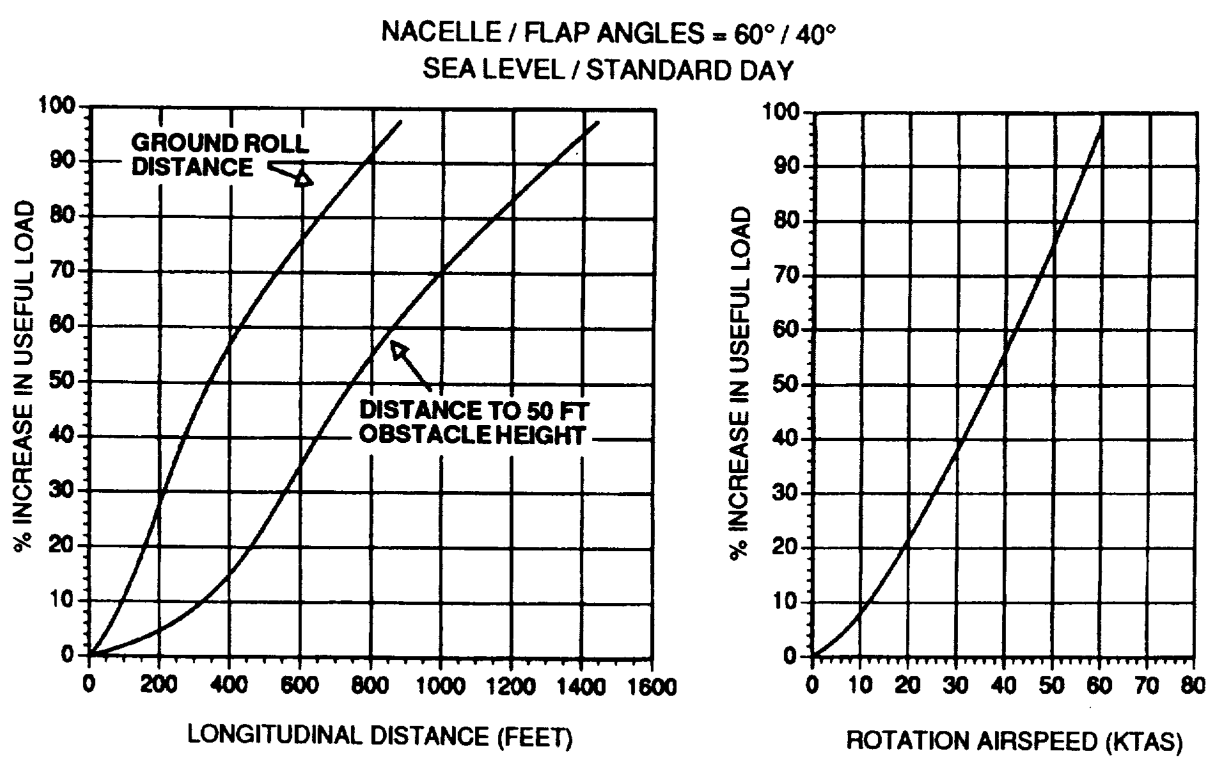

Figure B-39. Rolling Takeoff Performance - Civil Tiltrotor

Civil Tiltrotor Propulsion System

Drive System Description

The high-speed civil tiltrotor has wingtip mounted engines for maximum separation between the cabin and the engines. The engines are non-tilting to avoid hot high-velocity exhaust impingement on the landing pad and surrounding surfaces. This is also important for ground support personnel who may be in the vicinity of the rotorcraft at the gate with engines running. Non-tilting engines also avoid the additional certification procedures which would be required of tilting engines.

Figure B-40 shows a schematic diagram of the high-speed civil tiltrotor drive system. The 30-degree forward swept wing requires an additional gearbox at the wing tip to provide the desired orientation for the tilt-axis gearbox. An overall transmission efficiency of 0.98 was used for this system, representing losses between the engine and the rotor.

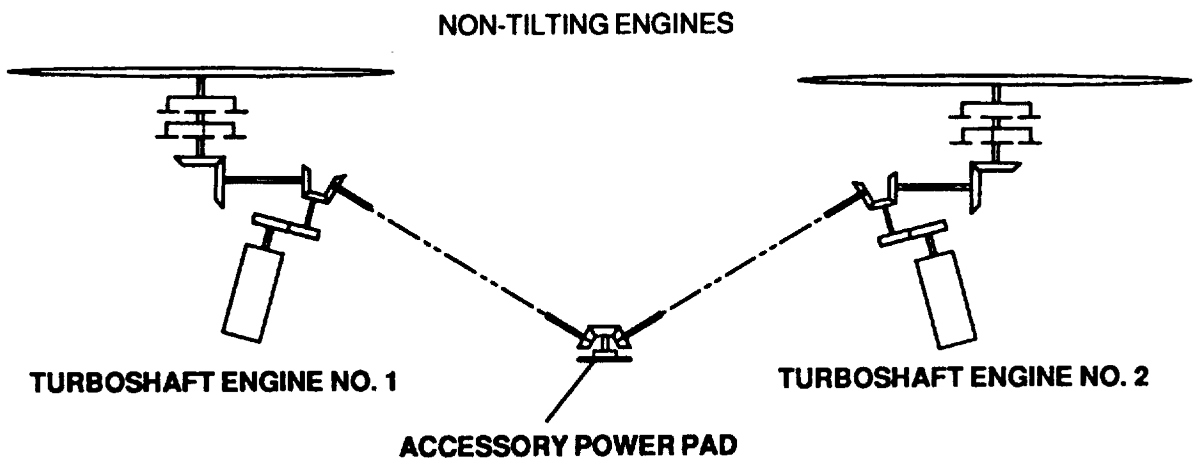

Figure B-40. High-Speed Civil Tiltrotor Drive System Schematic Diagram

Engine Characteristics

Performance and weight characteristics of the baseline turboshaft engine considered for the high-speed civil tiltrotor are consistent with turbomachinery technology available for a 1991 demonstrator engine program, leading to an initial operational configuration (IOC) in the year 2000. The technology is compatible with Phase I of the IHPTET program (Integrated High Performance Turbine Engine Technology), the tri-services/NASA sponsored research and development effort to achieve major improvements in propulsion system fuel consumption and weight. Compressor pressure ratio and turbine-inlet temperature; and hot section material properties are reflected in overall engine characteristics for the uninstalled engine:

- Design-point specific fuel consumption, SFC = 0.38 lb/hr/shp
- Power-to-weight ratio, shp/weight = 6.9 shp/lb

Installation Losses

The tiltrotor engines are located in wing-tip nacelles coupled by cross shafting which is essentially unloaded.

Inlet losses include the effects of the rotor blade hub cuff on recovery of dynamic pressure at the nacelle inlet, and pressure losses in the inlet passage and in the airframe inlet particle separator. Exhaust losses incorporate the effect of a variable area tailpipe to produce hover/cruise thrust optimization. The net effect of the installation losses results in the following installed performance effects at the hover point: a 4.5% shp reduction and a 0.5% fuel flow reduction

Power Available

Installed power available at the takeoff rating is presented in Figure B-41 for 100-percent rotor speed. Sea level, ISA takeoff power is 8,679 shp.

The aircraft drive system limit is 10,670 rotor horsepower, at the rotor shaft, 5,335 rhp per side. This corresponds to a somewhat larger value of engine shaft horsepower. Figure B-41 illustrates that the aircraft is drive-system limited below 12,000-ft altitude.

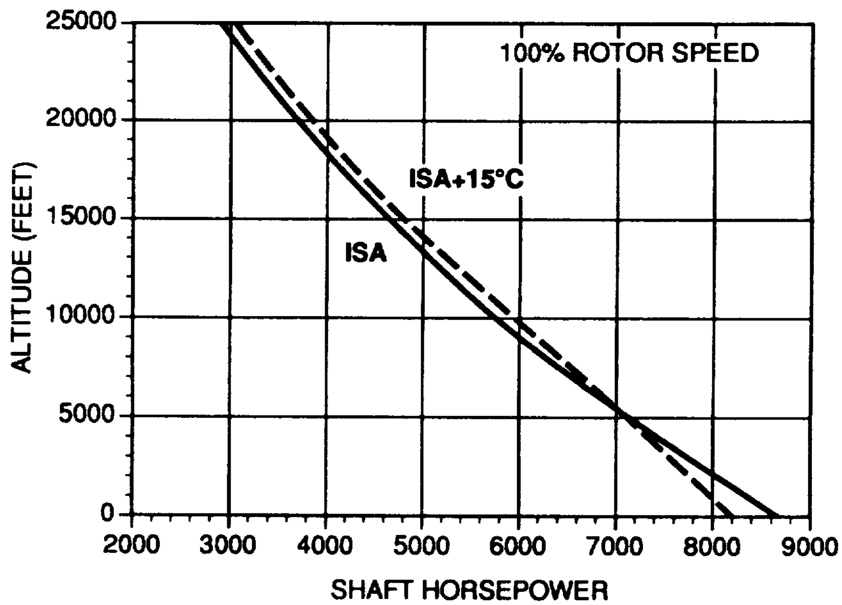

Figure B-41. Turboshaft Engine Installed Takeoff Power

Figure B-42 presents maximum continuous power installed as a function of altitude to 25,000 ft., flight speed to 450 kt., at ISA and ISA + 15°C, for 80 percent rotor speed.

The drive system limit at 80-percent rotor speed is 8,535 rhp, 4268 rhp per side. Figure B-42 indicates that the aircraft is drive-system limited in cruise up to very high altitudes.

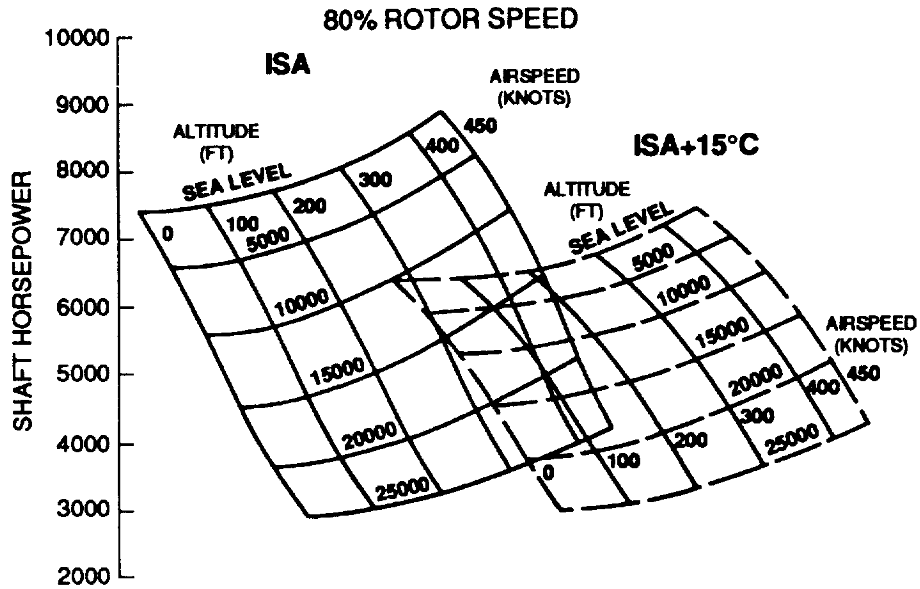

Figure B-42. Turboshaft Engine Maximum Continuous Power Available

Specific Fuel Consumption

Figure B-43 presents installed specific fuel consumption as a function of referred optimum shaft horsepower, and Figure B-44 presents optimum output shaft speed as a function of referred optimum shaft power. The effect of non-optimum output speed on power is expressed as a second order equation. Consequently, at a selected output shaft speed,

$$SHP\ N_2 = SHP_{opt} * [1\text{-}(1\text{-}N_2/N_{2opt})^2]$$

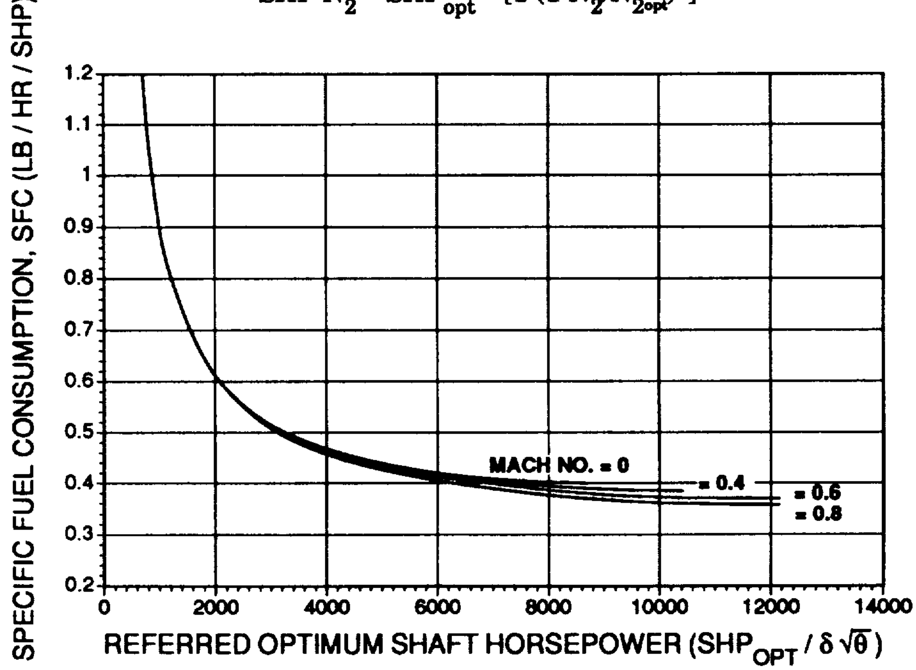

Figure B-43. Turboshaft Engine Specific Fuel Consumption

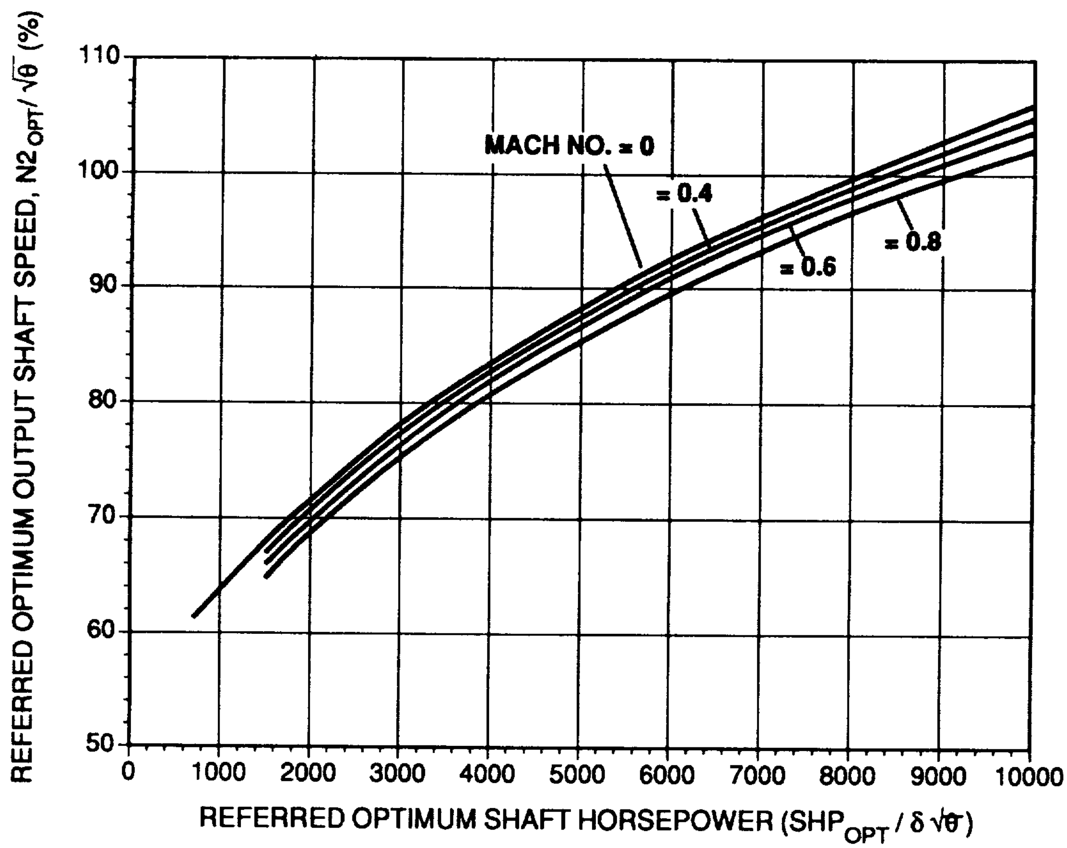

Figure B-44. Turboshaft Engine Optimum Output Shaft Speed

Folding Rotor System

A general description of the folding rotor system and its design constraints were given in Section 2; see Figures 58 and 59. The folding process is diagrammed in Figure B-45 showing a typical blade loading distribution in the stopped mode prior to folding. In addition to the flexbeam elastomeric hub shown in Figure 58 of the main text, Figures B-46 and B-47 show alternative lubricated bearing arrangements. Boeing's experience with the V-22 hub and the Model 360 all-composite hub have taught us which hub components can be designed with composites and which should be designed with metal. The rotor system is basically hover designed, but compromised for contour compatibility with the nacelle when in the folded configuration. A 20-degree linear twist was chosen on the basis of acceptable hover performance and reasonable contour compatibility. Thick airfoils are employed, as on the V-22, providing high lift coefficients and thereby reducing the required solidity. It is desirable to keep rotor solidity to a minimum to keep down the rotor system weight.

Rotor hover and cruise performance are not big drivers for the folding tiltrotor. The high-speed cruise is performed in the turbofan mode, which also sizes the convertible engine. Rotor efficiency affects hover fuel flow (not a big driver for the NASA transport mission) and drive system ratings, which translate into drive system weight. The rotor's hover and cruise performance was shown in the main text, Figures 57 and 60.

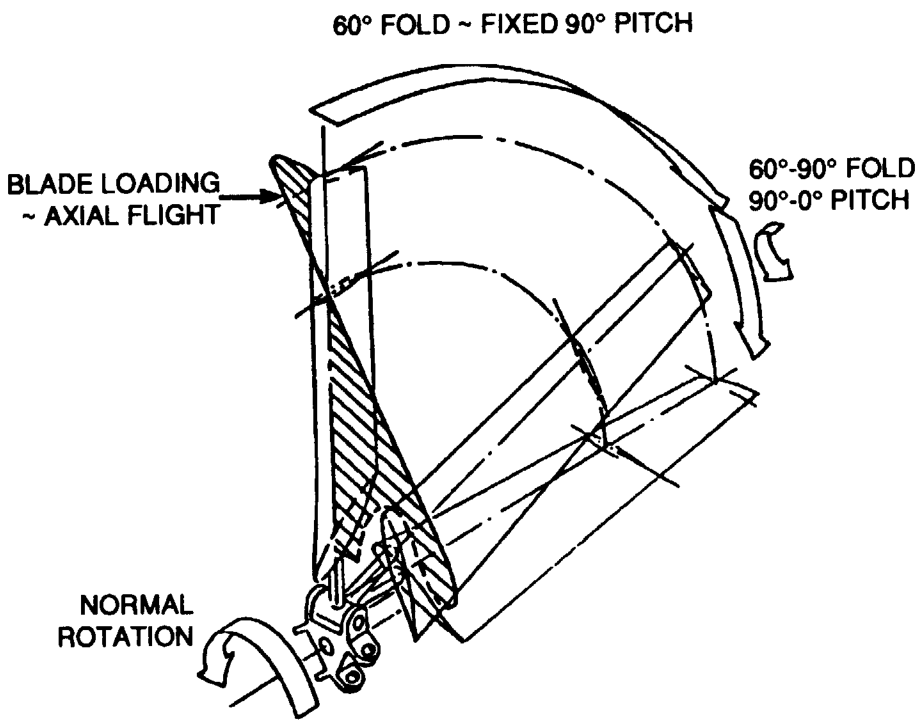

Figure B-45. Blade Fold Arrangement

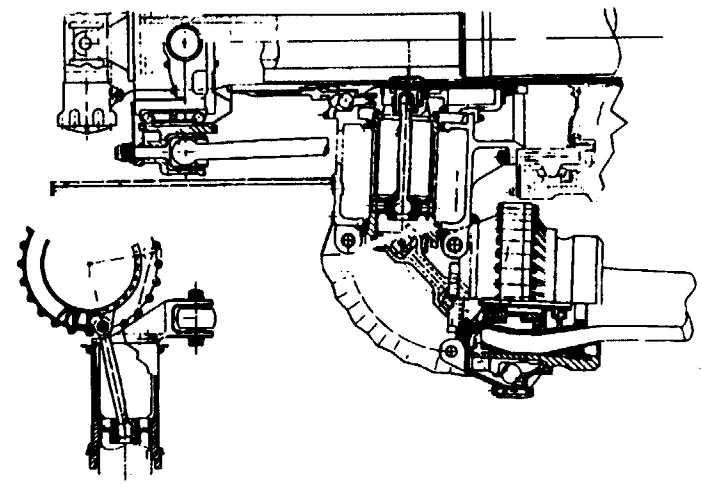

Figure B-46. Rigid Soft-in-Plane Folding Hub

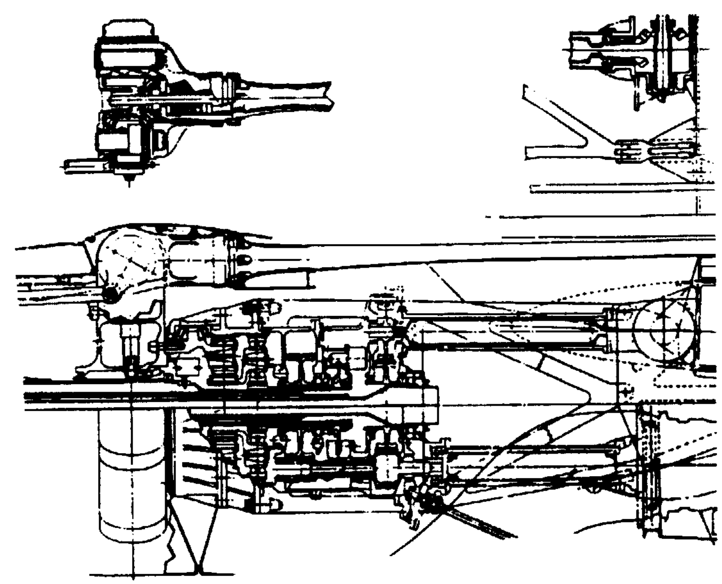

Figure B-47. Alternate Folding Rotor Hub System

Military Folding Tiltrotor General Performance

Hover Performance

The military folding tiltrotor hover ceiling is determined by transmission limits, not by installed power available (until high altitudes). The hover ceiling is shown in Figure B-48 for standard day and ISA + 15°C ambient conditions.

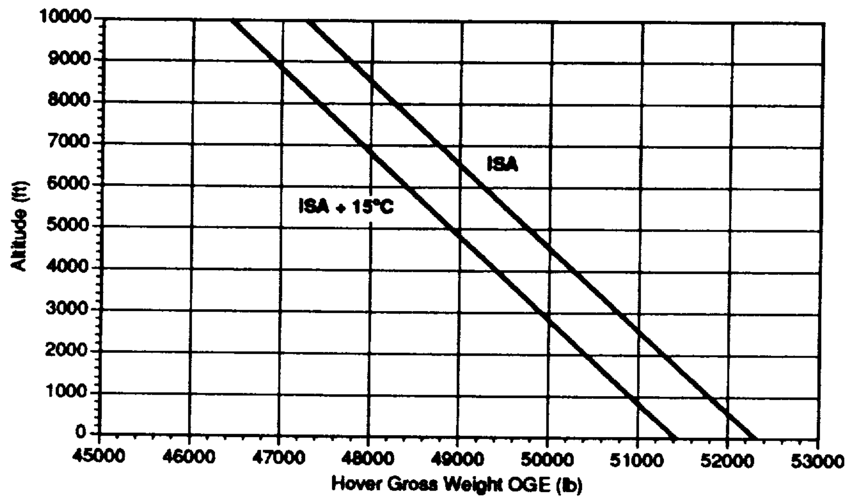

Figure B-48. Military Folding Tiltrotor Out-of-Ground Effect Hover Ceiling

Conversion Envelope

Figure 62 in the main text showed the conversion envelope for the military folding tiltrotor, indicating transmission limits and stall/attitude limits. Figure B-49 shows the corresponding power required versus airspeed for a range of nacelle angles. The dashed line indicates the transmission limit as determined by hover requirements.

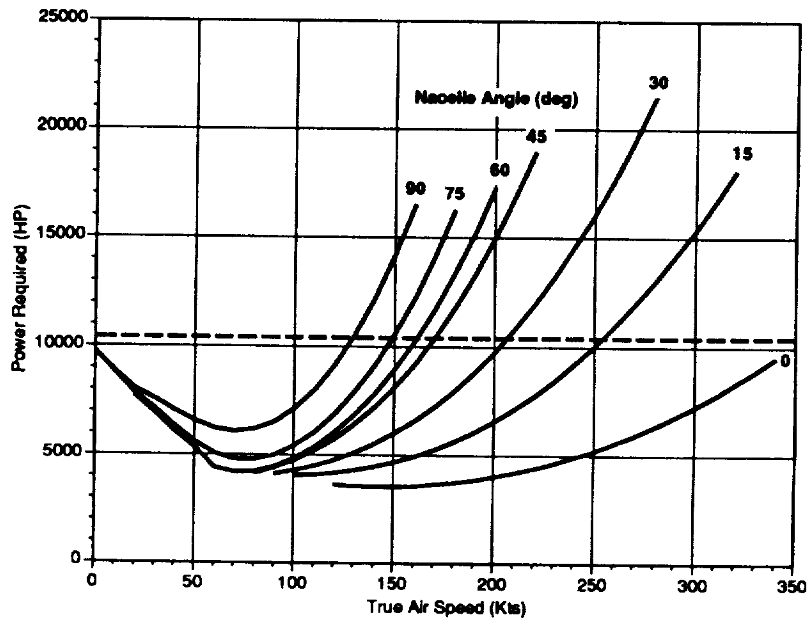

Figure B-49. Military Folding Tiltrotor Power Required in Conversion

Cruise Performance

Drag polars, lift-to-drag ratio curves and specific range curves were shown in the main text, Figures 63 through 65. Figure B-50 shows the parasite drag build-up for the military folding tiltrotor, for a total f_e of 13.78 sq.ft. Table B-6 shows the contributors to drag coefficient at the 450-knot cruise speed.

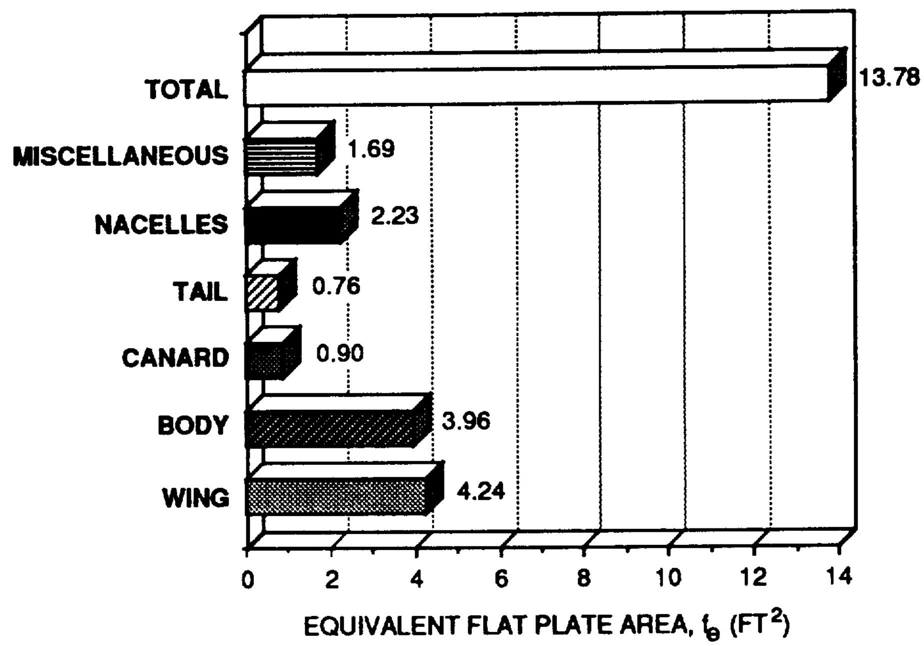

Figure B-50. Military Folding Tiltrotor Parasite Drag Build-Up

Table B-6. Military Folding Tiltrotor Cruise Drag Components

COMPONENT	DRAG COEFFICIENT (1g, 450 KTS, 25,000 FT)
Parasite Drag	0.02413
Induced Drag	0.00507
Compressible	0.0
Total	0.0292

Thrust required versus airspeed is shown in Figure B-51 as a function of altitude. The absolute magnitude of thrust required is less at 25,000-ft than at lower altitudes. Figure B-52 shows the ratio of power required to power available versus airspeed as a function of altitude.

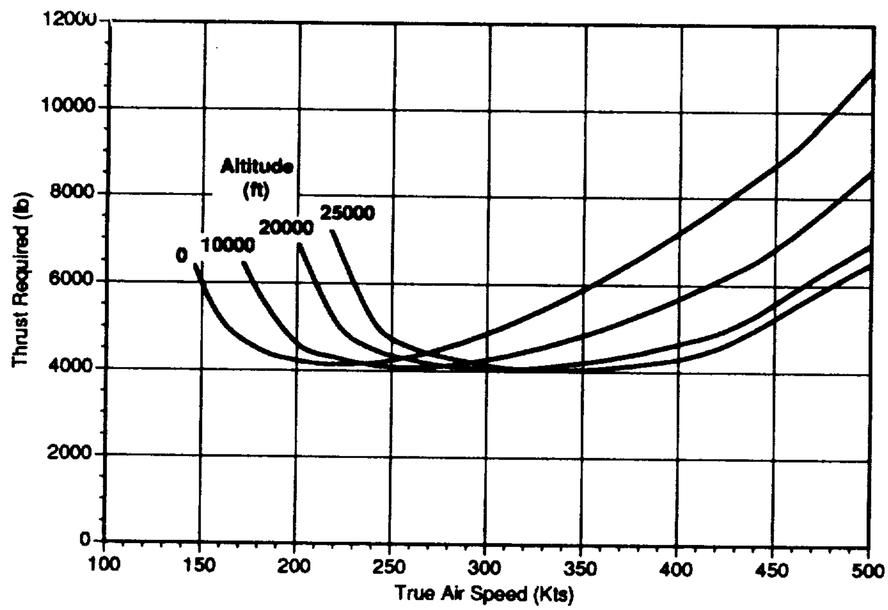

Figure B-51. Military Folding Tiltrotor Thrust Required (Standard Day)

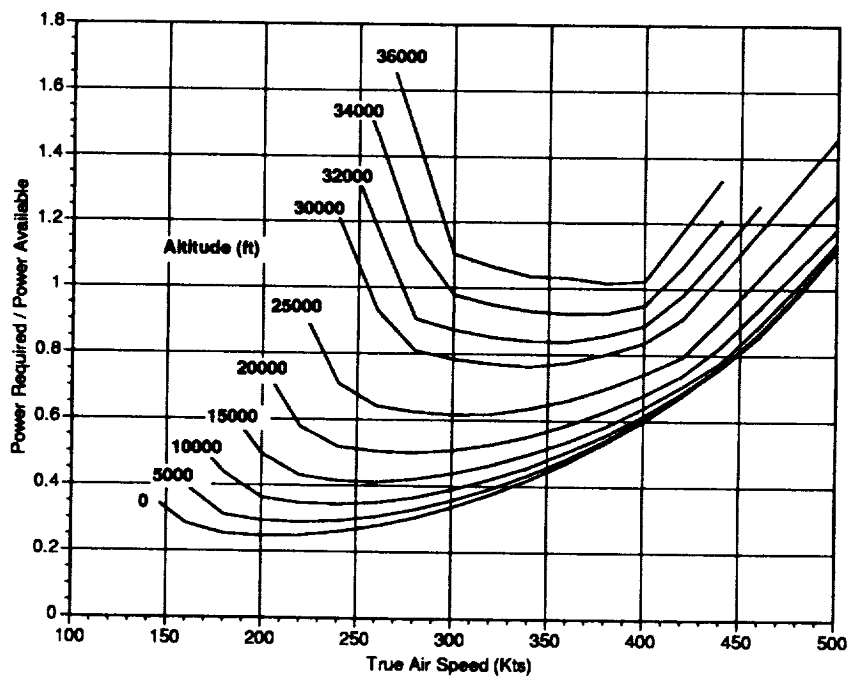

Figure B-52. Military Folding Tiltrotor Power Fraction vs. Speed

The percentage of lift sharing between the canard, wing, rotor & body, and tail surfaces was estimated and is shown in Figure B-53 at the stall speed and at the 450-knot cruise speed for both forward and aft CG limits. As for the civil tiltrotor, these calculations indicate a need to refine the canard design to decrease the amount of load it carries in the cruise mode. An 18% canard load suggests significant downwash on the main wing, which would almost certainly increase the main wing's induced drag. This area needs further development.

		LIFT / GW			
SPEED	CG	CANARD	ROTOR + BODY	WING	TAIL
Stall ($\delta_F = 0$)	Fwd (C_L)	14.4% (2.20)	6.9%	73.6% (1.60)	5.2% (0.51)
	Aft (C_L)	10.5% (1.62)	6.9%	73.6% (1.60)	9.0% (0.89)
450 Knots	Fwd (C_L)	18.5% (0.27)	0.5%*	77.4% (0.16)	3.6% (0.03)
	Aft (C_L)	14.6% (0.22)	0.5%*	77.4% (0.16)	7.5% (0.07)

*ROTORS STOWED

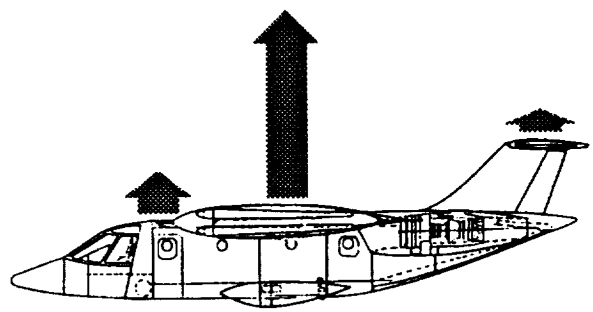

Figure B-53. Military Folding Tiltrotor Airplane Mode Lift Sharing

The rate of climb capability is shown in Figure B-54 for both standard day and ISA + 15° C ambient conditions.

Flight Envelopes

The flight envelope is shown is Figure B-55 for several values of normal load factor. The sustained maneuver envelope of Figure B-56 shows that the folding tiltrotor can meet or exceed the design criteria set forth in the main text, see Figure 43.

A continuous accelerated flight from hover to cruise is one of the strong suites of the folding tiltrotor concept. Figure B-57 shows a typical acceleration from hover to 140-knots, in turboprop mode, taking about 15 seconds. This level of performance is only slightly better than that demonstrated by the V-22. Transition to the turbofan mode should require another 6 seconds for rotor stopping and blade folding, as demonstrated by Bell and Boeing Helicopters scale model wind tunnel tests from the early 1970 time frame. Longitudinal acceleration may be continued during this transition so long as airspeed does not exceed the design airspeed for folding (about 250-knots). Figure B-57 shows an accelerating climb for the turbofan mode of operation, following transition. The folding tiltrotor could achieve a 400-knot airspeed in level flight at IRP power in slightly over 2 minutes from takeoff. Alternatively, at an 8-degree climb angle, it could reach about 270-knots and 8000-ft in just under 3 minutes after takeoff.

Based on Boeing's early test programs of scale model rotor blade stopping and folding, blade loads are not expected to be a hindrance to maneuver capability during transition to the turbofan mode.

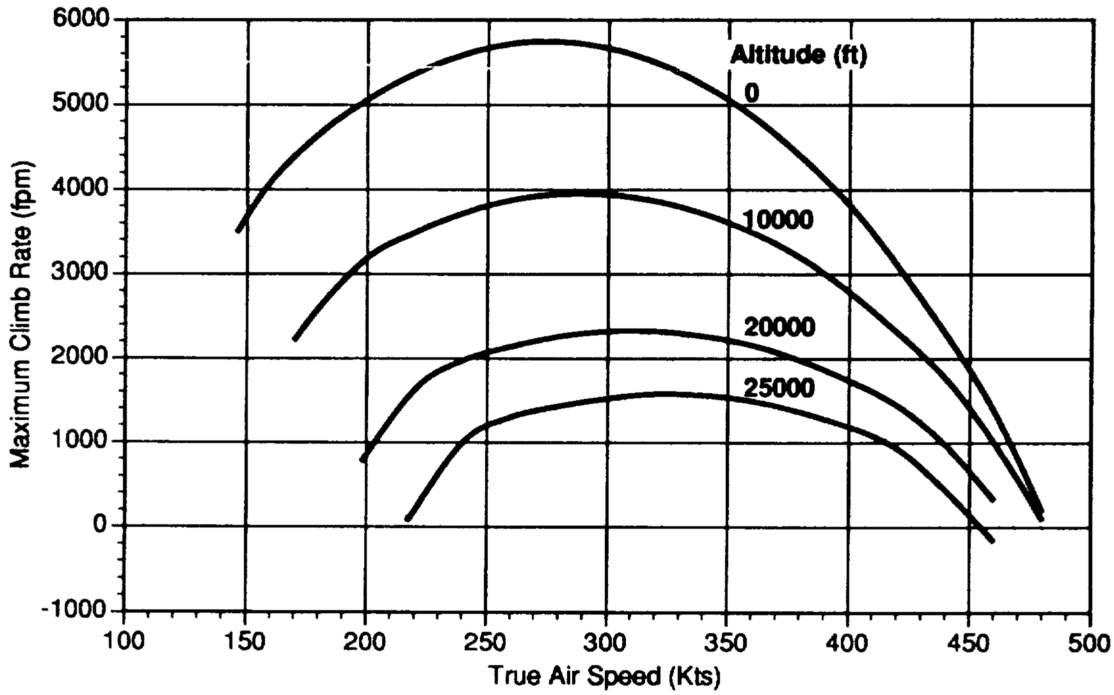

(a) Standard Day

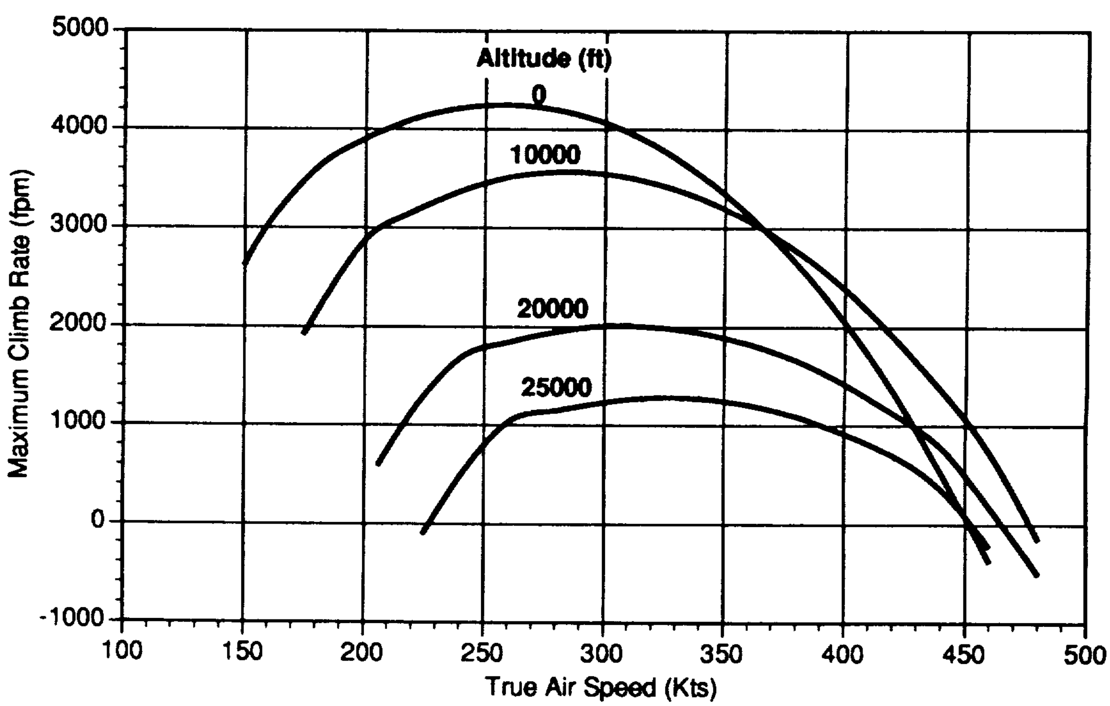

(b) ISA + 15°C Day

Figure B-54. Military Folding Tiltrotor Maximum Rate-of-Climb Capability

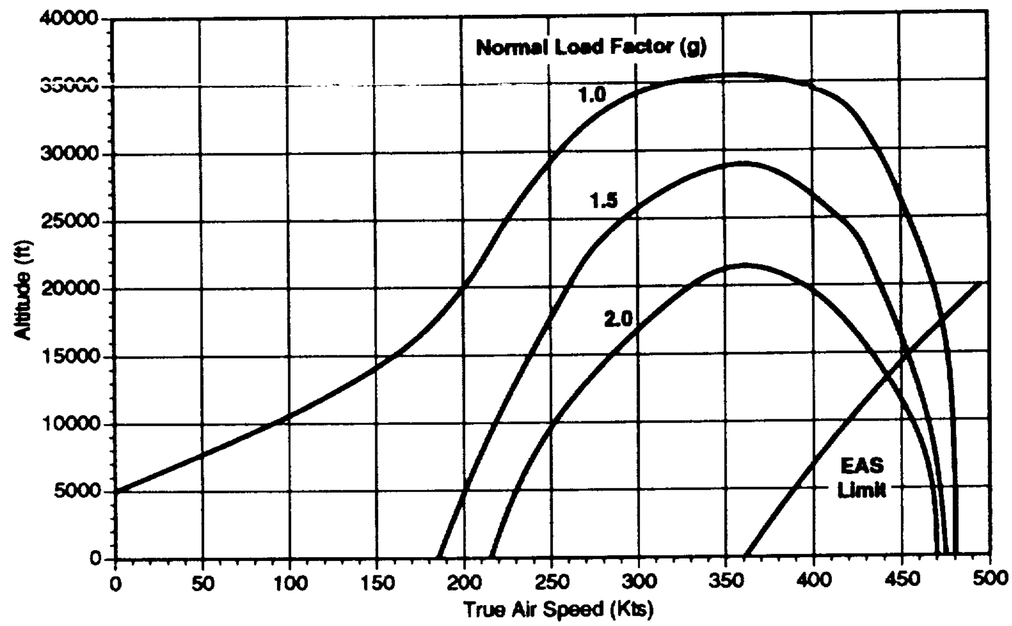

Figure B-55. Military Folding Tiltrotor Flight Envelope (Standard Day)

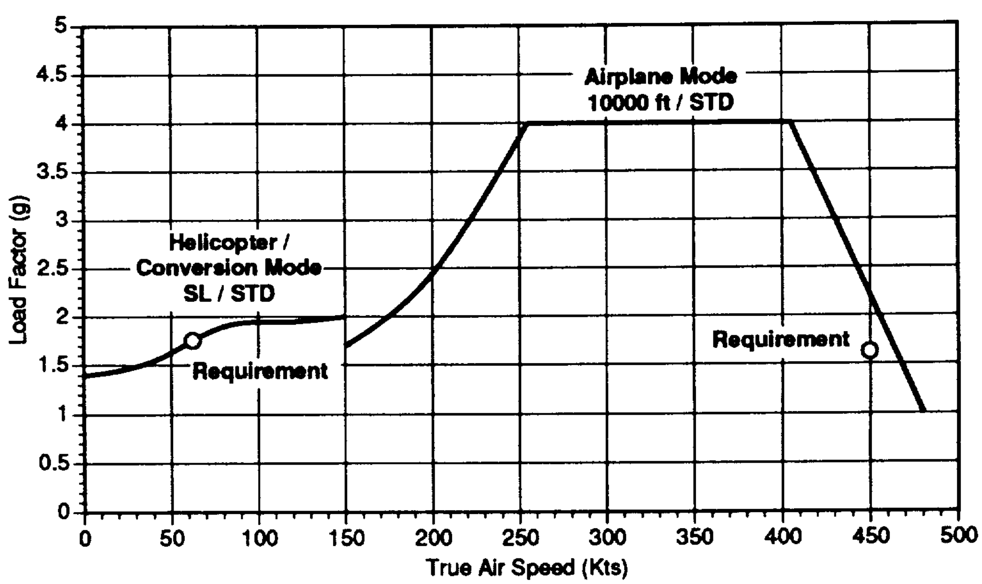

Figure B-56. Military Folding Tiltrotor Sustained Maneuver Capability

In general, these early tests identified that about 3 seconds were required to fold the blades back along the nacelle, requiring a total of about 6 seconds to be devoted to the stop/fold process. Development of an automated and reversible stop and fold process is one of the critical design issues discussed in Section 3 of the main report. Normal rotor blade design criteria would allow up to about 3-g loads (non-rotating), which would be within the maneuver capability of this military transport in the folding speed range from 140-knots to 220-knots, see Figure B-56. Higher maneuverability requirements normally associated with attack and tactical rotorcraft designs would have to be examined in more detail, considering the significance of the 6 second transition to total mission survivability. The rotor system and fold procedure would then be designed to the required operational capability.

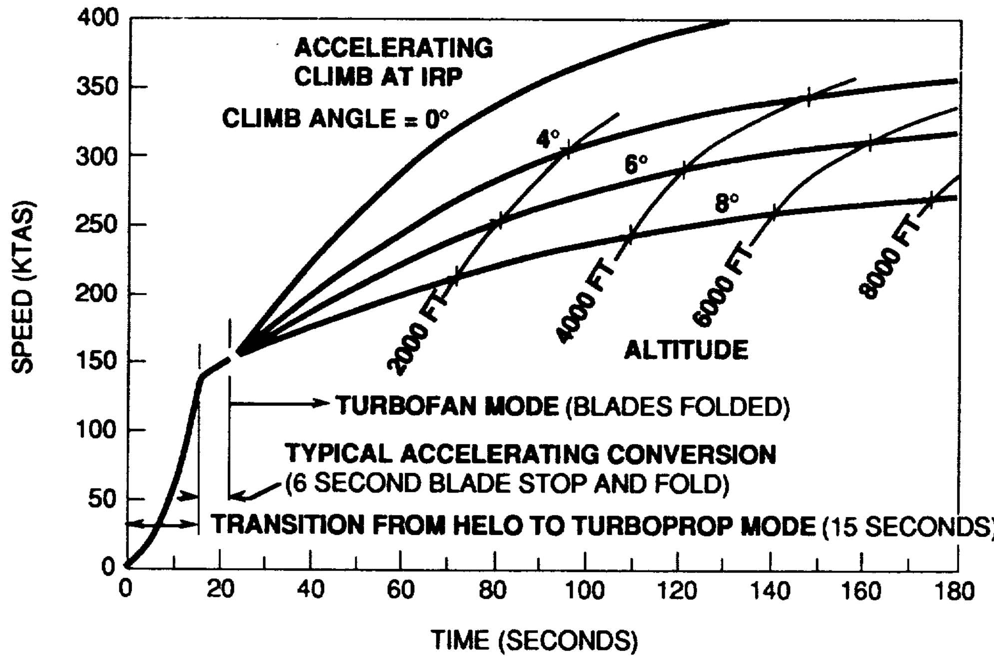

Figure B-57. Accelerating Transition, Conversion and Climb for the Military Folding Tiltrotor

Payload-Radius Curves

Figure B-58 shows the payload-radius curve for the military folding tiltrotor. It meets the design point of 6,000 pounds of payload at a 350-nm radius.

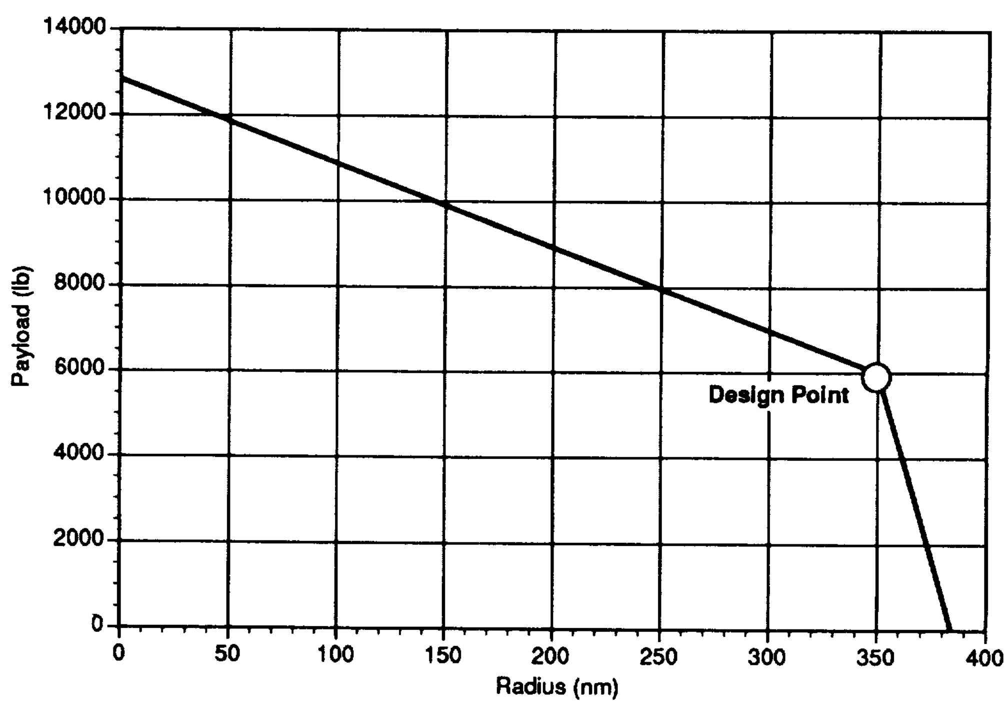

Figure B-58. Military Folding Tiltrotor Payload-Radius

Short Takeoff Performance

Short takeoff performance for the military folding tiltrotor is similar to the civil tiltrotor in every respect, except power. Whereas the civil tiltrotor had a prop-rotor and transmission designed for both hover power requirements and 450-knot cruise power requirements, the folding tiltrotor's transmission was sized only for hover. This is offset by the excess thrust available from the convertible engine when in the shaft power mode. The excess thrust is a significant benefit for STO by shortening the length of runway required for takeoff. Figure B-59 shows the percentage increase in useful load for STO operations. A 30% useful load increase requires only a 350-foot ground roll and a 750-foot distance to clear a 50-foot obstacle. This 30% useful load increase corresponds to about 5,200 pounds, or an 86% increase in payload.

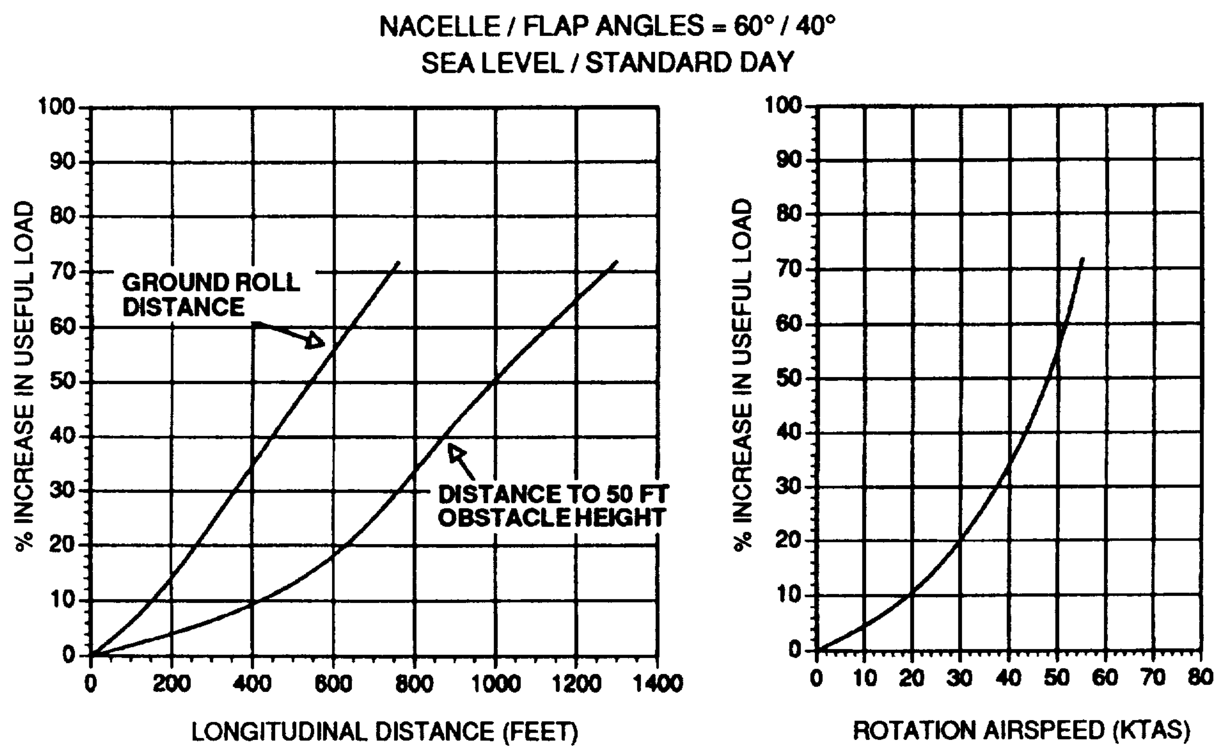

Figure B-59. Rolling Takeoff Performance - Military Folding Tiltrotor

Military Folding Tiltrotor Propulsion System

Drive System Description

A schematic diagram of the folding tiltrotor drive system layout is shown in Figure B-60. The 30-degree wing sweep of the folding tiltrotor requires an extra gearbox at the wingtip for proper alignment of the tilt-axis gearbox.

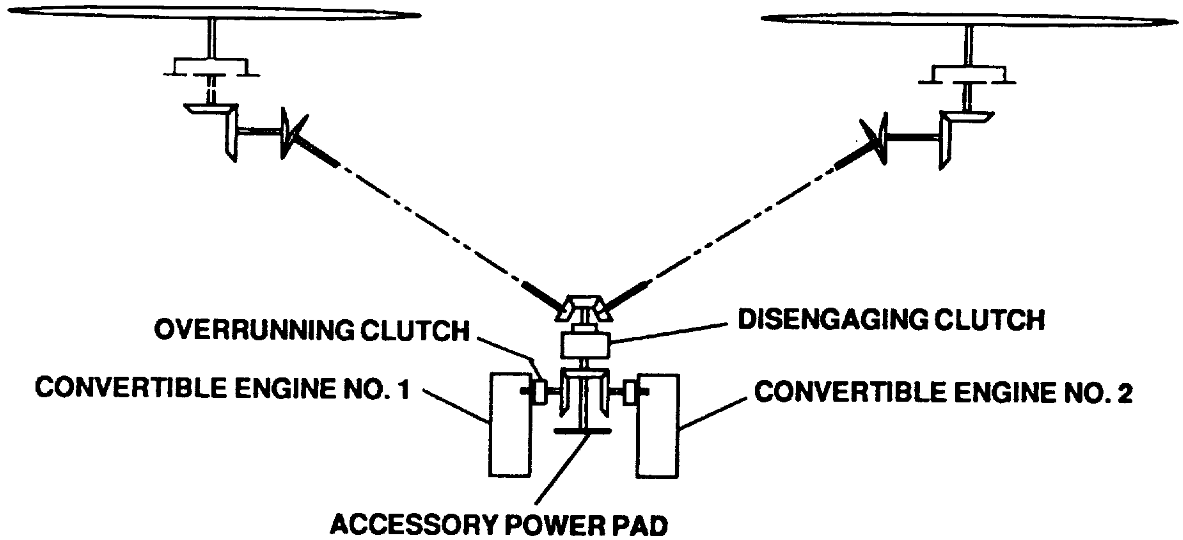

Figure B-60. Military Folding Tiltrotor Drive System Schematic Diagram

The two convertible engines are mounted on the sides of the fuselage. This small lateral thrust offset allows controlled flight in the turbofan mode in the event of a single engine failure. A single point disengaging clutch provides power transfer from the engines to the rotors. This single point power transfer eliminates the possibility of the clutch delivering power to only one rotor, which is possible by a single failure in a two clutch arrangement. Accessory power is taken from a power takeoff pad on the combining gearbox. Overrunning clutches on each engine allow for a single engine to drop off-line without disrupting continuous power transfer from the remaining engine.

Engine Characteristics

The propulsion system for the military folding tiltrotor is a convertible turbofan-turboshaft engine providing output shaft horsepower during hover, combined power and thrust during conversion to forward flight, and thrust during the cruise mode of operation. The powerplant has variable fan inlet and exit guide vanes (VIGV/VEGV) which minimize airflow through the fan flow passages during shaft operation, while the hub section of the fan rotor blade still supercharges the core gas generator. Some fan airflow is permitted during shaft operation to absorb the heat generated by windage losses in the fan, and this contributes to the residual thrust of the convertible engine while producing shaft horsepower.

The baseline convertible engine technology is consistent with 1990 turbomachinery technology leading to an IOC in the year 2000.

- Design-point thrust specific fuel consumption (S.L., 86°F, M=0), TSFC = 0.405 lb/hr/lb thrust
- Design-point thrust-to-weight ratio, = 6.1 lb thrust/lb weight
- Design-point thrust/shp = 1.47 lb thrust/shp

Installation Losses

The convertible engines are mounted in free-standing nacelles, close coupled to the aircraft fuselage. The only losses associated with the installation are assumed to be the losses in the VIGV/VEGV during hover and conversion operation, and these losses are inherent in the stated performance of the engine.

Turboshaft Performance

Installed power available at the maximum (10 minute) rating is presented in Figure B-61. Sea level, ISA maximum power is 7,785 shp.

The aircraft drive system limit is 10,390 rotor horsepower, at the rotor shaft, 5195 rhp per side, which corresponds to a larger value of engine shaft horsepower. Figure B-61 illustrates that the aircraft is drive-system limited below 10,000-ft altitude.

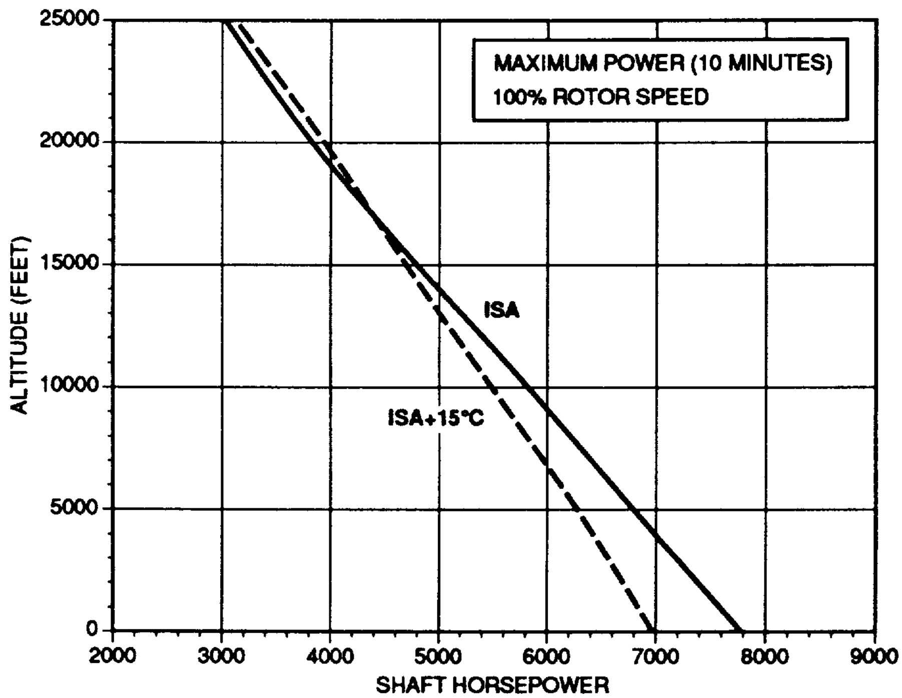

Figure B-61. Convertible Engine Maximum Installed Shaft Horsepower

At the relatively high powers for hover at sea level, 86°F, the shaft SFC is essentially constant and equal to 0.598 lb/hr/shp. The residual thrust of the convertible engine during shaft power operation, M = 0, at sea level, 86°F, is presented in Figure B-62.

Turbofan Performance

Figure B-63 presents the net thrust of the convertible engine in the turbofan operating mode at the maximum continuous rating. Net thrust is plotted as a function of altitude to 25,000-ft, flight speed to 450-knots, at ISA and at ISA + 15°C.

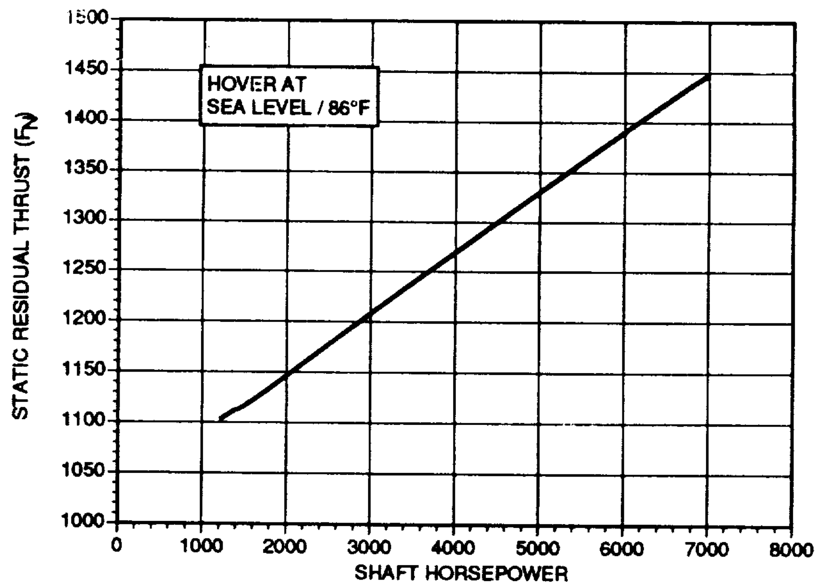

Figure B-62. Convertible Engine Static Residual Thrust

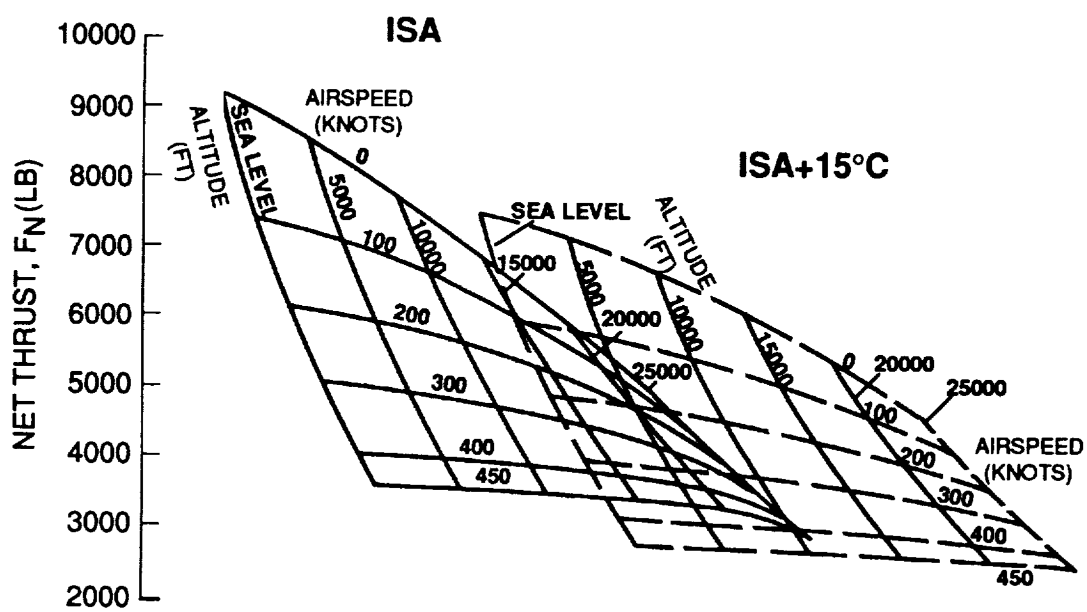

Figure B-63. Convertible Engine Maximum Continuous Thrust Available

Referred thrust specific fuel consumption, TSFC / $\sqrt{\theta}$, is presented as a function of referred net thrust and flight mach number in Figure B-64.

Conversion Mode Performance

Conversion mode performance of the convertible engine in the transition from shaft power to the rotor to thrust in forward flight is illustrated in Figure B-65. The convertible engine performance

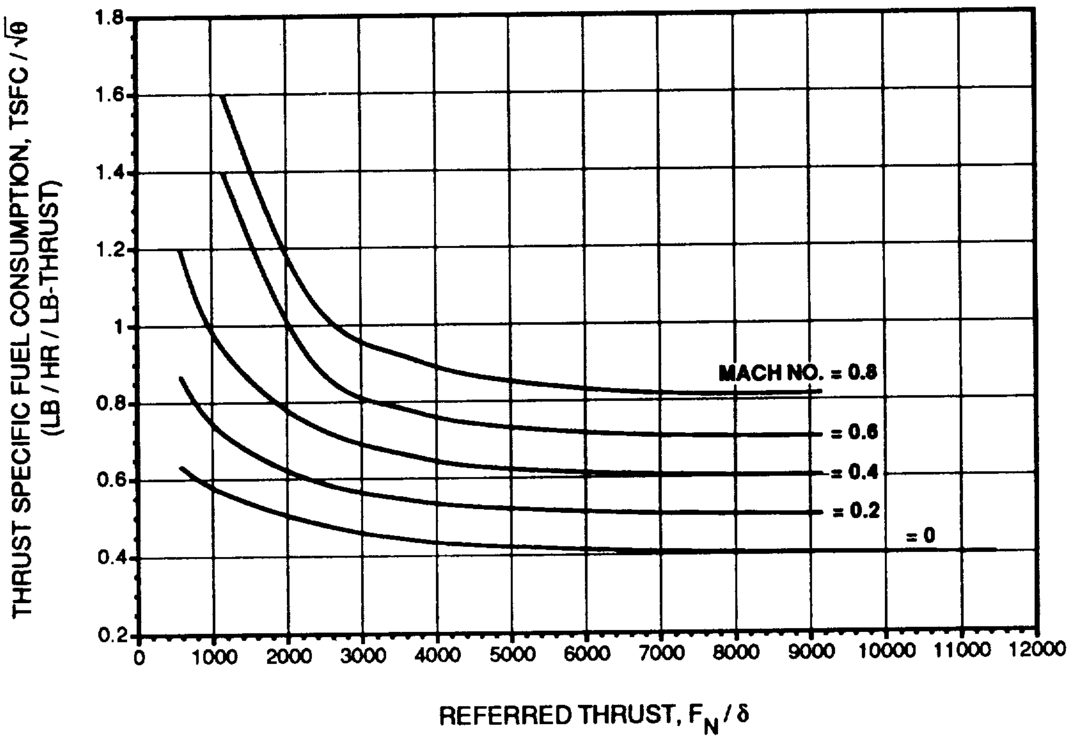

Figure B-64. Convertible Engine Thrust Specific Fuel Consumption

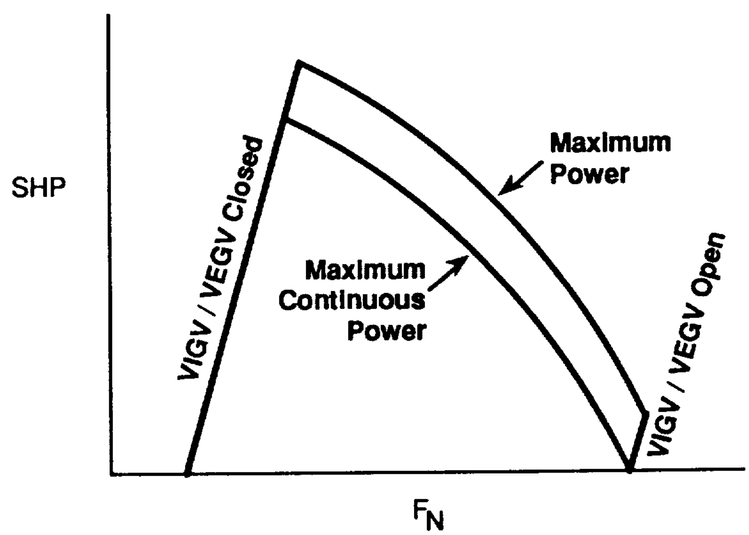

Figure B-65. Convertible Engine Conversion Mode Performance Diagram

envelope is bounded by the VIGV/VEGV closed line. The maximum rating shaft horsepower-thrust line, and the VIGV/VEGV open line for thrust performance. VIGV/VEGV and variable turbine temperature permit an infinite combination of thrust and shaft horsepower within these limits.

The military folding tiltrotor requires 2190-lb thrust and 975-shp during conversion, which is well within the performance capability of the convertible engine.

Relative Cost Analysis

Relative Life Cycle Cost (LCC) estimates were prepared for both military and civil high-speed configurations. (Refer to Appendix A, Task I Cost Comparison for a general discussion of LCC). Both cases examined 1990 and year 2000 technology scenarios. The baseline case for comparative analysis was the 450-knot configuration. The impact of enabling technology was assessed by estimating a year 2000 450-knot rotorcraft in comparison to the 1990 baseline.

Military and civilian configurations were estimated independently of each other. A relative comparison was made against the baseline design (the 1990 technology 450-knot configuration).

The LCCs used commercially available models to insure consistency. Research and Development (R&D) and Production costs were estimated with the PRICE H model. The PRICE-H model was supplemented with contractor developed cost estimating relationships for System Test and Evaluation (ST&E). Support Investment, i.e. Initial Spares, and Operating and Support (O&S) costs were estimated using the Modular Life Cycle Costs Model (MLCCM).

The impact of enabling technologies was assessed by applying the above methodology to the year 2000 450-knot configuration and comparing that to the 1990 baseline 450-knot design.

A summary of results was given in Section 2 of this report

Parametric Model Overview

Price-H Model

Widely accepted as a consistent predictor of cost, the PRICE-H model was the primary estimating model for this study. The model was developed by RCA and later acquired by General Electric. PRICE-H is commercially available on a time share basis. One of the strengths of the model is its database of industry average empirical factors. These factors are continually updated for advancements in technology. In addition, the user may calibrate his own database of complexity factors from actual program histories.

Actual histories for most Boeing Helicopter (BH) programs reside on the Executive Information Database. The databases are used to produce calibrated complexities for the PRICE-H model. BH developed a comprehensive set of complexity values derived from the V-22 Osprey, CH-47D and UTTAS programs. Depending on the definition of each Work Breakdown Structure (WBS) element, both calibrated and industry average complexity values were used.

Technological improvement trends are built into the PRICE-H model. The year of technological state controls the trend. The effect of the trend is to cause engineering and manufacturing processes to become easier over time. Thus, a consistent methodology for modeling technology improvement for the year 2000 450-knot aircraft was established, including the impact of design and manufacturing process improvements. In parallel, the reduction in aircraft weight made possible by enabling technology development was modeled.

System Test and Evaluation (ST&E) is not handled well by the PRICE-H model. Therefore, the model was supplemented with ST&E cost estimating relationships developed from the V-22 Osprey development program.

The key parameters required for the PRICE-H model are:

- Quantity
- Schedules for development and production
- Hardware geometry consisting of size, weight of electronic and structural elements, and electronic packaging density
- Amount of new design required and complexity of the development engineering task
- Operational environment and specification requirements for the hardware (distinguishes between MIL-SPEC airborne and FAA commercial)
- Type and manufacturing complexity of structural/mechanical and electronics portions of the hardware
- Fabrication used for production
- Technological improvement

MLCCM Overview

The MLCCM is a computerized parametric estimating methodology for predicting and conducting aircraft life cycle cost trade studies at the subsystem level during the conceptual and preliminary design stages of a new aircraft development program. The primary technical data sources for aircraft Life Cycle Cost Estimating Relationship (LCCER) development were the standard aircraft characteristics, group weight statements, technical orders, and the manufacturer of various aircraft developed in the 60s and 70s. The SAC charts were used to obtain data on engine design and performance, fuel and tankage, armament, loading and aircraft performance, development dates, etc.

The model is dependent on 122 discrete variables that comprehensively describe the performance, material, schedule and configuration of the aircraft under study. The cost estimating relationships are arranged in the general categories of airframe, avionics and engines and further subdivided by subsystem. Put another way, a unique cost estimating relationship was developed for each cost element by subsystem offering good visibility into potential cost drivers.

The model was used to estimate costs in the following support investment and O&S areas:

Support Investment	O&S
- Initial Spares & Spare Parts	- Maintenance Personnel, Aircrew
- Support Equipment Data	- Petroleum, Oil & Lubricants
- Training Equipment & Services	- Support Personnel
- War Reserve Material (Military)	- Logistics Support
	- Depot Supply Sustaining Investment
	- Replacement Raining Personnel

Life Cycle Cost Phases

A general discussion of Life Cycle Cost and its component parts was given in Appendix A, Task I Cost Comparison.

Research and Development

R&D areas estimated include Design, ST&E, Data, Prototypes and Tooling. All categories were estimated using PRICE-H except ST&E. Boeing developed cost estimating relationships for the ST&E estimate. Figures B-66 and B-67 summarize the results of the R&D estimates for both military and civil tiltrotors relative to their baselines.

Military - Figure B-66 depicts R&D comparisons relative to the 1990 technology 450-knot baseline for the 350 knot, the 500 knot and the year 2000 technology 450-knot military configurations. The 350-knot configuration showed a 11% decrease in R&D costs, the 500-knot configuration showed a 13% increase in R&D costs and the year 2000 technology 450-knot configuration showed a 3% increase in R&D costs.

Civil - Figure B-67 depicts R&D comparisons relative to the 1990 technology 450-knot baseline for the 350 knot, the 500 knot and the year 200 technology 450-knot civil configurations. The 350-knot configuration showed a 13% decrease in R&D costs, the 500-knot configuration showed a 33% increase in R&D costs and the year 2000 technology 450-knot configuration showed a 8% increase in R&D costs.

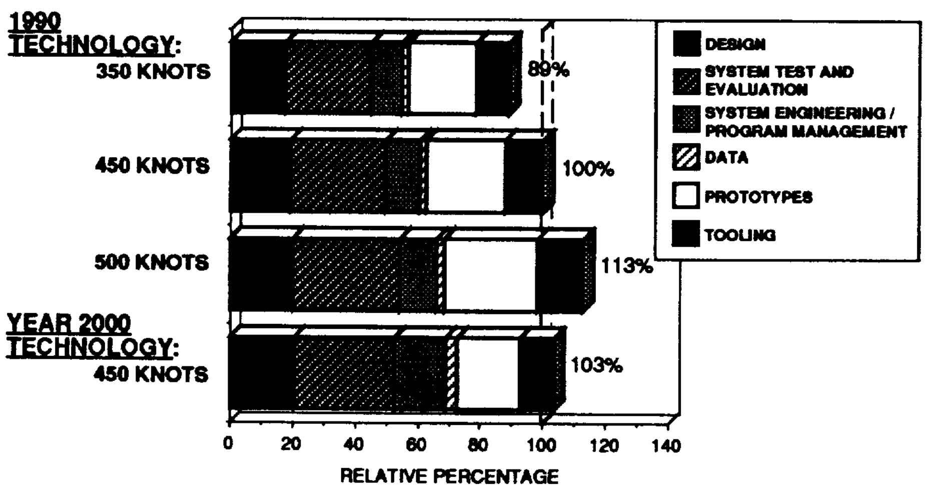

Figure B-66. Military Folding Tiltrotor Research and Development Cost

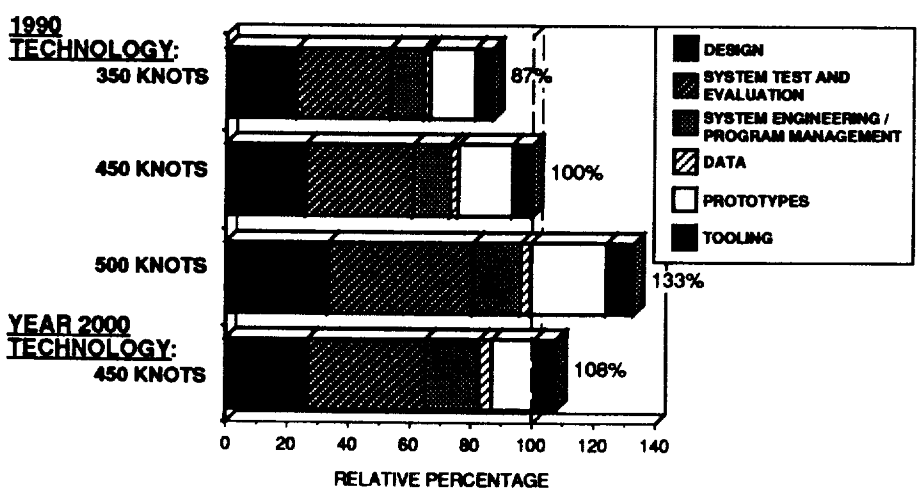

Figure B-67. High-Speed Civil Tiltrotor Research and Development Cost

Production

Military - Figure 75 in the main text gave recurring production cost comparisons relative to the 1990 technology 450-knot baseline for the 350 knot, the 500 knot and the year 2000 technology 450-knot military configurations. The potential savings in production costs due to development of enabling technology, are great. For military programs, a year 2000 technology 450-knot configuration yielded cost savings of 30% under the 1990 technology 450-knot baseline. In comparison, the 350-knot 1990 technology configuration saves 14%, while the 500 knot 1990 technology configuration increases costs 24% over the baseline. In essence, enabling technologies allow development of a year 2000 technology 450-knot high-speed rotorcraft costing less than the 1990 technology 350-knot high-speed rotorcraft.

Civil - The same trend is evident for the high-speed civil tiltrotor in Figure 77 of the main text. The year 2000 technology 450-knot configuration yielded a 31% reduction in production costs over the 1990 technology 450-knot baseline. In comparison, a 15% reduction in production costs was evidenced for the 350-knot configuration while the 500-knot configuration had an increase in production costs of 51%.

Figure 69 of the main text showed the relationship of production costs to aircraft power and empty weight. All results were plotted relative to a 450-knot 1990 technology baseline. For both military and civil configurations, increases in production costs track to increases in weight, which is driven by power. Therefore, enabling technologies that reduce weight are desirable.

Effect of Enabling Technologies on R&D and Production

Military - All comparisons are relative to the military 1990 technology 450-knot baseline configuration. Assuming that enabling technologies are funded and developed between the present and year 2000, a net increase of 3% in Research and Development costs can be expected. This 3% increase was comprised of an 8% rise in nonrecurring and a 5% cost reduction in prototype cost. Production costs experience a net cost reduction of 37%.

Civil - In comparison to the civil 1990 technology 450-knot baseline configuration, a net R&D increase of 8% was comprised of an 11% increase in nonrecurring and a 3% decrease in prototype costs. Production costs experience a net cost reduction of 25%.

As evidenced by the above two paragraphs, continued investment in aerospace technologies between 1990 and the year 2000 will result in substantial cost benefits early in the life cycle.

Support Investment

Airframe support investment costs are largely functions of takeoff maximum gross weight (Data), fuselage volume (support equipment), total wetted area and maximum speed (initial spares). Engine support investment is a function of total thrust (data); engine thrust to weight ratio (support equipment); engine production cost and spares factor (initial spares); and avionics weight and fuselage density (training equipment). The total thrust of an engine is a measure of engine size, complexity and sophistication. The more complex engine requires more data. Similarly, thrust/weight ratio is directly related to complexity and therefore the number of repairs on engine is likely to have. The number of repairs is related to the amount and type of support equipment required. This type of explanation and reasoning is generally consistent throughout all cost elements.

Military - Significant variation was found in the initial and engine spares among the four variants examined. The recurring unit production cost drove initial engine spares in the analysis. Spare engines and engine modules were 38% lower in the 350-knot configuration, relative to the baseline, and 39% higher in the 500-knot configuration. All other support investment elements' costs varied less than 5% above or below the baseline value. A significant reduction in cost was also noted when the year 2000 technology 450-knot configuration was analyzed. Though marginally higher costs were indicated for data and support equipment, overall support investment costs for the year 2000 technology aircraft were lower than the baseline. A larger (16%) total wetted area and higher engine thrust in the baseline design were the primary cost drivers. War Reserve Material is estimated at a constant 30% of initial spares.

Civil - The basic trend in the support investment costs of the civil configurations was similar to that exhibited by the military aircraft. Overall support investment costs were 8% lower in the 350-knot configuration and 19% higher in the 500-knot configuration compared to the baseline aircraft. For the 350-knot configuration, data and support equipment indicated a reduction of less than 1% from the baseline, initial spares contributed a 5% reduction and engine spares a 41% reduction. The civil transport powerplant maintains a relatively high technology when compared to its military counterpart as a function of high thrust-weight ratios achieved at a lower turbine inlet temperature. Engine production cost (a key variable in estimating repair parts cost) is a function of engine thrust which, in the case of the 350-knot civil aircraft, decreases 45% from the baseline. The 500-knot aircraft reflects a thrust increase of 126% over the baseline with the associated increase in engine spares accounting for 106% growth. Overall, engine spares and parts accounted for 69% of the support investment cost differential between the 500-knot aircraft and the 450-knot baseline.

The year 2000 technology 450-knot civil configuration reflected higher data (14%) and support equipment (30%) but somewhat lower initial spares cost.

Operating and Support

O&S costs are estimated in the three categories indicated for support investment, namely airframe, avionics and engine. Maintenance related costs are further estimated at the subsystem level. Aircrew costs are estimated as a function of crew size and quantity of aircraft. Utilization rate, a key parameter in O&S calculation, is a contributing factor to command staff (military) and management/administrative staff (civil). Support personnel are a factored estimate off of the direct operator, maintenance and management costs predicted earlier.

Military - O&S costs for the military were generally quite stable fluctuating approximately ±10% around the baseline. The 350- and 500-knot designs varied marginally 6% below and 8% above the baseline aircraft, respectively. Fuel consumption in 350-knot configuration was 23% below that found in the 450-knot baseline. Conversely, the 500-knot configuration had 23% higher consumption accounting for comparable movement in fuel cost. Other O&S cost had similar, albeit smaller movements. The year 2000 technology 450-knot rotorcraft was 7.5% less expensive generally due to lower specific fuel consumption.

Civil - O&S costs for commercial aircraft were markedly higher on the basis of utilization rate (1,936 hours versus 240 hours per year per aircraft). Variation in O&S costs among variants was more pronounced; a 16% increase in O&S for the 450-knot aircraft relative to the 350-knot aircraft. A 33% increase was indicated for the 500-knot configuration. Contributing factors include a 45% increase in specific fuel consumption coupled with a 226% increase in thrust per engine. Year 2000 technology gave a 15% decrease in O&S cost over the system life cycle.

Materials and Manufacturing Methods

The structures challenge for high-speed civil tiltrotors is to combine the attributes of several competing technologies such as materials, manufacturing and design-to-cost into a single structural concept. The resulting concept must achieve its goal to maximize its structural performance at minimum cost and weight. Lightweight, minimum gauge structure is required for VTOL characteristics. Manufacturing defects and impacts which occur in in-flight and service environments mandates that low velocity damage tolerance be a part of the design. Military applications must provide for special features integrated into the structural design. Acquisition and operating costs determine the economic health of any concept.

Materials and process improvements can accommodate the competing requirements for lightweight and damage tolerance, however, the current costs are high. Reliability, in the form of defect tolerance, will limit the performance of lightweight structure by limiting the strains. Improved confidence in design methods for airframe structures are required before the long-sought improvements in performance can follow. State-of-the-art design concepts for VTOL (Vertical Take-Off and Landing) structures have not taken full advantage of potential material improvements. More development is needed to establish confidence in design of two-dimensional laminated composites in three-dimensional structural applications. Therefore, new aggressive methods for design and analysis, which reduce the risk of out-of-plane loading in laminated composites, must be developed and validated in order to provide a solution for high-speed rotorcraft.

The application of new materials and manufacturing methods usually requires a prototype program. This by itself still falls short of validating the production costs of new systems because the total number of aircraft built seldom extends to the amounts required to take full advantage of the learning curve. The question as to whether any real improvements are realized in a prototype program will tend to limit the application of new structures manufacturing concepts into existing programs. How, then, can the structural design process proceed in parallel paths for the application of new technologies with those of the other essential elements for aircraft development?

The answer lies in the aggressive use of materials and methods which have exhibited the potential for high payoff at an acceptable level of risk. This idea goes against current thinking of very low-risk in an effort to guarantee the initial success of any new program. Under the current business climate, the rate of failure for full-scale prototype aircraft is expected to be zero or at most, extremely low. The corresponding rate of improvement might, therefore, be lower still due to the lack or risk-taking in the design. Critical areas for technology improvements are identified below and should be worked in the near term in order to reverse the trend away from progress in small steps.

New materials such as pitch fiber composites with higher moduli (55-100 Msi) than is the current norm for polyamilnitrile (PAN)-based fibers (30-40 Msi) should be investigated for forward swept wing application. The higher moduli will be beneficial for stiffness-critical wing design. The corresponding lower strain-to-failure of pitch fibers will have to be addressed. One possible solution lies in the use of hybrid materials which increase the moduli of the laminates while, at the same time, have acceptable strength margins. The same holds true for new resins such as thermoplastics and polyimides, which exhibit an improved damage tolerance to low velocity impacts. The lack of improvements in the compression strengths of these resins should be addressed especially in light of the fact that vastly differing values for compression strengths are derived from test specimens, which have differing geometries.

The correlation to coupon-level strength data to composite structures strength should be addressed in order to assess the effects of material allowables on the design and analysis process. A series of design concepts, which take full advantage of the in-plane properties of two-dimensional composites without the corresponding penalty for low out-of-plane strengths, should be developed.

Pure monocoque shells and improved postbuckled structures should be investigated. Membrane loading has usually been ignored in favor of the simpler differential bending approach in the design of structures, probably owing to the degree of confidence and experience in the latter. This single change can be a starting point for high-speed rotorcraft structures development. Improvements in the ability of the material to efficiently carry loads should be matched by methods to fabricate those components at low cost. All approaches must examine the processes and materials to be used in manufacture of the parts. Large, monocoque structures can eliminate fasteners and stress risers because the number of subassemblies are reduced. However, on the other hand, these large modules often require new and normally expensive process tools and equipment. Therefore, in order to create the right mix of new design developments and low producibility costs in manufacture, there is an urgent need to assess the most promising tooling and fabrication techniques for high-speed rotorcraft.

A case in point is given in the current NASA structures initiative (ATCAS) program in which Boeing is a major contractor. Clearly, for the aircraft studied under this NASA sponsored research, the use of new material systems is probably not the most cost effective from a manufacturing standpoint. Performance and cost attributes must be traded against manufacturing considerations to determine which combination of materials and processes will provide the right mix to optimize the design development. The use of textile composites holds great promise in this area as evidenced by its visibility on the ATCAS program. Boeing has begun to pursue this technology in both IR&D and contracted research efforts in order to support its inclusion in new aircraft design. The high-speed rotorcraft can leverage a large portion of this work into improved concepts for structure design and manufacture.

Ultra-Lightweight Design - The high-speed requirement for this program will force new, thin skin approach to the structure design. At the same time, the requirements for damage tolerance are expected to increase. Therefore, the design concept may be forced to erase the oxymoron of damage tolerant gossamer structures. This becomes more of a problem when embedded electronics are placed in the skins to widen the view angles for avionics and antennas. This mix of non-impact tolerant electronics and thin skins tends to further reduce the durability of the structural concept by the inclusion of defects in the materials as part of the manufacture process. Again, as is the case for almost all developmental programs, the criticality of defects in composite structures must be investigated and understood prior to the start of any design efforts.

Accessibility - The inclusion of access doors in the structure must be given a new approach in order to reduce weight and improve reliability. The use of load transfer cams and pre-fitted openings for all access should be considered as a first step. Numerous deign concepts proposed for LH should be studied for high-speed rotorcraft application.

Smart structures - These can be divided into at least two categories and probably many more. The active control of structural shape comes first to mind as does the use of embedded sensors to monitor loads, damage or fatigue. Electronic repackaging of sensors which are non-structural such as conformal antennas or windows located in the structure form another type of smart structure. For high-speed rotorcraft, this area must be addressed in order to eliminate much of the VTOL aircraft maintenance and improve reliability. NASA and university research into the use of embedded materials such as thin films or metallic shape-memory alloys provides the most useful insight into the technology available for structural skin and damage modeling from sensor inputs. The high-speed rotorcraft program should leverage these technologies into new approaches for skins and internal elements.

Design and Analysis - New concepts described earlier and being developed as part of the NASA ATCAS program will be included in the structures design development for high-speed rotorcraft. Integrally stiffened skins which use textile technologies and near net-shape preforms are part of the current Boeing program studies. Three-dimensionally reinforced composites are under study for improved performance. However, the analytical tools needed for the successful application of 3-D composites into aircraft structures are still in the infancy stage and need to be developed as part of an overall program requirement. The same applies to the development of material mechanical properties, which often are used to validate the actual design rather than to enhance the accuracy of predictive models which were used in the initial design and analysis.

These are the prime candidate structural technologies, which should be considered in the design process for high-speed rotorcraft. The most effective design exercise would be to apply these ideas in a prototyping experiment for new structures and materials concepts. Although producibility may not be adequately addressed by this approach, certainly the majority of structures design and analysis issues identified above could be studied in enough detail to determine their relative worth as a high risk/high payoff candidate.

Acoustic Analysis

High-Speed Civil Tiltrotor

ICAO Noise Levels

The tiltrotor has many varied options for approach, flyover and departure methods which could be used to reduce or redistribute noise. For the purpose of this report, the helicopter certification procedures have been followed. The resultant predictions show that the levels required for ICAO certification can be met by the tiltrotor, though consideration to engine noise and blade-vortex interaction noise is required. Results for the high-speed civil tiltrotor were summarized in the main body of the report, Section 2, Table 10.

Departure Noise Levels - The predicted departure EPNL (Effective Perceived Noise Level) for the high-speed civil tiltrotor with a normal engine installation was 101 EPNL, which is below the ICAO standard level of 102.5. The flight profile sound spectrum is presented in Figure B-68, as well as the centerline Perceived Noise Level time history. The ICAO procedure specifies that a microphone be placed in the flight path 1640 feet from the brake release point which has an altitude of 65 feet, and also two 500-ft sideline microphones. The EPNL time history shows that the rotor loading noise predominates, with the engine noise contributing only a small amount to the EPNL. The EPNL at each microphone was arithmetically averaged to arrive at the ICAO rating.

Flyover Noise Levels - The predicted flyover EPNL for the high-speed civil tiltrotor with a normal engine installation is 91 EPNL, which is well below the ICAO standard of 101.5. The ICAO procedure specifies that cruise mode is used in calculating 500-ft altitude flyover noise, so the airplane mode (0 degree nacelle angle) was used in calculating the flyover noise. A flight speed of 180-knots was used, according to the ICAO standard method of determining cruise speed. The flyover noise is dominated by the engine noise as shown by the acoustic spectrum of Figure B-69. The engine could be acoustically optimized either in design and/or with acoustic treatments. Assuming a modest engine noise reduction of 6-dB, the ICAO flyover noise would then be 84.6 EPNL.

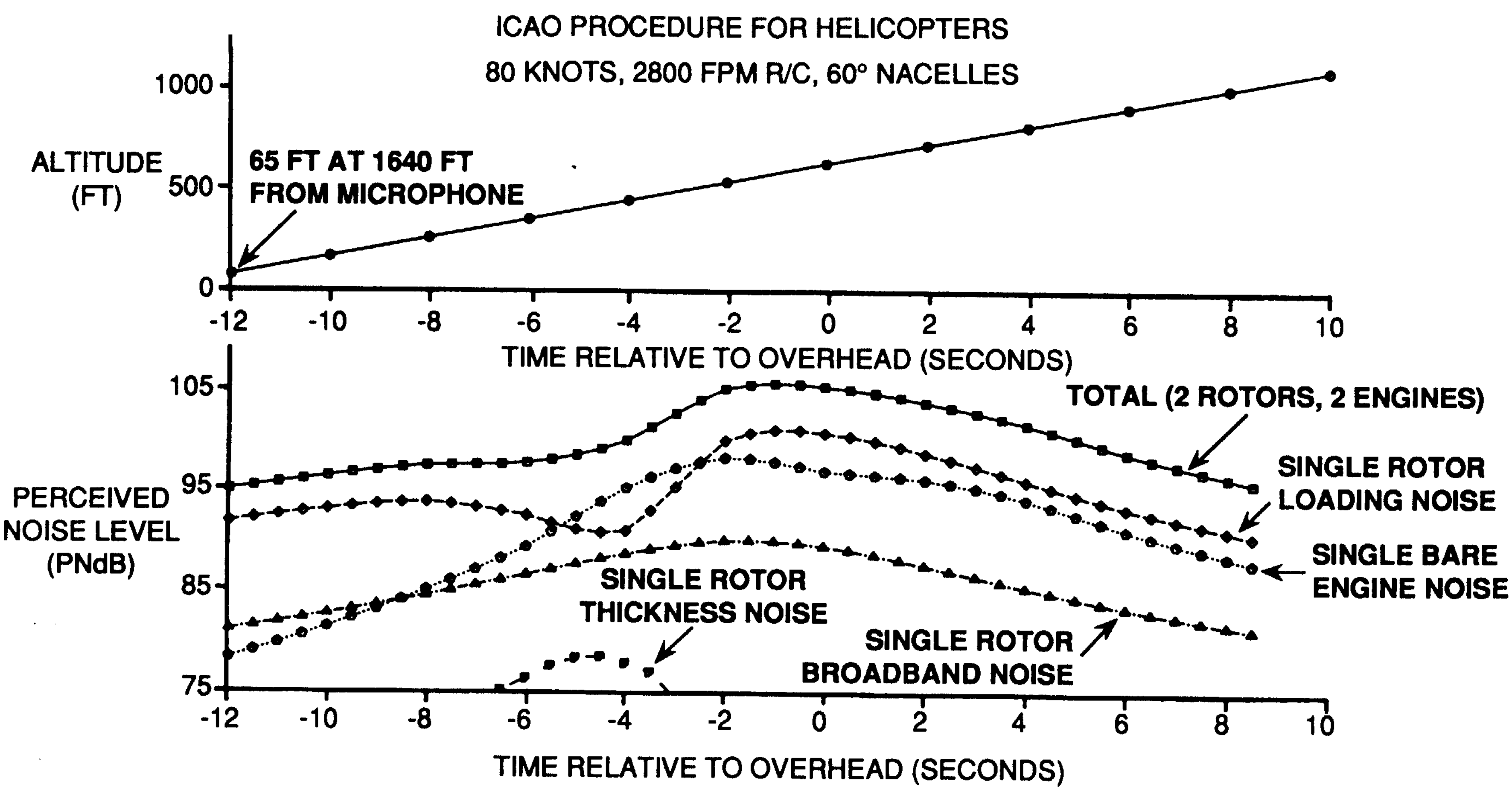

EFFECTIVE PERCEIVED NOISE LEVELS (EPNdB)		
WITH BARE ENGINE: **103**	WITH NORMAL ENGINE INSTALLATION: **101**	ICAO STANDARD: **102.5**

Figure B-68. Predicted Civil Tiltrotor Departure Noise Levels

ICAO PROCEDURE FOR HELICOPTERS

180 KNOTS, 500 FT ALTITUDE, 0° NACELLES

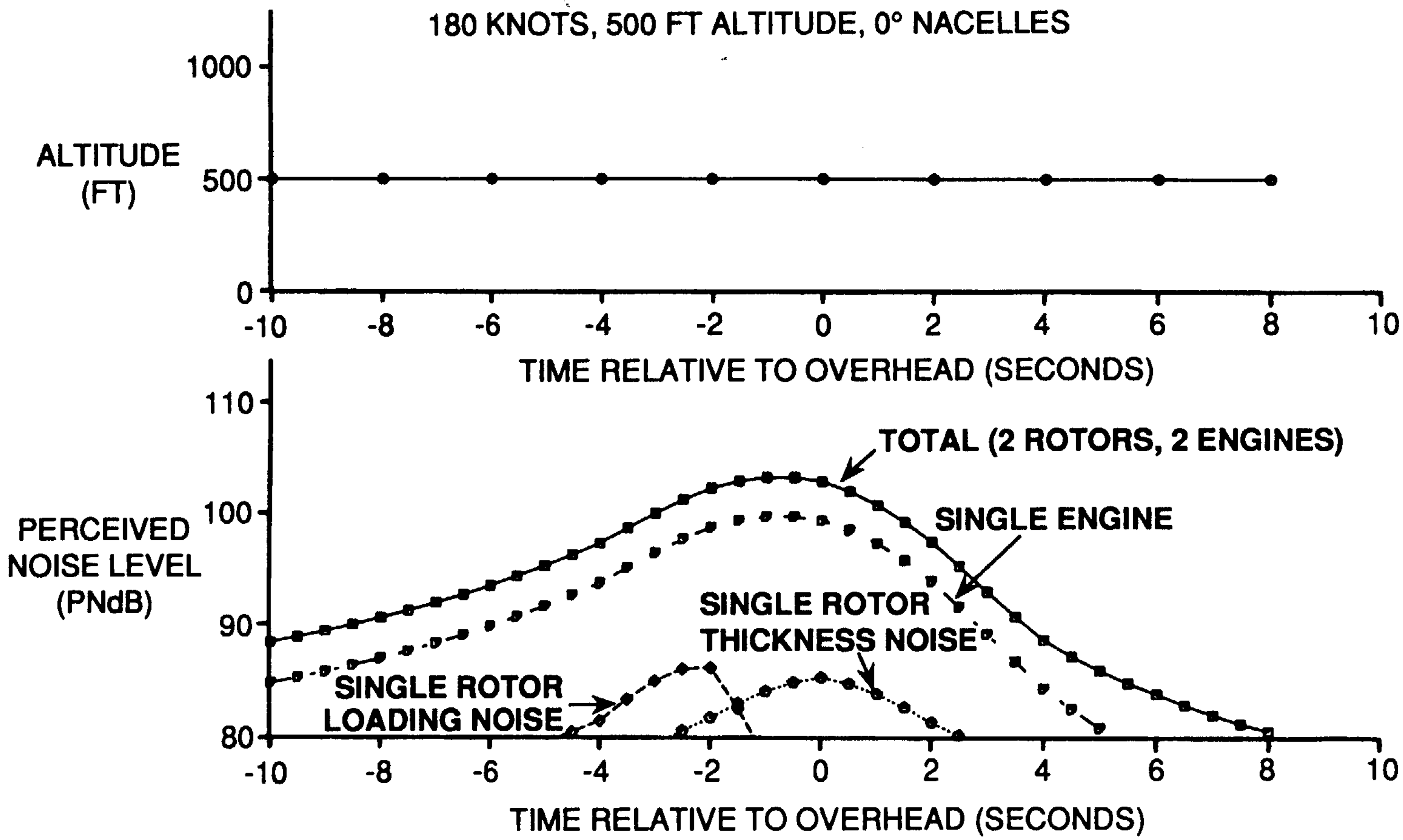

EFFECTIVE PERCEIVED NOISE LEVELS (EPNdB)			
WITH BARE ENGINE: 93.6	WITH INSTALLED ENGINE: 91.0	WITH TREATED ENGINE: 84.6	ICAO STANDARD: 101.5

Figure B-69. Predicted Civil Tiltrotor Flyover Noise Levels

Approach Noise Levels - The predicted approach EPNL for the high-speed civil tiltrotor with a normal engine installation and assuming no Blade-Vortex Interaction (BVI) noise is 103.7, which would nominally meet the ICAO standard level of 103.5. The ICAO procedure specifies that a 6-degree glide slope be used at the best rate-of-climb airspeed (80-knots for this design), and the centerline microphone be 490-ft below the flight path at overhead. Figure B-70 shows the predicted noise time history at the centerline microphone. The rotor loading noise is the dominant contributor to the EPNL, but the engine noise and blade-vortex interaction noise components are seen to be significant contributors. The engine noise can be reduced as discussed in the previous sections. Blade-vortex interaction noise results when a vortex from a preceding rotor blade are encountered by another blade. This situation can be encountered in descent conditions when the rotor wake can be swept up through the rotor disc. The tiltrotor has the potential of using a large number of possible operating modes and techniques to minimize or avoid BVI conditions. Possible noise abatement approach procedures could also reduce and/or redistribute the resulting noise 'footprint'.

Hover Sideline Noise

The predicted 500-ft sideline sound spectrum for the high-speed civil tiltrotor hovering at a 100-ft altitude is shown in Figure B-71. The engine noise, rotor loading noise, rotor broadband noise, and blade-vortex interaction noise are all seen to be contributors to the total noise levels. The resulting dBA and dBC levels were presented in Section 2 of the main body of this report.

Assuming normal engine installations, the total predicted levels with rotor BVI assumed is 90.5-dBA and 95.3-dBC. The engine used in the calculations has close inlet guide vane-to-rotor spacing. The engine compressor noise could be reduced by increasing this spacing, or inlet duct acoustic treatment could be considered. If a moderate reduction of 6-dB in the engine noise is achieved, then the predicted levels would be reduced to 88.1-dBA and 93.9-dbC. Further reductions in the sound pressure levels could be obtained by reducing the blade-vortex or blade-wake interaction noise. Preliminary investigation of devices which could be used to alleviate, delay the formation of, or displace trailed vortices were being investigated under a NASA contract by Boeing Helicopters (Reference B-5). Assuming reductions in the levels by engine acoustic optimization and BVI avoidance, the predicted levels would be reduced by 3-dBA and 2.5-dBC. If additional reductions were necessary, the rotor disc loading would have to be reduced. By going to a disc loading of 20-psf, the A-weighted rotor noise level would be reduced by 2-dBA, which would give an aggregate reduction of 5-dBA. To reduce the rotor noise level by 2.5-dBC, a disc loading of 1-psf would be required. A decrease in the disc loading to 20-psf would increase the rotor diameter by approximately 3.7-ft., and a reduction to 19-psf would increase the rotor diameter by 4.6-ft. Increases to the rotor diameter would also require an increase in wingspan and weight.

Military Folding Tiltrotor

Hover Sideline Noise - The predicted 500-ft sideline sound spectrum for the folding tiltrotor hovering at a 100-ft altitude is shown Figure B-72. The total third octave levels are shown, as well as the contribution by each component. The resultant levels with various combinations of acoustical improvements were summarized in the main body of this report, Section 2, Table 11. The resultant A-weighted level for the baseline design is 97.3-dBA. Since A-weighted levels give a greater weighting to high-frequency noise, the low-frequency levels produced by rotorcraft may not be adequately represented, so the C-weighted levels have also been included. The resultant C-weighted level for the military folding tiltrotor is 101.5-dBC. Both of these levels assumes a 'normal' engine installation where the engine is enclosed in an untreated nacelle.

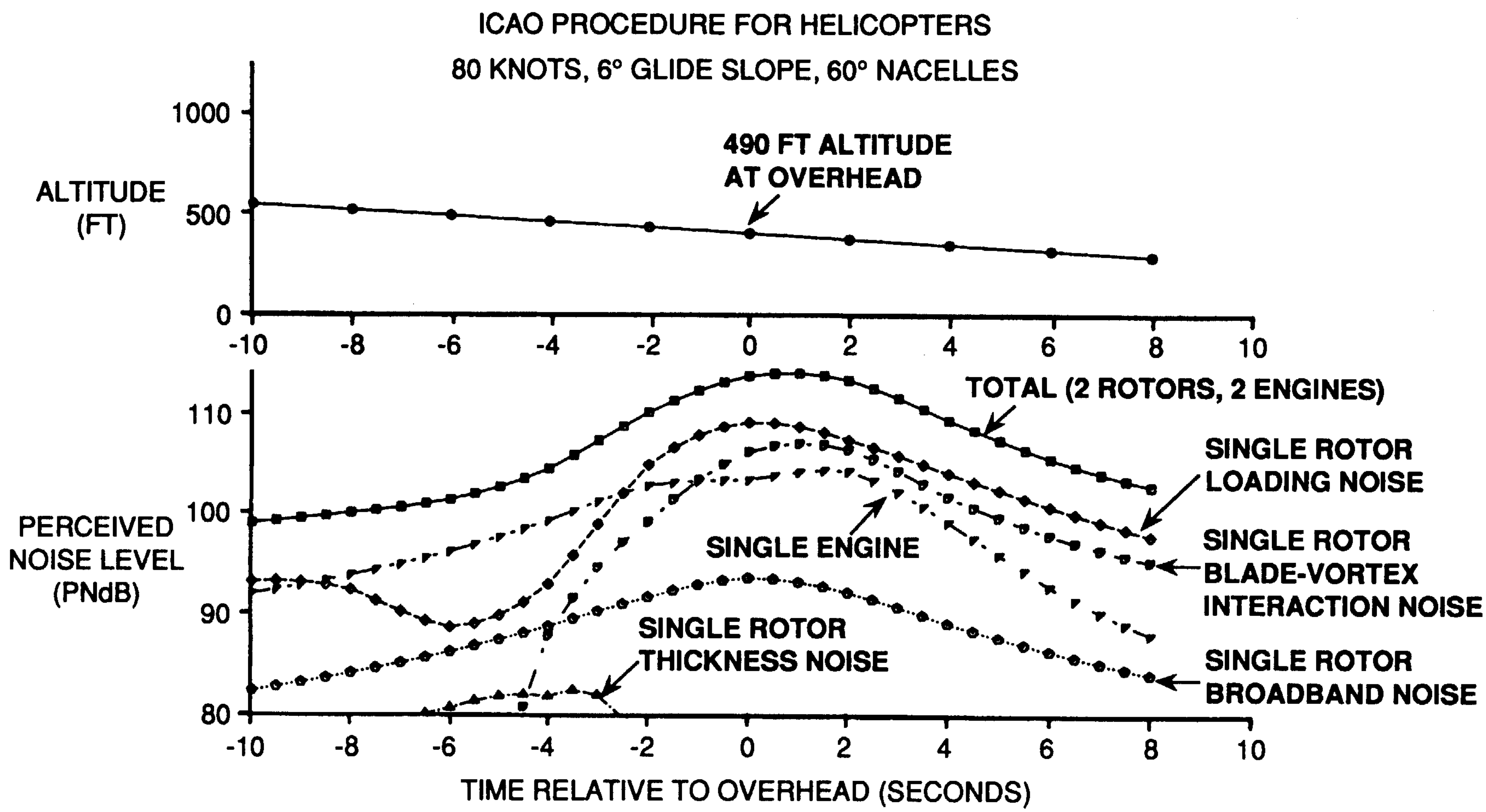

EFFECTIVE PERCEIVED NOISE LEVELS (EPNdB)			
WITH BARE ENGINE AND BVI: **106.4**	WITH INSTALLED ENGINE AND BVI: **105.3**	WITH INSTALLED ENGINE; NO BVI: **103.7**	ICAO STANDARD: **103.5**

Figure B-70. Predicted Civil Tiltrotor Approach Noise Levels

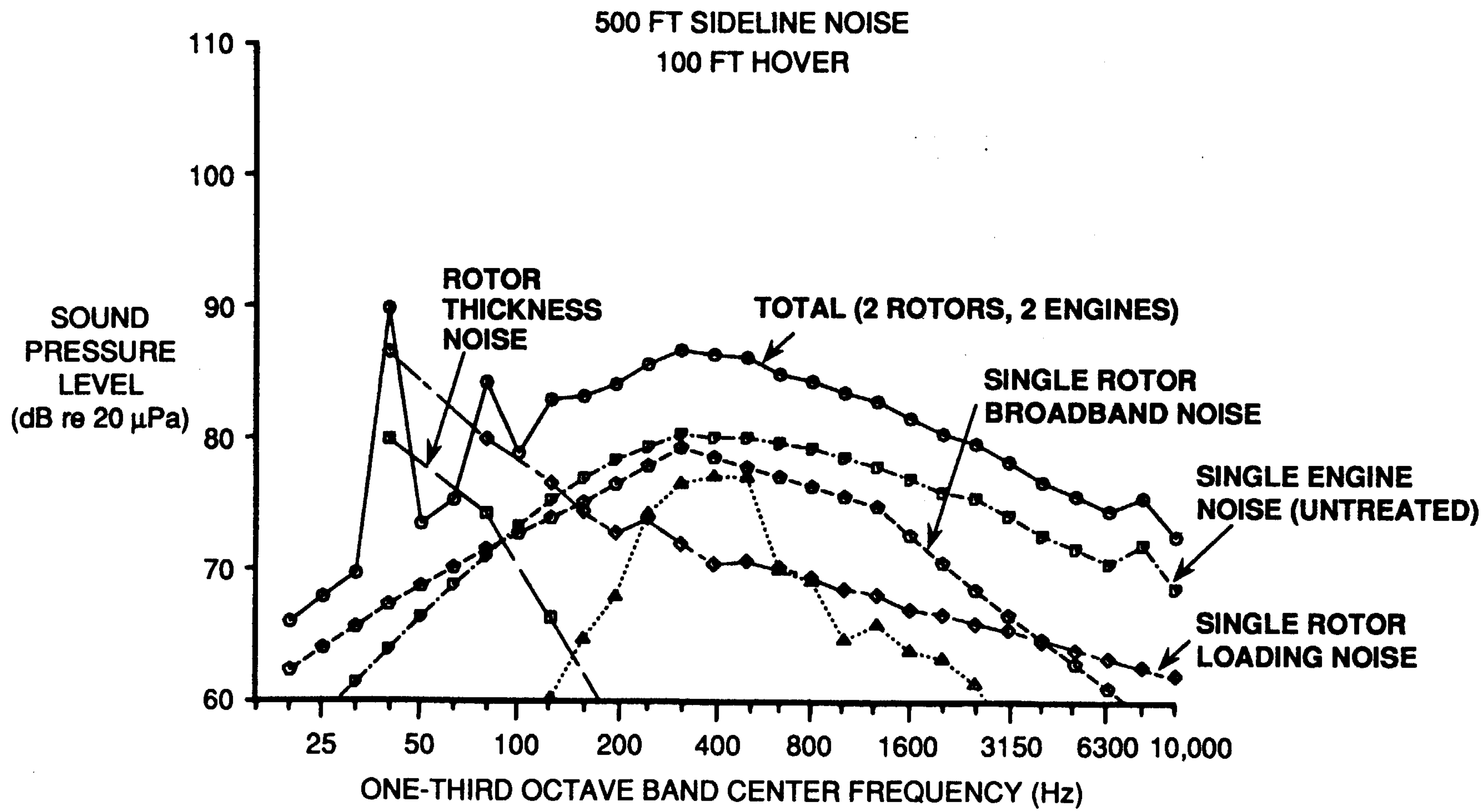

INSTALLED ENGINE WITH BVI	TREATED ENGINE WITH BVI	TREATED ENGINE NO BVI	TREATED ENGINE NO BVI DL = 20 psf
90.5 dBA	**88.1 dBA**	**87.6 dBA**	**85.5 dBA**

Figure B-71. Predicted Civil Tiltrotor Hover Sideline Acoustic Spectrum

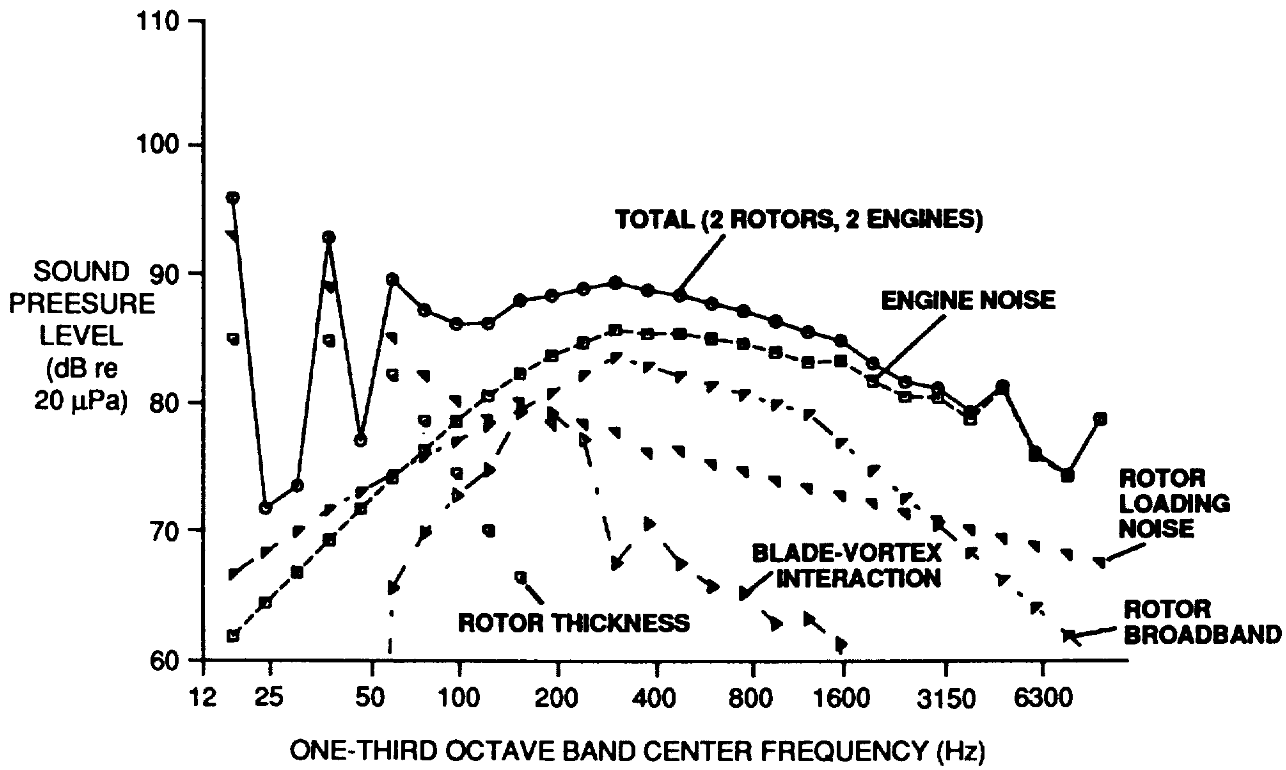

Figure B-72. Predicted Military Folding Tiltrotor Hover Sideline Acoustic Spectrum

The engine combustor noise dominates both the A-weighted and C-weighted levels. If a "moderate" amount of noise reducing treatment to the nacelle is assumed to reduce the engine combustor radiated noise by 3-dB, then the resultant A- and C-weighted levels are reduced to 95.6 and 100.5, respectively. These calculations assumed rectangular planform blades; if tapered blades were used, then the rotor noise would be reduced by approximately 2-dB. The resultant predicted A- and C-weighted levels with a normal engine installation are 96.7 and 100.4, and noise reducing treatment to the nacelles would result in 94.7-dBA and 99.2-dBC. With treatment to the nacelles to reduce the combustor noise, the engine compressor noise would become the dominant contributor. As suggested in Reference B-6, to account for the close VIGV/blade/VEGV spacing a correction value of 8-dB has been added to the compressor noise levels predicted by the methodology given in Reference B-7. This convertible engine (based on the GE38/CE4 engine) has a spacing as low as 0.5 chords, whereas the data which the prediction procedure of Reference B-7 was based on 2.0 chords minimum spacing. If the design of the engine was optimized for noise (increased VIGV/blade/VEGV spacings) the compressor noise could be reduced by 8-dB. The reduction of the compressor noise in conjunction with the reduction of the radiated combustor noise and the tapered rotor blades results in predicted levels of 92.5-dBA and 98.2-dBC. Relative to the baseline design, this gives a reduction of approximately 5-dBA, and approximately 3-dBC. The total reduction is less when using the C-weighting due to the low-frequency rotor noise. To achieve a total reduction of 5-dBC would require reducing the rotor noise by 2-dBC, which could be done by reducing the disc loading from 25 lb/sq. ft to approximately 20 lb/sq. ft. This reduction in the disc loading would require an increase in the rotor diameter from 31.4-ft to approximately 35-ft and require an increase in wingspan and hence weight.

REFERENCES

B-1. George, M., et al, *Downwash Environment for the Boeing Model 160 V/STOL Aircraft*, DCR-268, Dynasciences Corp., 1968.

B-2. Wernicke, R. K., *Prediction of Tilt Rotor Outwash*, AIAA Paper 81-0013, AIAA 19th Aerospace Sciences Meeting, 1981.

B-3. Schoen, A. H., et al, *User's Manual for VASCOMP II, The V/STOL Aircraft Sizing and Performance Computer Program*, Boeing Vertol Company, Report D8-0375, Volume IV, 1980.

B-4. Prouty, R., *Helicopter Performance, Stability and Control*, PWS Publishers, 1986.

B-5. Carlin, G., et al, *Results of a Powered Model Wind Tunnel Test of Helicopter Rotor Blade Vortex Alleviation Devices*, NASA CR 181969, 1990

B-6. McArdle, J. G., *Fan Acoustic Characteristics of a Turbofan/Turboshaft Convertible Engine with Variable Inlet Guide Vanes*, NASA TM 100207, 1987.

B-7 Heidmann, M. F., *Interim Prediction Method for Fan and Compressor Source Noise*, NASA TM X-71763, 1975.

NASA
National Aeronautics and Space Administration

Report Documentation Page

1. Report No.	2. Government Accession No.	3. Recipient's Catalog No.
NASA CR-177585		

4. Title and Subtitle	5. Report Date
Technology Needs for High-Speed Rotorcraft (1)	May 1991
	6. Performing Organization Code

7. Author(s)	8. Performing Organization Report No.
J. B. Wilkerson, J. J. Schneider, and K. M. Bartie	A-91159
	10. Work Unit No. 532-06-37
9. Performing Organization Name and Address: Boeing Helicopters, P. O. Box 16858, Philadelphia, PA 19142	11. Contract or Grant No. NAS2-13041
12. Sponsoring Agency Name and Address: Ames Research Center, Moffett Field, CA 94035-1000	13. Type of Report and Period Covered: Contractor Report
	14. Sponsoring Agency Code

15. Supplementary Notes

Point of Contact: P. D. Talbot, Ames Research Center, MS 237-5, Moffett Field, CA 94035-1000
(415) 604-5108 or FTS 464-5108

16. Abstract

The study identified high-speed rotorcraft concepts and the technology needed to extend rotorcraft cruise speeds up to 450 knots, while retaining the helicopter attributes of low downwash velocities. Task I identified 20 concepts with high-speed potential. These concepts were qualitatively evaluated to determine the five most promising ones. These five concepts were designed with optimum wing loading and disc loading to a common NASA-defined military transport mission. The optimum designs were quantitatively compared against 11 key criteria and ranked accordingly. The two highest ranking concepts were selected for further study in Task II: the canard tiltrotor and the folding tiltrotor. In Task II, the folding tiltrotor was chosen for the military transport mission since it had the highest speed potential and best survivability. The canard tiltrotor was chosen for the 30-passenger civil mission since it had the lowest gross weight and lowest estimated cost to build. Vehicle sensitivity to design speed and technology level was estimated as part of Task II. The combination of year 2000 structural, aerodynamics and propulsion potential improvements was projected to decrease vehicle gross weight by 25%. Task III identified design issues and technologies critical for concept maturity. One example is the development of a prop-rotor capable of efficient cruise at 450 knots; another is the development of an automated, reversible stop/fold procedure for the folding tiltrotor. An enabling technology plan was developed around each critical technology, to prepare for low-risk full scale development by the year 2000.

17. Key Words (Suggested by Author(s))	18. Distribution Statement
VTOL, High speed rotorcraft, Civil transport, Tilt rotor, Variable diameter tilt rotor, Tilt wing, Folding tilt rotor, Technology tasks, Conceptual design, Convertible engine	Unclassified-Unlimited Subject Category – 05

19. Security Classif. (of this report)	20. Security Classif. (of this page)	21. No. of Pages	22. Price
Unclassified	Unclassified	250	A11

NASA FORM 1626 OCT 86

For sale by the National Technical Information Service, Springfield, Virginia 22161